

RECOVERY OF LITHIUM FROM KAOLIN MINING WASTE MATERIAL

BY

ZUBERA IQBAL

A thesis submitted to

The University of Birmingham for the degree of

DOCTOR OF PHILOSOPHY

School of Chemical Engineering

University of Birmingham

May 2015

UNIVERSITY OF
BIRMINGHAM

University of Birmingham Research Archive

e-theses repository

This unpublished thesis/dissertation is copyright of the author and/or third parties. The intellectual property rights of the author or third parties in respect of this work are as defined by The Copyright Designs and Patents Act 1988 or as modified by any successor legislation.

Any use made of information contained in this thesis/dissertation must be in accordance with that legislation and must be properly acknowledged. Further distribution or reproduction in any format is prohibited without the permission of the copyright holder.

Abstract

Lithium is considered a borderline strategically important metal for the UK due to the limited availability of primary deposits, of sufficient grade, for economic processing (Naden, 2012). The rising demand, of approximately 10% yearly, has promulgated investigations for the development of secondary sources of lithium in order to secure long term reserves for the UK and Europe (Jaskula, 2015).

The British Geological Survey (1987) estimated that the St Austell granite contained up to 3.3 million tonnes of recoverable lithium. Imerys Ltd also identified lithium-bearing mineral in their kaolin waste material in Beauvoir, containing up to 0.89 wt.% Li_2O . The lithium-bearing minerals identified were; lepidolite ($\text{K}(\text{Li},\text{Al})_3(\text{Si},\text{Al})_4\text{O}_{10}(\text{F},\text{OH})_2$) and zinnwaldite ($\text{KLiFeAl}(\text{AlSi}_3)\text{O}_{10}(\text{F},\text{OH})_2$), which can contain between 3.0 to 7.7 wt.% Li_2O and 2.0 to 5.0 wt.% Li_2O , respectively (Garrett, 2004).

Lithium flotation concentrates containing up to 5.0 wt.% Li_2O were optimised for the Beauvoir waste material with up to 80% lithium recoveries, whereas a lower flotation grade of 0.5 wt.% Li_2O was found for the St Austell material. The St Austell waste materials did not prove viable to process via conventional flotation routes hence a novel process route for the bio-recovery of lithium from lithium rich micas was developed. Extraction of lithium by bioleaching has demonstrated the ability of fungi, of *Aspergillus niger* group, to leach lithium from the lepidolite in significant quantity, achieving 125mg/L of lithium in solution after twelve weeks of bio-leaching, at a recovery of 45%. Following this research, Imerys are applying to build a pilot plant, securing funding through the Innovative UK grant.

Acknowledgements

Firstly, I would like to thank my lead supervisor Professor Neil Rowson for his support and guidance throughout the PhD, without him this journey would never have started. Thank you for your pearls of wisdom and support throughout the PhD.

I would also like to thank Allah (swt) for blessing me with this opportunity and to everyone who helped make this thesis possible, including my family and friends who have played an important role in the making. I can't forget to mention the friendly staff at Starbucks and Costa who helped provide the much needed energy to keep me going.

Finally I would like to express my gratitude to my industrial supervisor Mr Anthony Phillips at Imerys Lt, as well as the Engineering and Physical Science Research Council for providing funding for the research to take place.

TABLE OF CONTENTS

ABSTRACT	II
ACKNOWLEDGEMENTS	IV
CHAPTER 1	1
1.1 The importance of Lithium	1
1.2 Aims of the thesis	3
1.3 Thesis chapters	4
CHAPTER 2	7
2.1 Background on lithium	7
2.1.1 Lithium deposits	8
2.1.2 Lithium production	13
2.1.3 Applications of lithium	18
2.1.4 Future	20
2.2 Kaolin	21
2.2.1 Kaolinisation Grade Classification	22
2.2.2 Kaolin production	24
2.3 Imerys Ltd	25
2.3.1 Beauvoir, France	25
2.3.2 Saint Austell, UK	29
2.4 Froth flotation separation	36
2.4.1 The effect of particle size on processing	38
2.4.2 Effect of pH on froth flotation	39
2.4.3 The effect of collector dosage and type on froth flotation	39
2.4.4 The effect of depressant addition on froth flotation performance	41
2.5 Overview of potential extraction processes for lithium	42
2.5.1 Acid leaching process	43
2.5.2 Gypsum process	44
2.5.3 Bioleaching	49

CHAPTER 3	56
3.1 Introduction	56
3.2 Materials	57
3.2.1 Mica Specimen Analysis	57
3.2.2 Kaolin waste material	58
3.3 Sample preparation	60
3.4 Physical Separation techniques	61
3.4.1 Froth flotation separation	61
3.4.2 Wet High Intensity Magnetic Separation (WHIMS)	63
3.4.3 Dry High Intensity Magnetic Separation	65
3.4.4 Electrostatic Separation	66
3.5 Analytical techniques	67
3.5.1 Particle size distribution	67
3.5.2 X-Ray Diffraction (XRD)	67
3.5.3 X-Ray Fluorescence (XRF)	68
3.5.4 Scanning Electron Microscopy (SEM)	69
3.5.5 Mineral Liberation Analysis (MLA)	70
3.5.6 Inductively Coupled Plasma (ICP)	70
3.5.7 Atomic Absorption Spectroscopy (AAS)	71
3.5.8 Flow cytometry	71
CHAPTER 4	73
4.1 Introduction	73
4.2 Beauvoir Mica Wastes	73
4.2.1 Introduction	73
4.2.2 Hydrocyclone underflow waste material	74
4.2.3 Beauvoir lithium mica concentrate	77
4.2.4 Mineral grade specimen pure lepidolite	80
4.3 St Austell, UK lithium mica deposits	81
4.3.1 Introduction	81
4.3.2 New Sink Grade 5	83
4.3.3 New Sink, Grade 4	88
4.3.4 Stope 13, Grade 4	91

4.3.5 Blackpool, Grade 4	94
4.3.6 Summary of St Austell deposit	97
CHAPTER 5	98
5.1 Introduction	98
5.2 Froth Flotation Separation of Kaolin Waste Material From Beauvoir in France	99
5.2.1 Introduction	99
5.2.2 Particle Size Distribution (PSD) of Beauvoir waste material	103
5.2.3 Change of design of experiments	104
5.2.4 Margin of experimental errors	105
5.2.5 Experimental procedure	105
5.2.6 Results and discussion	106
5.2.7 Conclusion of Beauvoir material	124
5.3 Froth Flotation Separation of Kaolin Waste Material from St Austell in the UK	125
5.3.1 Introduction	125
5.3.2 Experimental procedure	126
5.3.3 Results and discussion	126
5.3.4 Summary of froth flotation separation	156
5.4 Magnetic Separation of Kaolin Waste Material From St Austell in the UK	157
5.4.1 Introduction	157
5.4.2 Experimental procedure	158
5.4.3 Results and discussion	158
5.4.4 Summary on magnetic separation technique	166
5.5 Electrostatic separation of kaolin waste material from St Austell, UK	167
5.5.1 Introduction	167
5.5.2 Experimental procedure	167
5.5.3 Results and discussion	168
5.6 Overall conclusion of the separating techniques	169
CHAPTER 6	171
6.1 Introduction	171
6.2 Gypsum process	172
6.2.1 Introduction	172

6.2.2 Experimental procedure	173
6.2.3 Results and discussion	173
6.2.4 Summary of gypsum process	186
6.3 Organic acid leaching of lithium micas	187
6.3.1 Introduction	187
6.3.2 Experimental procedure	188
6.3.3 Results and discussion	188
6.3.4 Summary of organic acid process	206
6.4 Mine water analysis from kaolin sites	210
6.4.1 Introduction	210
6.4.2 Experimental procedure	211
6.4.3 Beauvoir mine water analysis	211
6.4.4 St Austell mine water analysis	214
6.4.5 Using mine water as a leachant	217
6.5 Biological leaching	225
6.5.1 Introduction	225
6.5.2 Preliminary research (carried out by TUKE)	226
6.5.3 Bioleaching with <i>A. niger</i>	231
6.5.4 Summary of bioleaching results	245
CHAPTER 7	248
7.1 Conclusion	248
7.2 Characterisation	249
7.3 Recovery	249
7.4 Extraction	251
7.5 Recommendations	253
REFERENCES	254
APPENDIX	267

List of Figures

Figure 2:1 The mineral petalite (taken from Northern Geological Supplies Ltd, 2014). . .	8
Figure 2:2 Primary sources of lithium production (WS, 2013).....	10
Figure 2:3 The Lithium Triangle surrounding Chile, Bolivia and Argentina. The three salars; Salar de Atacama, Salar de Uyuni and the Salar de Hombre Muerto, represent smaller brines (Roskill, 2012).	11
Figure 2:4: Extraction processes for lithium (Ebensperger, 2005).....	14
Figure 2:5 Lithium applications for the year 2014 (Jaskula, 2015).....	19
Figure 2:6: Global Lithium Carbonate Demand and Forecast (Astle, 2009).	20
Figure 2:7 Kaolinised rock (Camm, 2005).	21
Figure 2:8 Type of primary deposit where the two kinds of alteration are visible (Hirtzig, 2010).	22
Figure 2:9 Images of varying grades of kaolin decomposition (Lanzi, 2008).	23
Figure 2:10 Geological map of Beauvoir mine site in France taken from Google Earth, the red balloon locates the Imerys Ceramic centre and below it is the open cast mine. .	25
Figure 2:11 Flow diagram of the processing route for Beauvoir material (adapted from Thompson, 2012).....	28
Figure 2:12 Map of St Austell shows the UK Hydrous Kaolin Platform operations site taken in 2010 (Hirtzig, 2010).	30
Figure 2:13 Primary lithological variation in the kaolinised St Austell granite, UK (Hirtzig, 2010; Manning, 1996).....	31
Figure 2:14 Mineral Liberation Analysis of the Treviscoe hydrocyclone underflow (Ancia, 2010).....	33

Figure 2:15 Mineralogy of the Treviscoe material compared to other locations owned by Imerys (Ancia, 2010).....	34
Figure 2:16 Schematic diagram of flotation cell	37
Figure 2:17 Interrelated components of a flotation system (Kawatra, 2011).....	38
Figure 2:18 Typical Collector types used in minerals processing (Kawatra, 2011).....	40
Figure 2:19: Cationic Collector Structure (Bulatovic, 2007)	41
Figure 2:20 Gypsum process for lithium adapted from ANZAPLAN ltd. (Anzaplan, 2013).....	45
Figure 2:21 Mechanism of bacterial leaching (a) bacteria can either oxidise ferrous ions in the solution (b) attach to the bacteria to oxidise the ferric ions (c) the bacteria directly oxidise the mineral using only micro-organisms, (Crundwell, 2003).	50
Figure 2:22 SEM Image of spodumene after 30 days of leaching with <i>A. niger</i> , Magnification x 500 (Rezza, 2001).	52
Figure 2:23 Dissolved lithium detected in the leach liquor by AAS, each value was an average of three experiments with standard deviation less than 15% (Rezza, 2001).....	54
Figure 3:1 Mineral grade specimen of (a) Biotite mica, (b) Muscovite mica, (c) Lepidolite mica (lithium-rich mice).	57
Figure 3:2 The Beauvoir mining site in France, this photo was taken in April 2011. ...	58
Figure 3:3 Schematic representation of a hydrocyclone, spiral flow, taken from (Rowson, 2010)	59
Figure 3:4 Principle of operation of froth flotation cell	62
Figure 3:5 Image of flotation cell taken from sepor.com.	62
Figure 3:6 Principal of operation of wet high intensity magnetic separator.	64

Figure 3:7 Boxmag-Rapid, Wet high intensity magnetic separator.	64
Figure 3:8 Induced roll magnetic separator	65
Figure 3:9 Principal of operation of electrostatic separator.	66
Figure 3:10 Electrostatic separator	66
Figure 3:11 Muffle furnace used for loss on ignition tests.....	69
Figure 4:1 MLA image analysis of waste material for 315-630 μ m size fraction, the key is found in table 1.3 (Ancia, 2010).	75
Figure 4:2 Particle size distributions for Li ₂ O wt.% (Ancia, 2010).	76
Figure 4:3 Thin section microscopy image of lepidolite mineral obtained from Beauvoir, France, magnification x10.	79
Figure 4:4 SEM image of lepidolite mineral obtained from Beauvoir, France, 10KV, Mag: 500, Det: SE, WD 10mm.	79
Figure 4:5 Geological map of St Austell showing the UK Hydrous Kaolin Platform operations site taken in 2010.	81
Figure 4:6 Selected face of New Sink G5 material (Hooper, 2012).....	84
Figure 4:7 Hand specimen of New Sink Lithium Mica granite G5 (Hooper, 2012).	84
Figure 4:8 Lithium concentrations in varying particle size fraction for the New Sink G5 material.	86
Figure 4:9 Particle Size Distribution of New Sink G5 material after classification into size fractions (a) 53 μ m to 250 μ m and (b) 250 μ m to 500 μ m, obtained by laser-sizer...	87
Figure 4:10 Selected face of New Sink G4 material (Hooper, 2012).....	89
Figure 4:11 Hand specimen of New Sink Lithium Mica granite G4 (Hooper, 2012).	89

Figure 4:12 Lithium concentration in varying particle size fraction for the New Sink material.	90
4:13 Selected face of Stope13 G4 material (Hooper, 2012).	92
4:14 Hand specimen of Stope 13 Lithium Mica granite G4 (Hooper, 2012).	92
Figure 4:15 Lithium concentration in varying particle size fraction for the St Austell kaolin mining waste material.	93
4:16 Selected face of Blackpool G4 material (Hooper, 2012).	95
4:17 Hand specimen of Blackpool Lithium Mica granite G4 (Hooper, 2012).	95
Figure 4:18 Lithium concentration in varying particle size fraction for the St Austell kaolin mining waste material.	96
Figure 5:1 Process flow sheet for the Beauvoir waste material. (a) Addition of H ₂ SO ₄ (b) addition of collector (Ancia, 2010).	100
Figure 5:2 Li ₂ O concentrate grade and recovery for the Beauvoir waste material using froth flotation separation, experimental number is shown in Table 5:1.	102
Figure 5:3 Particle Size Distribution of the Beauvoir waste material after classification into the size fraction of 53µm to 400µm. Determined by laser-sizer.	103
Figure 5:4. Process flowsheet for the Beauvoir waste material. (a) addition of H ₂ SO ₄ (b) addition of collector and/or depressant (an additional conditioning period was added if depressant was used).	105
Figure 5:5 Froth flotation separation results for Beauvoir material, an average of two experiments was taken. The conditions of the experiments are given in table 5.3.	107
Figure 5:6 Metal concentrations detected in the Beauvoir lithium concentrates, average of two experiments.	109

Figure 5:7 Metal oxide correlations for the Beauvoir granite (Ancia, 2010).	111
Figure 5:8 Recovery of Li_2O at different pulp acidity using froth flotation as a function of 200g/t collector, 80g/t depressant for the particle size fraction of 250 μm to 400 μm	113
Figure 5:9 Recovery of Li_2O at different pulp acidity using froth flotation as a function of 200g/t collector, 80g/t depressant for the particle size fraction of 53 μm to 250 μm	113
Figure 5:10 Concentrate grade of Li_2O at different pulp acidity using froth flotation as a function of 200g/t collector, varying depressant dosages and pH levels for the particle size fraction of 250 μm to 400 μm	116
Figure 5:11 Recovery of Li_2O using froth flotation at different pulp acidity as a function of 200g/t collector, varying depressant dosages and pH levels for the particle size fraction of 250 μm to 400 μm	116
Figure 5:12 Concentrate grade of Li_2O using froth flotation at different pulp acidity as a function of 200g/t collector, varying depressant dosages and pulp pH levels for the PSD of 53 μm to 250 μm	118
Figure 5:13 Recovery of Li_2O using froth flotation at different pulp acidity as a function of 200g/t collector, varying depressant dosages and pulp pH levels for the particle size fraction of 53 μm to 250 μm	119
Figure 5:14 Lithium concentrate grade of Li_2O at different pulp acidity using froth flotation as a function of 250g/t depressant, varying collector dosages and pH levels for the particle size fraction of 250 μm to 400 μm	121

Figure 5:15 Recovery of Li_2O using froth flotation at different pulp acidity as a function of 250g/t depressant, varying collector dosages and pH levels for the particle size fraction of 250 μm to 400 μm	121
Figure 5:16 Recovery of Li_2O as a function of 250g/t depressant, varying collector dosages and pulp pH levels for the particle size fraction of 53 μm to 250 μm	123
Figure 5:17 Recovery of Li_2O as a function of 250g/t depressant, varying collector dosages and pulp pH levels for the particle size fraction of 53 μm to 250 μm	123
Figure 5:18 Li_2O concentrate grades in varying particle size fraction for the St Austell kaolin mining waste materials used in this study.	129
Figure 5:19 PSD of New Sink G5 material after classification into size fractions (a) 53 μm to 250 μm and (b) 250 μm to 500 μm , determined by laser-sizer.	130
Figure 5:20 Recovery/ grade of Li_2O using froth flotation at different particle size distributions as a function of 200g/t collector, 250g/t depressant at pH 1.5.	132
Figure 5:21 XRD pattern of the lithium concentrate for the PSD between 53 μm to 250 μm , (a) zinnwaldite, (b) quartz.	135
Figure 5:22 XRD pattern of the tailings for the PSD between 53 μm to 250 μm , (b) quartz.	135
Figure 5:23 Recovery of Li_2O from New Sink G5 at different pulp acidity as a function of 200g/t collector, 250g/t depressant and particle size fraction of 53 μm to 250 μm ...	137
Figure 5:24 Recovery of Li_2O from New Sink G5 at different pulp acidity as a function of 200g/t collector, 250g/t depressant and particle size fraction of 250 μm to 500 μm	137

Figure 5:25 Recovery of Li_2O of New Sink G5 at different depressant dosage as a function of 200g/t collector at pH 1.5 for the particle size fraction of 53 μm to 250 μm	138
Figure 5:26 Recovery of Li_2O of New Sink G5 at different collector dosage as a function of 250g/t depressant and pulp pH 1.5 for the particle size fraction of 53 μm to 250 μm	140
Figure 5:27 Li_2O grades in varying particle size fraction for the St Austell kaolin mining waste materials used in this study.....	141
Figure 5:28 Recovery of Li_2O for New Sink G4 using froth flotation at different particle size distributions as a function of 200g/t collector, 500g/t depressant at pulp pH 1.5.	144
Figure 5:29 Recovery/ grade of Li_2O for New Sink G4 using froth flotation at as a function of 200g/t collector, 250g/t depressant at pulp pH 1.4 - 2.3.....	146
Figure 5:30 Recovery of Li_2O for New Sink G4 using froth flotation as a function of 200g/t collector, 250g/t depressant at pulp pH 1.4 - 2.3.....	146
Figure 5:31 Li_2O grade for New Sink G4 using froth flotation as a function varying collector and depressant dosages at pH 1.5.	149
Figure 5:32 Li_2O recoveries for New Sink G4 using froth flotation as a function varying collector and depressant dosages at pH 1.5.	149
Figure 5:33 Li_2O grade for New Sink G4 using froth flotation as a function varying collector and depressant dosages at pH 1.5.	150
Figure 5:34 Li_2O recovery for New Sink G4 using froth flotation as a function varying collector and depressant dosages at pH 1.5.	151

Figure 5:35 Li ₂ O recovery for Stope 13 G4 using froth flotation as a function 500g/t depressant and 400g/t collector at pulp pH 2.0	152
Figure 5:36 Li ₂ O recovery for Stope 13 G4 using froth flotation as a function 250g/t depressant and 200g/t collector for PSD (53µm to 250µm).....	153
Figure 5:37 Li ₂ O recovery for Stope 13 G4 using froth flotation on various reagent dosages, pulp pH 2.0.	154
Figure 5:38 Li ₂ O recovery for Blackpool G4 using froth flotation on various reagent dosages, pulp pH 1.5.	155
Figure 5:39 Schematic of two-stage separation process using WHIMS.	157
Figure 5:40 Lithium concentrations for varying particle size fractions using WHIMS (0.8 Tesla).....	159
Figure 5:41 XRD pattern of New Sink G5 material showing magnetic fractions after WHIMS separation, (a) zinnwaldite, (b) quartz, (a*) zinnwaldite and quartz.	161
Figure 5:42 XRD pattern of New Sink G5 material showing non-magnetic fractions after WHIMS separation, (a) zinnwaldite, (b) quartz, (a*) zinnwaldite and quartz.	161
Figure 5:43 XRD pattern of New Sink G5 material showing magnetic fractions after dry magnetic separation, (a) zinnwaldite, (b) quartz, (a*) zinnwaldite and quartz.	163
Figure 5:44 XRD pattern of New Sink G5 material showing non-magnetic fractions after dry magnetic separation, (a) zinnwaldite, (b) quartz, (a*) zinnwaldite and quartz.	163
Figure 5:45 Lithium concentrate grades for the ore sample from St Austell (UK) using WHIMS.	165

Figure 6:1 Crystal structure of the lepidolite taken from Crystal Structure Gallery, National Institute of Advanced Industrial Science and Technology (Nomura, 2002).	174
Figure 6:2 Optical microscope image of Beauvoir lithium concentrate untreated, magnification x10, scale 2.65cm.	175
Figure 6:3 Optical microscope image of Beauvoir lithium concentrate heat treated at 850°C for 60 minutes, magnification x10, scale 2.65cm.	175
Figure 6:4 XRD pattern of Beauvoir lithium concentrate (untreated) for the PSD 53µm to 250µm, (a) zinnwaldite.	177
Figure 6:5 XRD pattern of Beauvoir lithium concentrate heat treated to 850°C for 60 minutes, for the PSD 53µm to 250µm, (a) zinnwaldite.	177
Figure 6:6 Results for the gypsum process with Beauvoir lithium concentrate at varying calcination temperatures.	178
Figure 6:7 XRD pattern of Beauvoir lithium concentrate and CaSO ₄ calcined at 900°C for 60 minutes, (a) CaSO ₄ , (b) oxides.	182
Figure 6:8 XRD pattern of Beauvoir lithium concentrate and CaSO ₄ calcined at 900°C for 60 minutes and then leached with water at 90°C for 30 minutes, (a) CaSO ₄ , (b) oxides.	182
Figure 6:9 XRD pattern of mineral specimen grade pure lepidolite untreated, (a) lepidolite.	184
Figure 6:10 XRD pattern of pure lepidolite and CaSO ₄ after calcination at 850°C for 60 minutes, (a) lepidolite, (b) CaSO ₄ .	184
Figure 6:11 XRD pattern of pure lepidolite and CaSO ₄ calcined at 850°C and then water leached at 90°C for 30 minutes, (a) lepidolite, (b) CaSO ₄ .	184

Figure 6:12 Metal extraction results for the gypsum method for lepidolite, the experiments were analysed three times, RSD <105%.....	185
Figure 6:13 Extraction of lithium mica using water as a leachant, RSD <10%.....	189
Figure 6:14 Lithium concentration in solution for the Beauvoir lithium concentrate leached at 25°C, with oxalic acid at varying acid concentrations, RSD < 10%.....	190
Figure 6:15 Lithium recovery for the Beauvoir lithium concentrate leached at 25°C, with oxalic acid at varying acid concentrations.....	191
Figure 6:16 Lithium concentration in solution for the Beauvoir lithium concentrate leached with oxalic acid (1% w/v) at varying temperatures, RSD <10%.	193
Figure 6:17 Lithium concentration in solution for the Beauvoir lithium concentrate leached with oxalic acid (5% w/v) at varying temperatures, RSD <10%.	193
Figure 6:18 Lithium recovery for the Beauvoir lithium concentrate leached with oxalic acid (1% w/v) at varying temperatures.....	194
Figure 6:19 Lithium recovery for the Beauvoir lithium concentrate leached with oxalic acid (5% w/v) at varying temperatures.....	194
Figure 6:20 Lithium concentration in solution for the Beauvoir lithium concentrate leached with 1% (w/v) oxalic acid, the concentrate was heat treated (HT) and untreated (UT) prior to leaching at 25°C, RSD <10%.	196
Figure 6:21 Lithium concentration in solution for the Beauvoir lithium concentrate leached with 5% (w/v) oxalic acid, the concentrate was heat treated (HT) and untreated (UT) prior to leaching at 25°C, RSD <10%.	196

Figure 6:22 Lithium recovery for the Beauvoir lithium concentrate leached with 1 wt.% oxalic acid, the concentrate was heat treated (HT) and untreated (UT) prior to leaching at 25°C.....	197
Figure 6:23 Lithium recovery for the Beauvoir lithium concentrate leached with 5 wt.% oxalic acid, the concentrate was heat treated (HT) and untreated (UT) prior to leaching at 25°C.....	197
Figure 6:24 Lithium concentration in solution for the Beauvoir lithium concentrate (heat treated) leached with oxalic acid (1% w/v) at varying temperatures, RSD <10%.	199
Figure 6:25 Lithium concentration in solution for the Beauvoir lithium concentrate (heat treated) leached with oxalic acid (5% w/v) at varying temperatures, RSD <10%.	199
Figure 6:26 Lithium recovery for the Beauvoir lithium concentrate (heat treated) leached with oxalic acid (1% w/v) at varying temperatures.....	200
Figure 6:27 Lithium recovery for the Beauvoir lithium concentrate (heat treated) leached with oxalic acid (5% w/v) at varying temperatures.....	200
Figure 6:28 Lithium concentration for the Beauvoir lithium concentrate leached with oxalic acid (5% w/v) at varying temperatures RSD <10%. Heat treated (HT) and untreated (UT) Beauvoir concentrates.....	202
Figure 6:29 Lithium concentration and recovery for the Beauvoir lithium concentrate (untreated) leached with citric acid (5% w/v) at varying temperatures, RSD <10%. .	203
Figure 6:30 Comparison of lithium concentration for the Beauvoir lithium concentrate (untreated) leached with oxalic and citric acid (5% w/v) at 40°C, RSD <10%.	203

Figure 6:31 Lithium concentration in solution for the Beauvoir lithium concentrate (Heat treated) leached with citric acid (5 % w/v) at varying temperatures, RSD <10%.	205
Figure 6:32 Lithium recovery for the Beauvoir lithium concentrate (Heat treated) leached with citric acid (5% w/v) at varying temperatures.	205
Figure 6:33 Comparison of lithium concentration in solution for the Beauvoir lithium concentrate (Heat treated) leached with oxalic and citric acids (5% w/v) at 70°C, RSD <10%.	207
Figure 6:34 Comparison of lithium recovery for the Beauvoir lithium concentrate (Heat treated) leached with oxalic and citric acids (5% w/v) at 70°C.	208
Figure 6:35 Comparison of lithium concentration for the Beauvoir lithium concentrate (heat treated) leached with oxalic and citric acid (5% w/v) at 40°C, RSD <10%.	208
Figure 6:36 Comparison of lithium recovery for the Beauvoir lithium concentrate (heat treated) leached with oxalic and citric acid (5% w/v) at 40°C.	209
Figure 6:37 Left image: Mine site in Beauvoir, France. Right image: lake near the mine in Beauvoir, France.	212
Figure 6:38 Density plot of (a) Mine water and (b) Lake water from Beauvoir stained with SYTO62 showing DNA count (FL4A) vs cell size (FSC-A).	213
Figure 6:39 Map of St Austell showing the UK Hydrous Kaolin Platform operations site taken in 2010 (Hirtzig, 2010).	214
Figure 6:40 Iron and lithium analysis of the mine water samples taken from Imerys Ltd St Austell sites.	216

Figure 6:41 Lithium concentration in solution for the Beauvoir lithium concentrate contacted with mine water at 25°C RSD <10%.	220
Figure 6:42 Iron concentration in solution for the Beauvoir lithium concentrate contacted with mine water at 25°C RSD <10%.	220
Figure 6:43 Lithium concentration in solution and DNA count for the Beauvoir lithium concentrate contacted with mine water at 25°C RSD <10%.	221
Figure 6:44 Lithium in solution when bioleaching New Sink G5 sample in Trebal refinery water, each data point is an average of three experiments.....	223
Figure 6:45 Lithium in solution when bioleaching Beauvoir lithium concentrate in Dubbers dam, each data point is an average of three experiments.....	224
Figure 6:46 Lithium content observed in a low-nutrient medium containing a culture of acidophilic bacteria was used to leach lithium from the Beauvoir lithium concentrate, carried out in collaboration with TUKE.	228
Figure 6:47 <i>A. niger</i> grown on Sabouraud agar taken from (JGI, 2012).	229
Figure 6:48 pH changes observed in a low-nutrient medium containing <i>A. niger</i> bioleaching the Beauvoir lithium concentrate over 42 days, carried out in collaboration with TUKE.	230
Figure 6:49 SEM of Beauvoir lithium concentrate before bioleaching with <i>A. niger</i> , taken in TUKE.....	231
Figure 6:50 SEM of Beauvoir lithium concentrate after bioleaching <i>A. niger</i> taken in TUKE.	231
Figure 6:51 Lithium in solution when direct bioleaching mineral specimen grade pure lepidolite with <i>A. niger</i> at 25°C <10% RSD, S: sterilised, NS: non-sterilised.....	234

Figure 6:52 Lithium in solution when directly bioleaching mineral specimen grade pure lepidolite with <i>A. niger</i> at 25°C. <10% RSD, S: sterilised, NS: non-sterilised.....	236
Figure 6:53 Lithium in solution for direct bioleaching under aerobic conditions Beauvoir lithium concentrate with <i>A. niger</i> at 25°C, <10% RSD, S: sterilised, NS: non-sterilised.....	237
Figure 6:54 Lithium in solution for direct bioleaching under aerobics condition of the Beauvoir lithium concentration using <i>A. niger</i> 12 weeks. RSD<10%. S: sterilised, NS: non-sterilised.	239
Figure 6:55 Direct Bioleaching of the Pure lepidolite using <i>A. niger</i> over a period of 4 weeks, each data points is an average of three experiments, which are each analysed three times RSD<10%.	241
Figure 6:56 Schematic diagram for indirect leaching using dialysis tubing (adapted from SOS03, 2011).	242
Figure 6:57 Indirect bioleaching mineral specimen grade pure lepidolite using <i>A. niger</i> . Each data points is an average of three experiments, which are each analysed three times RSD<10%.	244
Figure 6:58 Indirect bioleaching Beauvoir lithium concentrate using <i>A. niger</i> . Each data points is an average of three experiments, which are each analysed three times RSD<10%.	245

List of Tables

Table 2:1 Global in-situ lithium resource, Mt: Million ton, ^a Producing, ^b Lowest estimate (Gruber, 2011).	8
Table 2:2 World Mine Reserve for lithium (Jaskula, 2015).....	12
Table 2:3 Commercial Lithium-bearing minerals, ^a high grade deposit, ^b low grade deposit, ^c theoretical values, Garrett, 2004; Siame, 2011).....	13
Table 2:2:4 Lithium resource and production assessment, Mt = Million ton ^a estimate (MIR, 2008).....	15
Table 2:5 World Mine Reserve for lithium (Jaskula, 2015).....	16
Table 2:6 Global Lithium markets demand for lithium applications *combined (Jaskula, 2008 - 2014).	19
Table 2:7 Magnetic product grade and recovery using WHIMS (Siame, 2011).....	35
Table 2:8 Magnetic product grade and recovery at a magnetic field strength of 0.94 Tesla. (Siame, 2011).....	35
Table 2:9 Partial chemical analysis of sample materials (Distin, 1982).	44
Table 2:10 Cost of bulk roasting additives (Siame, 2011).	47
Table 2:11 Additives used in the study (Yan, 2012).....	47
Table 2:12 Chemical composition of the leach liquor.....	47
Table 2:13 Comparison of conditions and results of different studies, *estimate, adapted from (Luong, 2013).	48
Table 2:14 Results from a study by Rezza (2001) when leaching lithium from the mineral, spodumene using <i>A. niger</i> as the leachant.....	53

Table 4:1 MLA, Mineralogy of the waste material for 315-630µm size fraction (Ancia, 2010; Watson, 1962).	75
Table 4:2 Chemical analysis of the Beauvoir waste material by particle size classification (Ancia, 2010).	77
Table 4:3 Chemical analysis of the lithium mica concentrate for the particle size fraction of 53 to 400µm. *tested by ICP ^a (Ancia, 2010), ^b (Garrett, 2004).	78
Table 4:4 Chemical analysis of a mineral specimen grade pure lepidolite, *tested by ICP.	80
Table 4:5 Mineralogy of the New Sink G5 material [For the mineral Tourmaline, X may be Na or Ca and Y may be Mg, Fe or Li] (Garrett, 2004; Hooper, 2012).	84
Table 4:6 Chemical analysis of New Sink G5, for the size fraction 53µm to 500µm. *tested by ICP.	86
Table 4:7 Mineralogy of the New Sink G4 material [For the mineral Tourmaline, X may be Na or Ca and Y may be Mg, Fe or Li, for Feldspar X may be K, Ca or Na] (Garrett, 2004; Hooper, 2012).	88
Table 4:8 Chemical analysis of New Sink G4, for the size fraction 250µm to 500µm. *tested by ICP.	90
Table 4:9 Mineralogy of the Stope 13 G4 sample [For the mineral Tourmaline, X may be Na or Ca and Y may be Mg, Fe or Li, for Feldspar X may be K, Ca or Na] (Garrett, 2004; Hooper, 2012).	91
Table 4:10 Chemical analysis of Stope 13 G4, for the size fraction 250µm to 500µm. *tested by ICP.	93

Table 4:11 Mineralogy of the Blackpool G4 material [For the mineral Tourmaline, X may be Na or Ca and Y may be Mg, Fe or Li, for Feldspar X may be K, Ca or Na] (Garrett, 2004; Hooper, 2012).	94
Table 4:12 Chemical analysis of Blackpool G4, for the size fraction 53µm to 250µm. *tested by ICP.	96
Table 4:13 Summary of chemical and mineralogical compositions for St Austell samples.	97
Table 5:1 Results from both of the froth flotation processes on Beauvoir kaolin waste (Ancia, 2010).	102
Table 5:2 The variables used in the froth flotation separation of Beauvoir hydrocyclone underflow and their experimental ranges.	104
Table 5:3 Recovery of Li ₂ O grade as a function of pH 1.5 for the particle size fraction of 53µm to 400µm.	107
Table 5:4 XRF analysis of Beauvoir lithium concentrates for experiments 1 to 4, *tested by ICP.	108
Table 5:5 Recovery of metal oxides grade as a function of pH 1.5 for the particle size fraction of 53µm to 400µm.	110
Table 5:6 Average of metal oxide results for the Beauvoir granite data obtained from Imerys.	111
Table 5:7 Comparison of the recovery for Li ₂ O using froth flotation as a function of 200g/t collector, 80g/t depressant.	114
Table 5:8 Comparisons of the recovery for Li ₂ O using froth flotation as a function of 200g/t collector for the PSD 250µm to 400µm.	115

Table 5:9 Comparisons of the recovery for Li ₂ O using froth flotation as a function of 200g/t collector for the PSD 53µm to 250µm.	118
Table 5:10 Comparisons of the recovery for Li ₂ O using froth flotation as a function of 250g/t depressant for the PSD 250µm to 500µm.	120
Table 5:11 Comparisons of the recovery for Li ₂ O using froth flotation as a function of 250g/t depressant for the PSD 53µm to 250µm.	122
Table 5:12 Mineral proportions of St Austell geological samples (Hooper, 2012).	129
Table 5:13 Chemical composition for New Sink G5, particle size fraction 53µm to 500µm.	131
Table 5:14 Metal oxides using froth flotation separation for the particle size distribution 53µm to 250µm.	133
Table 5:15 Chemical analysis of New Sink G5 concentrate and feed *tested by ICP .	133
Table 5:16 Mineral proportions of New Sink G5 sample after froth flotation separation at pH 1.5, depressant dosage 250g/t, collector dosage 200g/t for the particle size fraction 53µm to 250µm, *estimated, + form of tourmaline.	134
Table 5:17 Chemical analysis using froth flotation at different pulp acidity as a function of 200g/t collector and 250g/t depressant.	136
Table 5:18 Chemical analysis using froth flotation at different depressant dosage as a function of 200g/t collector at pH 1.5 for the particle size fraction of 53µm to 250µm.	139
Table 5:19 Chemical analysis using froth flotation at different collector dosage as a function of 250g/t depressant and pH 1.5 for the particle size fraction of 53µm to 250µm.	140

Table 5:20 Chemical analysis of New Sink G5 and G4 material (PSD 53µm to 500µm) *tested by ICP.....	142
Table 5:21 Mineral proportions of New Sink samples (Hooper, 2012).	143
Table 5:22 Recovery of Li ₂ O for the New Sink G4 using froth flotation as a function of 200g/t collector, 500g/t depressant at pulp pH 1.5	144
Table 5:23 Chemical analysis of New Sink G4 concentrate *tested by ICP.....	145
Table 5:24 Chemical analysis of New Sink G4 lithium concentrate for PSD 53-250µm *tested by ICP.....	147
Table 5:25 Optimum recoveries using froth flotation at pulp pH 1.5 for PSD (53µm to 250µm) in New Sink G4.....	148
Table 5:26 Optimum recoveries for New Sink G4 using froth flotation as a function varying collector and depressant dosages at pulp pH 1.5.....	150
Table 5:27 Recovery for Stope 13 G4 material via froth flotation on various pH pulp as a function 500g/t depressant and 400g/t collector at pulp pH 2.0	152
Table 5:28 Recovery for Stope 13 G4 material via froth flotation on various pH pulp as a function 200g/t depressant and 250g/t collector for PSD (53µm to 250µm).	153
5:29 Recovery for Stope 13 G4 material via froth flotation on various reagent dosages, pulp pH 2.0.	154
Table 5:30 Recovery for Blackpool G4 material via froth flotation on various PSD. .	155
Table 5:31 Magnetic product grade and recovery of New Sink G5 using WHIMS (0.8 Tesla).	159
Table 5:32 Chemical analysis of the G5 material separation products at magnetic field of 0.8 Tesla for WHIMS, *tested by ICP.	160

Table 5:33 Chemical analysis of the G5 material separation products at magnetic field of 1.2 Tesla for dry magnetic separation, *tested by ICP.	162
Table 5:34 Magnetic product grade and recovery of lithium concentrate using WHIMS (0.8 Tesla).....	165
Table 5:35 Electrostatic separation technique employed to recovery lithium bearing minerals for New Sink G5 samples.	168
Table 5:36 Chemical composition of New Sink G5 material electrostatically separated *tested by ICP.....	168
Table 6:1 Comparison of lithium extraction processes from various studies, using the gypsum method, * estimate.....	180
Table 6:2 Comparison of the effect of temperature on lithium recovery via gypsum process.	181
Table 6:3 Extraction of lithium mica using water as a leachant.....	189
Table 6:4 Size of lepidolite crystal at various heat-treatment temperature (Fang, 2002).	201
Table 6:5 Summary of the results for mine water sampled from Beauvoir, France, *tr: trace.	213
Table 6:6 Analysis of the mine water samples taken from various locations within St Austell (UK), RSD <10%, *tr: trace.	215
Table 6:7 Results for water and soil residue samples, analysed by Guardian labs, UK. The iron content was analysed at the University of Birmingham. *tr: trace.	217
Table 6:8 DNA count detected within the leach liquors during the mine water leaching extraction process, an average of three experiments, RSD < 10%.....	219

Table 6:9 Analysis of the mine water samples taken from Dubbers dam, within St Austell (UK) , each data point is an average of three readings, RSD <10%.....	223
Table 6:10 Lithium-bearing minerals and their lithium concentrations ^a theoretical maximum (Garrett, 2004).	226
Table 6:11 Results for direct bioleaching experiment under aerobic conditions, S = sterile and NS= non-sterile.	236
Table 6:12 Results for direct bioleaching experiment under aerobic conditions, S = Sterile and NS = Non-sterile.....	238
Table 6:13 Results for the direct bioleaching experiment for lepidolite under anaerobic conditions for week 4, S = Sterile and NS = Non-sterile.	241
Table 6:14 Chemical analysis of indirect bioleaching for mineral specimen grade of pure lepidolite.	243
Table 6:15 Chemical analysis of indirect bioleaching for Beauvoir lithium concentrate	244

Abbreviations

AAS	Atomic Absorption Spectroscopy
ICP	Inductively Coupled Plasma
LOI	Loss on Ignition
MLA	Mineral Liberation Analysis
PSD	Particle Size Distribution
SEM	Scanning Electron Microscopy
WHIMS	Wet High Intensity Magnetic Separation
XRD	X-ray diffraction
XRF	X-ray fluorescence

CHAPTER 1

INTRODUCTION

1.1 The importance of Lithium

Lithium has been categorised as a borderline strategic metal for the UK in a report published by the National Engineering Research Council (Naden, 2012), this is due to the decreasing availability of primary deposits, of sufficient grade, for economic processing, increasing demand for lithium in electronic devices and the lack of exploitable reserves in the UK. The complexity of the lithium battery recycling process route also adds to the strategic importance of lithium to the UK (and Europe).

From 2013 to 2020, the United States Geological Survey (2015) reported that the average annual growth in the world consumption of lithium can be expected to be around 10%. Recent years have seen an increase in the number and type of lithium usage, including technology driven devices which use lithium-ion batteries.

Lithium is the lightest metal with the greatest electrochemical potential of 3.04 V and high energy density. Baylis (2013) estimated that lithium-ion battery manufacture would consume 90,000 tonne (Lithium metal equivalent) per annum by 2017. Jaskula (2015) estimated that the total world reserves were 13,500,000 tonnes and reported that in 2014, the global mine production was approximately 36,000 tonnes per annum, without including the United States production to avoid disclosing company data.

As lithium is a finite global resource, it can be concluded that if processes are not investigated to recover lithium from secondary sources, problems with its availability and price may soon limit the development of lithium's current and future applications.

This thesis investigated the feasibility of recycling secondary sources of lithium in the form of lithium rich mica deposits discarded as a waste material from kaolin mining in France and the UK to recover lithium on a commercial scale, thus making it a sustainable resource for future generations and create a contribution to supply line of lithium in the UK. Through the economical recovery of lithium from existing waste material which has been stockpiled for many years, a valuable new lithium resource could be accessed.

The research was carried out in collaboration with Imerys Ltd, a world leader in mineral based specialist solutions. Imerys identified lithium-bearing minerals in their kaolin mining waste material at their mine sites in France and in the UK, this waste had been previously stockpiled for many decades at mine sites and represents considerable reserves if exploitable.

The French Administration in charge of the Geological Survey of France (1985) identified approximately 1.0 wt.% Li_2O in kaolin deposits in the Beauvoir area of central France, whereas for the St Austell area of kaolin mining in the UK, the British Geological Survey report (1987) provided detailed research on the mineralogy of the St Austell granite and estimated up to 3.3 million tonnes of recoverable lithium.

1.2 Aims of the thesis

The main aims for the research into the recovery of lithium from kaolin mining waste materials was to get a better understanding of the containing lithium deposits and then to develop a commercial process to recovery and extract lithium from the secondary resources. For this study two mine sites were investigated; St Austell mine sites in the UK and Beauvoir mine site in France, both were owned by Imerys Ltd. The objectives of this research can be summarised as;

1. Characterisation of the kaolin waste material for lithium recovery for the various Imerys Ltd deposits in St Austell, UK. To include detailed analysis on the chemical composition, mineralogy and the ease of recovery using various separation techniques.
2. To re-visit the froth flotation recovery process previously carried out on the Beauvoir (France) deposit to optimise lithium mica recovery and grade, in order to produce on a commercial scale.
3. To investigate the current extraction processes for lithium, such as the gypsum process, acid leaching process and bioleaching, and to establish the optimum leaching conditions to develop an economically viable process in order to produce marketable lithium products.
4. To develop a novel (low cost) technique to recover lithium from kaolin (also known as china clay) waste materials.

1.3 Thesis chapters

This thesis consists of seven chapters; each provides detail on different areas of the research, a summary of each chapter is given below.

Chapter 1: Introduction

This chapter provides a brief background into the strategic importance of lithium in the 21st century, providing information on the recovery of lithium from kaolin waste material and briefly outlining the objectives of the thesis.

Chapter 2: Literature review

The chapter provides the background into the research carried out in this thesis; including primary sources of lithium, lithium applications and the reasons behind its increasing demand over the past years. The chapter also provided an overview on the kaolin mine sites visited in this study and the current techniques used to recovery lithium from the waste material.

Chapter 2 also highlights the difficulties encountered when recovering lithium from lithium-bearing minerals; the impact on the environment, high extraction costs of extracting lithium from the mineral when using the current techniques as well as the limited supply of current resources in the UK.

Chapter 3: Materials and methods

In this chapter the experimental techniques used in order to recovery lithium from the lithium-bearing minerals can be found. As well as analytical techniques such as; X-ray fluorescence (XRF), X-ray diffraction (XRD), Inductively Coupled Plasma (ICP) and Atomic Absorption Spectroscopy (AAS), to better understand the efficiency of the recovery and extraction processes.

Chapter 4: Characterisation of lithium rich mica wastes

This chapter provides a background on the location of the kaolin waste material investigated, detailing the representative sampling techniques, the chemical and mineralogical characteristics, using various techniques including; Mineral Liberation Analysis (MLA) and Scanning Electron Microscopy (SEM).

Chapter 5: Recovery of lithium-bearing minerals

Chapter 5 investigated the kaolin waste materials obtained from Imerys Ltd using a number of mineral processing concentration techniques to increase the lithium content of the concentrate prior to any chemical treatment.

The separation techniques included; froth flotation, magnetic separation and electrostatic separation; the objectives being to obtain a high recovery of lithium rich mica species exploiting differences in surface chemistry, mineral magnetic

susceptibility and conductivity, respectively. The efficiency of the lithium concentration stage was optimised to achieve at least 4.0 wt.% Li₂O to make it a saleable commodity for the glass or ceramics industry (Amarante, 1999).

Chapter 6: Extraction processes for lithium concentrate

This chapter investigated extraction processes for the lithium concentrate using gypsum and leaching processes. A novel extraction process routes for the lithium-bearing mineral lepidolite $K(Li,Al)_3(Si,Al)_4O_{10}(F,OH)_2$ was investigated; bioleaching of lithium concentrate using micro-organisms; *A. niger*, as well as optimising the operating conditions such as; heat treatment, solution temperature, concentration and agitation for lithium selectivity. The bioleach process has the potential to be low cost, as it does not require additional processing costs for the kaolin waste material before extraction of lithium.

Chapter 7: Conclusions and recommendations

This chapter provides an overall summary of the research, which presents the main findings and it provides recommendations for future work.

CHAPTER 2

LITERATURE REVIEW

2.1 Background on lithium

Lithium is estimated to be the 25th most abundant element in the earth's crust (Meshram, 2014). The British Geological Survey risk level report (2013) stated that the crustal abundance was 16ppm, thus it is rated as a medium-risk on a global scale. It is a relatively rare in mineable deposits whilst the current and future demand for lithium in electrical goods has created some concern regarding securing viable lithium supply chains in the UK and EU. In appearance lithium metal is silvery white; it is the lightest metal with an atomic number of 3 and density of 0.534g/mL at room temperature (Hawkes, 1987). Lithium is a highly reactive metal, when in contact with water it reacts violently forming lithium hydroxide, as a safety precaution it is stored under liquid paraffin. Lithium is also the most electropositive of all the metals, it has a high standard electrode potential of 3.05 V when compared to other group 1 metals; 2.71 V for sodium and 2.92V for potassium (Garrett, 2004).

Lithium was first discovered in 1817 by Auguste Arfvedson in the mineral petalite ($\text{LiAlSi}_4\text{O}_{10}$), it was described as a stone from the Earth, see figure 2.1. The name was derived from the Greek word *lithos* which is translated to *a stone*. In 1818, Sir Humphrey Davy was the first to isolate lithium by electrolysis of lithium oxide (Hawkes, 1987).



Figure 2:1 The mineral petalite (taken from Northern Geological Supplies Ltd, 2014).

2.1.1 Lithium deposits

There are three main types of lithium deposits found in the world (Figure 2:2); brines, pegmatite (hard rock) and sedimentary rocks. Gruber (2011) investigated the in-situ resources for lithium deposits worldwide. As shown in Table 2:1 the study estimated that brines form 66% of the global lithium resource whereas pegmatites and sedimentary rocks form 26% and 8%, respectively.

Table 2:1 Global in-situ lithium resource, Mt: Million ton, ^aProducing, ^bLowest estimate (Gruber, 2011).

Deposit	Country	Type	Average concentration (% Li)	In-situ resource (Mt Li)
Uyuni	Bolivia	Brine	0.05	10.2
Atacama ^a	Chile	Brine	0.14	6.30
Kings Mountain Belt	US	Pegmatite	0.68	5.90
Qaidam ^a	China	Brine	0.03	2.02
Kings Valley	US	Sedimentary rock	0.27	2.00
Zabuye ^a	China	Brine	0.07	1.53

Manono/Kitotolo	Congo	Pegmatite	0.58	1.15
Rincon	Argentina	Brine	0.03	1.12
Brawley	US	Brine	-	1.00
Jadar Valley	Serbia	Sedimentary rock	0.01	0.99
Hombre Muerto ^a	Argentina	Brine	0.05	0.80
Smackover	US	Brine	0.02	0.75
Gajika	China	Pegmatite	-	0.59
Greenbushes ^a	Australia	Pegmatite	1.59	0.56
Beaverhill	Canada	Brine	-	0.52
Yichun.a	China	Pegmatite	-	0.33
Salton Sea	US	Brine	0.02	0.32
Silver Peak ^a	US	Brine	0.02	0.30
Kolmorzerskoe	Russia	Pegmatite	-	0.29
Maerking ^a	China	Pegmatite	-	0.23
Maricunga	Chile	Brine	0.09	0.22
Jiajika ^a	China	Pegmatite	0.59	0.20
Daoxian	China	Pegmatite	-	0.18
Dangxiongcuo ^a	China	Brine	0.04	0.18
Olaroz	Argentina	Brine	0.07	0.16
Other ^a (8 deposits)	Brazil, Canada, China, Portugal	Pegmatite	-	0.15
Goltsovoe	Russia	Pegmatite	-	0.14
Polmostundrovsk- oe	Russia	Pegmatite	-	0.14
Ulug-Tanzek	Russia	Pegmatite	-	0.14
Urikskoe	Russia	Pegmatite	-	0.14
Koralpe	Austria	Pegmatite	-	0.10
Mibra	Brazil	Pegmatite	-	0.10
Bikita ^a	Zimbabwe	Pegmatite	1.40	0.06 ^b
Dead Sea	Israel	Brine	0.001	-
Great Salt Lake	US	Brine	0.004	-
Searles Lake	US	Brine	0.005	-
Total				38.68

2.1.1.1 Brines

Lithium brines are a primary source of lithium, making up an estimated 66% of the global lithium resource; they are formed due to geothermal waters leaching lithium from solid clays and volcanic ash. The three types of brine deposits are; continental, geothermal and oil field, Figure 2:2 (Evans, 2008).

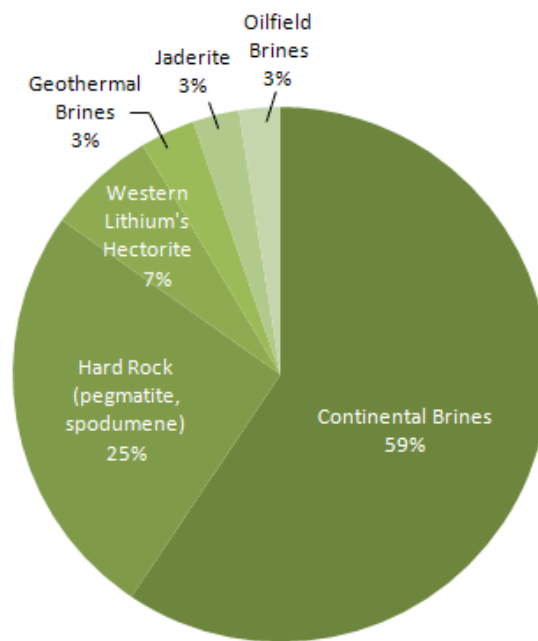


Figure 2:2 Primary sources of lithium production (WS, 2013).

The continental brines form 59% of the global lithium production and are commonly known as: salt lakes, lake waters, salt flats or salars. Salt lakes generally hold between 0.06 to 0.15% of lithium, they are formed of sand, mineral with brine and saline water containing high concentrations of salt (Pistilli, 2012). They are created in basins, which entrap lithium-containing water leached from nearby rocks (Evans, 2008).

2.1.1.1.1 Location

The main brines that are mined for lithium are located within South America and China (MIR, 2008). In South America the lithium deposits are found in; Chile, Argentina and Bolivia, a triangle is shown to represent the locality of the lithium production which is known as the Lithium Triangle, Figure 2:3.

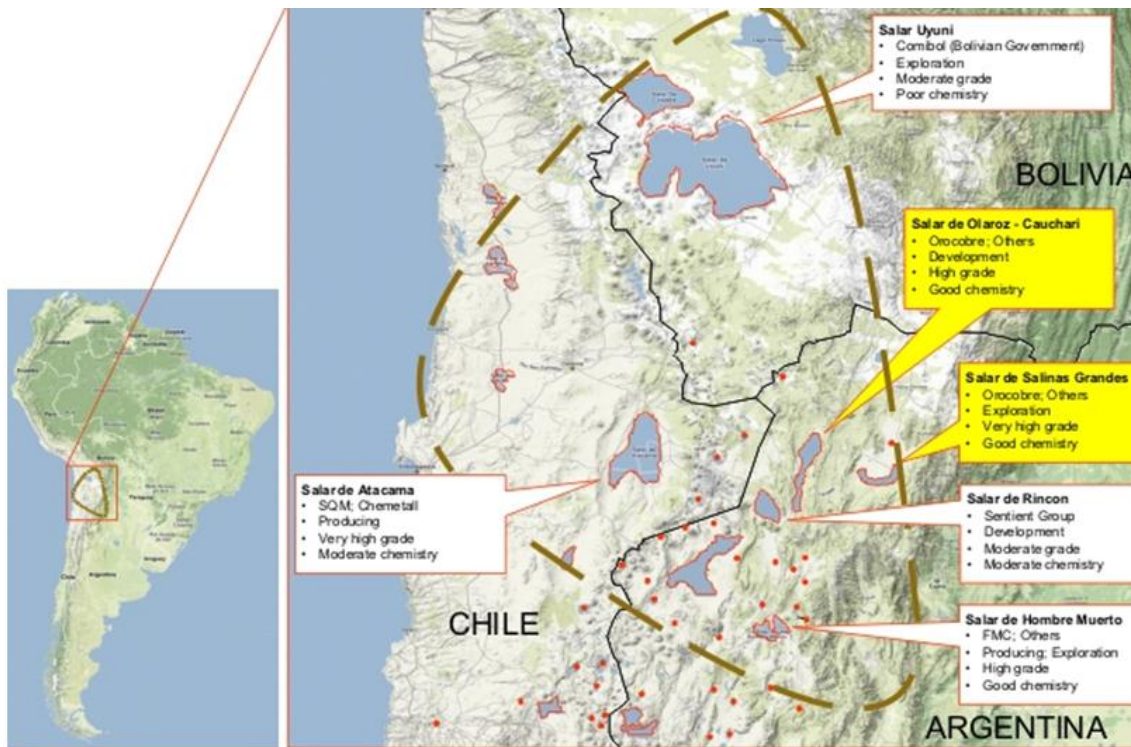


Figure 2:3 The Lithium Triangle surrounding Chile, Bolivia and Argentina. The three salars; Salar de Atacama, Salar de Uyuni and the Salar de Hombre Muerto, represent smaller brines (Roskill, 2012).

The U.S. Geological Survey (2015) estimated the global reserves and identified resources for lithium which are shown in Table 2:2 World Mine Reserve for lithium (Jaskula, 2015). The reserves in Chile and China contained the highest reserve estimates of 7,500,000 and 3,500,000 tonnes, respectively. The reserves for Bolivia are unknown, as Bolivia does not process the resource due to political issues.

The known reserves were calculated from the reserve bases, depending on a specified criteria including; grade, quality, thickness, and depth, which could be economically produced at the time of determination. The reserve bases were estimated from the identified resources, location, grade, quality and quantity are estimated from specific geological evidence, which were reported in the U. S. Geological Survey (Jaskula, 2015).

Table 2:2 World Mine Reserve for lithium (Jaskula, 2015).

Country	Reserve (tonne)	Identified resource (tonne)
Chile	7,500,000	> 7,500,000
China	3,500,000	5,400,000
Bolivia	-	9,000,000
Australia	1,500,000	1,700,000
Argentina	850,000	6,500,000
Portugal	60,000	-
United States	38,000	5,500,000
Brazil	48,000	180,000
Zimbabwe	23,000	-

2.1.1.2 Pegmatite (hard rock)

Pegmatites are hard rocks containing minerals such as; quartz (Si_2O), feldspar (aluminosilicate) and mica (phyllosilicates). Lithium can be contained within pegmatites minerals; formed due to highly soluble lithium concentrating in flowing magma and eventually crystallising. The Li_2O content in the mineral varies according to the source of the rock; due to the compact structure it is difficult to extract lithium. Garrett (2004) reported that there are 43 commonly known minerals containing lithium as a major component. Siame (2011) stated that there are only six commercially viable

lithium-bearing, shown in Table 2:3. The most abundant mineral, spodumene, was found in two types of deposit; high grade and low grade, containing 2.9 to 7.7 % Li₂O and 0.6 to 1.0 % Li₂O, respectively (Garrett, 2004). Deposits containing between 3.0 to 4.0% Li₂O were considered to be economically viable to process using the present extraction techniques; froth flotation and chemical recovery (Bauer, 2000).

Table 2:3 Commercial Lithium-bearing minerals, ^ahigh grade deposit, ^blow grade deposit, ^ctheoretical values, Garrett, 2004; Siame, 2011).

Mineral	Chemical formula	Li ₂ O (%)	Locations of the deposits
Spodumene	LiAlSi ₂ O ₆	2.9 - 7.7 ^a	Australia, Canada, China,
		0.6 - 1.0 ^b	Zimbabwe
Lepidolite	K(Li,Al) ₃ (Si,Al) ₄ O ₁₀ (F,OH) ₂	3.0 - 7.7 ^c	Canada, Zimbabwe, Portugal
Zinnwaldite	KLiFeAl(AlSi ₃)O ₁₀ (F,OH) ₂	2.0 - 5.0 ^c	Germany, Czech Republic
Petalite	LiAlSi ₄ O ₁₀	3.0 - 4.7	Zimbabwe, Canada,
			Namibia, Brazil
Amblygonite	LiAl(PO ₄)(F,OH)	7.5 - 9.5	Canada, Brazil, Surinam
Eucryptite	LiAlSiO ₄	4.5 - 6.5	Zimbabwe

2.1.2 Lithium production

Lithium can be commercially extracted from the two types of deposits; brines and pegmatites containing lithium-bearing minerals. Overviews of the processes are shown in Figure 2:4. Lithium is typically traded in its carbonate form (Li₂CO₃) due to the pure metal being dangerously reactive in water and air. Other compounds such as lithium chloride, lithium hydroxide and spodumene are traded to lesser degrees. A unit called Lithium Carbonate Equivalent (LCE) is used to equate these different forms and give a baseline figure for total demand. The extraction cost from brines is estimated to be £840 to £1500 per tonne of LCE; the extraction cost from spodumene is estimated to be

£2500 to £2900 per tonne of LCE (Khaykin, 2009). The lithium carbonate price was on average £4,311 per tonne in the United States and £3,724 to £4,449 per tonne in China (UGSG, 2015).

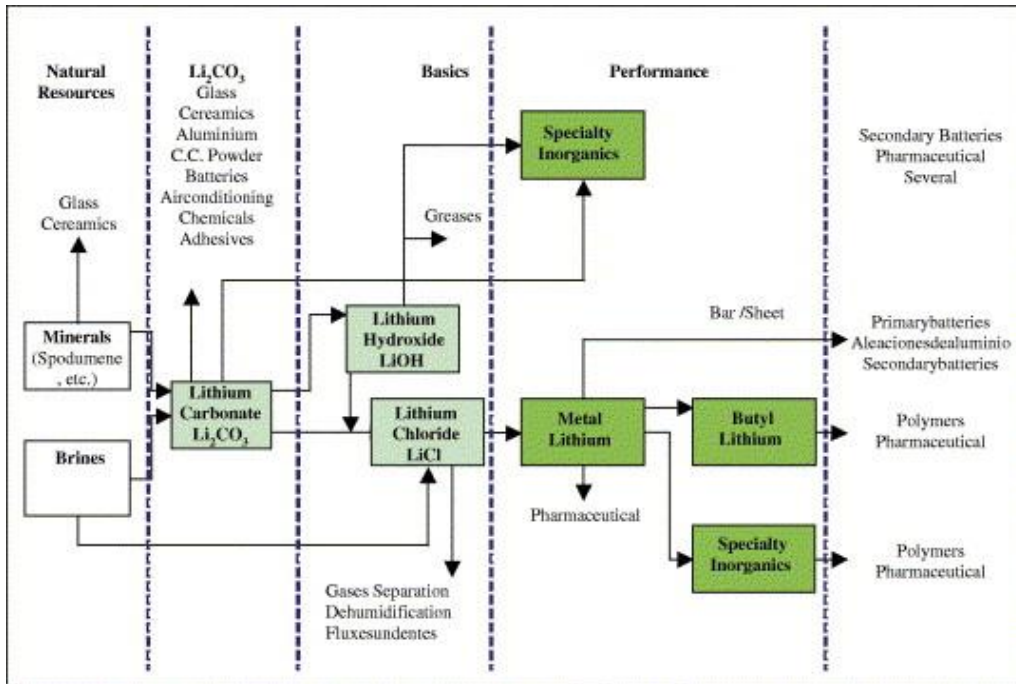


Figure 2:4: Extraction processes for lithium (Ebensperger, 2005).

2.1.2.1 Production from brines

Lithium produced from brines is the main source of extraction for lithium; it is formed through natural evaporation of the salt lakes, which in turn concentrates the lithium through precipitation to produce lithium carbonate. The process route has been favoured due to the relatively simplicity and economic advantages of the process (Evans, 2008). There was around 50% reduction in the global price of lithium due to the production from brines being more economically viable process as well as produced in large volumes (Smith, 2011).

Meridian International Research (Independent Strategy Research and Technology Consultancy) conducted a study on lithium resources and production in 2008. In Table 2:2:4 the lithium resources for the main brines deposits are shown along with the LCE Production. The table is not inclusive of all of the brine production sites.

Table 2:2:4 Lithium resource and production assessment, Mt = Million ton ^aestimate (MIR, 2008).

Location	Deposit (Salar de)	Lithium metal (Mt)		Lithium Carbonate Equivalent Production (tonne)		
		Resource	Reserve	2007	2010 ^a	2020 ^a
Chile	Atacama	3.0	1.0	42,000	60,000	100,000
Bolivia	Uyuni	5.5	0.6	-	-	30,000
China	Zhabuye	1.3	0.8	5,000	10,000	20,000
Argentina	Hombre Muerto	0.8	0.4	15,000	15,000	25,000
Argentina	Rincon	0.5	0.3	-	10,000	25,000
Nevada	Clayton lake	0.3	0.1	9,000	9,000	8,000

More recently (2015) the US Geological Survey report provided estimates for lithium mine production as well as current reserves, which are shown in Table 2:5. Chile still dominates the production of lithium with reserves estimates of 7,500,000 tonne in 2015. Chile is followed by China and Australia with reserves of 3,500,000 tonne and 1,500,000 tonne, respectively.

Table 2:5 World Mine Reserve for lithium (Jaskula, 2015).

Country	Lithium Production		Reserves (tonne)
	2013	2014	
Chile	11,200	12,900	7,500,000
China	4,700	5,000	3,500,000
Australia	12,700	13,000	1,500,000
Argentina	2,500	2,900	850,000
Portugal	570	570	60,000
United States	870	Withheld	38,000
Brazil	400	400	48,000
Zimbabwe	1,000	1,000	23,000

2.1.2.2 Production of lithium from pegmatites

The production of lithium from pegmatites is a difficult, energy intensive process with considerably higher production costs due to more complex process flow sheets the higher processing temperatures (approximately 1100°C) that are required for the extraction process (MIR, 2008). The hard rock pegmatite also needs crushing and milling prior to initial separation and then is chemically extracted to obtain the lithium metal. Previously processes such as acid leaching and the gypsum process have been used, which require strong acids and high temperatures to extract the metal. This process route is not as commercially attractive to produce lithium on a commercial scale when compared to the brine extraction process, although China does process spodumene to produce lithium carbonate following the sulphuric acid leaching method; crushed and ground before being physically separated using froth flotation separation followed by heating to temperatures of around 1100°C (Siame, 2011).

Many sites processing pegmatites have been forced to close, due to the higher process costs and the relatively low market price of lithium carbonate which is price capped by the brine process operators.. This supply/demand issue has created concern in the UK and EU regarding the strategic supply of lithium for the production of the next generation of electrical goods for European countries (Garrett, 2004). However, as the consistent increase in demand for lithium year on year has put a strain on the current lithium supply from brine reserves, hence more research is being carried out into new processing techniques for commercially viable ores or recycling options for lithium production (Garrett, 2004; Siame, 2011).

2.1.2.3 Other studies

To meet the current demand for lithium production, and due to the relative scarcity of the primary resources (particularly in Europe), studies have started to investigate recycling lithium from secondary sources such as; lithium-ion batteries and lithium-bearing minerals from mining waste material. These process routes are potentially favourable as they not only met the strategic demand for lithium but also provide a sustainable future for the metal.

Several studies have been made to try to minimise the physical separation process costs and to increase the recovery rates. Amarante (1999) investigated processing spodumene using froth flotation separation whereas Bale (1989) extracted lithium from a spodumene which was concentrated using gravity separation and magnetic separation techniques; although successful the processes were not economically viable at the time of publication. Other novel concepts for extracting lithium minerals from pegmatite ores

include using electrodynamic fragmentation and optical sorting (Ryu, 2015; Brandt, 2010). Brandt (2010) used a pegmatite that was placed underwater and shockwaves used to break the rock down into its component minerals ensuring good liberation of the lithium minerals from the gangue. This allowed for other minerals such as feldspar and quartz to be cleanly separated and processed separately rather than discarded as waste. Also, Demirbar (1999) reported the extraction of up to 400 mg/L of lithium in solution when water leaching borogypsum at temperatures between 20 to 90°C for up to 160 minutes. Borogypsum is a by-product of boric acid, which mainly consists of $\text{CaSO}_4 \cdot 2\text{H}_2\text{O}$ around 11.0 % B_2O_3 and 0.04 % Li.

2.1.3 Applications of lithium

Lithium has the highest electrochemical potential of all the metals, providing longer shelf life. In recent years the applications for lithium have increased greatly, typically 6% per annum (Jaskula, 2015). The U.S. Geological Survey reported the global lithium market for the lithium applications in the year 2014, as shown in Figure 2:5. For the glass and ceramic industry, the addition of lithium provides many advantages including; increasing the melt rate of the glass and lowering the viscosity which in turn improve the strength and quality of the products. The lithium cation is small thus can easily fit within the existing molecular structure of other compounds, providing greater strength and reduced thermal expansion coefficient (Garrett, 2004).

Lithium has many favourable properties such as higher energy density as well as low weight; this has developed a demand for rechargeable batteries in electrical and electronics as well as in the current development of electric cars. Table 2:6 shows a

comparison of the applications over the last few years (USGS, 2013; Gruber, 2011; Ebensperger, 2005). In 2008, 70% of the total rechargeable battery market used lithium-ion batteries (USGS, 2010).

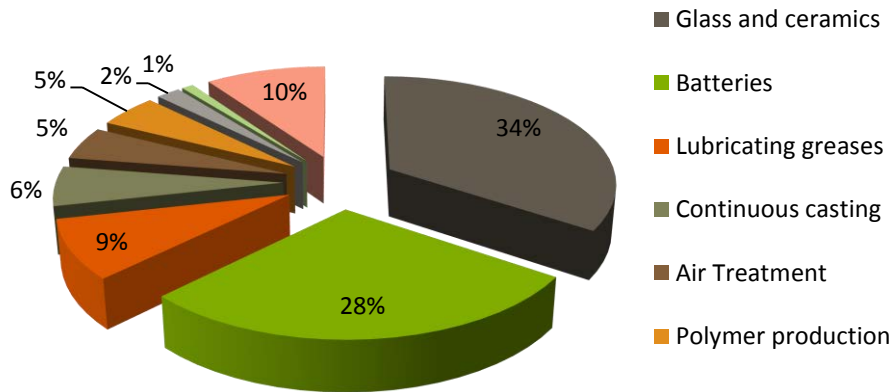


Figure 2:5 Lithium applications for the year 2014 (Jaskula, 2015).

Table 2:6 Global Lithium markets demand for lithium applications *combined (Jaskula, 2008 - 2014).

Application (%)	2008	2010	2012	2014
Glass and ceramics	20	31	29	35
Batteries	20	23	27	29
Lubricating greases	16	10	12	9
Continuous casting	-	4	5	6
Air Treatment	8	5	4	5
Polymer production	9*	-	3	5
Pharmaceutical	9*	-	2	2
Primary aluminium production	6	3	2	1
Other uses	21	24	16	10

2.1.4 Future

Clarke (2012) forecasted world lithium consumption through 2015 to 2020, indicating that there is likely to be an increase to approximately 280,000 tonnes per annum of LCE by 2020, see Figure 2:6. From 2013 to 2020 the average annual growth in the world consumption is expected to be around 9.5% (Jaskula, 2015). The lithium for lithium-ion battery was expected to account for 90,000 tonne of LCE by 2017 (USGS, 2013). At present, lithium carbonate is sourced from brine deposits to produce lithium-ion batteries, due to the costs involved in the processing route. It is needed for the cathode material and the electrolyte in the lithium battery (MIR, 2008).

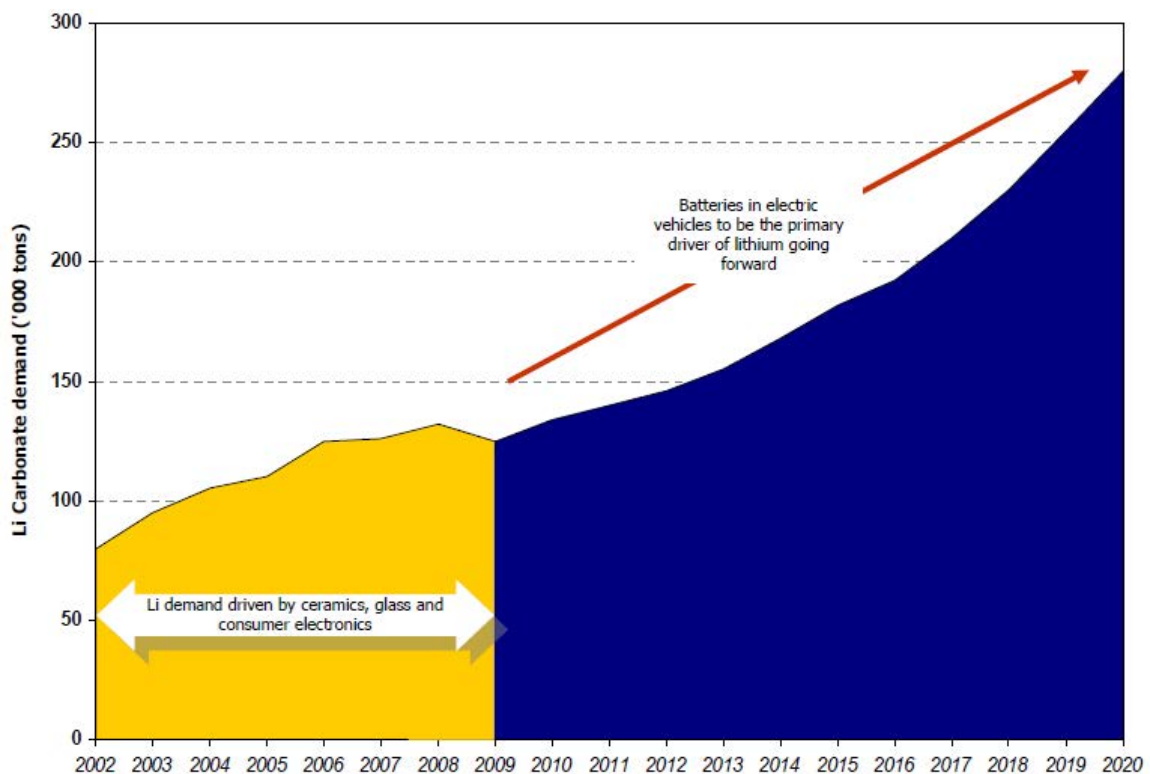


Figure 2:6: Global Lithium Carbonate Demand and Forecast (Astle, 2009).

2.2 Kaolin

Kaolin, also known as china clay, is used in the ceramics, paper, paint, rubbers and chemical industries, Figure 2:7. Kaolin can be formed through hydrothermal processes which caused the alteration from the base of the deposit upwards, or weathering of felsic rocks such as granite which allowed alteration from the surface downwards or a combination of both processes.



Figure 2:7 Kaolinised rock (Camm, 2005).

The kaolinisation process involves the hydrolysis of the aluminosilicates (e.g. feldspars) which changes the structure of the hard felsic rock to become soft and clay-like. The reaction equations shown represent the chemical reactions with feldspar forming kaolinite (Lanzi, 2008). Kaolinite is then mined and extracted via physical mineral processing techniques. Due to the fine particle size of the kaolin minerals, size separation (thickening, hydrocyclones and centrifuges) are mainly used to produce a fine particle size range clay product. The coarse (unkaolinised) granite is discarded to stockpile or sometimes sold as a building material locally.

➤ *Orthoclase + water → kaolinite + quartz + potassium oxide*



➤ *Albite + water → kaolinite + quartz + sodium oxide*



Orthose + water → kaolinite + quartz + potassium oxide

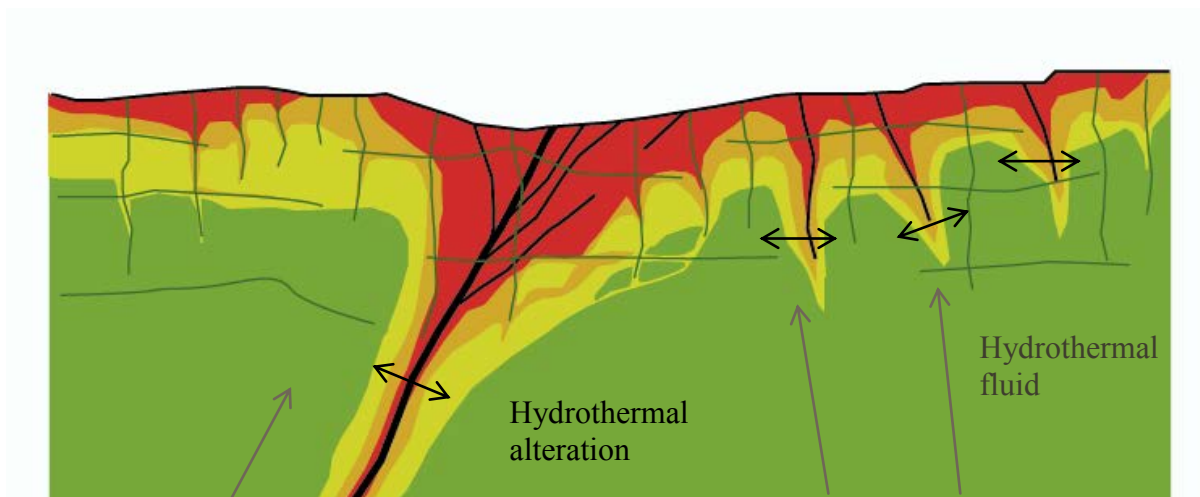
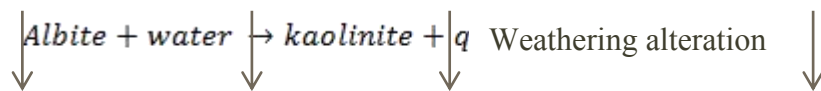


Figure 2:8 Type of primary deposit where the two kinds of alteration are visible (Hirtzig, 2010).

2.2.1 Kaolinisation Grade Classification

Lanzi (2008) classified kaolin into decomposition grades I to V depending on their relative degree of kaolinisation. Grade I, the fresh granite, is where the minerals are not visibly altered. In Figure 2:9 Images of varying grades of kaolin decomposition can be seen, illustrating the physical properties of the material as the kaolinisation process takes place.

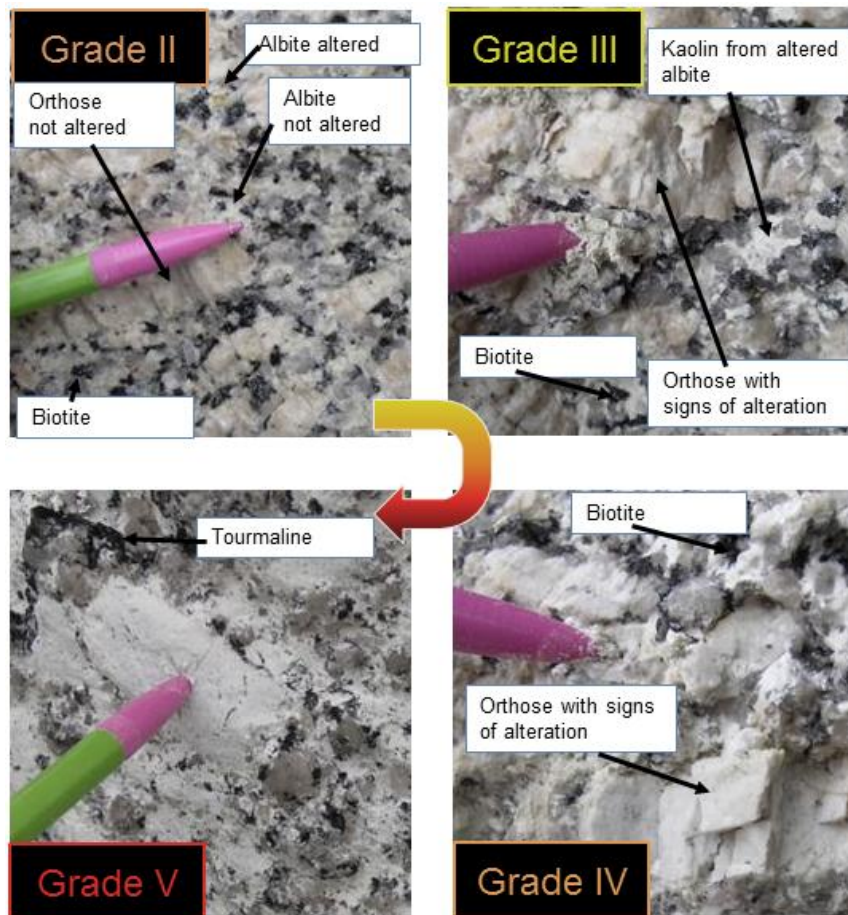


Figure 2:9 Images of varying grades of kaolin decomposition (Lanzi, 2008).

In figure 2.8 the grades II to V classifications of the material were characterised by the mineral alteration of the feldspar.

- II. Albite began to kaolinise, orthoclase was unaltered.
- III. Albite continued to alter, orthoclase began to kaolinise.
- IV. Both albite and orthoclase increasingly kaolinised.
- V. Fully kaolinised, all feldspars are completely altered.

As the minerals alter, the grades IV and V can be easily broken by hand; due to the feldspar being almost completely kaolinised thus the material can be described as completely malleably. Thus a greater efficiency of the recovery of lithium-bearing minerals can be achieved by froth flotation separation of grade IV and V, due to improved liberation of the mica containing minerals as kaolinite is known to be hydrophilic (Hirtzig, 2010).

2.2.2 Kaolin production

Kaolin is typically extracted by hydraulic mining; high-pressure water jets, which results in a slurry of sand, mica and kaolin flowing down to the pit of the mine. Other dry mining techniques have been used to separate the unaltered material, such as; digging, drilling and blasting (BGS, 2009). The kaolinised granite is then transported to a screening area where oversized material is removed from the process. The remaining undersize material is then hydraulically blasted and processed in the aforementioned fashion. The British Geological Survey (2009) reported that approximately 45% of Imerys Ltd total production was produced by dry mining techniques.

2.3 Imerys Ltd

A mineral-based specialist solution for industries has many operations worldwide. It operates kaolin production plants in Beauvoir, France and St Austell in the UK.

2.3.1 Beauvoir, France

2.3.1.1 Introduction

The kaolin production plant located in Beauvoir, France has been operating since 1880 and continues on a part time basis today. Beauvoir is located within the French Massif Central, Echassiere, France as seen in Figure 2:10 Geological map of Beauvoir mine site in France taken from Google Earth, the red balloon locates the Imerys Ceramic centre and below it is the open cast mine.



Figure 2:10 Geological map of Beauvoir mine site in France taken from Google Earth, the red balloon locates the Imerys Ceramic centre and below it is the open cast mine.

2.3.1.2 Geology

The rocks surrounding the granite intrusions in Beauvoir are mica schist and there are multiple intrusions; Colette granite, Beauvoir granite and La Bosse granite. The Beauvoir granite is found at the surface and located to the south of the Colette granite, (400 x 300 m). The granite is classified as albite-lepidolite granite; it is a fine to medium grained (Thompson, 2012).

2.3.1.3 Deposit

The Beauvoir deposits are mined in depths of 20 to 40m. Lithium is formed in the form of the pegmatite minerals lepidolite and amblygonite (Cuney *et al.*, 1992). As the albite-lepidolite granite becomes finer, average grain size of 40µm, a lower recovery rate of kaolin is observed, 25%, in comparison to the coarse grained biotite granite which has a recovery of 35%, average grain size 23µm.

Cassiterite is the main by-product produced and the majority is found associated with quartz and disseminated in the albite-lepidolite Beauvoir Granite, and occasional cassiterite within greisen veins, average grain size is 80-300 µm (Thompson, 2012).

2.3.1.4 Production

The deposit was primarily formed of; kaolin granite, dry sand (unkaolinised granite) and a tin concentrate. Beauvoir produced an average of 16,000 tonnes of kaolin per annum and approximately 100 tonnes per day, forming two ceramic products from the Beauvoir granite (BIP) and Colette granite (BIO). The ceramic products for the granite

were dependent on the colour of the material; BIP clay was used for fine quality tableware as it had a brighter whiteness whereas BIO was primarily used for sanitary ware (Lestang, 2013). When compared to other French deposits, the kaolin from Beauvoir had a highly refined purity, typically kaolin contained 0.8% of Fe_2O_3 (hematite) which formed a red/brown coat on the surface of SiO_2 (quartz), whereas the kaolin from Beauvoir, had a brighter whiteness as it only contained 0.4% Fe_2O_3 (Imerys, 2012).

Two other products are also sold from Beauvoir; dry sand (unkaolinised granite) and a tin concentrate, in the following quantities: 11 000 tonnes per annum and 60 tonnes per annum, respectively. The dry sand was separated into a fine and a coarse fraction and then used in the glass wool industry, whereas the SnO_2 concentrate (Tin/Cassiterite), containing; 43% Sn, 5% Nb_2O_5 (columbite) and 9% Ta_2O_5 (tantalite), was smelted. Other applications of kaolin included; porcelain, paper coating, fillers, paints and agriculture (Murray, 2000; Siame, 2011).

2.3.1.5 Processing

The flow diagram of the processing route for kaolin, cassiterite concentrate, dry sand and gravel waste can be seen in Figure 2:11. The initial stages of the process included; crushing, washing and classifying the material in order to liberate the kaolin from the less weathered and larger particles, which formed the gravel waste (>5mm). The materials were separated following into; kaolin (<0.04mm), cassiterite concentration, fine sand (100 μm to 1mm) and coarse sand (2 to 5mm). The kaolin was then filtered and dried so that the final product contained between 12 to 15% moisture.

2.3.2 Saint Austell, UK

2.3.2.1 Introduction

The lithium containing potential of the St Austell region has been examined by the British Geological Survey in 1987, estimating that the area contained up to 3.3 million tonnes of recoverable lithium within the upper 100 m region of an 8 km² recognised area (Hawkes, 1987). The report also concluded that the St Austell granite contained a sufficient resource of lithium for commercial production. This lithium was mostly found in the form of lithium-bearing mica pegmatites dispersed throughout the granite. Figure 2:12 Map of St Austell shows the UK Hydrous Kaolin Platform operations site taken in 2010 (Hirtzig, 2010).

2.3.2.2 Deposit

The kaolin deposits in St Austell have been defined as a primary deposit by Hirtzig (2010), as the deposits have experienced hydrothermal and weathering conditions causing alteration of the granite in situ. The structure and composition of the ore deposits vary across the area due to differences in hydrothermal alteration and weathering. Four sites investigated in this study were chosen due to their lithium extraction potential; three were taken from the Karslake site and one from the Blackpool site.

- New Sink, Grade 5
- New Sink, Grade 4
- Stope 13, Grade 4
- Blackpool, Grade 4

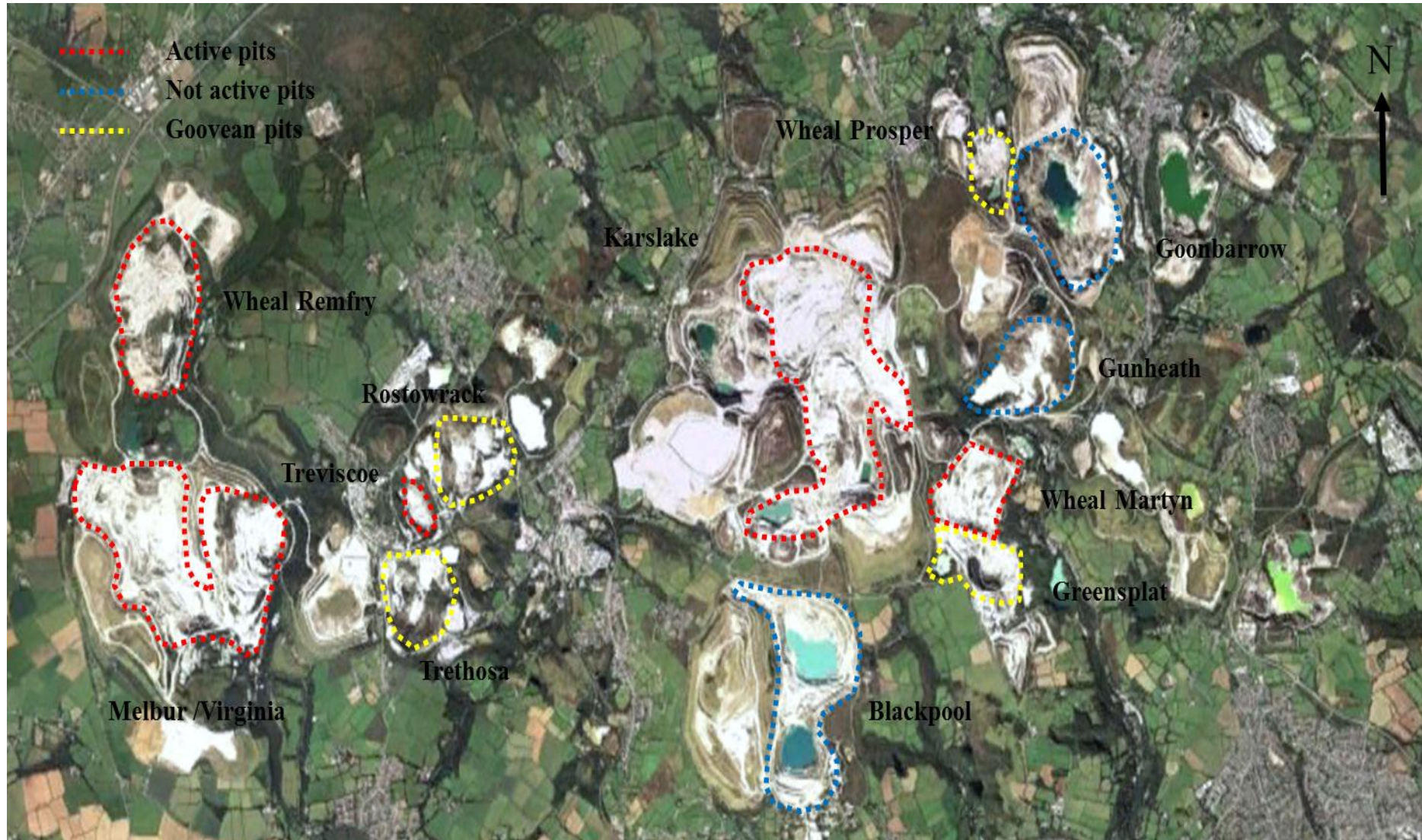


Figure 2:12 Map of St Austell shows the UK Hydrous Kaolin Platform operations site taken in 2010 (Hirtzig, 2010).

2.3.2.3 Geology

Manning (1996) identified four granite classifications occurring throughout St. Austell and the South West of England:

- Biotite granite
- Lithium mica granite
- Tourmaline granite
- Topaz granite

The lithium mica granite was identified mainly in the Karslake, Blackpool and Melbur/Virginia site in St Austell as can be seen in Figure 2:13.

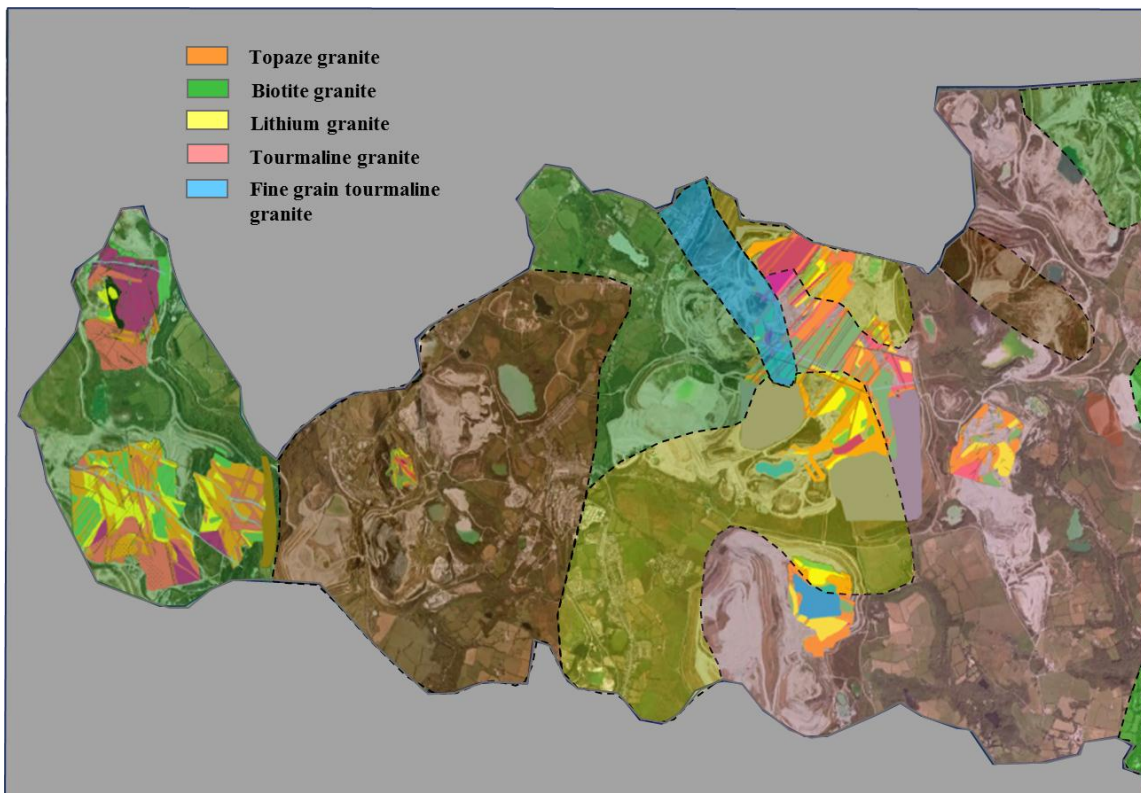


Figure 2:13 Primary lithological variation in the kaolinised St Austell granite, UK (Hirtzig, 2010; Manning, 1996).

2.3.2.4 Potential lithium recovery routes from kaolin waste

The first step of beneficiation is to reduce and classify the size of the weathered pegmatite into a finely divided suspension. Once the particle size has been reduced to a suitable level to the order of micrometres froth flotation is commonly used to concentrate the lithium-bearing minerals. Froth flotation separation utilises surface chemistry along with certain collector and depressant reagents to help separate out the lithium containing minerals from the gangue materials (Siame, 2011; Amarante, 1999; May, 1989). To develop an economically viable feed stream for the production of lithium-based materials, 4.0 wt.% Li_2O is required (Bauer, 2000).

Examples of previous studies on mineral recovery of lithium rich minerals from pegmatites deposits include; Jandova (2010), utilisation of dry magnetic separation to recover zinnwaldite from wastes material processed in the Czech Republic and Siame (2011) consecutive use of froth flotation and magnetic (dry) for recovery and separation of multiple lithium-bearing minerals (zinnwaldite) from hydrocyclone underflows from kaolin operations in St Austell owned by Goonvean Ltd (at the time of the study).

2.3.2.5 Treviscoe pit

In St Austell, investigations have been carried out in the Treviscoe pit, the granite used in the study was taken from the hydrocyclone underflow. The particle size was greater than $53\mu\text{m}$ which contained 0.5 wt.% of Li_2O . After froth flotation separation a final concentrate of 1.4 wt.% Li_2O was achieved, giving a recovery of 95% (Ancia, 2010). The low lithium concentration was stated to be due to undesirable mineral contaminants

discovered in the kaolin mined in this region. The impurities had an impact on separation processes, mainly due to their properties these include; muscovite mica, iron (titane), potash, smectite, tin and columbo-tantalite.

Mineral liberation analysis, a SEM-based mineral liberation analyser, was carried out on the material. The method is described in section 3.5.5. MLA identified the presence of 28 wt.% of the mica muscovite ($\text{KA}_3\text{Si}_3\text{O}_{10}(\text{OH})_{1.8}\text{F}_{0.2}$), see Figure 2:14. It was suggested that the mineral structure of muscovite was altered due to weathering of lithium-bearing minerals (Manning, 1996). Further upgrading of the concentrate was carried out using dry magnetic separation on the particle size range above $100\mu\text{m}$, achieving 2.08 wt.% Li_2O and a recovery of 95%. As muscovite is a non-magnetic mineral, any unaltered mineral was separated from the magnetic lithium-rich fraction (Ancia, 2010).

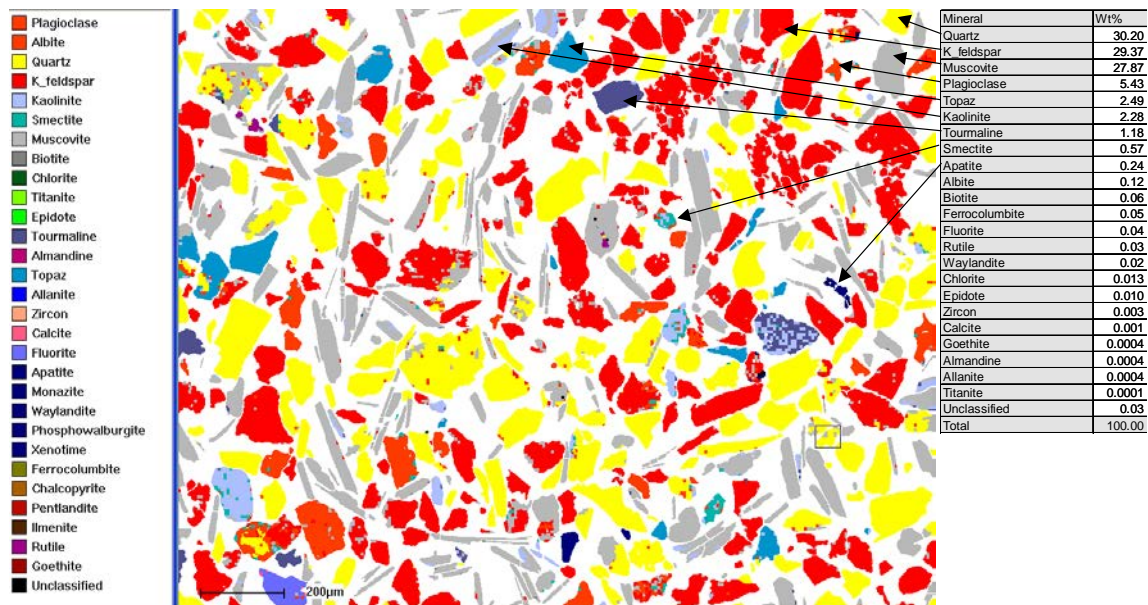


Figure 2:14 Mineral Liberation Analysis of the Treviscoe hydrocyclone underflow (Ancia, 2010).

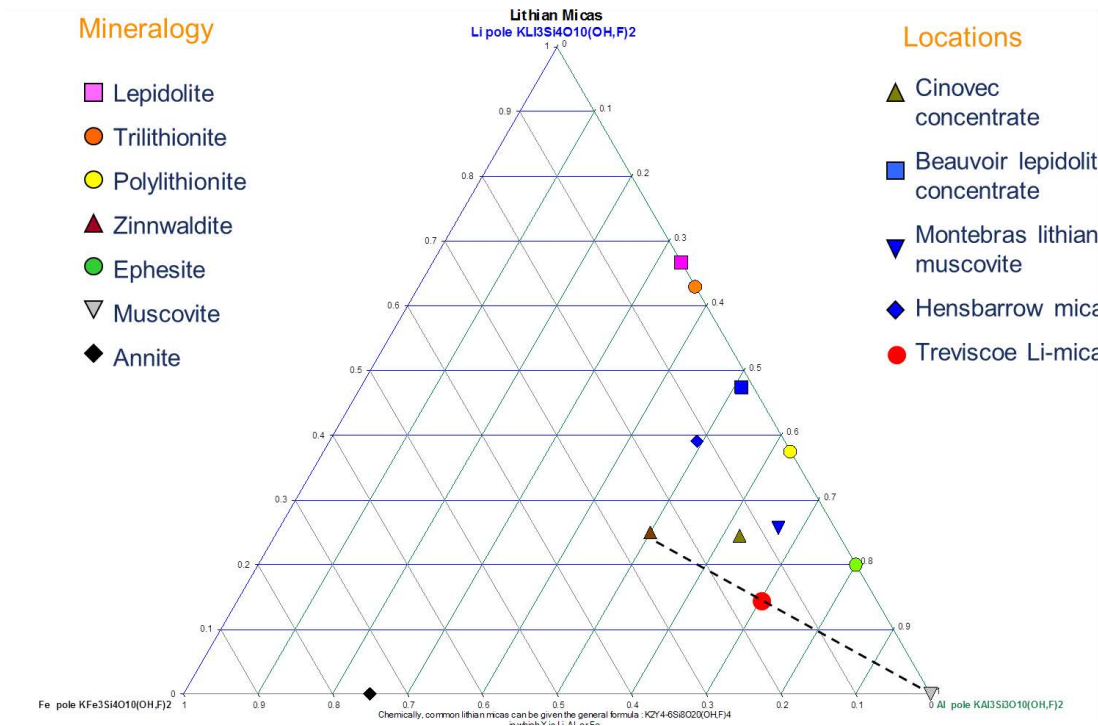


Figure 2:15 Mineralogy of the Treviscoe material compared to other locations owned by Imerys (Ancia, 2010).

2.3.2.6 Goonvean pit

A study by Siame (2011) carried out for Goonvean and Rostorock estimated that 100,000 tonne per annum of micaceous residues were produced from Goonvean pit containing biotite granite (Manning, 1996). The material was obtained from the underflow of the hydrocyclones, containing an approximately of 0.84 wt.% Li_2O .

The lithium bearing mineral was identified as zinnwaldite mica, which was concentrated up to 2.07% Li_2O using froth floatation separation and magnetic separation. Siame (2011) reported a steady decrease of the lithium grade, in the magnetic fraction, as the magnetic field strength was increased from 0.94 Tesla to 2.06 Tesla, that recovering zinnwaldite using the particle size fraction $53\mu m$ to $150\mu m$. In Table 2:7 it can be seen

that the recovery was increased as the magnetic field strength was increased. The magnetic separation processes were limited to the strength of the magnetic field, the samples displayed weaker magnetic properties thus requiring stronger fields, due to instrumental limitations further investigations at higher magnetic fields was not studied.

Table 2:7 Magnetic product grade and recovery using WHIMS (Siame, 2011).

Tesla	Li₂O Grade (%)		Li₂O Recovery (%)	
	<i>Magnetic</i>	<i>Non-magnetic</i>	<i>Magnetic</i>	<i>Non-magnetic</i>
0.94	2.2	1.3	26	74
1.40	2.3	1.1	43	57
1.95	2.2	0.8	68	32
2.06	2.1	0.7	73	27

Table 2:8 Magnetic product grade and recovery at a magnetic field strength of 0.94 Tesla. (Siame, 2011)..

	Grade (%)			Recovery (%)		
	Li ₂ O	Rb ₂ O	Fe ₂ O ₃	Li ₂ O	Rb ₂ O	Fe ₂ O ₃
Magnetic	2.2	0.8	5.4	26	25	25
Non-magnetic	1.3	0.5	3.3	74	75	75
Feed	1.5	0.5	3.6	100	100	100

Overall a number of factors were considered including the effects of pH, particle size, collector dosage on flotation recovery and magnetic field strength used in the high intensity magnetic separator, although the study did not investigate the effects of using a depressant, as well as an electrostatic separation as a general separation technique. The second part of the study investigated the extraction of lithium, following the gypsum process, with the additive sodium sulphate, the leach solution showed potential of

achieving a purity of >90% for Li_2O_3 product deeming the product suitable for the glass and ceramic industry (Siame, 2011).

2.4 Froth flotation separation

Froth flotation separation is the most widely used method of ore beneficiation to physically separate minerals from gangue material (Amarante, 1999). Flotation processes are relatively cheap, thus widely used by many manufacturing industries to separate minerals, see Figure 2:16.

Flotation can be considered to be chemically-assisted gravity separation (Howe-Grant, 1999). The mineral particles are separated by utilising the differences in their surface chemistry and consequently the mineral to water interface (Backhurst, 2002; Siame, 2011). The pulp is aerated so that hydrophobic particles selectively adhere to air bubbles entering the cell by forming weak bonds to the hydrogen molecules. Consequently, they form a froth layer at the surface of the pulp. The hydrophilic particles remain in the gangue (Rowson, 2010; Siame, 2011). Degner (1986) stated that any flotation machine must provide four functions:

1. Provision of good contact between solid particles and air bubbles.
2. It must maintain a stable froth/pulp interface.
3. It must adequately suspend the solid particles in the slurry.
4. It must provide sufficient froth removal capacity.

The laboratory flotation cell used promote: air dissemination in the pulp, bubble-particle collisions, stability of bubble-particle aggregate. Froth flotation is a balance between buoyancy and gravitational forces. Improved flotation is by addition of non-polar oils, for example kerosene, added to the pulp as an emulsion. The oil droplets collect on the non-polar surfaces and increase their hydrophobicity.

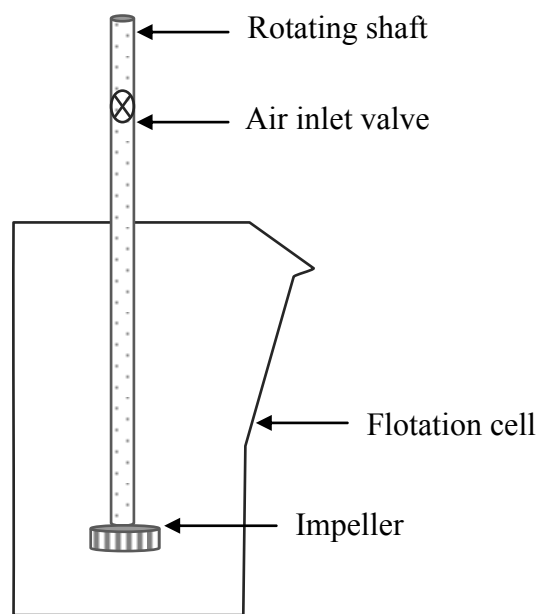


Figure 2:16 Schematic diagram of flotation cell

The flotation process variables can be divided into three components; chemistry, operations and equipment (Kawatra, 2011). Factors within these categories can be manipulated to optimise the process for a particular application, as shown in Figure 2:17. Flotation reagents are described as interfacial surface tension modifiers (Crozier, 1992) and are added to maximise recovery of desirable material. There are five different types: collectors, frothers, activators, depressants and pH modifiers. Frothers create a stable froth and encourage a fine dispersion of bubbles in the pulp (Howe-Grant, 1999).

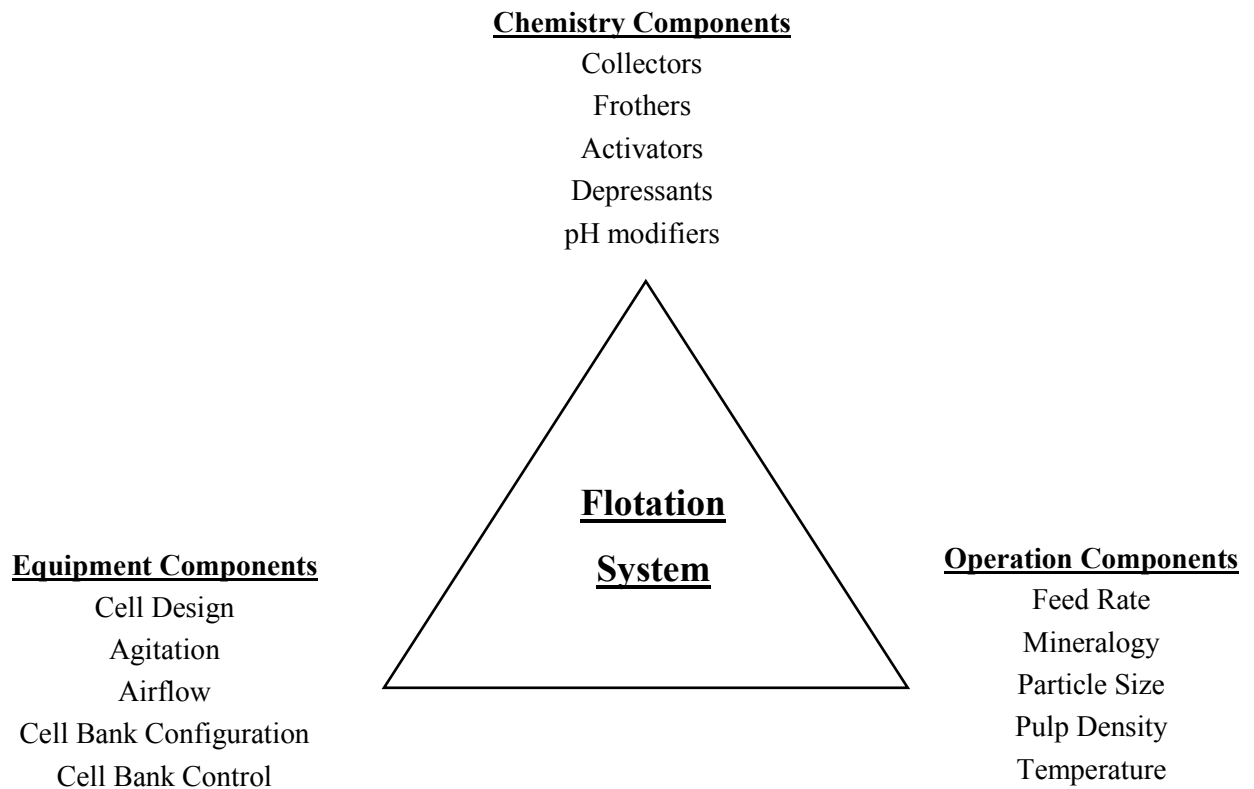


Figure 2:17 Interrelated components of a flotation system (Kawatra, 2011).

2.4.1 The effect of particle size on processing

The particle size distribution of the feed material in a flotation process plays an important role in achieving a higher recovery rate. The selectivity process is greater for smaller particle sizes due to an increase in the liberation of the desirable hydrophobic minerals from the gangue. However, the presence of finer particles can cause entrainment, thus transporting unwanted particles that are trapped between these bubbles into the froth layer; there will always be some gangue material in the floated fraction (Forsberg, 1988). Kaolin in particular has shown to be particularly susceptible for its tendency to entrain (Mortland, 1978).

In addition to entrainment, gangue material can collect in the float by being physically attached to the desired particles. This is particularly true for pegmatite minerals such as lepidolite that are an intrusive material in a gangue matrix. By increasing the comminution of the feed and decreasing the average particle size, it is more likely that the desired material will be liberated from the gangue matrix, thus allowing for a more selective float.

2.4.2 Effect of pH on froth flotation

The critical pH value for each flotation regime depends on the nature of the mineral, the particular collector and its concentration (Wark, 1995). In general, under acidic conditions minerals can develop a positive surface charge and vice versa under basic conditions. Hence, by manipulating the pH, hydrophobicity can be induced when the charge on the desired minerals surface is neutral (Ullman, 2005). Siame (2011) described altering the pH of a system as the simplest method of modifying surface chemistry as all minerals change from a negative-charge to a positive-charge at a particular pH, stating that conventionally mica is floated through amine addition at pH 2.5 to 3.5.

2.4.3 The effect of collector dosage and type on froth flotation

Collectors are reagents that can selectively adsorb onto the surfaces of particles, changing the nature of a minerals surface and are highly selective. They form a froth layer on the surface of the pulp, containing a thin film of non-polar hydrophobic hydrocarbons. The valuable minerals are physically separated from the gangue, containing the impurities which remain in the pulp (Siame, 2011).

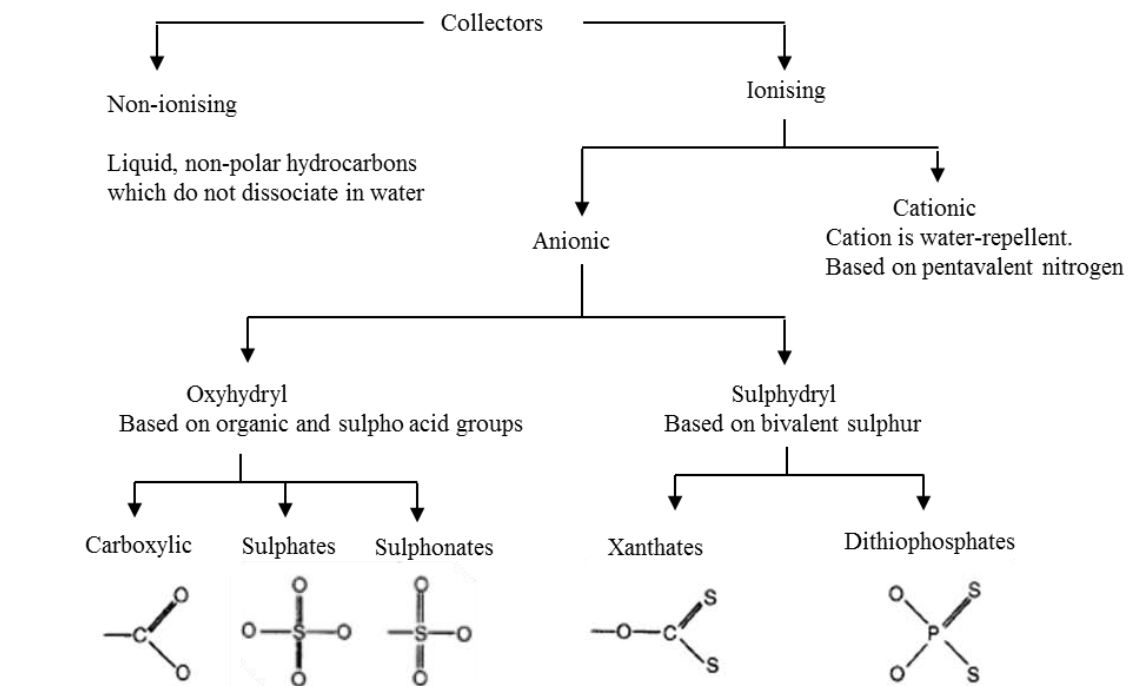


Figure 2:18 Typical Collector types used in minerals processing (Kawatra, 2011).

Figure 2:18 categorises the types of collectors; ionising, non-ionising, anionic and cationic. Collectors can either chemically or physically bond to the surface of a mineral; the surfactants form a monolayer around the mineral which destabilises the hydrated layer separating the mineral from the air bubble which allows for favourable adhesion to the bubble compared to the water phase (Napier-Munn, 2011).

Non-ionising collectors are non-polar hydrocarbon which do not dissociate in water, whereas the ionising collectors contain a polar end that can attach to mineral surfaces. The variation in collector types depends on the mineral of interest. Siame (2011) found that mica floated in acid suspensions were better when a cationic collector was used, whereas an anionic collector was preferred in an alkaline system. For the separation of lithium mica, amine collectors are recommended by Cytec Industries.

All cationic collectors contain an amine group with unpaired electrons and overall positive charge, Figure 2:19. The hydrocarbon ‘R’ groups covalently bonded to the amine can be altered to manipulate the properties of the collector for specific applications (Bulatovic, 2007).

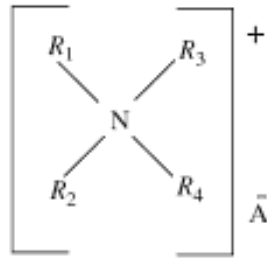


Figure 2:19: Cationic Collector Structure (Bulatovic, 2007)

2.4.4 The effect of depressant addition on froth flotation performance

Depressants inhibit the adsorption of collectors onto the surface of gangue (Napier-Munn, 2011). This increases the selectivity of the process, as the impurities remain hydrophilic. Depressants work in a variety of ways depending on their chemistry; from polymer coating particles to forming complexes on the mineral surface reducing any physical interactions or chemical reactions between the mineral and collecting agent (Kawatra, 2009).

2.5 Overview of potential extraction processes for lithium

Two established processes outlined for lithium extraction from ground pegmatites are the acid and alkali process (Averill, 1978). The acid process has been investigated by Distin and Phillips on the St Austell pegmatite. The mineral ores were leached using strong acids (Distin & Phillips, 1982) through heap leach or process leach (Wills, 2006). The alkali process, also known as the gypsum process, involves heating the physically concentrated lithium mineral with calcium carbonate. Previous studies that have used this extraction method include Alex and Suri (1996), Jandova and Vu (2008), Jandova, (2009, 2010), Yan, et al., (2012) and Siame (2011).

Various process parameters are also considered to have significant impact towards the leaching processes. The studies have looked at various parameters to optimise the leaching effects, such as; temperature, pressure, pH, agitation speed, variables such as temperature (Distin & Phillips, 1982), pH (Rezza, 1997), agitation speed (Yan, 2012), particle sizes and solid to liquid ratio (Jandova, 2009) have been reported to play a certain role in optimizing the efficiency of the leaching process. Therefore, using these parameters as our controlled variables for the leaching process, we can achieve greater efficiency toward the extraction of lithium from the mineral samples by manipulating these variables in our process control.

The main disadvantages with the current processes available were that, when compared to extraction lithium through brines, lithium extraction from mineral ores was not as cost effective. Further research was needed to develop the mineral processing routes in order to meet the increasing demand of commercial lithium.

2.5.1 Acid leaching process

The acid leaching processes involved thermal pre-treatment of spodumene; typically at high temperature around 1100°C, which changed the structure of the mineral from alpha (α) to beta (β) type spodumene. The β -spodumene increased the reactivity when leached with acids such as sulphuric, hydrochloric and nitric acid at 250°C. The product formed was lithium sulphate. Lithium sulphate was dissolved in water and passed through several filtration steps to remove impurities before the lithium is precipitated using sodium carbonate. This precipitate is lithium carbonate (Averill & Olson, 1978; Dresler, 1998; E. Siame, 2011). Studies by Alex and Suri (1996) recovered lithium from sintering zinnwaldite at temperatures of 700°C with sulphuric acid and they were able to achieve 90% extraction efficiency.

2.5.1.1 St Austell

Distin and Philips (1982) identified a number of potential stockpiles of material amenable to upgrading in and around St Austell; Meldon granite, Godolphin granite and St. Austell pegmatite. The materials were non-kaolinised pegmatite and the typical lithium content was between 0.5 to 0.7 % prior to any up-grading via physical concentration, Figure 2:8. The St Austell pegmatite was leached with sulphuric acid up to 260°C, recovering up to 70% of the lithium content being dissolved to produce up to 3 g/L in the final leach liquors. Leaching of the material was quite efficient however these are known to release toxic gases and the waste solution that is harmful to the environment. Li (2013) reported that toxic gases such as Cl₂, SO₃ and NO_x were produced.

Table 2:9 Partial chemical analysis of sample materials (Distin, 1982).

Sample material	Li (%)	Na (%)	K (%)	Rb (%)	Ca (%)	Mg (%)	Al (%)	Fe (%)
Meldon granite	0.5	5.5	2.3	0.2	0.6	0.01	7.1	0.11
Godolphin granite	0.07	4.8	3.4	0.06	0.02	0.02	7.1	0.58
St Austell pegmatite	0.65	1.1	5.7	0.44	0.23	0.40	11.7	11.5

2.5.2 Gypsum process

Crocker (1988) from the US Bureau of Mines proved that it was possible to extract high recoveries (>85%) of lithium from montmorillonite-type clays (0.3 to 0.6 % Li). The process involved roasting the ore with either KCl and CaSO₄ or CaCO₃ and CaCO₃, water leaching the calcine then precipitating the lithium carbonate (99%) from the liquor using potassium or sodium carbonate. This had the advantage of using water as the leaching material, rather than aggressive acids.

Studies have investigated the extraction from lithium-bearing mineral such as; spodumene, zinnwaldite, petalite and lepidolite (Bauer, 2008). The gypsum process involved calcining the lithium concentrate with calcium sulphate (CaSO₄) and calcium hydroxide (Ca(OH)₂) at temperatures of up to 1000°C to produce water soluble lithium-containing salts, such as; LiKSO₄. The calcined material was then water leached and purified by precipitation using potassium carbonate (K₂CO₃) to form lithium carbonate (Li₂CO₃). Siame (2011) reported that for efficient precipitation of lithium carbonate, the leach liquor should contain at least 9 g/L of lithium concentration. The commonly desired product in lithium extraction is lithium carbonate, due to relative chemical inertness in powder form and being an industrial standard, (Garrett, 2004).



Figure 2:20 Gypsum process for lithium adapted from ANZAPLAN ltd. (Anzaplan, 2013)

The economics of this process are substantially affected by the energy requirements of the mining, grinding, physical separation and high temperature roasting, so costs can be brought down significantly through optimisation of these processes (Siame, 2011).

2.5.2.1 Czech Republic Process

Jandova (2010) investigated several studies on zinnwaldite waste stream (0.21% Li, 0.20% Rb) in the Cinovec area in Czech Republic. Previous studies reported that 1.40% Li was extracted from the zinnwaldite waste, achieving 96% extraction when roasting at 950°C and then leaching at 90°C in a liquid-to-solid ratio of 10:1 and reaction time of 10 minutes (Jandova, 2009). The 2010 study showed that 1.21% Li and 0.84% Rb were extracted from the zinnwaldite wastes roasting at 825°C, achieving about 90% extraction efficiency.

Jandova (2009) observed that the gypsum method had the main advantage over the limestone method of producing liquor with relatively high lithium concentrations, even when leaching the calcine at ambient conditions. However, the disadvantages of the gypsum method are reduced rubidium extraction rates and higher concentrations of calcium in the leach liquors; rubidium extraction is not a requirement for this investigation. Jaskula (2013) reported that a 3.5% increase in rubidium usage was

observed in 2012 from 2011, due to increases in lithium exploration creating rubidium as a by-product and it can be expected that the commercial applications for rubidium will expand. At present uses of Rb are increasing, with the main use in atomic clocks for global positioning satellites. Other uses include: glass manufacturing, magneto-optic modulators, phosphors and lasers (Jandová and Vu, 2013; Wagner,). An estimate of the world demand for rubidium was about 2 to 4 tonnes per annum (Thompson, 2011; Wagner, 2006).

2.5.2.2 Studies on St Austell Deposits

Siame (2011) investigated the effectiveness of the roasting and water leach procedure using the reagent systems considered by Jandova (2010) as well as the additive sodium sulphate (Na_2SO_4). The techniques were applied to a tailing sample containing 0.84% Li, the mica-rich waste product from the kaolin production site from the St Austell granite. The lithium-bearing mica mineral found was zinnwaldite; other minerals also present in the sample were predominantly muscovite and kaolinite with smaller amounts of K-feldspar and quartz. Siame found that when roasting with sodium sulphate, the recovery rates were up to 97% Li_2CO_3 at 850°C. When using gypsum an extraction efficiency of 84% was achieved at 1050°C. The process was not effective when using limestone, as the additive the extraction process was not successful as of the formation of eucryptite in St Austell, which was not very soluble in water.

The formation of lithium products such as KLiSO_4 and $\text{Li}_2\text{KNa}(\text{SO}_4)_2$ were identified when roasting at 900°C; although KLiSO_4 had a low solubility and was regarded as the controlling factor of the release of lithium into water in the leaching stage. At higher

temperatures of 1050°C, KLiSO_4 formed a new mineral phases and was water soluble. Although more efficient extraction rates were achieved from sodium sulphate, it was significantly more expensive than gypsum, as shown in Table 2:10.

Table 2:10 Cost of bulk roasting additives (Siame, 2011).

Additive	Approximate cost (£/T)
Sodium sulphate	123
Gypsum	20

2.5.2.3 China

Yan (2012) studied lithium extraction from lithium-bearing mineral lepidolite, which contained a relatively high content of lithium 2 wt.%. The sample was obtained from Jiangxi Province in China. Following sulphation roasting and then water leaching, the study was successful in obtaining an extraction efficiency of 92% at 850°C for 30 minutes. The additives used in this study are shown in Table 2:11.

Table 2:11 Additives used in the study (Yan, 2012).

Additive	Lepidolite	Na_2SO_4	K_2SO_4	CaO
Ratio	1	0.5	0.1	0.1

Table 2:12 Chemical composition of the leach liquor

Leaching Solution (g/L)	Li	Na	K	Rb	Ca	Cs	Si	Al	Fe	Mn
	4.36	22.19	8.51	2.18	0.77	0.43	0.017	0.008	0.0001	0.0006

The chemical composition of the leaching solution is shown in Table 2:12. A lithium concentration of 4.36 g/L was reported in the leaching solution, with a few impurities were found from the process; Al and Si in the leach liquor. Although this study was

successful at achieving good recoveries, high temperatures were used to achieve this, hence it would not be commercially viable to scale up the process.

2.5.2.4 Korea

Luong (2013) investigated the lithium extraction from lepidolite concentrate (2.55% Li) on roasting with Na_2SO_4 in a 2:1 ratio (Na_2SO_4 :Li) at 1000°C for 30 minutes and then water leached at 85°C for 3 hours, water to calcine ratio of 15:1. The leach liquors contained up to 3 g/L Li and an extraction efficiency of 90%.

2.5.2.5 Summary

Key performance data for the most developed processes are given in Table 2:13. Most techniques give >90% recovery rates, but rely on high temperature calcination of the mineral concentrate, which may prove prohibitive in terms of energy costs.

Table 2:13 Comparison of conditions and results of different studies, *estimate, adapted from (Luong, 2013).

	Jandova (2009)	Jandova (2010)	Siame (2011)	Yan (2012)	Luong (2013)
Mineral	Zinnwaldite	Zinnwaldite	Zinnwaldite	Lepidolite	Lepidolite
Lithium (%)	1.40	1.21	0.96	2.0	2.55
Additives	CaSO_4 , Ca(OH)_2	CaCO_3	Na_2SO_4	Na_2SO_4 , CaO	Na_2SO_4
Calcination temperature ($^\circ\text{C}$)	950	825	850	850	1000
Calcination time (minutes)	60	60	60	30	30
Leach temperature ($^\circ\text{C}$)	90	90-95	85	ambient	85
Leach time (minutes)	10	30	30	30	30
Water-to-calcine ratio	10:1	5:1	10:1	2.5:1	2-18:1

Recovery rate (%)	96	90	>90	~90	~90
Liquor Li concentration (g/L)	0.7	0.4	~1.0*	4.39	1-3

2.5.3 Bioleaching

Bioleaching of pegmatite ores utilises naturally occurring microorganisms to extract the metal of interest. It has a similar concept to that of traditional chemical leaching, except for the part that the process is induced by the microbial metabolisms through a direct and indirect mechanism of extractive bio-hydrometallurgy (Buckley, 2012; Devasia & Natarajan, 2004). A few studies have investigated bioleaching processes for lithium from pegmatite ores, and to extract the metals into solution microorganisms alter the oxidation states of metals.

2.5.3.1 Acidophilic bacteria

A mixed culture of acidophilic bacterial (*A. ferrooxidans* and *A. thiooxidans*) have been investigated previously, as these can act as a catalyst to improve the efficiency of the bioleaching processes for spent lithium-ion batteries (Karimi2010; Mishra, 2008). Acidithiobacillus are rod shaped bacteria commonly found in acid mine drainages, they are described as acidophilic iron and sulphur oxidising bacteria (Buckley, 2007). Karimi (2010) stated that when bioleaching copper using *A. ferrooxidans* the mechanism involved the extraction of iron into solution. The aerobic bacteria can oxidise via direct and indirect leaching processes. The direct leaching process occurs when metal in the

mineral is oxidised into its ionic state, hence releasing the metal from the mineral formation into the leach solution (Buckley, 2007).



For the indirect leaching processes a continuous reaction of the metals with the leach solution can be observed. In Figure 2:21 the mechanism of bacterial leaching can be seen, showing direct and indirect bioleaching.

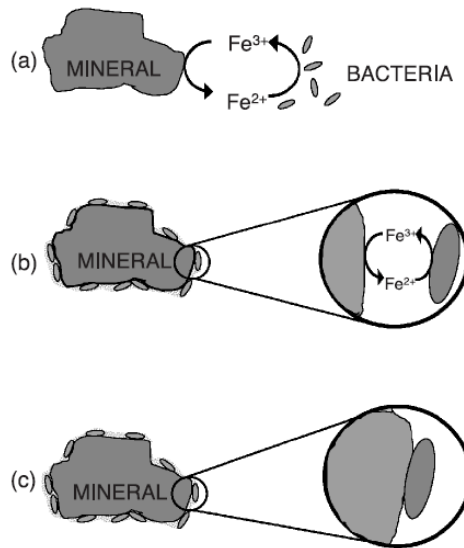
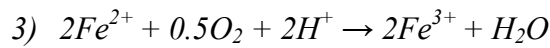
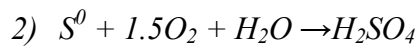
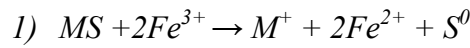


Figure 2:21 Mechanism of bacterial leaching (a) bacteria can either oxidise ferrous ions in the solution (b) attach to the bacteria to oxidise the ferric ions (c) the bacteria directly oxidise the mineral using only micro-organisms, (Crundwell, 2003).

2.5.3.2 Spodumene

Rezza (1997; 2001) investigated extracting lithium from spodumene ($\text{LiAlSi}_2\text{O}_6$) taken from a deposit in San Luis (Argentina) which contained between 6 to 9 % Li_2O . The mineralogical composition of the mineral was 96% spodumene and the rest was made up of plagioclase-albite, quartz, feldspar-microcline and granite.

In a study by Rezza (2001) micro-organisms were used to facilitate the extraction of lithium from the mineral spodumene, as in previous studies by Karavaiko (1980) and Rossi (1990) reported that micro-organisms were involved in bioleaching aluminosilicates such as spodumene to extract lithium. Rezza (1997) identified the fungal strains isolated from the mineral as;

- *Penicillium purpurogenum* (*P. purpurogenum*)
- *Aspergillus niger* (*A. niger*)
- *Rhodotorula rubra* (*R. rubra*)

In previous literature it was reported that an organic acid such as *Aspergillus* degrades and solubilise mineral compounds. The study by Rezza (1997) investigated the organic acids. (Torre, 1993) had reported that *Aspergillus* was capable of producing organic acids such as oxalic citric and gluconic and citric in media with low glucose content. Rezza (2001) found that under these conditions *A. niger* was found to be less effective than *P. Puropurogenum* and *R. Rubra* at lithium extraction.

In 2001 Rezza reported that oxalic acid and citric acid were the two organic acids present, with oxalic acid being present in the largest concentration, *A. niger* was found

to be more effective at leaching lithium than *P. purpogenum*. This indicates that oxalic acid is possibly the key organic acid in the leaching of lithium using *A. niger*. The bioleaching mechanism for *A. niger* was related to the ability to excrete abundant concentrations of organic acids; oxalic and citric acid (Burgstaller, 1993). As organic acids do not produce toxic gases and can be easily degraded, they are seen as environmentally friendly and are less likely to cause diseases to humans (Li et al., 2013).

Furthermore, *A. niger* is a common fungus found in soil as well as a common contaminant of food. It is cheap and easy to grow in the laboratories, thus the extraction process would be economically viable on a larger scale.

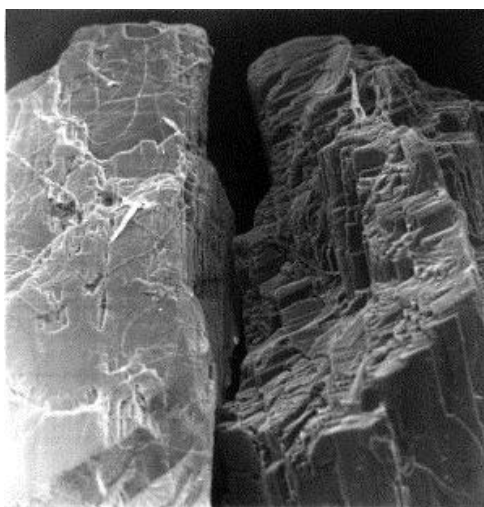


Figure 2:22 SEM Image of spodumene after 30 days of leaching with *A. niger*, Magnification x 500 (Rezza, 2001).

The research investigated for direct and indirect leaching, both under aerobic conditions. For the indirect process the mineral was placed in a dialysis tube and then placed into the medium. Rezza (2001) found the production of metabolites such as organic acids; oxalic, citric and gluconic acid, through both direct and indirect processes

when bioleaching spodumene. Metabolites are known to dissolve the metal from the mineral by displacement of the ion with hydrogen ions (Burgstaller, 1993).

In Table 2:14 the results from the study are shown, the organic acid production was slightly higher for the indirect process. After 30 days of leaching 11mM of oxalic acid was produced in the indirect process compared to 8mM in the direct process. A smaller difference was observed in the production of citric acid, 0.01mM. In Figure 2:23 interestingly after 30 days, the direct process solubilised a greater amount of lithium, 400 µg/L, compared to the indirect process, 223 µg/L, with a difference of 177 µg/L. This suggests that the mechanism prefers a direct contact between the mineral and the microorganism. To understand the mechanism better, the effect of the organic acids on lithium extraction were investigated.

Table 2:14 Results from a study by Rezza (2001) when leaching lithium from the mineral, spodumene using *A. niger* as the leachant.

Time (d)	Oxalic acid (mM)		Citric acid (mM)		Dissolved lithium (µg/L)	
	<i>Indirect</i>	<i>Direct</i>	<i>Indirect</i>	<i>Direct</i>	<i>Indirect</i>	<i>Direct</i>
7	6.96	2	0.21	0.2	50	40
15	16	11.2	0.42	0.3	133.3	240
30	11	8	0.10	0.09	223	400

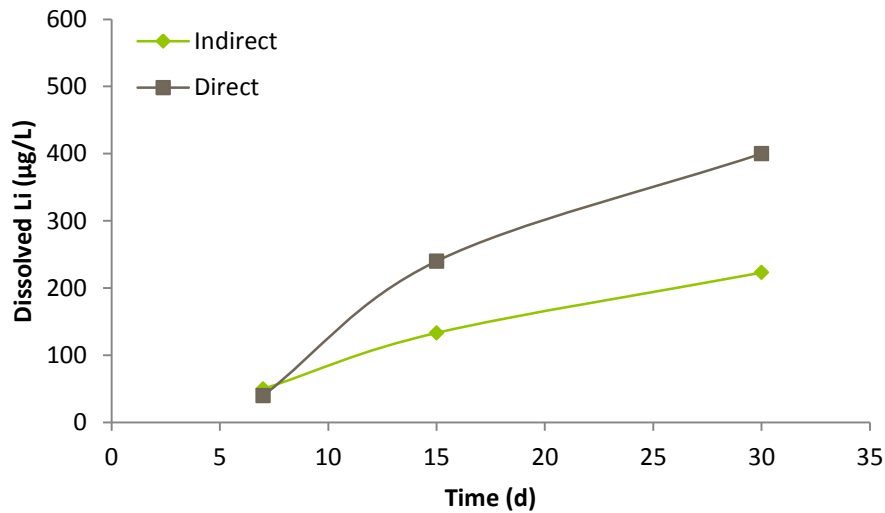


Figure 2:23 Dissolved lithium detected in the leach liquor by AAS, each value was an average of three experiments with standard deviation less than 15% (Rezza, 2001).

It is interesting to note that after 15 days of leaching, Rezza (2001) observed that the solubilised aluminium levels fell significantly (~50%) for both the direct and indirect mechanisms. The oxalic acid concentration also fell after 15 days, so it was assumed that an insoluble aluminium oxalate had precipitated; XRD analysis to detect aluminium oxalate crystals was not possible due to the presence of an amorphous precipitate. It was concluded that leaching of lithium from spodumene is independent of the leaching of aluminium and organic acid production, possibly due to the presence of non-lithium species such as; albite and feldspar. Higher lithium extraction rates were achieved under direct mineral-microorganism contact, which was also suggested by (Karavaiko, 1980). It was established that the attack mechanism of *A. niger* was mediated by organic acids, the maximum concentrations reached were 16mM oxalic acid and 0.42mM citric acid. After investigating the effect of bioleaching from spodumene, (Rezza, 1997)

hypothesises that metabolic adaptation to low nutrient conditions by the microorganisms present are an important factor in the extraction and accumulation of lithium, as suggested by (Neijssel, 1993), as they induce the synthesis of binding proteins for depleted elements and these subsequent proteins to have an affinity for other elements is well known, (Rezza, 1997).

2.5.3.3 Summary of the bioleaching processes

Many studies have been carried out on minerals containing lithium, such as; spodumene, Rezza (2001) was able to successfully identify *A.niger* to assist the lithium extraction for spodumene, extracting 400 µg/L of lithium into solution after 30 days. Other studies such as Tsuruta (2005) also investigated the extraction of lithium but from water containing lithium chloride and found that gram positive bacteria (*Arthrobacter nicotianae* and *Brevibacterium Helovolum*) were able to utilise lithium as a substrate. Utilising micro-organisms for the recovery of lithium has been further investigated using organic acid such as oxalic acid, citric and malic acids. These studies recovered lithium and cobalt from spent lithium-ion batteries and found oxalic acid to be most ideal due to higher solubility in water and environmentally friendly as it is a weak acid, it found recoveries of up to 98% of LiCoO_2 were achieved (Li, 2010; Sun, 2012).

Micro-organisms provide an environmentally friendly solution to extraction when compared to other harsher treatment such as the gypsum process which uses high temperatures of 900°C, thus is not a cost-effective process in the long run. The main disadvantage with bio-recovery process would be the longer process periods, which could potentially be months.

CHAPTER 3

MATERIALS AND METHOD

3.1 Introduction

This chapter describes the methods used to characterise and process the kaolin waste arising from St Austell and Beauvoir as well as the various mineralogical samples of micas obtained during this study. The kaolin waste deposits were selected by geologists at Imerys ltd. as being the most likely to contain significant quantities of lithium rich mica and were sourced from two main Imerys ltd. mining sites in the UK and in France. This study initially investigated the mineralogy of the samples using various techniques such as X-ray diffraction (XRD) and X-ray fluorescence (XRF) to quantify the minerals present and the bulk chemical analysis of the samples.

Particle size distributions were generated and the lithium content of each sample was determined by Inductively coupled plasma spectroscopy (ICP). These techniques were then used to monitor the recovery and grade of the samples as they went through the various upgrading processes used in the study. The final stages investigated various methods to extract the metal in an economic viable process.

3.2 Materials

3.2.1 Mica Specimen Analysis

Mineral specimen grade of pure mica mineral samples; biotite ($K(Mg,Fe)_3[AlSi_3O_{10}(OH,F)_2]$), muscovite ($KAl_3Si_3O_{10}(OH)_{1.8}F_{0.2}$) and lepidolite ($K(Li,Al)_3(Si,Al)_4O_{10}(F,OH)_2$) can be seen in Figure 3:1.



Figure 3:1 Mineral grade specimen of (a) Biotite mica, (b) Muscovite mica, (c) Lepidolite mica (lithium-rich mice).

The minerals were purchased from Northern Geological Supplies Ltd. and analysed to gain a better understanding of the mineralogy and chemical make-up of these minerals that are present in the kaolin mining wastes from both St Austell and Beauvoir sites.

The mica had flat surfaces, composed of layers tightly compact together. Biotite was dark brown/black in colour, due to iron being present in the structure, Muscovite was silvery/white in colour and lepidolite was silvery/lilac in colour and lepidolite had a flaky structure, which was relatively easy to crush. The mineral samples were crushed and milled in a Tema Mill (manganese steel pot) to a particle size range between 10 to 150 μm for subsequent analysis.

3.2.2 Kaolin waste material

Samples were taken from two mine sites in Europe which were thought to contain significant quantities of mica (lithium rich mica lepidolite or zinnwaldite), owned by Imerys Ltd. The two mine sites were Beauvoir in France and St Austell in the UK.

To take a representative geological sample suitable for laboratory testing the British Standard EN 932-1 was followed. The samples were then delivered in individual plastic drums containing 50 kg of the sample in a raw unprocessed form (Michel, 2010). The samples were then representatively sampled and screened ready for laboratory test work.

3.2.2.1 Beauvoir material

Imerys own a small scale kaolin production site in Beauvoir, France. Previous studies in 1985 by the French Administration in charge of the Geological Survey of France (Bureau de Recherches Geologiques et Minieres) identified the presence of significant quantities lithium in their waste material.



Figure 3:2 The Beauvoir mining site in France, this photo was taken in April 2011.

For these investigations two large containers of 50kg were received; the waste material obtained from the hydrocyclone underflow and the Beauvoir lithium concentration (produced in a pilot scale froth flotation study, which was processed by the French Administration in charge of the Geological Survey of France in 1985).

The hydrocyclone waste material had already undergone mining and grinding stages which generally accounts for a large proportion of the ore beneficiation cost (Levich, 2009). Hydrocyclones are used in the mineral industry as a classifier to separate fine particles by density or size (Napier-Munn, 2006). A schematic representation of a hydrocyclone can be seen in Figure 3:3. The kaolin slurry is introduced to the system at a tangential inlet at the top; inside the cyclone a spiralling rotation of slurry creates a vortex. The particles then experience either a drag or centrifugal force which determines the particles pathway to either the overflow (kaolin) or underflow exit (quartz/mica) (Goodbody, 2014). The balance of forces separate the particles according to their particle size and specific gravity (Napier-Munn, 2006). The liberated clay particles exit through the overflow as a dilute suspension. The coarser and denser particles (e.g. cassiterite, coarse quartz and mica) move towards the walls of the cyclone where the velocity is lower, they eventually exit through the bottom outlet forming the underflow.

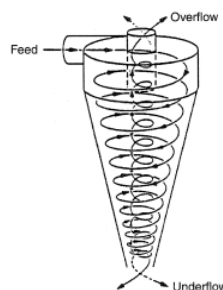


Figure 3:3 Schematic representation of a hydrocyclone, spiral flow, taken from (Rowson, 2010)

3.2.2.2 St Austell material

The St Austell mining area in the UK, also owned by Imerys, was investigated. The granite was reported to have lithium potential according to the British Geological Survey report of 1987. Selected material was chosen in collaboration with a team of Imerys geologists, which was classified into different grades depending on the amount of kaolinisation the material has undertaken (Lanzi, 2008). Mainly grade 4 or 5 materials were selected as they would ensure a better efficiency of separation from the mineral due to the liberation of the ore (Hooper, 2012), due to a higher degree of kaolinisation of the granite liberating the micas from the granite matrix. It should be noted that grade 5 is the highest degree of kaolinisation possible and represents a higher malleable material. Four samples of 50kg each were received from the St Austell site after a sampling campaign was undertaken. The sample were then sampled and prepared for laboratory test trials.

1. New Sink grade 5
2. New Sink grade 4
3. Stope 13 grade 4
4. Blackpool grade 4

3.3 Sample preparation

The 50 kg sample bins were emptied and sampled before a particle size classification was carried out using sieve screens. The particle size ranges used in this study were between 53 μ m to 500 μ m, particles less than 53 μ m were discarded as they contained low lithium contents of approximately 0.02wt. Li₂O.

3.4 Physical Separation techniques

3.4.1 Froth flotation separation

A laboratory scale self-aerated flotation cell with a 2.5L capacity cell was used (Denver LF6797A, Denver Equipment Company), Figure 3:4 and Figure 3:5. The experiments were performed at an impeller speed of 1500 revs per minute, the quantity of kaolin waste material used was up to 500g and 2L of tap water, to give solids by weight of up to 20%.

The pH was checked using a HI-98103 Pocket Checker¹ from Hanna Instruments, resolution of 0.01. The pH was adjusted to varying levels from 1.5 to 3.5 using H₂SO₄ (concentration of 5%). A conditioning period of 5 minutes was applied before the collector and depressant were added. The collector and depressant used were recommended by Cytec Industries. A cationic amine collector Aeromine 3030C and depressant, Cyquest 40E were used; a conditioning period of 5 minutes was applied between each addition. After the air valve was opened, a froth layer formed at the top of the cell. The froth layer was collected for 5 minutes, as the froth is scrapped off the water level decreased thus to maintain a steady froth layer extra water was added. The concentrate and tailings were filtered and dried at a temperature of 80°C in an air atmosphere ready to be weighed and then analysed for lithium by ICP-OES at Imerys ltd. The samples were also analysed using XRF and XRD to determine their chemical and mineralogical data analysis, respectively. The grade and recovery of the lithium and other key elements were then calculated from the resultant data.

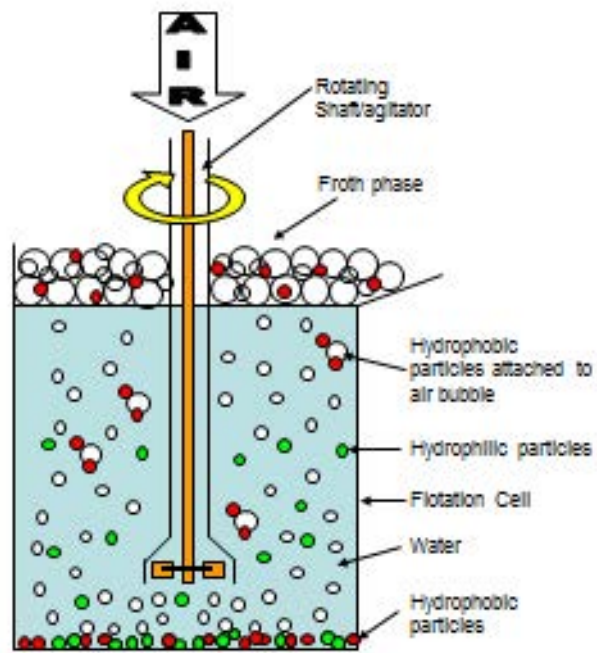


Figure 3:4 Principle of operation of froth flotation cell

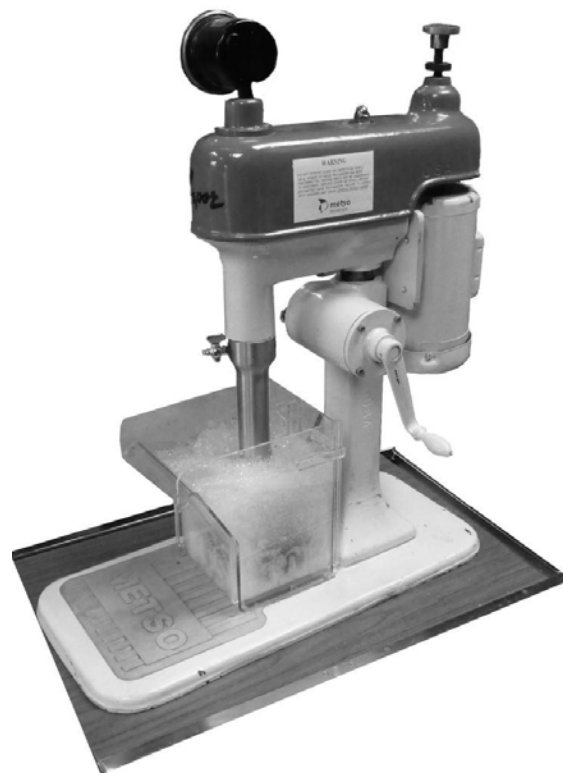


Figure 3:5 Image of flotation cell taken from sepor.com.

3.4.2 Wet High Intensity Magnetic Separation (WHIMS)

Wet High Intensity Magnetic Separation (WHIMS) was used (BoxMag-Rapid, Rapid Magnetic Ltd, England), shown in Figure 3:6 and Figure 3:7. The separator was operated at 0.8 Tesla and a current of 5 amps, in the open gap of the unit. A 1 mm metal wedge wire matrix was inserted into the gap to give capture sites for any paramagnetic mineral particles (iron rich micas, iron oxides and tourmaline) and to provide the magnetic field gradient necessary to achieve a separation.

The suspension (15% by weight), consisted of mineral particles in tap water, was poured in a controlled manner through the magnetic matrix. The material was separated into two fractions; magnetic and non-magnetic, which were dried and weighed. The fractions were analysed for lithium by ICP-OES, for other metals by XRF and for other mineral phases via XRD.

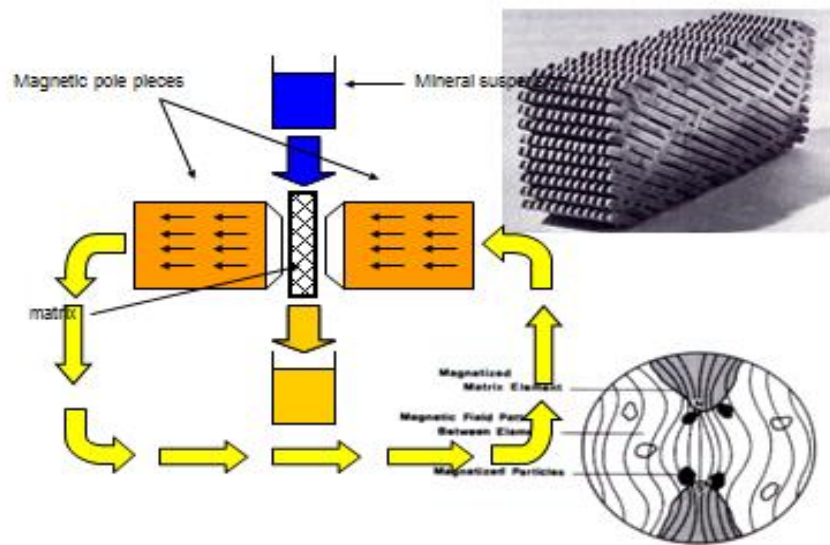


Figure 3:6 Principal of operation of wet high intensity magnetic separator.



Figure 3:7 Boxmag-Rapid, Wet high intensity magnetic separator.

3.4.3 Dry High Intensity Magnetic Separation

A sample was passed through a dry magnetic separation Induced Roll Separator produced by Rapid Magnetic Ltd, Birmingham, UK (Figure 3:8). The separator operated at a magnetic field strength of 1.2 Tesla in the roll/pole gap area, this was the maximum magnetic field strength possible with this machine and was aimed at capturing any weakly paramagnetic mica particles (e.g. biotite, zinnwaldite) plus any iron oxides or tourmaline particles. Samples were collected in two separate containers; magnetic and non-magnetic, and then weighed and analysed by ICP-OES/XRF/XRD.

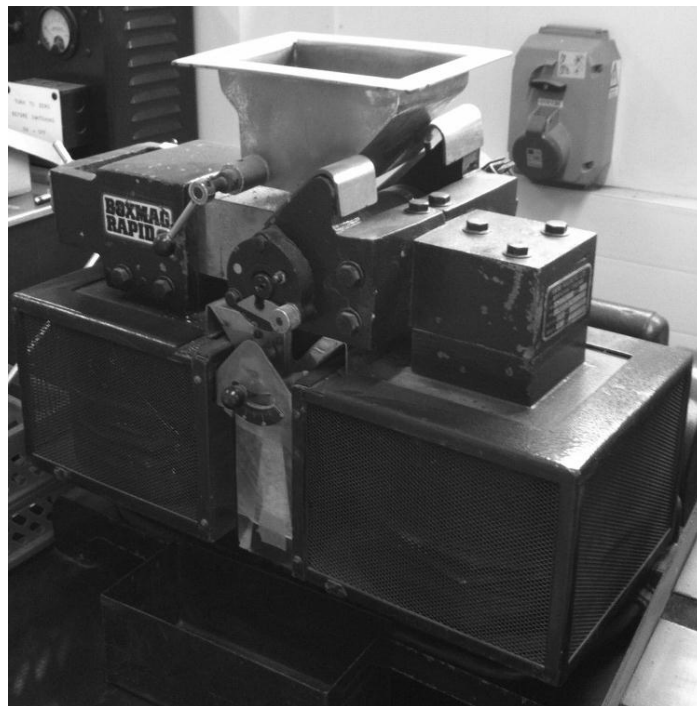


Figure 3:8 Induced roll magnetic separator

3.4.4 Electrostatic Separation

An electrostatic separator (HT Electrostatic separator, BoxMag-Rapid Ltd., England), see Figure 3:9, was used to separate the minerals at an operating voltage of 12keV. Dry material was fed into the vibratory hopper connected to the electrostatic separator, and two fractions were collected; non-conductive (insulator) and conductive. The samples were analysed by ICP-OES/XRF/XRD.

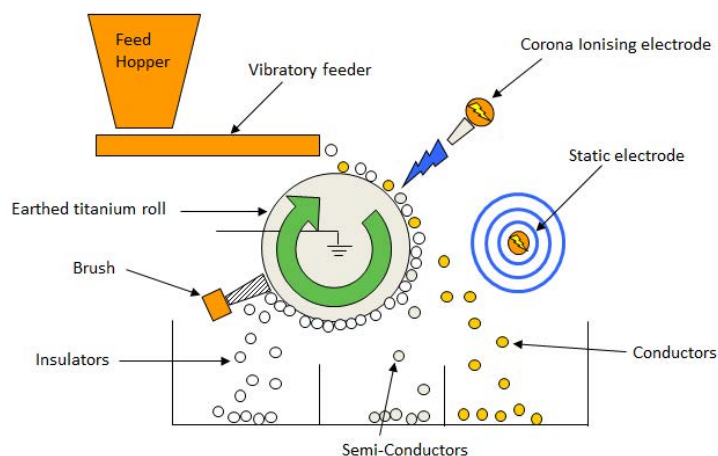


Figure 3:9 Principal of operation of electrostatic separator.



Figure 3:10 Electrostatic separator

3.5 Analytical techniques

3.5.1 Particle size distribution

The particle size distribution was analysed using an image analyser (Quicpic, Sympatec GmbH Inc., Clausthal-Zellerfeld, Germany). The dry particles were fed into the high speed disperser, to obtain statistically representative results the minimum amount used was 1 gram. During the process the particles were dispersed by the gravity disperser and centrifugal forces which are caused by velocity gradients. The laser diffraction sensor for samples was between 0.1 to 875 μm . The images of the particles were captured by a high-speed camera detecting the size of the particles. The analysis was carried out using Windox 5.0 software.

3.5.2 X-Ray Diffraction (XRD)

An X-ray diffractometer (Bruker D8 Advance Powder, Bruker Ltd, Germany) was used to determine the mineralogy of the material. XRD is a qualitative analytical technique used to identify different phases and material composition. It is based on the constructive interference of monochromatic X-rays with a powder sample. Samples for analysis were prepared by pulverising and homogenising the recovered materials with a pestle and mortar. Approximately 0.1 grams of the pulverised sample was evenly spread on a transparent insert. The insert was then placed in the diffractometer and analysed for 30 minutes. The current was set at 30 mA and the voltage at 40 kV. The samples were scanned through a broad range of angles that cover all possible diffraction directions. The analysis of the results was carried out using EVA v2 software, the peak intensity graphs were compared against a reference database.

3.5.3 X-Ray Fluorescence (XRF)

An X-ray fluorescence spectrometer (Bruker S8 Tiger wavelength dispersive, Bruker Ltd, Germany) was used to provide the chemical analysis of the minerals. XRF can quantify the majority of elements in bulk and trace amounts; it is limited to elements with atomic numbers, greater than 5. The X-rays causes molecules to become ionised by striking them and ejecting an electron to a higher energy level. The instability of the ions results in the electron falling back down to the lower energy level. Each element's orbital structure and energy levels are unique and can be used for analysis and classification of materials. Samples were analysed using a rhodium tube with voltage (60kV) and current (67 mA) under a ten minute cycle. The analyser crystal LiF220 and 0.23° collimeter were used to achieve a good separation of the elements (Bruker, 2006). The pressed pellets were fixed into an 8mm mask and placed into the Bruker S8 Tiger and analysed on the QUANT-EXPRESS software.

3.5.3.1 Sample preparation

The samples were prepared by mixing 0.5g of the sample with 0.1g of grinding additive, wax (SpectroBlend 660, Chemplex Industries Inc.). A thin-film sample support (Mylar sheets, Chemplex Industries Inc) was used to prevent adhesion to the 13mm die. The mechanical tester (Zwick, Roell Z030, Germany) was then used to compress the samples ensuring homogeneity, at a force of 10mN.

3.5.3.2 Loss on ignition (LOI)

The loss on ignition procedure was carried out to determine the weight loss of material upon heating. The sample was placed within a muffle furnace at 1050°C for up to 60 minutes in an air atmosphere. After cooling the samples in ceramic crucibles, the percentage of the dry weight lost on ignition was then calculated.



Figure 3:11 Muffle furnace used for loss on ignition tests

3.5.4 Scanning Electron Microscopy (SEM)

Scanning electron microscopy (JSM-6060, JEOL, Germany) was carried out to analyse the mineral surface of the samples. In the instrument a beam of electron are emitted through the electron gun directed towards the sample, they are controlled by a series of electromagnetic lenses and apertures. As the beam hits the sample, electrons are ejected from the sample and produce signals which can determine the samples' morphology and composition. The detectors can determine the X-rays; backscattered electrons illustrate the contrast in composition in the samples and the secondary electrons show the

morphology and topography on the samples. The X-rays are then converted into a signal and displayed as SEM images.

The samples used were prepared in a vacuum chamber using gold or platinum coating. The analysis was carried out using Oxford Inca Energy Dispersive Spectroscopy (EDS) software, the mode used for the samples was secondary electrons and the accelerating voltage was 10kV.

3.5.5 Mineral Liberation Analysis (MLA)

Mineral liberation analysis (MLA) of the waste material was carried out to gain a better understanding of its mineralogical composition. MLA measurements are based on backscattered electron image analysis for determining grain boundaries and locations for X-ray spectral acquisition, thus MLA can provide a quantitative analysis on the particle size, shape and mineralogy of sample (Sylvester, 2010).

3.5.6 Inductively Coupled Plasma (ICP)

Lithium analysis was performed using Inductively coupled plasma spectroscopy (ThermoScientific iCAP 6000 Series ICP, Thermo Scientific, England) at Imerys. ICP is a highly sensitive analytical used for determining the elemental composition of materials. It detects and measures elements by the light emitted at specific wavelengths. It initially promotes electron excitation thus the electrons inside the atom move towards a higher energy level. As the electron relax it drops back down to the lower energy level emitting light. This energy difference of the electron is measured by wavelength, thus element analysis can be calculated by the intensity of the emissions.

3.5.6.1 Sample preparation

The powder samples were prepared by mixing 0.1g of the sample with 0.95g of sodium tetraborate and then heated to 1000°C for 10 minutes. After cooling, 50mL of nitric acid (concentration of 3 wt.%) was added and then further cooled in a water bath for 30 minutes. The solids were filtered and then diluted with distilled water to analyse. The weight percentages of the sample were returned to within 1/100 of one percent accuracy.

3.5.7 Atomic Absorption Spectroscopy (AAS)

Atomic absorption spectroscopy was performed using an AAnalyst 300 Spectrometer by Perkin Elmer Instruments to analyse the lithium concentration of the samples. Acetylene was used as fuel for the flame, burning at 2300°C. The sample solution was aspirated by a nebuliser and transformed into an aerosol. The fine aerosol droplets then entered the flame, the concentration of the elements was analysed by measuring the absorbance of emitted wavelength from the sample using lamp detector, for the lithium lamp (20mA) was detected between 0 to 3ppm. The results were analysed on the Winlab Reformat software.

3.5.8 Flow cytometry

Flow cytometry (CFlow Plus, BD Accuri C6 flow cytometer) was used to detect the presence of micro-organisms in the mine water samples. The particles were fluorescently labelled using a DNA staining dye to identify the DNA particles, SYTO 62 (concentration of 200µm). The fluid stream was then transported to a laser beam;

where up to 10,000 particles were measured. The particles excited by the laser emitted light at varying wavelengths. Data was collected on each particle and the characteristic of those particles was determined based on their fluorescent and light scattering properties. The light signals detected were changed into electronic pulses that a computer can process, displaying the data in the form of a dot plot, contour plot or density plot. The results were analysed on the CFlow Plus software.

CHAPTER 4

CHARACTERISATION OF THE LITHIUM-RICH MICA WASTES

4.1 Introduction

This study investigated the processing of lithium mica rich waste streams from the Beauvoir mining site in France, as well as various sites of interest in the St Austell kaolin mining area of Cornwall, UK. Both sites were owned by Imerys, a world leader in the production of specialty minerals for industrial applications. This chapter presents in greater detail the characterisation of a number of kaolin waste materials studied, using various analytical techniques including; X-ray fluorescence, X-ray diffraction and Scanning electron microscopy to analysis the chemical composition, mineralogy and the mineral surface, respectively.

4.2 Beauvoir Mica Wastes

4.2.1 Introduction

For this study, a mica rich kaolin waste material was investigated. It was produced as a hydrocyclone underflow in an earlier stage of the process flowsheet at the Beauvoir kaolin mining operation. This chapter gives a detailed analysis of the chemical and

mineralogical characteristics carried out on this material. For the Beauvoir kaolin waste material two samples were investigated;

- Hydrocyclone underflow waste material; *taken from the hydrocyclone underflow on the existing plant.*
- Lithium mica concentrate; *taken from a bulk flotation concentrate produced previously by Imerys.*

4.2.2 Hydrocyclone underflow waste material

4.2.2.1 Production of waste material

The waste material investigated in this study was taken from hydrocyclone underflow product. At the time of commencement of this study, the waste material from the kaolin production plant was stockpiled on site as a waste material.

4.2.2.2 Mineralogical analysis of Beauvoir waste material

Figure 4:1 and Table 4:1 detail the MLA of the Beauvoir waste material carried out by Imerys (Ancia, 2010) using the particle size fraction of 315 to 630 μ m. The majority of minerals found in the samples were; albite, lepidolite and quartz, making up 84.9% of the waste material. The majority of the lithium was present as the lithium-bearing mineral lepidolite ($\text{KLi}_2\text{Al}(\text{Si}_4\text{O}_{10})(\text{OH},\text{F})$) representing 25.1% of the total mass. There was 1.0% of the mineral amblygonite ($\text{Li}(\text{F},\text{OH})\text{AlPO}_4$) also present in the waste material. Lepidolite was present as coarse particles of average size 364 μ m, hence it reported in the hydrocyclone underflow. The mineral was partially liberated (23%) indicating that the further downstream processing of the material of lithium mica would

be difficult. It was interesting to note that only 2.2% of the material is kaolinite, thus indicating that the hydrocyclone was performing efficiently.

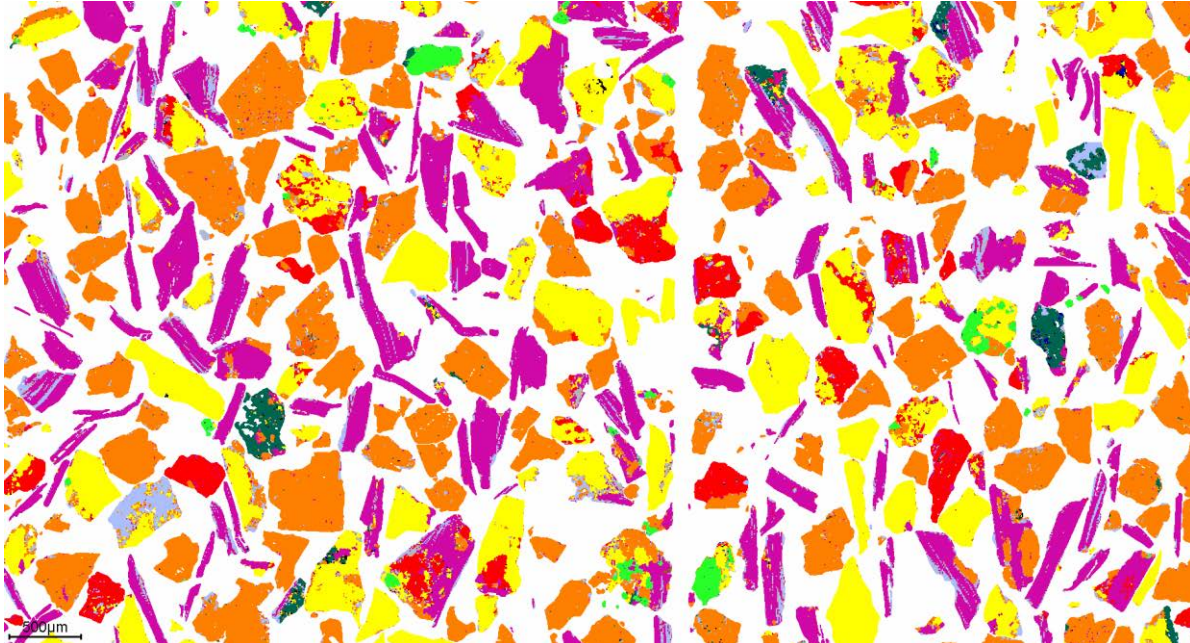


Figure 4:1 MLA image analysis of waste material for 315-630µm size fraction, the key is found in table 1.3 (Ancia, 2010).

Table 4:1 MLA, Mineralogy of the waste material for 315-630µm size fraction (Ancia, 2010; Watson, 1962).

Key	Mineral	Chemical formula	Content (%)	Particle size (µm)	Liberation (%)
	Albite	$\text{NaAlSi}_3\text{O}_8$	35.07	408	60
	Lepidolite	$\text{KLi}_2\text{Al}(\text{Si}_4\text{O}_{10})(\text{OH},\text{F})$	25.10	364	23
	Quartz	SiO_2	24.73	438	32
	K Feldspar	KAlSi_3O_8	6.90	296	2
	Topaz	$\text{Al}_2\text{F}_2\text{SiO}_4$	3.11	556	1
	Kaolinite	$\text{Al}_4\text{Si}_4\text{O}_{10}(\text{OH})_8$	2.17	116	1
	Muscovite	$\text{KAl}_2[(\text{AlSi}_3\text{O}_{10})].(\text{OH})_2$	1.74	40	0.01
	Amblygonite	$[\text{Li}(\text{F},\text{OH})\text{AlPO}_4]$	0.98	22	13
	Kyanite/sillimanite	Al_2SiO_5	0.11	13	0.01
-	Total	-	99.91	-	-

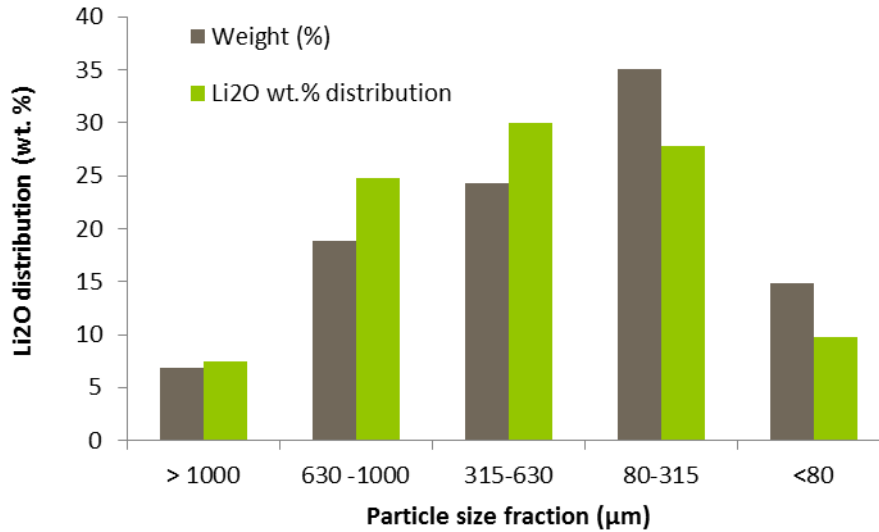


Figure 4:2 Particle size distributions for Li₂O wt.% (Ancia, 2010).

4.2.2.3 Chemical analysis of the waste material

In Table 4:2 the chemical analysis of a range of particle sizes can be seen, from less than 80µm to greater than 1000µm. The chemical analysis was carried out at Imerys Ltd Ceramic centre in France (Ancia, 2010). High concentrations of Si₂O of above 60% were found in all of the particle size fractions; which was due to hydrolysis of kaolin ores. The hydrolysis of the kaolin ore can be seen in the equation below;



In the waste material, the lithium concentrations were between 0.3 to 1.3 wt.% Li₂O for various particle size ranges. Higher concentrations of 1.3 wt.% Li₂O were found for the particle sizes 315 and 1000µm. Siame (2011) indicated that lepidolite generally contained between 3.0 and a theoretical maximum of 7.7 wt.% Li₂O. Low concentrations of Fe₂O₃ were found of up to 0.2 wt.% in all of the samples.

Table 4:2 Chemical analysis of the Beauvoir waste material by particle size classification (Ancia, 2010).

Particle size fraction (μm)	Oxide Concentration (wt.%)							LOI	Total
	SiO ₂	Al ₂ O ₂	Na ₂ O	K ₂ O	Li ₂ O	Fe ₂ O ₃	CaO	(%)	(%)
> 1000	81.5	11.0	1.2	2.8	1.1	0.2	0.1	1.4	99.2
630 - 1000	76.5	14.5	1.8	3.8	1.3	0.2	0.1	1.5	99.7
315 - 630	70.3	18.3	4.2	3.5	1.3	0.2	0.1	1.6	99.5
80 - 315	66.0	19.7	6.7	2.3	0.8	0.1	0.1	3.4	99.2
< 80	63.2	21.5	5.9	2.3	0.7	0.1	0.3	1.6	95.5

4.2.3 Beauvoir lithium mica concentrate

The lithium mica concentrate was processed by the French Administration in charge of the Geological Survey of France (Bureau de Recherches Geologiques et Minieres), in 1985.

4.2.3.1 Chemical analysis

The chemical analysis of the Beauvoir lithium concentrate can be seen in Table 4:3 Chemical analysis of the lithium mica concentrate for the particle size fraction of 53 to 400 μm . *tested by ICP). As the material was taken from a kaolin production unit, the majority of the chemical composition was made up of Si₂O and Al₂O₃ containing 51.2 and 26.2 wt.%, respectively. The lithium mica concentrate contained 4.1 wt.% Li₂O. Garrett (2004) identified that lepidolite concentrates obtained in China contain similar oxide concentrations of 55.3 and 23.6 wt.% for Si₂O and Al₂O₃, respectively.

Significant concentrations of Rb₂O were also observed in the Beauvoir lithium concentrate, (1.5 wt.%). An increase of Rb₂O during processing was also observed in the study by Garrett (2004) increasing from 0.3 to 1.2 wt.% in the final lithium concentrate. Rubidium could potentially provide a value added product to the lithium recovery stage.

Table 4:3 Chemical analysis of the lithium mica concentrate for the particle size fraction of 53 to 400µm. *tested by ICP ^a(Ancia, 2010), ^b(Garrett, 2004).

Chemical composition	Weight (%)	
	Beauvoir concentrate ^a	China concentrate ^b
SiO ₂	51.2	55.33
Al ₂ O ₃	26.2	23.64
K ₂ O	7.9	8.35
*Li ₂ O	4.1	4.65
Rb ₂ O	1.5	1.2
Fe ₂ O ₃	0.5	1.3
Na ₂ O	0.3	1.1
Cs ₂ O	0.2	-
MnO	0.2	-
P ₂ O ₅	0.1	-
LOI (1050°C)	4.4	-
SUM	96.6	96.9

4.2.3.2 Lepidolite mineral sample

Lepidolite is a translucent lilac colour mica mineral which has a monoclinic crystal structure. It has a complex and variable formula, which is dependable on its location. It has the general chemical formula; $\text{KLi}_2\text{Al}(\text{Si}_4\text{O}_{10})(\text{OH},\text{F})$, containing between 3.0 to a theoretical maximum of 7.7 wt.% Li_2O (Siame, 2011). In Figure 4:3 lepidolite can be seen under a thin section microscope, viewed under polarised light. Lepidolite is a vitreous mineral; it has a glass like sheen on the mineral surface which illuminates under a polarised microscope. The image shows the flat structure which is fractured in an uneven pattern. In Figure 4:4, a SEM image of lepidolite can be seen showing the platy structure of the surface which is composed of a stack of sheets, a common feature for micas.

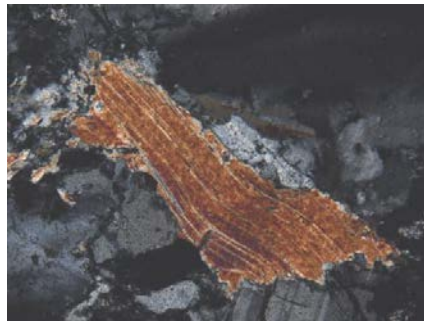


Figure 4:3 Thin section microscopy image of lepidolite mineral obtained from Beauvoir, France, magnification x10.

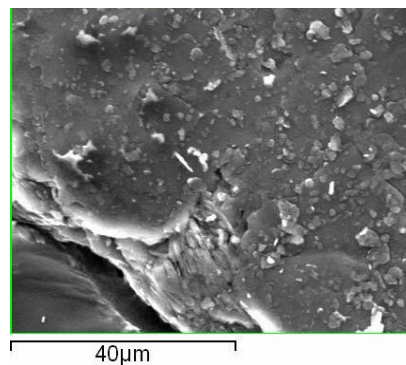


Figure 4:4 SEM image of lepidolite mineral obtained from Beauvoir, France, 10KV, Mag: 500, Det: SE, WD 10mm.

4.2.4 Mineral grade specimen pure lepidolite

4.2.4.1 Chemical analysis of mineral specimen grade pure lepidolite

To get a better understanding of the lithium potential for processing lepidolite, a sample of mineral specimen grade pure lepidolite was crushed and milled to a particle size fraction of 10 to 140 μ m using a hammer mill and a Tema mill. The chemical composition of this lepidolite sample can be seen in Table 4:4, which shows lepidolite to contain 5.6 wt.% Li₂O. Typically lepidolite has been reported to contain between 3.0 to a theoretical maximum of 7.7 wt.% Li₂O (Siame, 2011).

Table 4:4 Chemical analysis of a mineral specimen grade pure lepidolite, *tested by ICP.

Chemical composition	Weight (%)
SiO ₂	52.2
Al ₂ O ₃	18.3
K ₂ O	11.3
*Li ₂ O	5.6
Cs ₂ O	3.7
Rb ₂ O	2.6
Na ₂ O	0.4
MnO	0.4
Nb ₂ O ₅	0.1
LOI	4.0
SUM	98.6

4.3 St Austell, UK lithium mica deposits

4.3.1 Introduction

The British Geological Survey (1987) reported that St Austell had a lithium potential of up to 3.3 million tonnes of recoverable lithium within the upper 100 m region of an 8 km² recognised area. Manning (1996) identified several regions as lithium mica granite, from these Imerys identified the Karslake and Blackpool areas to investigate in this study, Figure 4:5.



Figure 4:5 Geological map of St Austell showing the UK Hydrous Kaolin Platform operations site taken in 2010.

Key for Karslake: (1) New Sink G5 (2) New Sink G4 (3) Stope 13 G4 (Hirtzig, 2010).

Four sites were chosen by Imerys as potentially containing lithium-bearing minerals. The geological samples were collected following the British Standard EN 932-1 which details methods for bulk sampling and sample size reduction.

The samples were named using the following standard code: XYGX where XY stands for the location and GX represent the grade type of the mineral. The following four samples were investigated in this study:

- Karslake area:
 - New Sink Grade 5 (*New Sink G5*)
 - New Sink Grade 4 (*New Sink G4*)
 - Stope 13 Grade 4 (*Stope 13 G4*)
- Blackpool area:
 - Blackpool Grade 4 (*Blackpool G4*)

4.3.2 New Sink Grade 5

4.3.2.1 Mineralogical analysis of the New Sink G5 Material

This sample formed part of the Lithium mica granite member (Manning, 1996) and was sampled near a working face within the Little Johns pit at New Sink. Hooper (2012) described the sample to contain a large selection of smaller unconsolidated scree around the main sample, which was relatively easy to excavate, as shown in Figure 4:6.

The New Sink G5 granite was fully kaolinised and classified as, high decomposition grade 5 (Lanzi, 2008). In the British Geological Survey report, it was reported to be a potential source of lithium due to the significant content of lithium mica found in this geological area (Hawkes, 1987). The sample was taken from deep within the lateritic vein and contained individual mineral crystals which were less than 4mm, on average. It was described as highly malleable off white material with some evidence of tourmalinisation, no iron staining, greisen or veining was reported (Hooper, 2012).

The mineralogical analysis of New Sink G5 is shown in Table 4:5, this indicates significant quantities of kaolin still present in the sample. The mica present is comprised of Muscovite ($\text{KAl}_2[(\text{AlSi}_3)\text{O}_{10}](\text{OH})_2$) and Zinnwaldite ($\text{KLiFe}^{+2}\text{Al}(\text{AlSi}_3)\text{O}_{10}(\text{F},\text{OH})_2$) making up 6%. Zinnwaldite ($\text{KLiFe}^{+2}\text{Al}(\text{AlSi}_3)\text{O}_{10}(\text{F},\text{OH})_2$) is a variant of lepidolite which contains a higher iron content. It is difficult to distinguish from other micas as they have similar characteristics, such as; layered structure forming sheets of silicate which are weakly bonded by potassium ions. Zinnwaldite contains between 2.0 to a theoretical value of 5.0 wt.% Li_2O (Siame, 2011).

Table 4:5 Mineralogy of the New Sink G5 material [For the mineral Tourmaline, X may be Na or Ca and Y may be Mg, Fe or Li] (Garrett, 2004; Hooper, 2012).

Mineral	Chemical Formula	Proportion (%)
Kaolinite	$Al_4Si_4O_{10}(OH)_8$	45
Quartz	SiO_2	44
Mica (Muscovite & Zinnwaldite)	$KAl_2[(AlSi_3)O_{10}](OH)_2$, $KLiFe^{+2}Al(AlSi_3)O_{10}(F,OH)_2$	6
Tourmaline	$XY_3B_3Al_3[(Al, Si)_3O_5]_3(OH, F)_4$	5



Figure 4:6 Selected face of New Sink G5 material (Hooper, 2012).



Figure 4:7 Hand specimen of New Sink Lithium Mica granite G5 (Hooper, 2012).

4.3.2.2 Chemical analysis of the New Sink G5 material

New Sink G5 was classified in various particle size fractions, ranging from 53µm to greater than 1700µm using a sieve screening deck. In Figure 4:8 the lithium oxide content for the various particle size ranges up to 17000µm can be seen.

The highest lithium content was found in the particle size range 53µm to 250µm, containing 0.07 wt.% Li₂O. The New Sink G5 samples contained a lower amount of lithium than expected for zinnwaldite (between 2.0 to 5.0 Li₂O), thus indicating that the proportion of zinnwaldite is very low in the mica composition or that the due to the weathering alteration of muscovite structure which contained small amounts of lithium.

The chemical analysis of the particle size fraction of 53µm to 500µm can be seen in Table 4:6. The chemical analysis was carried out by X-ray fluorescence at the University of Birmingham and ICP for Li₂O at Imerys. The Si₂O composition made up 82% of the final weight and the lithium oxide made up 0.09%. The low amount of lithium oxide is likely to indicate the presence of very little zinnwaldite and muscovite mica in the mica fraction. High levels of Fe₂O₃ indicated that tourmaline was present.

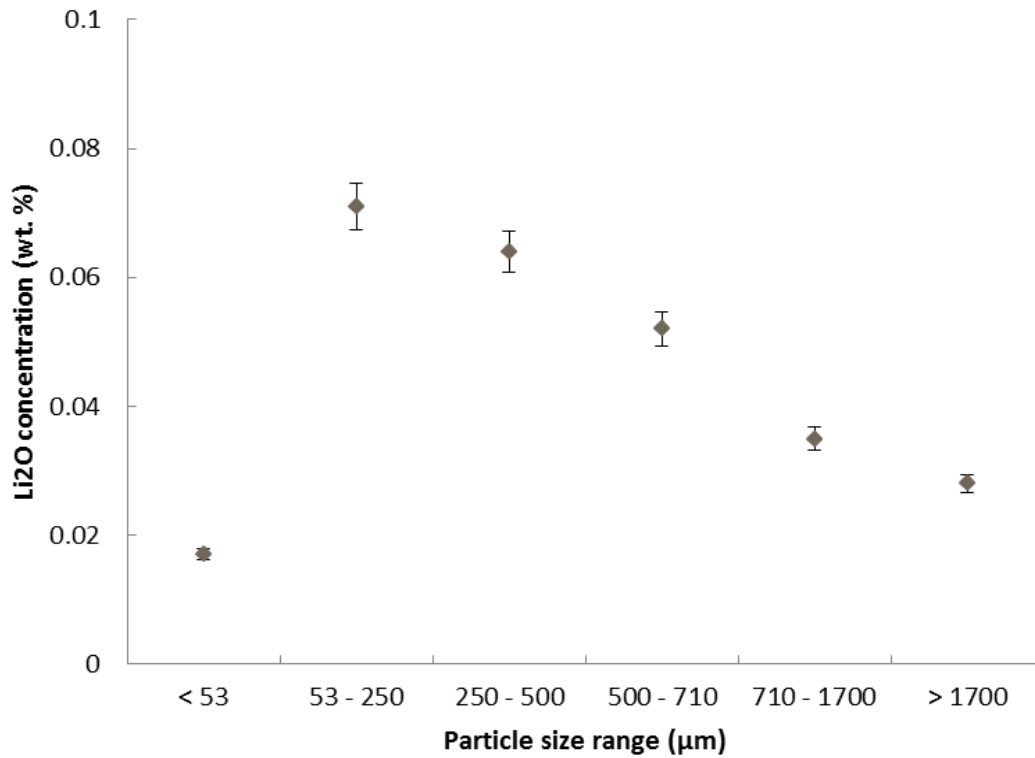


Figure 4:8 Lithium concentrations in varying particle size fraction for the New Sink G5 material.

Table 4:6 Chemical analysis of New Sink G5, for the size fraction 53µm to 500µm. *tested by ICP.

Chemical composition	Weight (%)
SiO ₂	81.0
Al ₂ O ₃	8.29
K ₂ O	4.00
Fe ₂ O ₃	3.81
TiO ₂	0.52
Rb ₂ O	0.14
*Li ₂ O	0.09
SUM	98.9

4.3.2.3 Particle Size Distribution

The particle size fractions between 53 μm to 500 μm were investigated further as they were suitable for flotation separation for lithium rich mica particles. Two particle size fractions were prepared in larger volumes; 53 μm to 250 μm and 250 μm , to 500 μm for potential upgrading processes such as froth flotation, Figure 4:9. The results show that an efficient separation was achieved in both particle size ranges, within acceptable limits.

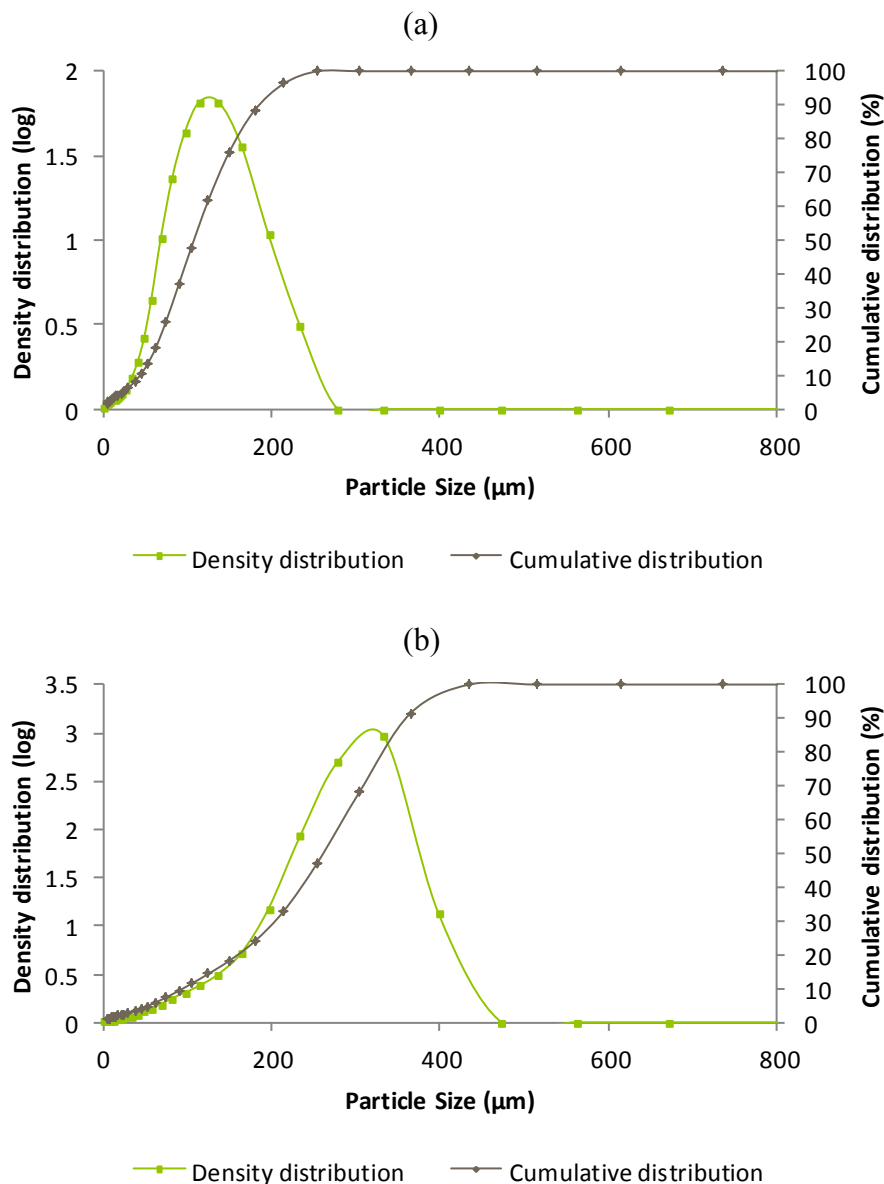


Figure 4:9 Particle Size Distribution of New Sink G5 material after classification into size fractions (a) 53 μm to 250 μm and (b) 250 μm to 500 μm , obtained by laser-sizer.

4.3.3 New Sink, Grade 4

4.3.3.1 Mineralogical analysis of the New Sink G4 material

The New Sink G4 sample also formed part of the lithium mica granite member (Manning, 1996) which was found within the Little Johns pit at New Sink. The New Sink G4 sample was of a lower grade and thus thought harder to recovery lithium-bearing minerals from due to its complex structure, on average the individual mineral crystals were less than 2mm.

New Sink G4, is lithium mica granite which is nearly fully kaolinised with a high decomposition grade 4 (Manning, 1996). According to Lanzi (2008) decomposition grades are defined as the amount of alteration the granite has experienced. The sample was highly malleable with some degree of friability. It had some evidence of tourmalinisation, no iron staining, greisen or veining. There were large amount of brown and white micas observed (Manning, 1996).

Table 4:7 Mineralogy of the New Sink G4 material [For the mineral Tourmaline, X may be Na or Ca and Y may be Mg, Fe or Li, for Feldspar X may be K, Ca or Na] (Garrett, 2004; Hooper, 2012).

Mineral	Chemical Formula	Proportion (%)
Kaolinite	$Al_4Si_4O_{10}(OH)_8$	42
Quartz	SiO_2	40
Mica (Muscovite & Zinnwaldite)	$KAl_2[(AlSi_3)O_{10}](OH)_2$ $KLiFe^{+2}Al(AlSi_3)O_{10}(F,OH)_2$	6
Tourmaline	$XY_3B_3Al_3[(Al, Si)_3O_5]_3(OH, F)_4$	3
Feldspar	$XAl_{(1-2)}Si_{(3-2)}O_8$	5



Figure 4:10 Selected face of New Sink G4 material (Hooper, 2012).



Figure 4:11 Hand specimen of New Sink Lithium Mica granite G4 (Hooper, 2012).

4.3.3.2 Chemical analysis of the New Sink G4 material

Lithium analysis was carried out on various particle size fractions for the New Sink G4 material, ranging from 53 μm to greater than 1700 μm . In Figure 4:12 it can be seen that low levels of lithium were detected in all of the size fractions, around 0.02 wt.% Li_2O . As the New Sink G4 material was not fully kaolinised, low levels of lithium were expected, but as the material was a high decomposition grade and the mineralogy indicated 6% mica presence it was expected to be higher than 0.02 wt.% Li_2O . Manning (1996) suggested that over time additional alteration effects to the lithium mica granite could include the replacement of zinnwaldite by tourmaline. In Table 4:8 it can be seen that Fe_2O_3 was present in the sample at around 0.05 %.

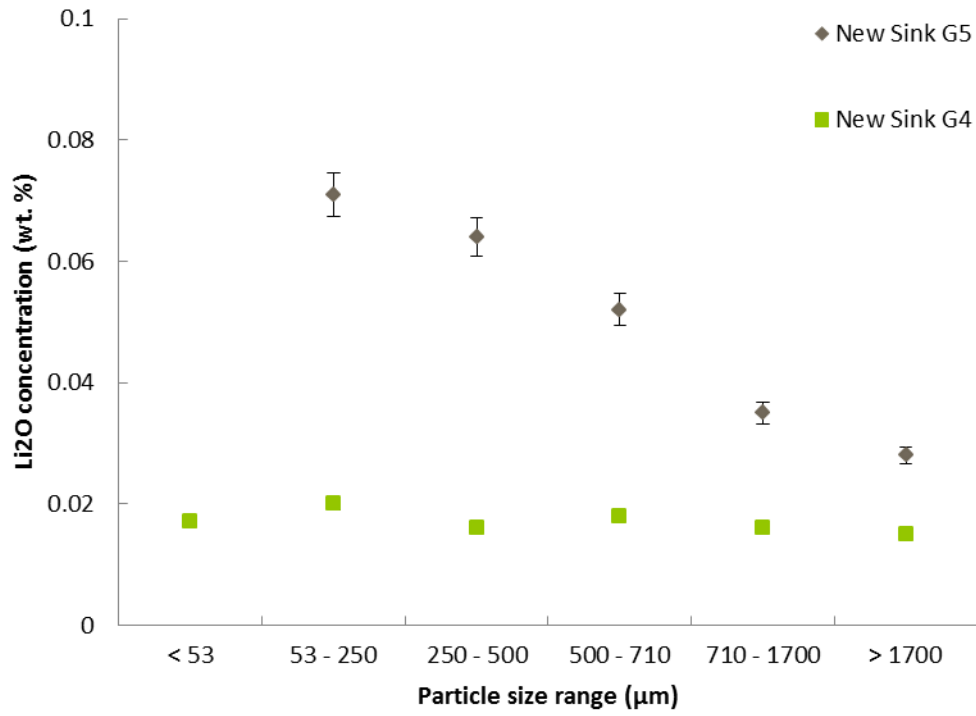


Figure 4:12 Lithium concentration in varying particle size fraction for the New Sink material.

Table 4:8 Chemical analysis of New Sink G4, for the size fraction 250µm to 500µm. *tested by ICP.

Chemical composition	Weight (%)
SiO ₂	75.8
Al ₂ O ₃	11.7
K ₂ O	0.01
Fe ₂ O ₃	0.05
TiO ₂	0.02
Rb ₂ O	0.17
*Li ₂ O	0.02
Total	87.8

4.3.4 Stope 13, Grade 4

4.3.4.1 Mineralogical analysis of the Stope 13 G4 material

Stope 13 Grade 4 was taken from the Karslake area of St Austell. It lies deep within the Lithium Mica granite within Little Johns pit (Manning, 1996). Stope 13 G4 is a lithium mica granite, described as partly-nearly fully kaolinised granite, low decomposition grade 4 (Lanzi, 2008). The individual mineral crystals were less than 4mm in size. The sample can be described as friable off white/brown material with no evidence of tourmalinisation, low iron staining, no greisen or veining, although there were several tourmaline veinlets observed, less than 1mm (Hooper, 2012).

Table 4:9 Mineralogy of the Stope 13 G4 sample [For the mineral Tourmaline, X may be Na or Ca and Y may be Mg, Fe or Li, for Feldspar X may be K, Ca or Na] (Garrett, 2004; Hooper, 2012).

Mineral	Chemical Formula	Proportion (%)
Kaolinite	$Al_4Si_4O_{10}(OH)_8$	40
Quartz	SiO_2	38
Mica (Muscovite & Zinnwaldite)	$KAl_2[(AlSi_3)O_{10}](OH)_2$ $KLiFe^{+2}Al(AlSi_3)O_{10}(F,OH)_2$	6
Tourmaline	$XY_3B_3Al_3[(Al, Si)_3O_5]_3(OH,F)_4$	6
Feldspar	$XAl_{(1-2)}Si_{(3-2)}O_8$	10



4:13 Selected face of Stope13 G4 material (Hooper, 2012).



4:14 Hand specimen of Stope 13 Lithium Mica granite G4 (Hooper, 2012).

4.3.4.2 Chemical analysis of the Stope 13 G4 material

In Figure 4:15 the lithium analysis for Stope 13 G4 showed low concentrations present in the material, of around 0.02 wt.% Li_2O . This could be potentially due to a number of reasons such as; a dyke found nearby the Little Johns pit at Stope 13, which contained K_2O which could have possibly acted as a contaminant in the sample, alterations of the mica due to weathering as well as the material containing relatively high amounts of feldspar (10%).

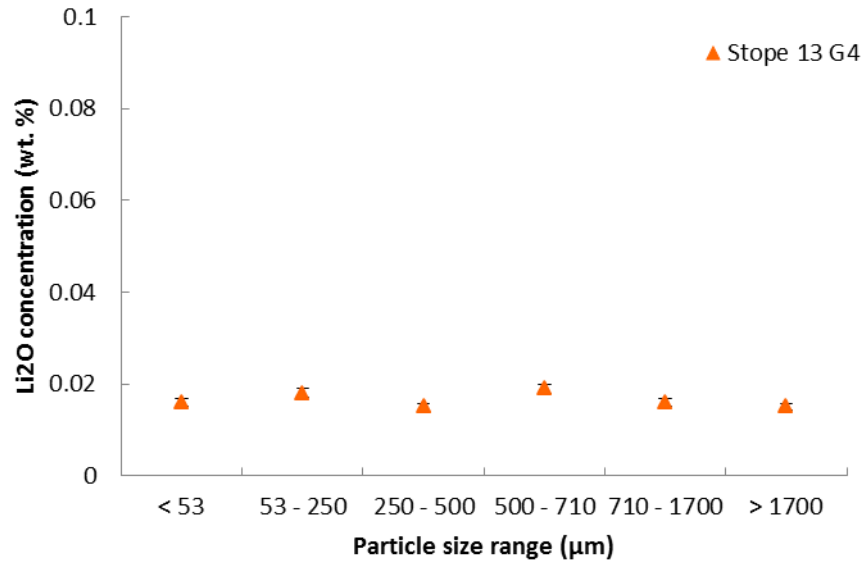


Figure 4:15 Lithium concentration in varying particle size fraction for the St Austell kaolin mining waste material.

Table 4:10 Chemical analysis of Stope 13 G4, for the size fraction 250µm to 500µm. *tested by ICP.

Chemical composition	Weight (%)
SiO ₂	50.7
Al ₂ O ₃	27.0
K ₂ O	8.90
Fe ₂ O ₃	6.50
TiO ₂	0.20
Rb ₂ O	0.30
*Li ₂ O	0.02
Total	97.6

4.3.5 Blackpool, Grade 4

4.3.5.1 Mineralogical analysis of the Blackpool G4 material

The Blackpool sample can be described as nearly fully kaolinised granite, high decomposition grade 4 (Lanzi, 2008). On average the individual mineral crystals were less than 4mm in size. The sample was an off white in colour with some evidence of Tourmalinisation, and no iron staining, greisen or veining. It contained small amounts of brown and white muscovite and zinnwaldite mica (6%), Table 4:11. The sample was near fully kaolinised for potassium feldspar incomplete kaolinisation of sodium feldspar (Manning, 1996; Hooper, 2012).

Table 4:11 Mineralogy of the Blackpool G4 material [For the mineral Tourmaline, X may be Na or Ca and Y may be Mg, Fe or Li, for Feldspar X may be K, Ca or Na] (Garrett, 2004; Hooper, 2012).

Mineral	Chemical Formula	Proportion (%)
Kaolinite	$Al_4Si_4O_{10}(OH)_8$	40
Quartz	SiO_2	42
Mica (Muscovite & Zinnwaldite)	$KAl_2[(AlSi_3)O_{10}](OH)_2$, $KLiFe^{+2}Al(AlSi_3)O_{10}(F,OH)_2$	6
Tourmaline	$XY_3B_3Al_3[(Al, Si)_3O_5]_3(OH,F)_4$	3
Feldspar	$XAl_{(1-2)}Si_{(3-2)}O_8$	5



4:16 Selected face of Blackpool G4 material (Hooper, 2012).



4:17 Hand specimen of Blackpool Lithium Mica granite G4 (Hooper, 2012).

4.3.5.2 Chemical analysis of the Blackpool G4 material

In Figure 4:18 the lithium concentrations for the various particle sizes can be seen, of up to 0.08 wt.% Li_2O for the particle size fraction 53 to 250 μm . Hooper (2012) indicated that the sample face showed signs of a high degree of recent weathering, at the time of sampling the Blackpool pit was dormant with no current workings taking place. It was of general interest to analyse the sample for potential lithium concentrations as it formed part of the lithium mica granite (Manning, 1996).

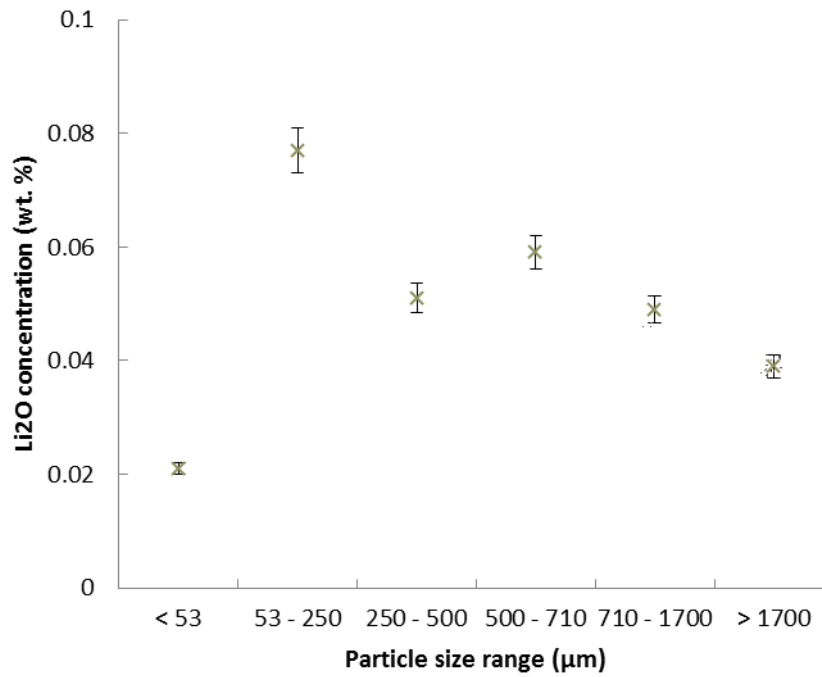


Figure 4:18 Lithium concentration in varying particle size fraction for the St Austell kaolin mining waste material.

Table 4:12 Chemical analysis of Blackpool G4, for the size fraction 53µm to 250µm. *tested by ICP.

Chemical composition	Weight (%)
SiO ₂	46.0
Al ₂ O ₃	30.8
K ₂ O	9.50
Fe ₂ O ₃	8.90
TiO ₂	0.50
Rb ₂ O	0.40
*Li ₂ O	0.08
Total	96.0

4.3.6 Summary of St Austell deposit

The following table contains the summary for the chemical and mineralogical compositions of the four samples obtained from St Austell. The mineralogy varied over the four samples, of different grades, although all samples contained approximately 6% mica. The Li₂O concentrations are approximately less than 0.1 wt% for the four samples.

Table 4:13 Summary of chemical and mineralogical compositions for St Austell samples.

	New Sink G5	New Sink G4	Stope 13 G4	Blackpool G4
Mineral composition	(Proportion, %)			
Quartz	44	40	38	42
Mica (Muscovite & Zinnwaldite)	6	6	6	6
Tourmaline	5	3	10	3
Feldspar	0	5	10	5
Chemical composition	(Weight, %)			
SiO ₂	81.0	75.8	50.7	46.0
Al ₂ O ₃	8.29	11.7	27.0	30.8
K ₂ O	4.00	0.01	8.90	9.50
Fe ₂ O ₃	3.81	0.05	6.50	8.90
TiO ₂	0.52	0.02	0.20	0.50
Rb ₂ O	0.14	0.17	0.30	0.40
*Li ₂ O	0.09	0.02	0.02	0.08
Total	98.9	87.8	97.6	96.0

CHAPTER 5

RECOVERY OF LITHIUM-BEARING MINERALS

5.1 Introduction

This chapter investigates the recovery of lithium-bearing minerals such as; lepidolite ($\text{K}(\text{Li},\text{Al})_3(\text{Si},\text{Al})_4\text{O}_{10}(\text{F},\text{OH})_2$) and zinnwaldite ($\text{KLiFeAl}(\text{AlSi}_3)\text{O}_{10}(\text{F},\text{OH})_2$), from kaolin mining waste material, mainly using froth flotation separation in an attempt to develop an economically viable lithium mica recovery process. Two main Imerys' mine sites were investigated in this study; Beauvoir granite in France containing 0.9 wt.% Li_2O and the St Austell granite in the UK, containing up to 0.08 wt.% Li_2O .

By attempting to recycle the waste material to recover lithium mica, a secondary resource for lithium would be provided for the UK and EU, thus reducing the rate at which primary lithium ores are presently utilised as well as maintaining an environment balance by reducing the volume of waste produced by the kaolin mining industries and producing an added value product for Imerys mining operations. For the recovery process route to be economically viable a lithium concentration of 4.0 wt.% Li_2O would be required to be generated (Amarante, 1999; Bauer, 2000).

The aims were to test the efficiency of lithium mica extraction for both deposits and to attempt to improve the recovery of lithium mica, taking into consideration the economic viability of any process employed and the critical and strategic nature of existing lithium deposits in the UK and Europe.

5.2 Froth Flotation Separation of Kaolin Waste Material From Beauvoir in France

5.2.1 Introduction

The waste material obtained from the hydrocyclone underflow of the kaolin production plant in Beauvoir reported a lithium grade of up to 0.9 wt.% Li_2O (Ancia, 2010). To upgrade the waste material, physical mineral separation methods were investigated. In a previous study at Imerys, a froth flotation process was developed to recover the lithium bearing minerals. In the Beauvoir material, lepidolite was identified as the lithium bearing mineral through various mineral analysis techniques including Mineral Liberation Analysis (MLA).

In Figure 5:1 the separation process can be seen in greater detail, an overview of the process can be summarised into the following stages;

- i. The particle size fraction of $53\mu\text{m}$ to $400\mu\text{m}$ was separated via a two-stage flotation process; rougher and scavenger float, to obtain the lepidolite pre-concentrate 1.
- ii. The pre-concentrate 1 underwent two cleaning stages, adjusting the pH only, to obtain a lepidolite concentrate of typically 4.5 wt.% Li_2O content at a recovery rate of 84%.
- iii. Any coarse particle size fraction $> 400\mu\text{m}$ was milled, for approximately 5 minutes the $53\mu\text{m}$ to $400\mu\text{m}$ fraction from this process was then processed via froth flotation to get lepidolite concentrate 2.

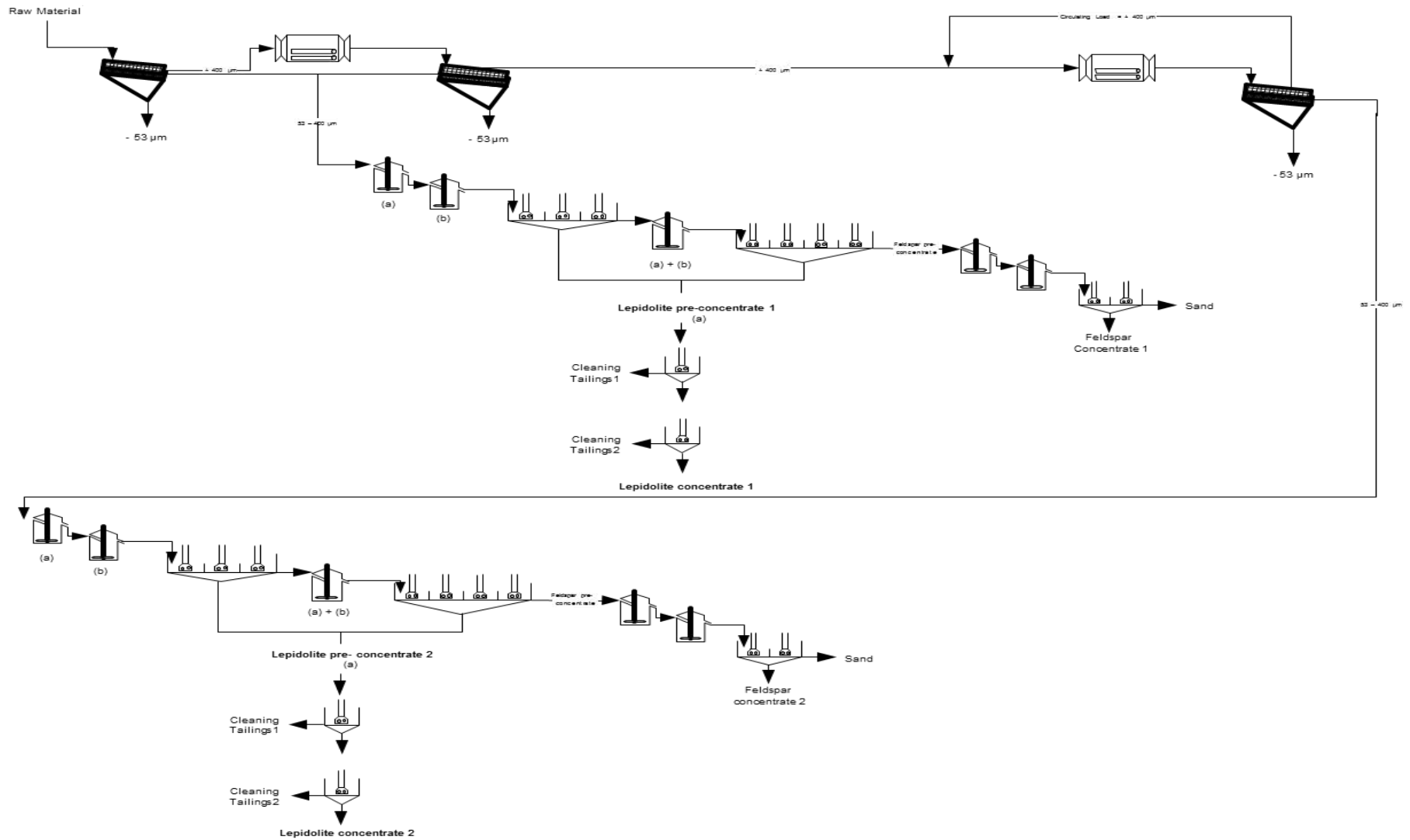


Figure 5: Process flow sheet for the Beauvoir waste material. (a) Addition of H_2SO_4 (b) addition of collector (Ancia, 2010).

The process can be separated into two stages; flotation 1 and flotation 2, both carried out at pH 1.5 using an amine acetate collector (Cataflot JCA 33, CECA, France). At pH 1.5 the lithium-bearing mineral lepidolite had a negative surface charge differentiating it from the impurities such as; muscovite and biotite mica, which were positively charged.

The study found that at a higher pH, the surface charge of the impurities also became negatively charged thus reducing the separation efficiency of the process, due to the increased reaction of H^+ ions with the particle surfaces. The first flotation stage in the study comprised of; wet sieving, milling and separating the lithium-bearing minerals using the particle size fraction of $53\mu m$ to $400\mu m$.

In Table 5:1 the parameters of the experimental variables along with the lithium concentrate grade and recovery rate can be seen. Flotation 1 concentrate contained 4.4 wt.% Li_2O and achieved a recovery rate of 63%. The recovery rate increased further by adding a milling stage for the particles greater than $400\mu m$ in order to liberate the locked lithium mica minerals, obtaining the particle size fraction $53\mu m$ to $400\mu m$. In flotation stage 2, Imerys were able to achieve 84% recovery with a lithium concentration of 4.5 wt.% Li_2O .

Table 5:1 Results from both of the froth flotation processes on Beauvoir kaolin waste (Ancia, 2010)..

	Flotation 1		Flotation 2	
	<i>Pre-concentrate</i>		<i>Pre-concentrate</i>	
	<i>1</i>	<i>Concentrate 1</i>	<i>2</i>	<i>Concentrate 2</i>
Experiment	<i>1</i>	<i>2</i>	<i>3</i>	<i>4</i>
Weight (%)	20.8	13.0	34.4	29.2
pH	1.5	1.7	1.5	1.7
Collector (g/t)	200	-	200	-
Li₂O grade (%)	3.3	4.4	4.2	4.5
Lithium recovery (%)	81	63	89	84

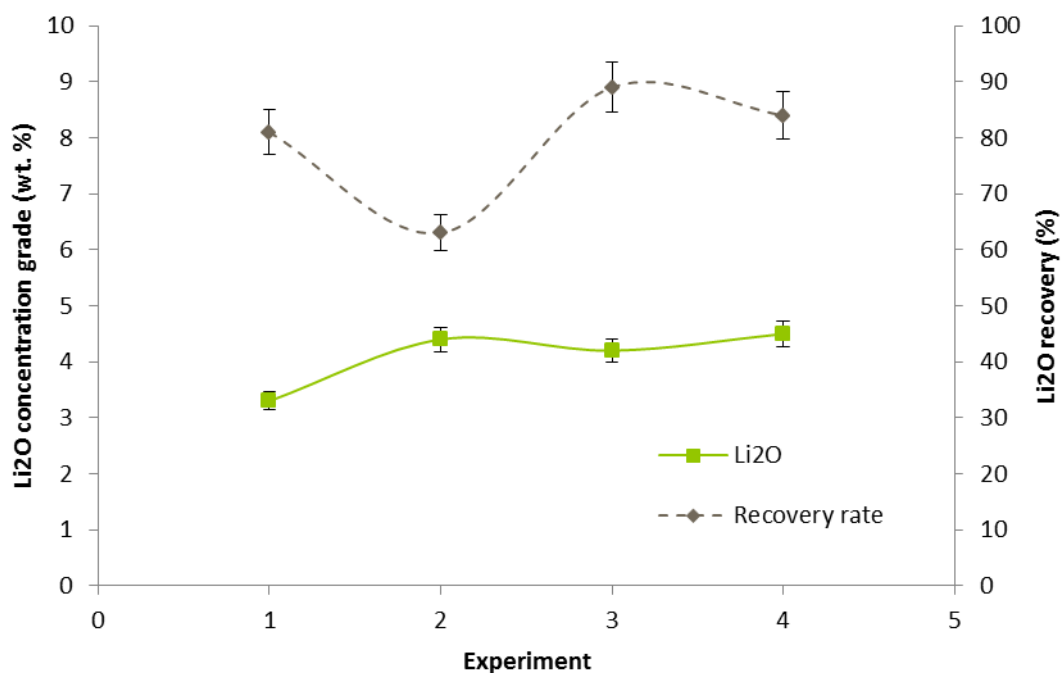


Figure 5:2 Li₂O concentrate grade and recovery for the Beauvoir waste material using froth flotation separation, experimental number is shown in Table 5:1.

5.2.2 Particle Size Distribution (PSD) of Beauvoir waste material

The Particle Size Distribution (PSD) of the raw material was analysed after classification. An image analyser (Quicpic, Sympatec GmbH Inc., Clausthal-Zellerfeld, Germany) and HELOS/BF (Sympatec) were used at the University of Birmingham to analyse the PSD. The results of this are shown in Figure 5:3, the efficiency of size separation was within the acceptable limits for this experiment.

The Particle Size Distribution for each percentile was: d_{10} , d_{50} and d_{90} was $59\mu\text{m}$, $171\mu\text{m}$ and $335\mu\text{m}$, respectively.

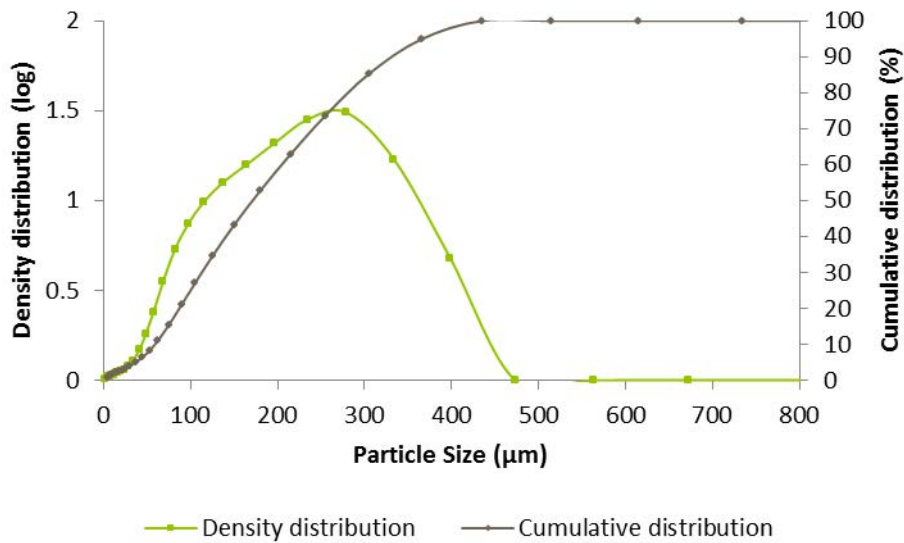


Figure 5:3 Particle Size Distribution of the Beauvoir waste material after classification into the size fraction of $53\mu\text{m}$ to $400\mu\text{m}$. Determined by laser-sizer.

5.2.3 Change of design of experiments

Following from the results obtained in the previous section, this study investigated the Beauvoir waste material (hydrocyclone underflow) in order to evaluate the effect of four variables; particle size fraction, pulp pH, collector and depressant dosages for the recovery of lithium-bearing minerals, see Table 5:2 for the experimental ranges investigated. The variables were investigated in order to ascertain the optimum efficiency levels for the process. The dosages of the reagents recommended by the manufacturer were between 100 to 500 grams per tonne (Cytec, 2002). The particle size fractions below 53 μm (containing 0.2 wt.% Li_2O) were discarded as they were of low lithium content and also increased entrainment, a non-selective process where small particles are suspended in the water present between the air bubbles thus are floated due to their size not their surface properties. Hence this would reduce the separation efficiency of the valuable material from the gangue (Konopacka, 2010; Siame, 2011) diluting the final lithium grade of the concentrate. Two particle size fractions of 53 μm to 250 μm and 250 μm to 400 μm were investigated. All of the flotation experiments were repeated for reliability. A process flowsheet can be seen in Figure 5:4 outlining the stages of the process.

Table 5:2 The variables used in the froth flotation separation of Beauvoir hydrocyclone underflow and their experimental ranges.

Variable	Minimum value	Maximum value
Particle Size fraction (μm)	53	400
pH	1.5	3.0
Collector (g/t)	70	400
Depressant (g/t)	0	500

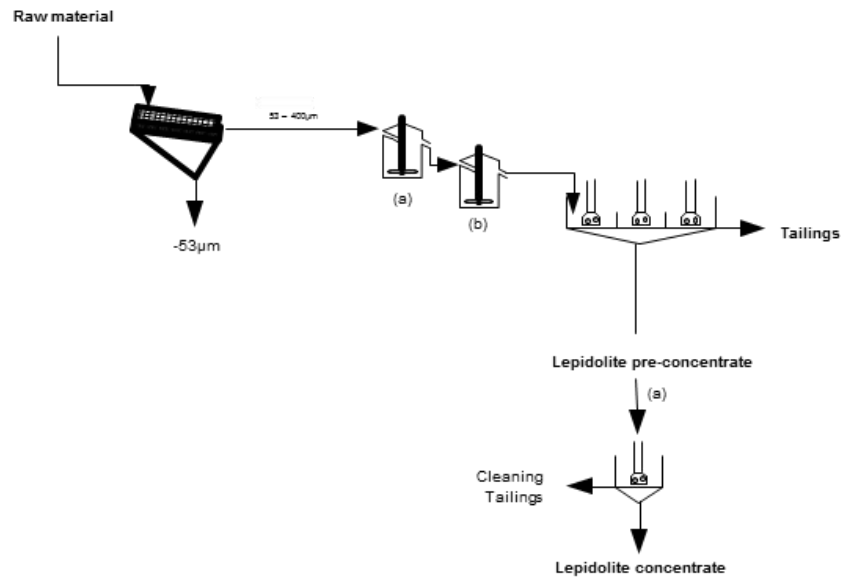


Figure 5.4. Process flowsheet for the Beauvoir waste material. (a) addition of H_2SO_4 (b) addition of collector and/or depressant (an additional conditioning period was added if depressant was used).

5.2.4 Margin of experimental errors

All of the experiments conducted were repeated at least twice, from which the standard deviation was calculated from the mean value. The error margins were calculated using Microsoft Excel 2010 software. The research concluded that the data points were given at 95% confidence levels, to the relative certainty of the error margins.

5.2.5 Experimental procedure

Froth flotation was investigated using the Beauvoir waste material (hydrocyclone underflow), containing 0.89 wt.% Li_2O . The flotation samples tested were up to 500g of material, particle size fraction of 53µm to 400µm, mixed with 2L of tap water in a Denver cell operated at an impeller speed of 1500 rpm to give a solids loading by weight of up to 20%. The pH was maintained using a dilute solution of H_2SO_4 of a

concentration of 5% w/w. A cationic collector (Aeromine 3030C, Cytec Industries Ltd, UK) and a depressant (Cyquest 40E, Cytec Industries Ltd, UK) were used in the study. A conditioning period of 5 minutes was applied after each reagent addition. The air valve was opened and the froth was collected for 5 minutes, the concentrate was re-floated with the addition of further H_2SO_4 to control the pH levels, producing the final lithium concentrate. The sample of the concentrate as well as the tailings were filtered, dried, weighed and then analysed for lithium by ICP-OES and for other metals by XRF.

5.2.6 Results and discussion

5.2.6.1 Preliminary data

Initial experiments were undertaken at pH 1.5, varying the collector and depressant dosages. In Figure 5:5 the results are shown when varying depressant and collector dosages between 0 to 250 g per tonne and 70 to 200 g per tonne, respectively. The most significant change observed was when the addition of a depressant was used, experiment 2 show an increase of lithium concentrate to 4.46 wt.% Li_2O , achieving a recovery rate of 88%. Previously without the depressant, only just over half of this recovery was achieved at a lower concentration of 2.2 wt.% Li_2O . Further increases to the amount of depressant dosage saw a smaller increase in the lithium concentration to 4.6 wt.% Li_2O , although a higher recovery rate of 94% was achieved. Experiment 4 investigated reducing the amount of collector to 70g/t, although the lithium concentration increased to 5.35 wt.%, the recovery was reduced to 79%. From this it can be concluded that as the collector dosage was reduced, less partially liberated lithium mica particles were floated, hence reducing the lithium recovery. From this study the

optimum results were found when using a combination of 80g/t depressant and 200g/t of collector recovering 88% with a lithium concentration of 4.46 wt.% Li_2O . As the economical grade of lithium of 4.0 wt.% Li_2O has been achieved, the lithium concentration has the potential to be extracted for lithium using further downstream processing (Amarante, 1999).

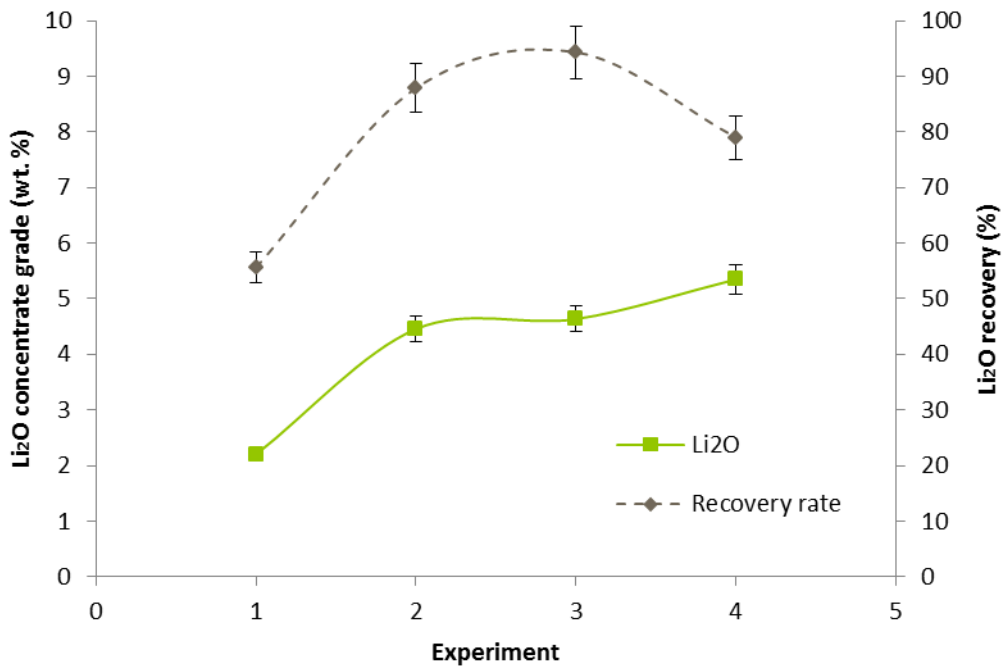


Figure 5:5 Froth flotation separation results for Beauvoir material, an average of two experiments was taken. The conditions of the experiments are given in table 5.3.

Table 5:3 Recovery of Li_2O grade as a function of pH 1.5 for the particle size fraction of 53 μm to 400 μm .

Experiment	1	2	3	4
pH	1.5	1.5	1.5	1.5
Depressant (g/t)	0	80	250	250
Collector (g/t)	200	200	200	70
Li_2O grade (wt.%)	2.20	4.46	4.64	5.35
Li_2O recovery (%)	56	88	94	79

5.2.6.2 Chemical analysis of Beauvoir lithium concentrate

The X-ray fluorescence (XRF) analysis of the Beauvoir lithium concentrate can be seen in Table 5:4. The waste material was taken from a kaolin production plant, thus through hydrolysis alteration of the aluminosilicates, high contents of SiO₂, Al₂O₃ and K₂O were observed. The oxides were present between 12 to 59 % in the material, when analysed in the particle size distribution of 53µm to 400µm. The reaction equations below represent the chemical reactions with feldspar forming kaolinite (Lanzi, 2008).

➤ *Orthoclase + water → kaolinite + quartz + potassium oxide*



➤ *Albite + water → kaolinite + quartz + sodium oxide*



Table 5:4 XRF analysis of Beauvoir lithium concentrates for experiments 1 to 4, *tested by ICP.

Metal oxide (%)	Experiment			
	1	2	3	4
SiO ₂	59.0	55.3	52.3	50.4
Al ₂ O ₃	22.3	21.1	22.1	23.4
K ₂ O	12.0	12.3	12.0	12.5
Rb ₂ O	1.3	2.6	3.7	3.8
Fe ₂ O ₃	1.4	1.5	1.9	1.9
TiO ₂	0.0	0.0	0.2	0.1
Li ₂ O*	2.2	4.46	4.64	5.35
SUM	98.2	97.3	96.8	97.5

The Beauvoir lithium concentrates (4.1 wt.% Li_2O) was also found to contain a high content of Rb_2O and Fe_2O_3 , as shown in Figure 5:6, the concentrations varied between 1.3 to 3.8 %. The optimum results, taking into consideration the operations costs, can be seen for experiment 2 where 80g/t of depressant and 200g/t of collector were used. The results for experiment 2 were: 4.5 wt.% Li_2O , 2.6 wt.% Rb_2O and 1.5 wt.% Fe_2O_3 at recoveries of 88%, 71% and 26%, respectively.

The study by Siame (2011) also found a positive correlation for Rb_2O and Fe_2O_3 in the flotation concentrates. Siame analysed the lithium mica zinnwaldite, a variant of lepidolite, which was reported to contain lower lithium content compared to lepidolite (Garrett, 2004). The material investigated was found in the St Austell area (hydrocyclone underflow) which was owned by Goonvean Ltd at the time of the study. Siame (2011) reported to concentrate up to 1.5% Li_2O and 0.6% Rb_2O and 4.5% Fe_2O_3 in the recoveries of 99%, 85% and 93%, respectively. The higher iron content found was mainly due to the mineral; zinnwaldite ($\text{KLiFeAl}(\text{AlSi}_3\text{O}_{10}(\text{F},\text{OH})_2)$), which was not found in the Beauvoir material, hence the operations produce a higher quality of kaolin. Siame (2011) estimated that low iron contents in kaolin waste material could be due to the quartz and feldspar minerals.

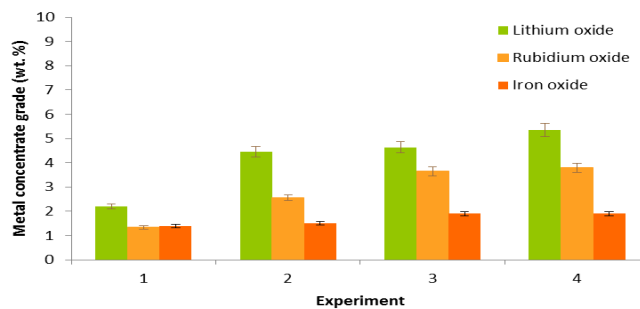


Figure 5:6 Metal concentrations detected in the Beauvoir lithium concentrates, average of two experiments.

Table 5:5 Recovery of metal oxides grade as a function of pH 1.5 for the particle size fraction of 53µm to 400µm.

Metal oxide (%)	1	2	3	4
Li ₂ O grade	2.20	4.46	4.64	5.35
Li ₂ O recovery	56	88	94	79
Rb ₂ O grade	1.3	2.6	3.7	3.8
Rb ₂ O recovery	38	71	70	59
Fe ₂ O ₃ grade	1.4	1.5	1.9	1.9
Fe ₂ O ₃ recovery	27	26	43	46

Rubidium can be seen as a value added product in the process, it has been a by-product of lithium chemicals productions and commercially available for around 40 years (USGS, 2013; Thompson, 2011). The uses of rubidium are increasing, with the main use in atomic clocks for global positioning satellites. Other uses include: glass manufacturing, magneto-optic modulators, phosphors and lasers (Jandová and Vu, 2013; Wagner,). An estimate of the world demand for rubidium was about 2 to 4 tonnes per annum (Thompson, 2011; Wagner, 2006). Jaskula (2013) reported that a 3.5% increase was observed in 2012 from 2011, due to increases in lithium exploration creating rubidium as a by-product it can be expected that the commercial applications for rubidium will expand.

Previously Imerys analysed the Beauvoir granite in the quarry, at different grades, prior to flotation or any other process separation the particles sizes were taken for the whole range. The analysis was carried out in the laboratories in Beauvoir ceramic centre. In Figure 5:7 a graph showing the correlation between Li₂O and Rb₂O can be seen. A positive correlation of 0.9 was found between the two oxides, at approximately 1.0 wt% Li₂O, 0.4 wt% Rb₂O was found, this can be seen in Figure 5:7.

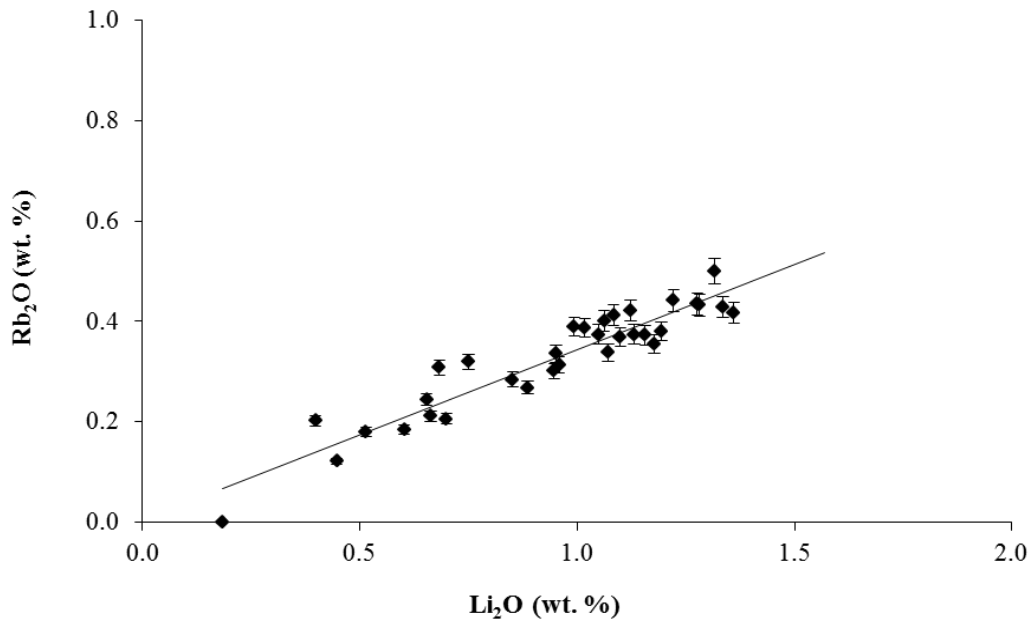


Figure 5:7 Metal oxide correlations for the Beauvoir granite (Ancia, 2010).

Furthermore a complete analysis of the Beauvoir granite data can be seen in Table 5.6. The particle size range from, less than 53 μ m to greater than 2000 μ m, was analysed for its' metal oxides, Li₂O, Rb₂O and Fe₂O₃. The samples were analysed prior to hydrocyclone separation. Higher Li₂O concentrations were found between particle size ranges from 315 to 2000 μ m, >1.0 wt.%.

Table 5:6 Average of metal oxide results for the Beauvoir granite data obtained from Imerys.

PSD (μm)	Li₂O (wt.%)	Rb₂O (wt.%)	Fe₂O₃ (wt.%)
> 2000	0.00	0.29	0.16
1000 - 2000	1.07	0.29	0.19
800 - 1000	1.25	0.17	0.21
500 - 800	1.33	0.27	0.22
315 - 500	1.15	0.37	0.20
53 - 315	0.71	0.23	0.16
< 53	0.49	0.10	0.31
Raw material	1.06	0.35	0.20

5.2.6.3 The effect of pH and particle size distribution on the recovery process

Further experiments were investigated changing the pulp pH between 1.5 and 3.0. By using a higher pH, lower quantities of the acid were required, thus when considering a scale up of the process it would be more advantageous to use higher pH as the process would be considered to be more economically efficient. The pH was maintained by the addition of dilute sulphuric acid, an acid system is preferred as it can produce greater froth levels thus potentially increasing the recovery rate of the flotation (Miller, 2002).

Two particle size fractions were investigated 250 μ m to 400 μ m and 53 μ m to 250 μ m, as shown in Figure 5:8 and Figure 5:9, respectively. The figures show lithium concentrations and recovery rates for varies pH when using 200g/t of collector and 80g/t of depressant. Figure 5:8 shows a positive correlation between the lithium concentration and recovery when increasing the pH. In Figure 5:9 a negative trend can be observed when increasing the pH value from 1.5 to 3.0 the lithium concentrations decrease from 4.8 to 2.6 wt.% Li₂O whereas the recovery rates for remain fairly consistent between 70 to 80%. This trend agrees with the findings by Ancia (2010), which suggested that the decrease in the lithium concentration was due to an increased number of impurities present in the final concentrate as fine particles can cause entrainment, transporting unwanted particles trapped between these bubbles into the froth layer (Forsberg, 1988).

From these results it can be concluded that the particle size distribution can have a significant impact on the optimal condition for froth flotation separation. In Table 5:7 it can be seen that for coarser particle size fraction higher lithium grades and recoveries were achieved at the pH values of pH 2.5 and 3.0, whereas for the finer particle size

fraction optimum results were found at a lower pH of 1.5, 4.8 wt.% of Li_2O and 70% recovery.

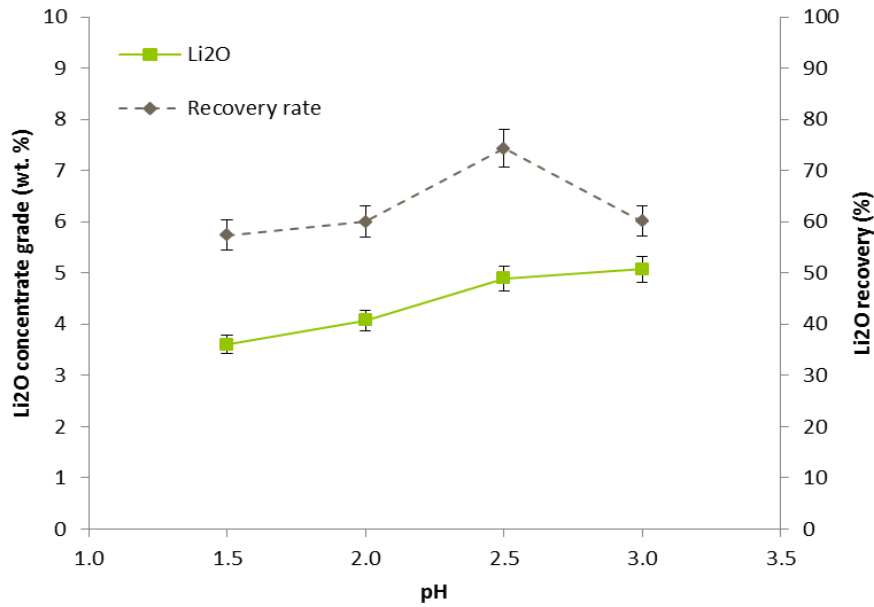


Figure 5:8 Recovery of Li_2O a different pulp acidity using froth flotation as a function of 200g/t collector, 80g/t depressant for the particle size fraction of 250µm to 400µm.

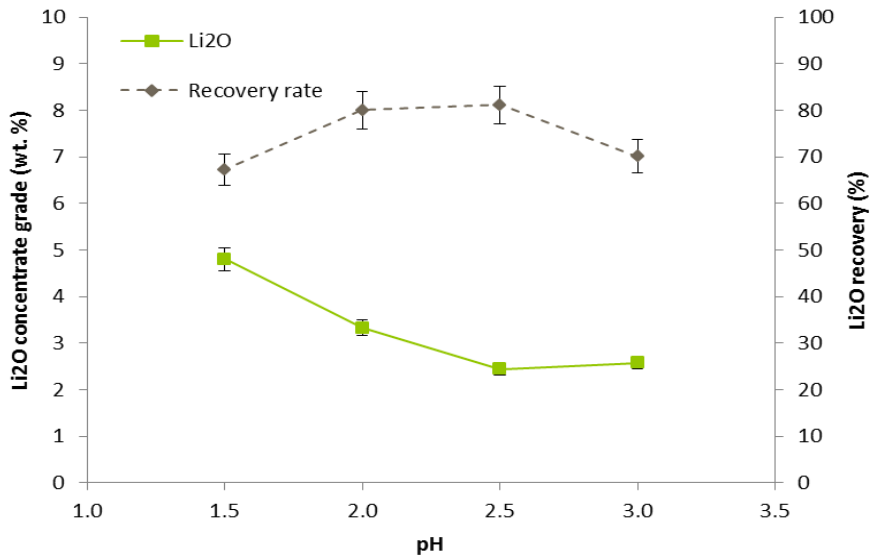


Figure 5:9 Recovery of Li_2O at different pulp acidity using froth flotation as a function of 200g/t collector, 80g/t depressant for the particle size fraction of 53µm to 250µm.

Table 5:7 Comparison of the recovery for Li₂O using froth flotation as a function of 200g/t collector, 80g/t depressant.

PSD	53 μm - 250 μm		250 μm - 400μm	
Li ₂ O	Grade (wt.%)	Recovery (%)	Grade (wt.%)	Recovery (%)
pH	1.5	4.8	70	57
	2.0	3.3	81	60
	2.5	2.5	20	74
	3.0	2.6	67	60

5.2.6.4 The effect of depressant dosage on flotation performance

5.2.6.4.1 Particle size 250μm to 400μm Beauvoir underflow

A depressant (Cyquest 40E, Cytec Industries, UK) was added to increase flotation selectivity, as the depressant was added before the collector it acted as a system modifier allowing the collector to selectively interact with the desired mineral, in this case lepidolite. Thus the addition of a depressant should increase the lithium concentration grade of the Beauvoir concentrate.

In Figure 5:10 the effect of the depressant can be seen, dosages varying between 0 to 250 g/t for pH 1.5 to 3.0 and collector dosage of 200 g/t. The lithium concentrations showed similar results when comparing the different experimental pulp pH values. Without the addition of a depressant, on average 1.6 wt.% Li₂O was detected in the final lithium flotation concentrate, when 80g/t of depressant was added a significant increase of an average of 4.41 wt.% Li₂O was observed. Further increases to the depressant dosages at 250 g/t showed a smaller change in the lithium concentration, for pH 1.5 and

2.0 the lithium concentrations increased to 4.1 and 4.7 wt.% Li₂O, respectively, whereas for pH 2.5 and 3.0 we observed decrease to, 3.9 and 4.3 wt.% Li₂O, respectively. The decrease could be explained by the depressant interacting with the lepidolite which in effect acted as a barrier between the collector and the mineral (Miller, 2007).

In Figure 5:11 the Li₂O recovery can be seen as a function of 200g/t collector, varying depressant dosages and pH levels for the coarser particle size fraction. The highest recovery obtained was for pH 2.5 at about 76%, 74% and 72% for depressant dosages of 0, 80 and 250 g/t. From Figure 5:11 it can be seen that the recoveries did not show significant changes over the pH range tested. From this study pH 2.5 was found to be the optimal condition for recovery of lithium at 80g/t depressant dosage and 200g/t collector; achieved 4.9 wt.% Li₂O and a recover of 74%. Although pH 3.0 achieved high lithium concentrations of 5.1 wt.% Li₂O, the lithium recovery showed that as the pH was increased the quantity of the minerals being floated was decreased achieving only 60% lithium recovery.

Table 5:8 Comparisons of the recovery for Li₂O using froth flotation as a function of 200g/t collector for the PSD 250µm to 400µm.

Li₂O	Grade (wt.%)			Recovery (%)		
	<i>0g/t</i>	<i>80g/t</i>	<i>250g/t</i>	<i>0g/t</i>	<i>80g/t</i>	<i>250g/t</i>
Depressant						
<i>1.5</i>	1.4	3.6	4.1	62	57	63
<i>2.0</i>	1.7	4.1	4.7	68	60	59
pH						
<i>2.5</i>	3.1	4.9	3.9	76	74	72
<i>3.0</i>	1.7	5.1	4.3	70	60	64

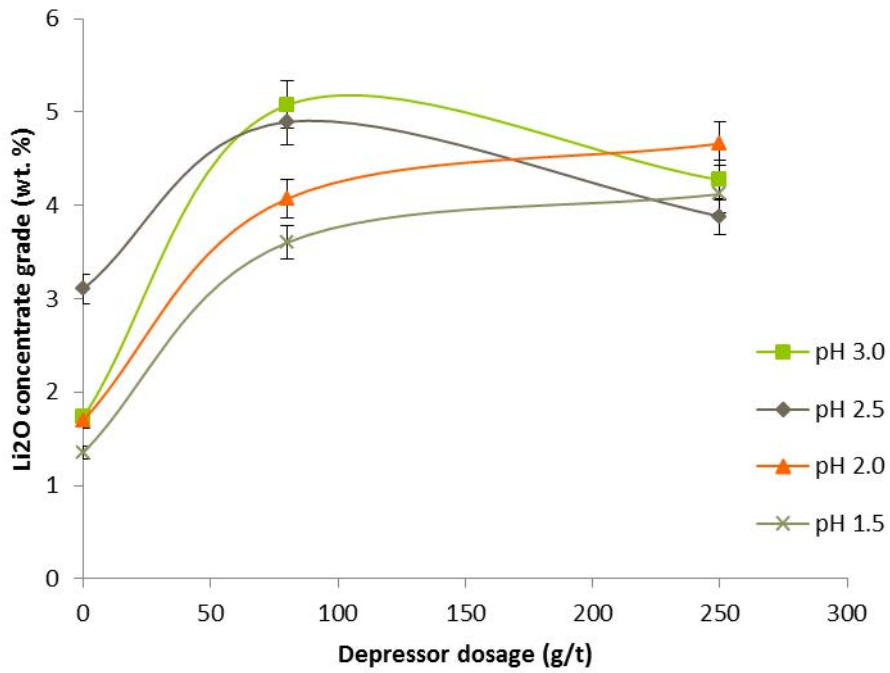


Figure 5:10 Concentrate grade of Li₂O at different pulp acidity using froth flotation as a function of 200g/t collector, varying depressant dosages and pH levels for the particle size fraction of 250µm to 400µm.

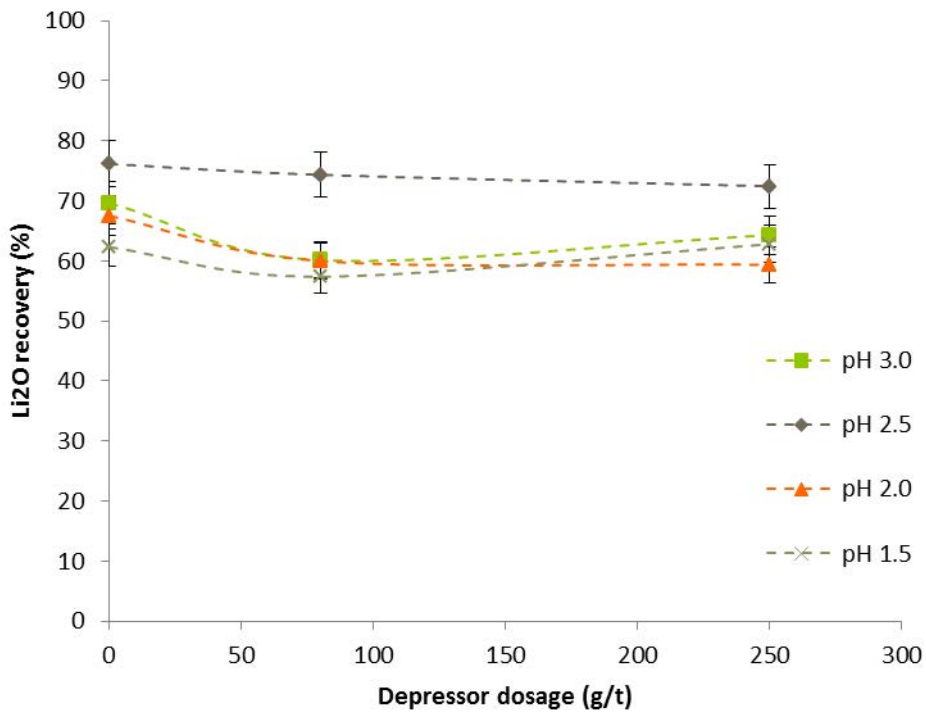


Figure 5:11 Recovery of Li₂O using froth flotation at different pulp acidity as a function of 200g/t collector, varying depressant dosages and pH levels for the particle size fraction of 250µm to 400µm.

5.2.6.4.2 Froth flotation of particle size 53 μ m to 250 μ m Beauvoir underflow

In Figure 5:12 and Figure 5:13 the lithium concentrate grade and recovery results for Beauvoir can be seen for varying pH levels and depressant dosages for the finer particle size fraction investigated. Without the addition of depressant, lithium concentration grades between 1.0 to 3.0 wt.% Li₂O with high lithium recoveries between 74% and 93% were observed. The addition of a depressant (80g/t) had a significant effect on the lithium concentrate grade for different pulp pH values, an increase was observed for all of the pulp pH values. The pulp pH values of 2.0 and 2.5 showed optimum efficiencies when considering the lithium concentrations (2.5 to 3.3 wt.% Li₂O) as well as the recoveries obtained (>80%).

Further experiments investigated higher dosages of depressant addition (250g/t), showing an increased for pulp pH values between 2.0 to 3.0 of up to 5.0 wt.% Li₂O with recoveries up to 95%. Although the pulp pH value of 1.5 showed a preference for the lower depressant dosage of 80g/t achieving a high lithium concentration of 4.8 wt.% Li₂O but a lower lithium recovery of 67%. The optimum conditions, when considering economical viable processes, were at pH 2.5, achieving 4.8 wt.% Li₂O with a relatively high recovery of 81%.

Table 5:9 Comparisons of the recovery for Li₂O using froth flotation as a function of 200g/t collector for the PSD 53µm to 250µm.

Li ₂ O	Grade (wt.%)			Recovery (%)			
	0g/t	80g/t	250g/t	0g/t	80g/t	250g/t	
pH	1.5	2.9	4.8	4.3	74	67	76
	2.0	1.8	3.3	5.0	96	80	76
	2.5	1.2	2.5	3.1	94	81	84
	3.0	0.9	2.6	4.8	97	70	78

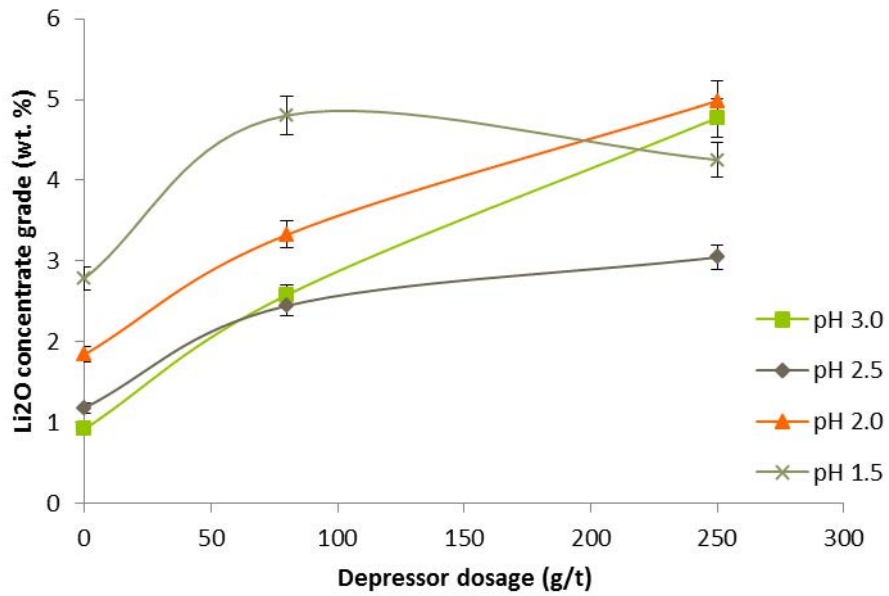


Figure 5:12 Concentrate grade of Li₂O using froth flotation at different pulp acidity as a function of 200g/t collector, varying depressant dosages and pulp pH levels for the PSD of 53µm to 250µm.

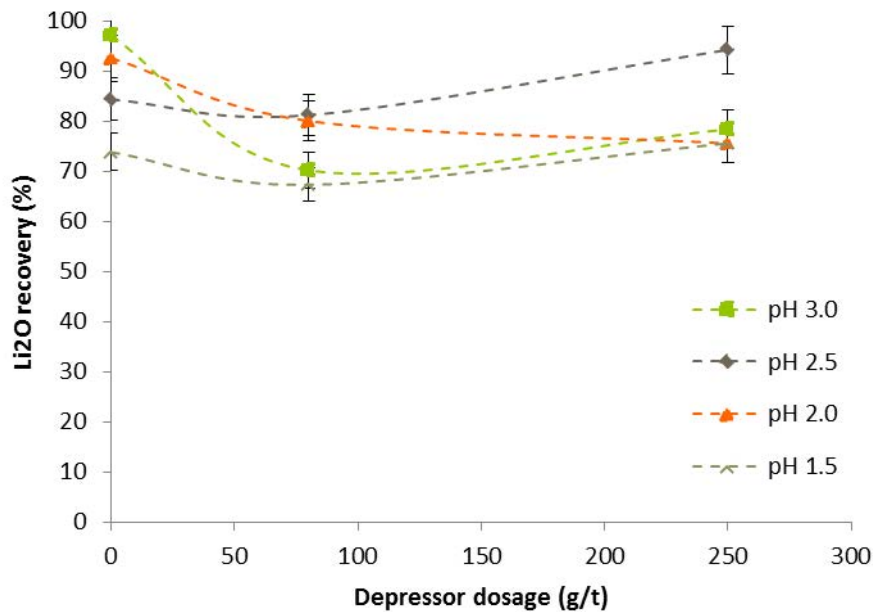


Figure 5:13 Recovery of Li₂O using froth flotation at different pulp acidity as a function of 200g/t collector, varying depressant dosages and pulp pH levels for the particle size fraction of 53µm to 250µm.

5.2.6.5 Effect of collector dosage on flotation efficiency for Beauvoir underflow

5.2.6.5.1 Froth flotation of particle size 250µm to 400µm

The effect of varying the dosage of cationic collector (Aeromine 3030C, Cytec Industries, UK) was investigated in dosages varying from 80 to 200g/t as recommended by the manufacturer. Collectors are chemicals that can adsorb onto particle surfaces enhancing the chances of binding to air bubbles making the particles hydrophobic. The hydrophobic particles formed a froth layer which was collected as the lithium concentrate.

In Figure 5:14 and Figure 5:15 the lithium recoveries for the coarser particle size fraction of 250µm to 400µm can be seen. The results for the pulp pH investigated for

1.5 and 2.5 showed a small decrease of 1.0 wt.% Li₂O, as the amount of collector dosage was increased from 80 to 200g/t. Although for pH 3.0, an increase in lithium concentrate grade was observed when increasing the collector dosage, from 2.9 to 4.3 wt.% Li₂O. At lower pH values there was reduced selectivity when increasing the collector dosage, this was possibly due to the fact that at lower pH levels the pulp will have a higher amount of H⁺ ions present in the solution. Thus, when overdosing with collector, undesired negatively charged particles are also attracted to the free H⁺ ions. Hence higher lithium recoveries were observed for all of the pulp pH values as shown in Figure 5:15.

Table 5:10 Comparisons of the recovery for Li₂O using froth flotation as a function of 250g/t depressant for the PSD 250µm to 500µm.

Li₂O	Grade (wt.%)		Recovery (%)		
	<i>70g/t</i>	<i>200g/t</i>	<i>70g/t</i>	<i>200g/t</i>	
Collector					
	<i>1.5</i>	<i>5.2</i>	<i>4.1</i>	<i>30</i>	<i>63</i>
	<i>2.0</i>	<i>4.6</i>	<i>4.7</i>	<i>48</i>	<i>59</i>
pH	<i>2.5</i>	<i>5.4</i>	<i>3.9</i>	<i>28</i>	<i>72</i>
	<i>3.0</i>	<i>2.9</i>	<i>4.3</i>	<i>34</i>	<i>64</i>

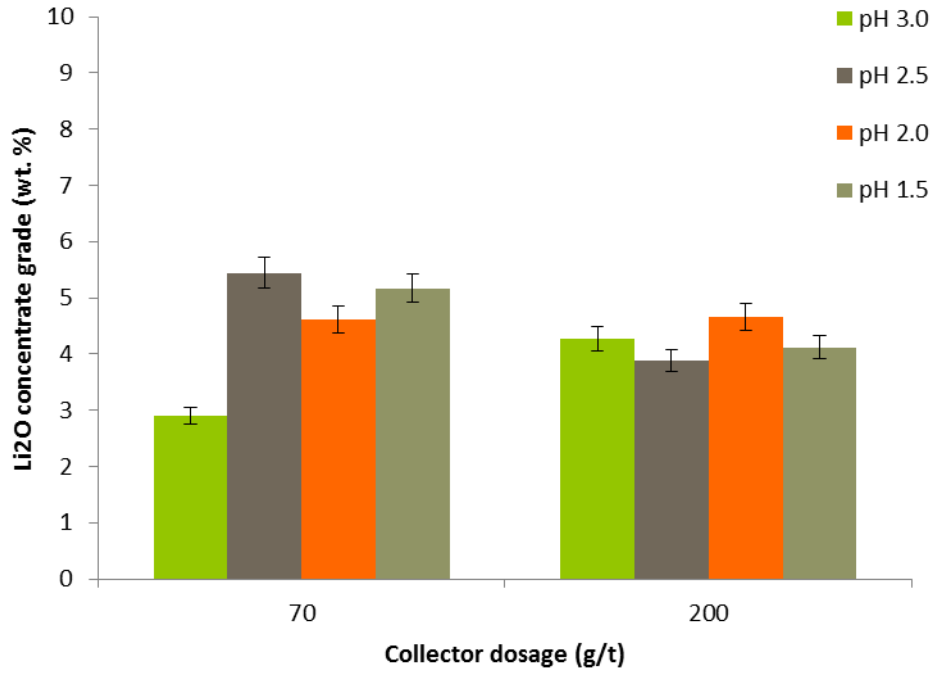


Figure 5:14 Lithium concentrate grade of Li_2O at different pulp acidity using froth flotation as a function of 250g/t depressant, varying collector dosages and pH levels for the particle size fraction of 250 μm to 400 μm .

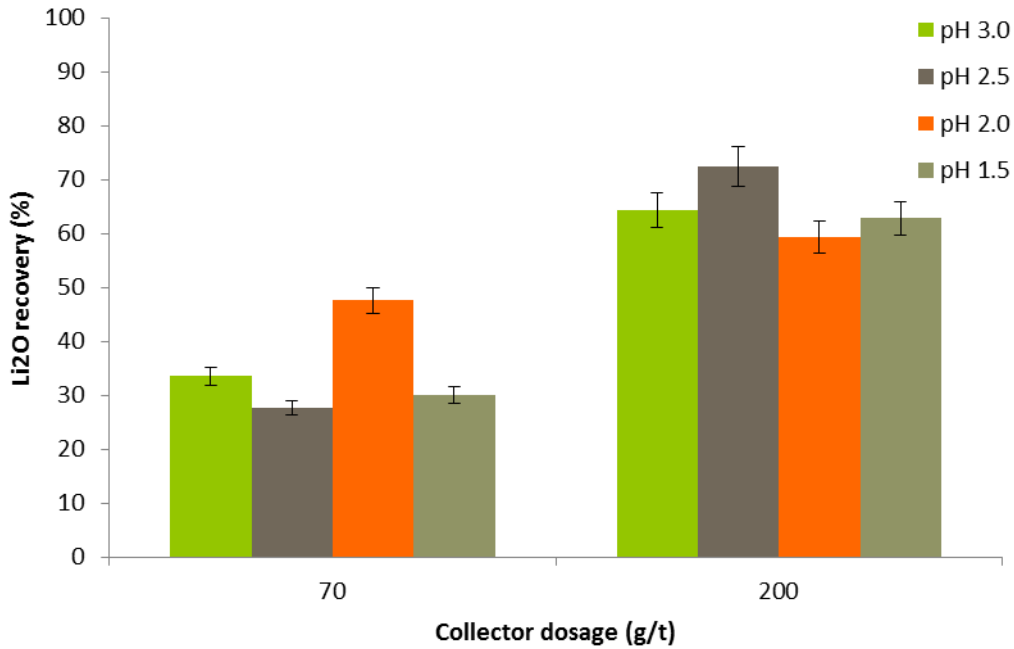


Figure 5:15 Recovery of Li_2O using froth flotation at different pulp acidity as a function of 250g/t depressant, varying collector dosages and pH levels for the particle size fraction of 250 μm to 400 μm .

5.2.6.5.2 Froth flotation of particle size 53µm to 250µm

In Figure 5:16 and Figure 5:17 the lithium concentrate grades and recoveries can be seen for the finer particle size fraction 53µm to 250µm. Optimum results are at pH 1.5, which 6.0 wt.% Li₂O achieved at a collector dosage of 70g/t with a 74% recovery. Although by increasing the pH to 2.0, a lower lithium concentration of 4.9 wt.% Li₂O is observed with a recovery of 74%, which would be more economically efficient.

Table 5:11 Comparisons of the recovery for Li₂O using froth flotation as a function of 250g/t depressant for the PSD 53µm to 250µm.

Li₂O	Grade (wt.%)		Recovery (%)		
	<i>70g/t</i>	<i>200g/t</i>	<i>70g/t</i>	<i>200g/t</i>	
Collector					
	<i>1.5</i>	6.0	4.3	74	76
	<i>2.0</i>	4.9	5.0	72	76
pH	<i>2.5</i>	1.0	3.1	73	84
	<i>3.0</i>	4.2	4.8	41	78

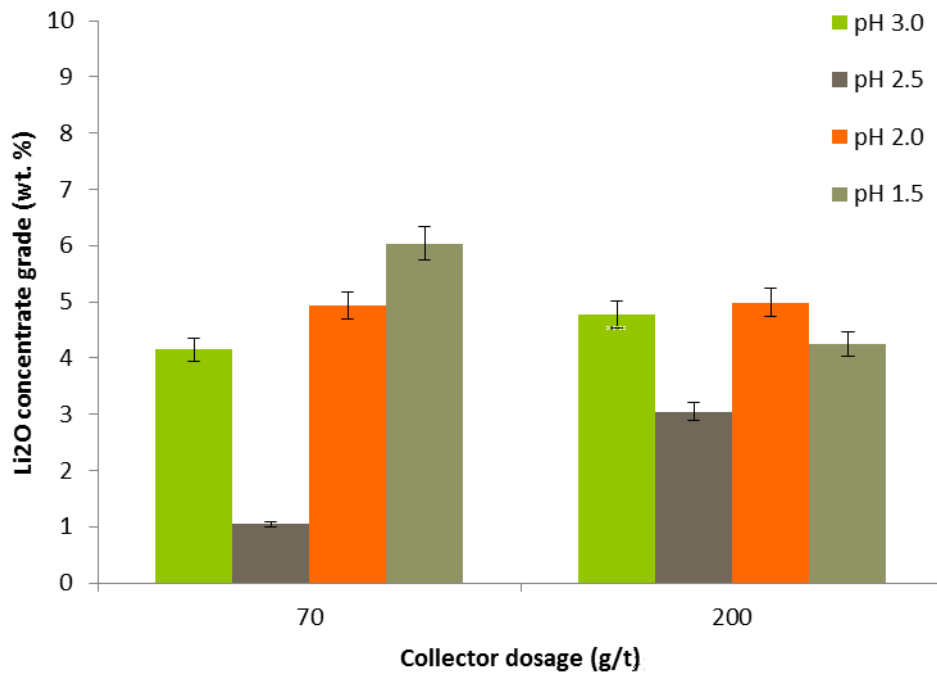


Figure 5:16 Recovery of Li_2O as a function of 250g/t depressant, varying collector dosages and pulp pH levels for the particle size fraction of 53 μm to 250 μm .

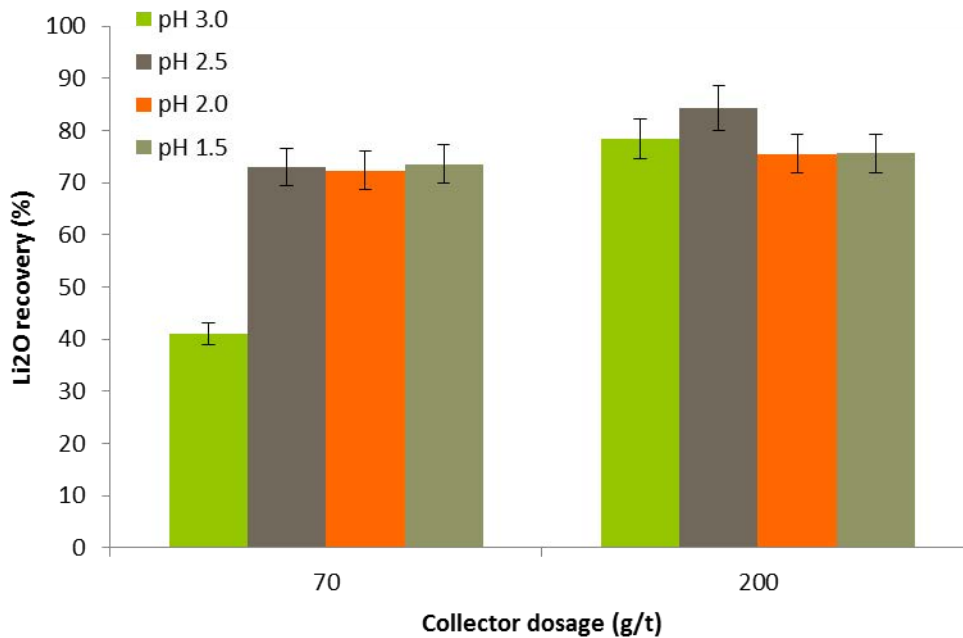


Figure 5:17 Recovery of Li_2O as a function of 250g/t depressant, varying collector dosages and pulp pH levels for the particle size fraction of 53 μm to 250 μm .

5.2.7 Conclusion of Beauvoir material

A froth flotation test programme showed that flotation concentrates containing over 4.0 wt.% Li_2O can be recovered from the hydrocyclone underflow for the Beauvoir deposits. The recoveries were selective dependent on the processing conditions used, the main difference was observed when investigating finer and coarser particle size fractions of $53\mu\text{m}$ to $250\mu\text{m}$ and $250\mu\text{m}$ to $400\mu\text{m}$, respectively. The conditioning parameters for the flotation were 80g/t of depressant and 200g/t collector. For the finer particle size fractions, a higher lithium concentrate grade was found at the lower pulp pH of 1.5, 4.8 wt.% Li_2O and a 70% recovery. In comparison the coarser particle size fraction achieved higher lithium recovery at pH 2.5, 4.9 wt.% Li_2O and a 74% recovery. Using a coarser particle size fraction and higher pH value has many advantages from an economical perspective; as lower reagents quantities would be used thus making the process more cost efficient.

The X-ray fluorescence results for the Beauvoir lithium concentrate identified Rb_2O as a by-product of lithium recovery. This could be a value added product could offer an extra income for Imerys. For a flotation concentrate using the particle size fraction of $53\mu\text{m}$ to $400\mu\text{m}$, pH 1.5, 80g/t depressant and 200g/t collector, the following oxides were recovered 4.5% Li_2O , 2.6% Rb_2O and 1.5% Fe_2O_3 in the recoveries 88%, 71% and 26%, respectively.

5.3 Froth Flotation Separation of Kaolin Waste Material from St Austell in the UK

5.3.1 Introduction

For the UK, the lithium potential of the St Austell Granite was suggested to be 3.3 million tonnes of recoverable lithium within the upper 100 m region of an 8 km² recognised area (Hawkes, 1987). According to Imerys the following sites were identified to contain lithium mica granite:

- New Sink Grade 5, (*New Sink G5*)
- New Sink Grade 4, (*New Sink G4*)
- Stope 13 Grade 4, (*Stope 13 G4*)
- Blackpool Grade 4, (*Blackpool G4*)

The materials were graded from one to five based on the malleability and coarseness of the sample ore, with grade 5 as the most malleable. The mineralogical proportions of the samples estimated approximately 6% of mica present in the samples (Hooper, 2012). The mica consisted of the lithium-bearing mineral zinnwaldite ($\text{KLiFeAl}(\text{AlSi}_3)\text{O}_{10}(\text{F},\text{OH})_2$) and muscovite ($\text{KA}_3\text{Si}_3\text{O}_{10}(\text{OH})_{1.8}\text{F}_{0.2}$). Zinnwaldite was identified in the lithium mica granite by lithological mapping carried out from 1985 to the year 2012 (Manning, 1996; Hooper, 2012). It is a variant of lepidolite, $\text{KLi}_2\text{Al}(\text{Si}_4\text{O}_{10})(\text{OH},\text{F})$, with a high iron content and can contain up to a theoretical value of 5.0 wt.% Li_2O (Siame, 2011). In order to separate the lithium mica minerals,

froth flotation separation was investigated along with high intensity magnetic separation and electrostatic separation.

5.3.2 Experimental procedure

The flotation test samples used were up to 500g of material, on two particle size fraction of 53 μ m to 250 μ m and 250 μ m to 500 μ m. The sample was mixed with 2L of tap water and impeller speed of 1500 rpm to give solids by weight of up to 20%. The pulp pH was maintained using a dilute solution of H₂SO₄ of a concentration of 5% w/w. A cationic collector (Aeromine 3030C, Cytec Industries Ltd, UK) and a depressant (Cyquest 40E, Cytec Industries Ltd, UK) were used in the study. A conditioning period of 5 minutes was applied after each addition. The air valve was opened and the froth was collected for 5 minutes, the concentrate was re-floated except only with the addition of H₂SO₄ to control the pulp pH levels, producing the final lithium concentrate. The sample of the concentrate as well as the tailings were filtered, dried, weighed and then analysed for lithium by ICP-OES and for other metals by XRF.

5.3.3 Results and discussion

5.3.3.1 Lithium potential of the kaolin mining waste material

The St Austell kaolin waste samples supplied by Imerys were investigated for their lithium mica extraction potential, ICP analysis was carried out on varying particle size fractions up to 1.7mm, shown in Figure 4:12. The greatest lithium potential (although still very low in comparison to Beauvoir) was observed in the two samples; New Sink

Grade 5 and Blackpool Grade 4 of up to 0.08 wt.% Li_2O and 0.07 wt.% Li_2O , respectively.

For the New Sink Grade 5 sample the highest lithium concentrations were found within the particle size fractions 53 μm to 250 μm and 250 μm to 500 μm , containing 0.07 and 0.06 wt.% Li_2O , respectively. A significant difference was observed in the lithium content for the New Sink Grade 5 and Grade 4 samples. It was suggested that as the Grade 4 material was not fully kaolinised, therefore it was less malleable and had some degree of friability (Hooper, 2012). The difference in grades suggested that the separation of the lithium-bearing minerals in the New Sink Grade 5 sample would achieve better recovery efficiency for the liberated minerals from the gangue, thus have the potential to be upgraded further. For particles sizes less than 53 μm , very low lithium concentrations of approximately 0.02 wt.% Li_2O were observed. As fine particles cause entrainment and subsequently decrease the recovery efficiency using froth flotation separation, particles less than 53 μm were discarded. (Kawatra, 2011). It was found that all the St Austell kaolin wastes supplied by Imerys were much lower in Li_2O concentration grades (0.08 wt.% Li_2O) than that of the Beauvoir material (0.89 wt.% Li_2O). The relatively low levels of lithium concentrations in the St Austell samples (0.08 wt.% Li_2O) were suggested to be due to alteration effects such as the replacement of zinnwaldite by either tourmaline or alterations to muscovite. Hooper (2012) confirmed that there was some evidence of tourmalisation occurring within all of the samples, except for in Stope 13.

The Beauvoir waste material containing 0.89 wt.% Li_2O had undergone several mineral liberation stages, (crushing and classification) in order to produce the hydrocyclone underflow. Thus the process allowed the lithium-bearing mineral to be liberated more efficiently via froth flotation due to the valuable mineral grains being released.

It was interesting to observe that the Blackpool Grade 4 material also achieved higher lithium concentrates of up to 0.08 wt.% Li_2O for the particle size fraction 53 μm to 250 μm . In Table 5:12 the approximate mineral proportions of the samples can be seen. It shows that approximately 5% of feldspar was present suggesting that the Blackpool Grade 4 was nearly fully kaolinised, thus it is classified as high decomposition grade 4 (Hooper, 2012). There was also some evidence of tourmalisation in the sample, approximately 3%, which could reduce the flotation efficiency as tourmaline has been suggested to alter the zinnwaldite mineral over time (Manning, 1996).

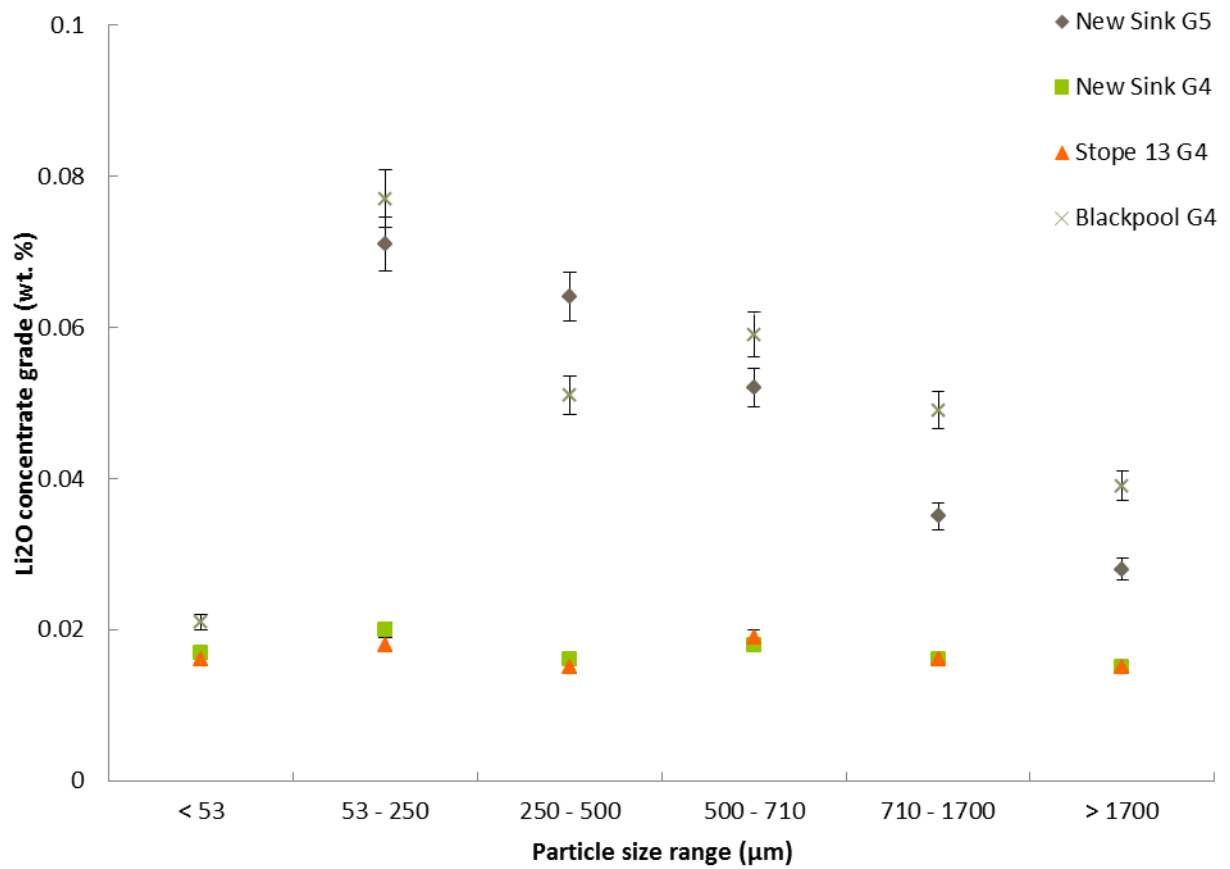


Figure 5:18 Li₂O concentrate grades in varying particle size fraction for the St Austell kaolin mining waste materials used in this study.

Table 5:12 Mineral proportions of St Austell geological samples (Hooper, 2012).

Mineral (%)	Geological Samples in St Austell			
	<i>New Sink G5</i>	<i>New Sink G4</i>	<i>Stope 13 G4</i>	<i>Blackpool G4</i>
Feldspar	0	5	10	5
Quartz	44	40	38	42
Mica (Zinnwaldite and Muscovite)	6	6	6	6
Tourmaline	5	3	6	3
Kaolinite	45	42	40	40

5.3.3.2 Particle Size Distribution (PSD) of New Sink G5

The PSD for the New Sink G5 sample can be seen in Figure 4:9, for 53 μm to 250 μm and 250 μm to 500 μm . The graphs show that a good separation was achieved when wet sieving the samples, d_{50} for the finer PSD of 53 μm to 250 μm was 108 μm and for the coarser PSD of 250 μm to 500 μm the d_{50} was 261 μm .

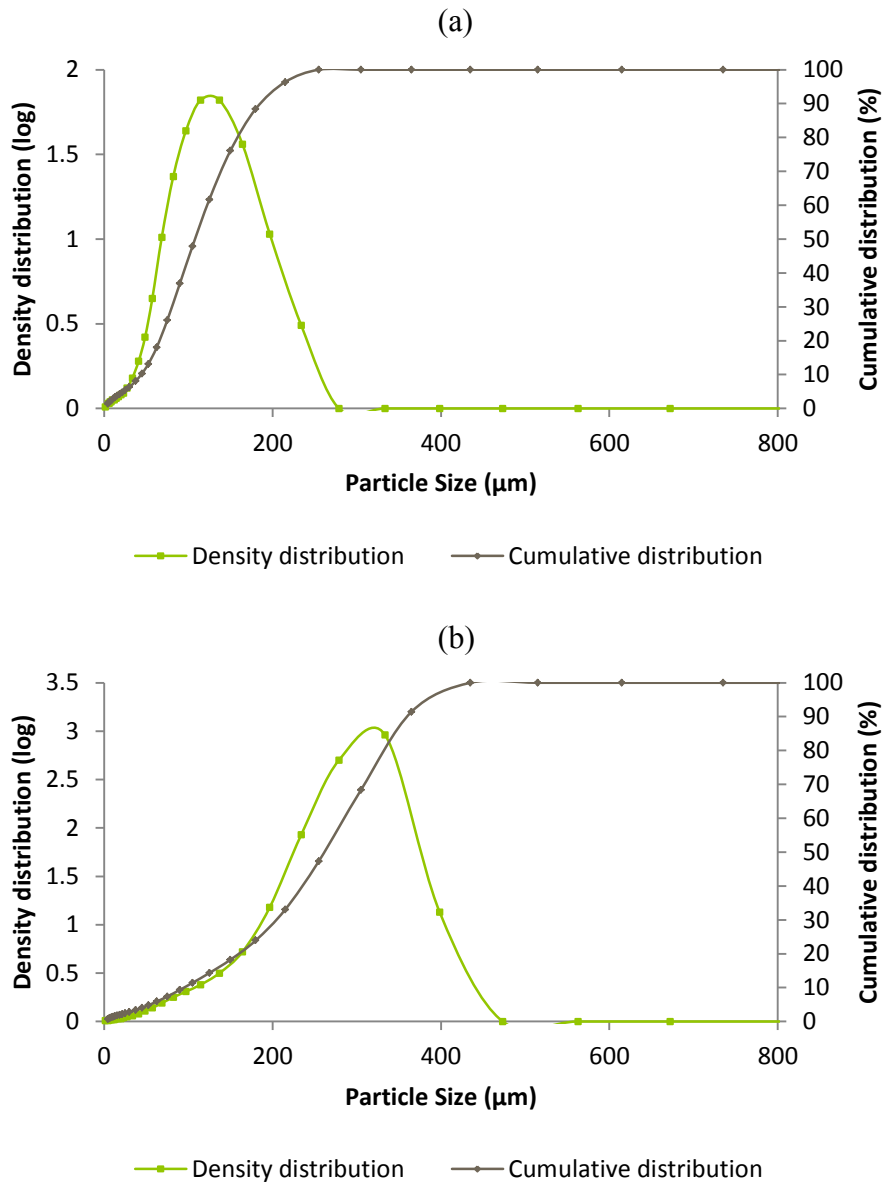


Figure 5:19 PSD of New Sink G5 material after classification into size fractions (a) 53 μm to 250 μm and (b) 250 μm to 500 μm , determined by laser-sizer.

5.3.3.3 Recovery of lithium from the New Sink G5 material

5.3.3.3.1 Chemical composition of the New Sink G5 material

The chemical composition for the New Sink Grade 5 sample can be seen in Table 5:13, for the particle size range between 53 μ m to 500 μ m. A high amount of iron was observed in the sample, 3.81% Fe₂O₃. The presence of iron could be due to either of the minerals; zinnwaldite or tourmaline, found within the sample (Hooper, 2012). XRD analysis was performed on the St. Austell New Sink G5 sample; it showed large peak intensity for kaolinite in the feed sample. The mica minerals; muscovite and biotite were also found along with tourmaline in the feed sample grades.

Table 5:13 Chemical composition for New Sink G5, particle size fraction 53 μ m to 500 μ m.

Chemical composition	Weight (%)
SiO ₂	82.00
Al ₂ O ₃	8.29
K ₂ O	4.00
Fe ₂ O ₃	3.81
TiO ₂	0.52
Rb ₂ O	0.14
Li ₂ O	0.09
SUM	98.85

5.3.3.3.2 The effect of varying the particle size fraction on the recovery of lithium-bearing minerals for the New Sink G5

The effects on lithium recovery efficiency using the two particle size fractions; 53µm to 250µm and 250µm to 500µm can be seen in Figure 5:20. All of the experiments were repeated for reliability. The finer particle size fraction was able to recover a higher lithium concentrate grades after froth flotation separation, achieving 0.5 wt.% Li₂O and a recovery of 90%, whereas for the coarser fraction it was much smaller, 0.2 wt.% Li₂O and a lithium recovery of 53%. This could be explained by the more liberated structure of the mineral allowing for a more efficient recovery. In Table 5:14 and Table 5:15 the chemical analysis for the two particle size fractions (53-250µm and 250-500µm) can be seen. It shows that the lithium grade was higher for the finer particle size fraction, 0.47 wt.% Li₂O with a higher recovery of 90%.

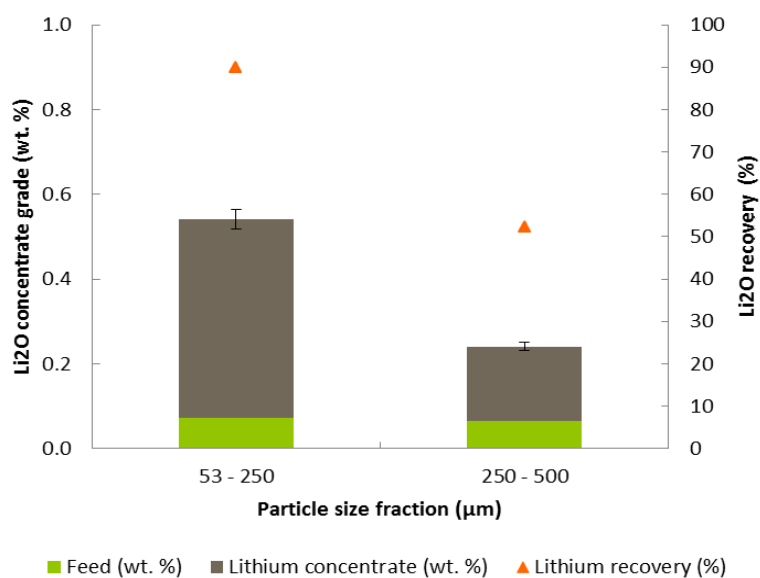


Figure 5:20 Recovery/ grade of Li₂O using froth flotation at different particle size distributions as a function of 200g/t collector, 250g/t depressant at pH 1.5.

Table 5:14 Metal oxides using froth flotation separation for the particle size distribution 53µm to 250µm.

PSD (µm)	Grade (wt.%)			Recovery (%)		
	Li ₂ O	Rb ₂ O	Fe ₂ O ₃	Li ₂ O	Rb ₂ O	Fe ₂ O ₃
53 - 250	0.47	0.5	12.9	90	94	90
250 - 500	0.2	0.4	10.6	52	90	89

In Table 5:15 the chemical analysis of the New Sink G5 feed material along with the flotation concentrates, for the PSD between 53µm to 500µm. As expected the SiO₂ content has significantly decreased in the lithium concentrates reducing by around 50%. An increase in the Li₂O, Rb₂O and Fe₂O₃ was observed for both of the particle size fractions. Using the finer PSD the metal oxide recovered were 0.47 % Li₂O, 0.5% Rb₂O and 12.9% Fe₂O₃ with the recoveries 90%, 94% and 90% respectively.

Table 5:15 Chemical analysis of New Sink G5 concentrate and feed *tested by ICP

Metal oxide (%)	PSD 53- 500(µm)	PSD (53-250µm)		PSD (250-500µm)	
	Feed	Concentrate	Tailing	Concentrate	Tailing
SiO ₂	82.0	44.8	95.9	40.1	54.3
Al ₂ O ₃	8.29	24.3	1.1	20.8	21.8
K ₂ O	4.00	12.2	0.9	5.9	10.2
Rb ₂ O	-	0.5	-	0.4	0.4
Fe ₂ O ₃	3.81	12.9	0.6	10.6	9.5
TiO ₂	0.52	1.3	-	0.8	0.9
SO ₃	-	2.3	-	0.5	0.6
CaO	-	-	0.73	0.2	-
Li ₂ O*	0.09	0.47	0.01	0.18	0.02
SUM	98.9	98.7	99.3	97.7	98.0

Table 5:16 shows the mineralogical proportion for the lithium concentrate and the tailings. The results are shown for the flotation carried out at pH 1.5 for the particle size fraction 53µm to 250µm. It can be seen that a greater amount of mica was present within the lithium concentrate, 74%, a loss of 15% was found within the tailings. The tailings were mainly composed of the quartz mineral (75%).

Table 5:16 Mineral proportions of New Sink G5 sample after froth flotation separation at pH 1.5, depressant dosage 250g/t, collector dosage 200g/t for the particle size fraction 53µm to 250µm, *estimated, +form of tourmaline.

Mineral (%)	Geological Samples in St Austell (New Sink G5)	
	<i>Flotation concentrate</i>	<i>Tailings</i>
Kaolin	4	0
Mica	74	15
Quartz	12	75
Feldspar	3	4
Schorl ⁺	7*	6*

In Figure 5.21 and Figure 5.22, the X-ray diffraction pattern can be seen for the lithium concentrate recovered during froth flotation as well as tailings, for the particle size fraction of 53µm to 250µm. In Figure 5.21 the mica mineral zinnwaldite has been identified through characteristic peaks shown, such as a large peak at 27 degrees with an intensity of 890 degrees. Other smaller peaks at 9, 18, 23, 25, 34, 39, 56, 62 degrees were representative of the mica mineral (Jandova, 2009). In both figures the peaks at 21, 27, 37 and 50 degrees were due to the quartz mineral, the estimated minerals proportions were 12% and 75% for the concentrate and tailings, respectively. The intensities of the peaks at 27 degrees reflect the proportion of quartz in the sample, the intensity for the tailings is 4900.

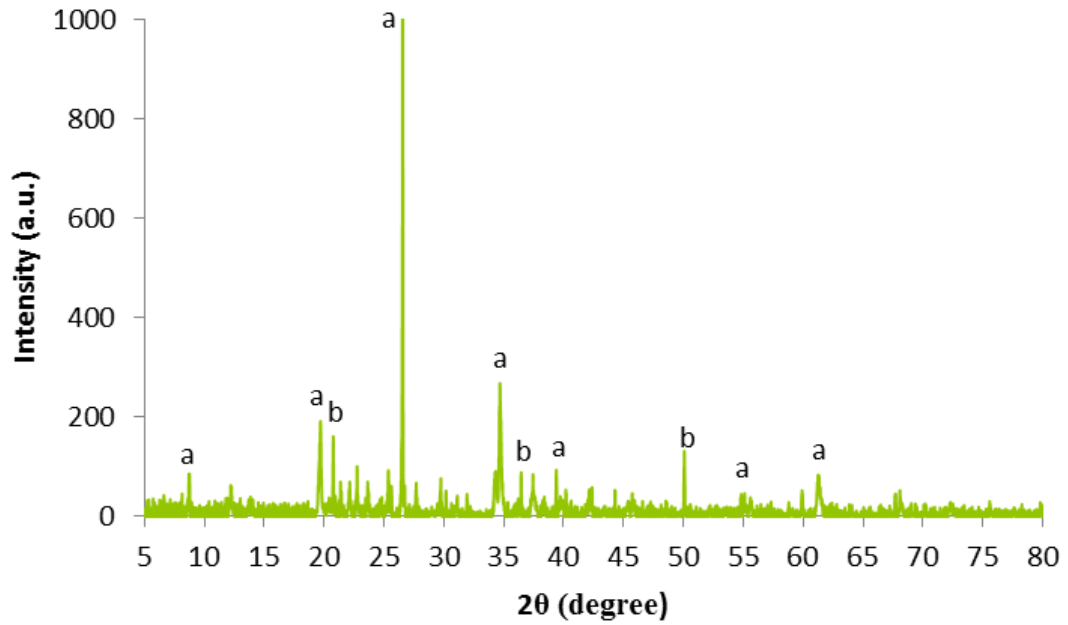


Figure 5:21 XRD pattern of the lithium concentrate for the PSD between 53 μ m to 250 μ m, (a) zinnwaldite, (b) quartz.

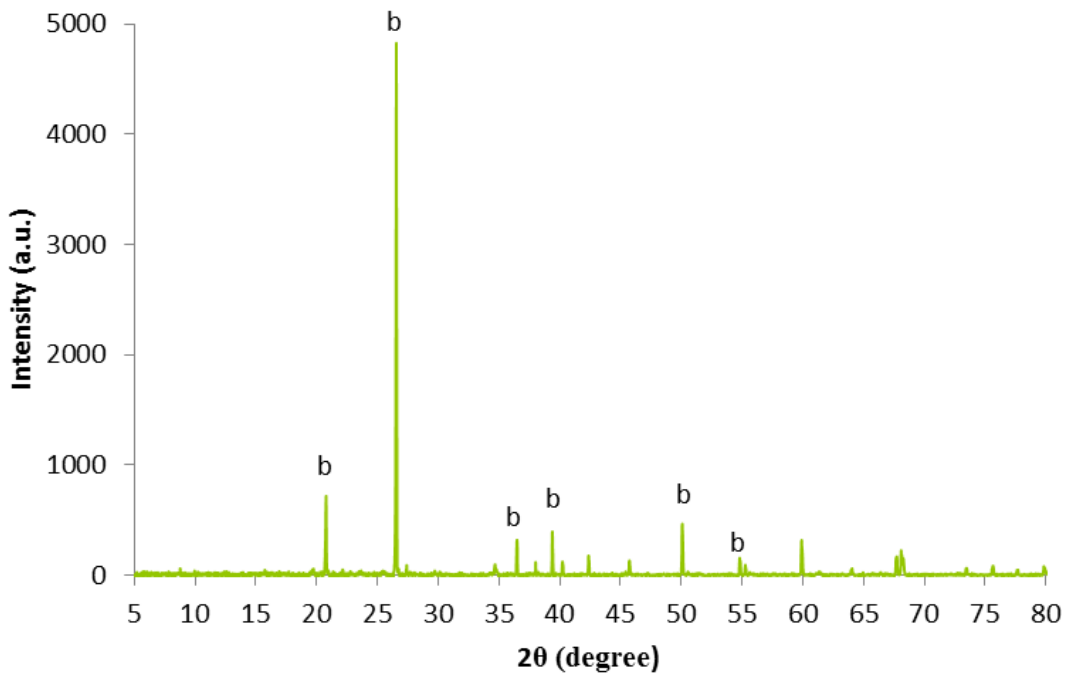


Figure 5:22 XRD pattern of the tailings for the PSD between 53 μ m to 250 μ m, (b) quartz.

5.3.3.3.3 The effect of varying the pH on the recovery of lithium-bearing minerals from New Sink G5

The chemical analysis can be seen in Table 5:17 using froth flotation at different pulp acidity as a function of 200g/t collector and 250g/t depressant. In Figure 5:23 and Figure 5:24 the lithium recoveries can be seen for the particle size fractions of 53µm to 250µm and 250 to 500µm, respectively. The pulp pH values were investigated between pH 1.4 to 2.0, as a higher pH value will result in an overall cost reduction in operating the process due to the lower content of acid required. Although in Figure 5:23 the optimum pulp pH value was found at pH 1.5, achieving 90% recovery and lithium concentration of 0.5 wt.%.The same results were observed for the coarser particle fraction as shown in Figure 5:24.

Table 5:17 Chemical analysis using froth flotation at different pulp acidity as a function of 200g/t collector and 250g/t depressant.

PSD (µm)	pH	Grade (%)			Recovery (%)		
		Li ₂ O	Rb ₂ O	Fe ₂ O ₃	Li ₂ O	Rb ₂ O	Fe ₂ O ₃
250-500	1.4	0.14	0.5	10.6	54	99	76
	1.5	0.47	0.5	12.9	90	94	97
	1.7	0.08	0.4	10.3	87	99	99
	2.0	0.11	0.4	8.9	40	99	64
53-250	1.4	0.18	0.4	10.6	89	95	80
	1.5	0.52	0.5	10.5	90	86	79
	1.7	0.15	0.3	6.01	36	99	30

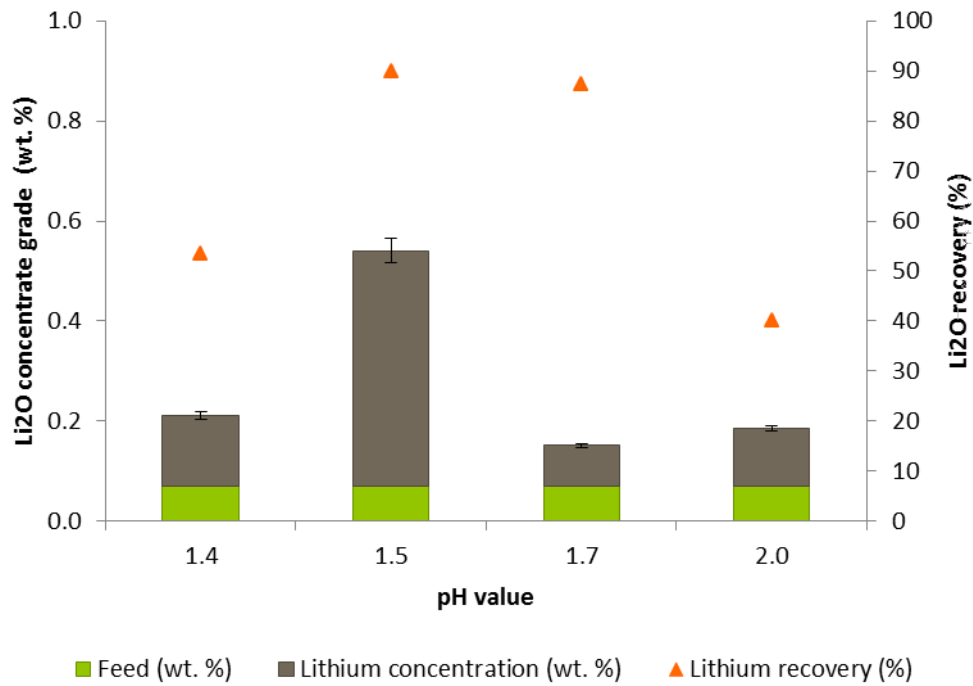


Figure 5:23 Recovery of Li₂O from New Sink G5 at different pulp acidity as a function of 200g/t collector, 250g/t depressant and particle size fraction of 53µm to 250µm.

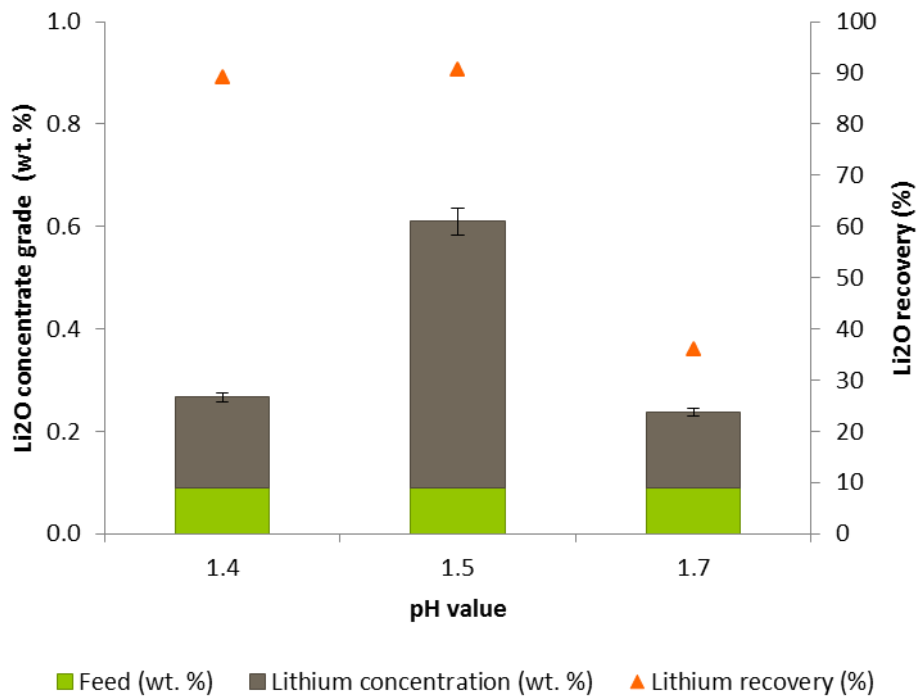


Figure 5:24 Recovery of Li₂O from New Sink G5 at different pulp acidity as a function of 200g/t collector, 250g/t depressant and particle size fraction of 250µm to 500µm.

5.3.3.3.4 The effect of varying the depressant dosages on the recovery of lithium-bearing minerals from New Sink G5

The effect of varying the depressant dosage for froth flotation separation can be seen in Figure 5:25. The effect of the addition of a depressant (Cyquest 40E, Cytec Industries, UK) can be seen when comparing depressant dosages of 0g/t and 250g/t, as an increase of 0.3 wt.% Li_2O was observed. The optimum concentration of depressant was found when using 250g/t of depressant to achieve 0.5 wt.% Li_2O and 90% recovery. Further addition of depressant of 500g/t saw a decrease in the lithium concentration of 0.3 wt.% Li_2O , as too high a concentration of depressant inhibits the collectors from attaching to the surface of the desired lithium-bearing minerals.

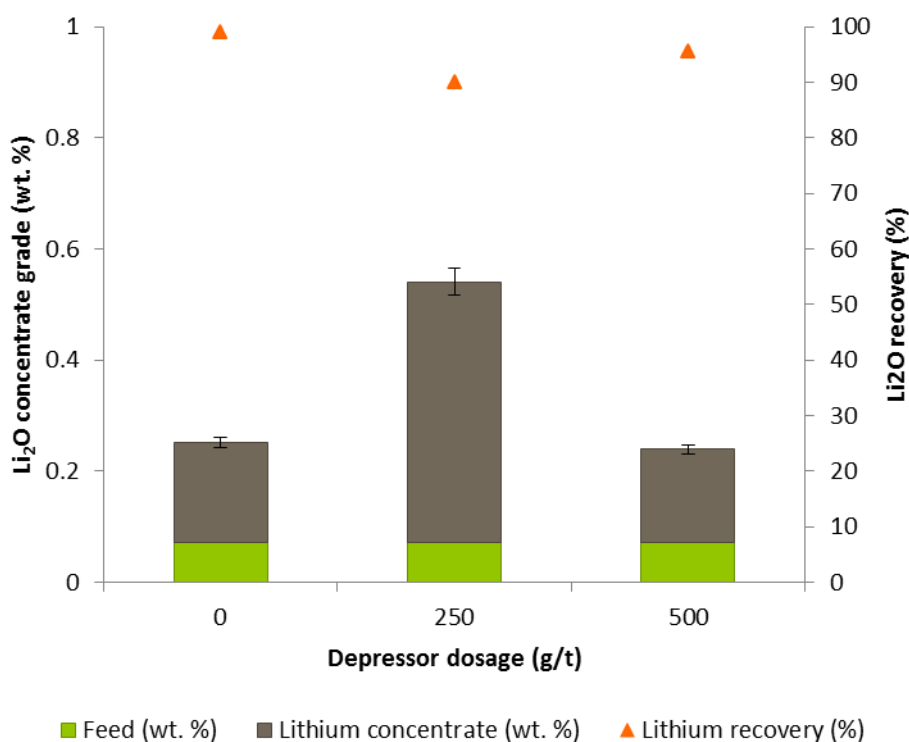


Figure 5:25 Recovery of Li_2O of New Sink G5 at different depressant dosage as a function of 200g/t collector at pH 1.5 for the particle size fraction of 53 μm to 250 μm .

Table 5:18 Chemical analysis using froth flotation at different depressant dosage as a function of 200g/t collector at pH 1.5 for the particle size fraction of 53 μ m to 250 μ m.

Depressant dosage (g/t)	Grade (%)			Recovery (%)		
	Li ₂ O	Rb ₂ O	Fe ₂ O ₃	Li ₂ O	Rb ₂ O	Fe ₂ O ₃
0	0.18	0.4	10.2	99	99	99
250	0.47	0.5	12.9	90	94	97
500	0.17	0.5	12.2	96	99	99

5.3.3.3.5 The effect of varying the collector dosages on the recovery of lithium-bearing minerals for New Sink G5

The effect of varying collector dosage levels, between 200g/t to 400g/t, on froth flotation performance can be seen in Figure 5:26. The separation was a function of 250g/t depressant, pH 1.5 and PSD of 53 μ m to 250 μ m.

A negative trend was found between the collector dosage and the lithium concentration, as when using 400g/t a Li₂O concentration grade of 0.25 wt.% was observed. This could be explained, as when over-saturating with collector the lithium content on the flotation concentrate can be reduced by reducing its overall selectivity of the separation process as well as increasing production costs of operating the process on a commercial scale. In Table 5:19 the chemical grades and recoveries can be seen for Li₂O, Rb₂O and Fe₂O₃. From the investigation optimum results were found when using 200g/t of collector, recovering 0.5 wt.% Li₂O, 0.5 % Rb₂O and 13 % Fe₂O₃.

Table 5:19 Chemical analysis using froth flotation at different collector dosage as a function of 250g/t depressant and pH 1.5 for the particle size fraction of 53µm to 250µm.

Collector dosage (g/t)	Grade (%)			Recovery (%)		
	Li ₂ O	Rb ₂ O	Fe ₂ O ₃	Li ₂ O	Rb ₂ O	Fe ₂ O ₃
200	0.47	0.5	12.9	90	94	97
400	0.25	0.5	13.9	93	92	92

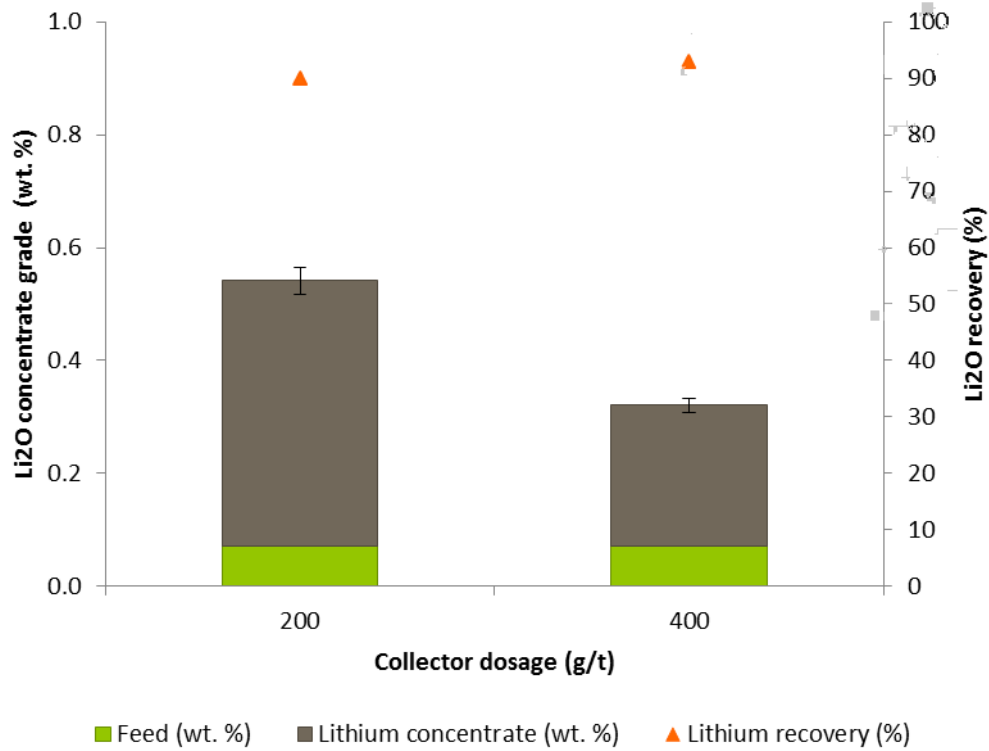


Figure 5:26 Recovery of Li₂O of New Sink G5 at different collector dosage as a function of 250g/t depressant and pulp pH 1.5 for the particle size fraction of 53µm to 250µm

5.3.3.4 Recovery of lithium from the New Sink G4 material

5.3.3.4.1 Chemical and mineralogical analysis of the New Sink G4 material

In Figure 5:27 the lithium grade for the New Sink G5 and G4 can be seen for the particle sizes in the range less than 53 μm to greater than 1700 μm . The lithium detected for the grade 4 sample was relatively low, averaging at 0.02 wt.% Li_2O , whereas for the grade 5 sample the up to 0.07 wt. Li_2O was observed.

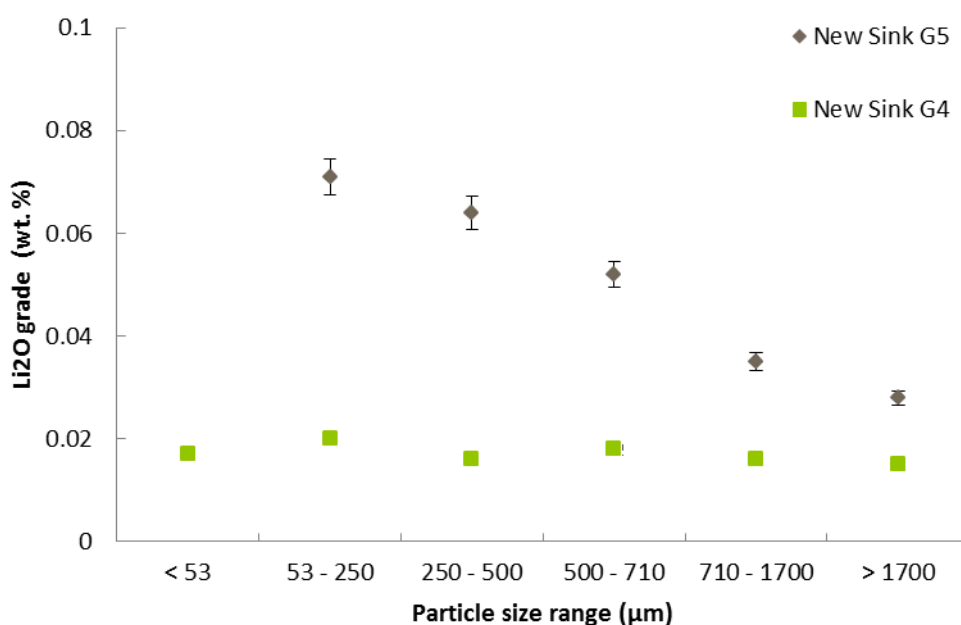


Figure 5:27 Li_2O grades in varying particle size fraction for the St Austell kaolin mining waste materials used in this study.

A comparison of the chemical analysis for the two grades (grade 5 and 4) can be seen in Table 5:20, for the particle size between 53 μm to 500 μm . It shows that a lower amount of Fe_2O_3 (0.1%) was detected for the grade 4 sample compared to 0.5% for grade 5. The presence of iron could be due to the minerals; zinnwaldite and tourmaline. In Table 5:21 the mineralogy of the grades is shown; the results confirm the low levels of tourmaline

present in the grade 4 sample (3%), as the mica mineral consisted of zinnwaldite and muscovite it was not possible to perceive a change in the zinnwaldite proportions. It can be suggested that a combination of low levels of Li_2O (0.02 wt.%) and Fe_2O_3 (0.1 wt.%) in the New Sink G4 sample indicate low levels of zinnwaldite. Also the mineral proportions for kaolinite were; 45% and 42% for the G5 and G4 sample, respectively. X-ray diffraction analysis showed smaller peak intensities for kaolinite when compared to New Sink G5, due to the lesser amount of weathering and kaolinisation experienced. Muscovite, biotite and tourmaline mineral were also found in the sample, which agreed with the results by Hooper (2012), who found approximately 6% mica and 3% tourmaline.

Table 5:20 Chemical analysis of New Sink G5 and G4 material (PSD 53 μm to 500 μm) *tested by ICP

Metal oxide	New Sink G5	New Sink G4
(%)		
SiO_2	82.0	80.8
Al_2O_3	8.3	11.7
K_2O	4.0	0.01
Rb_2O	3.8	0.2
Fe_2O_3	0.5	0.1
TiO_2	0.1	-
Li_2O^*	0.09	0.02
SUM	98.85	92.8

Table 5:21 Mineral proportions of New Sink samples (Hooper, 2012).

Mineral (%)	Geological Samples in St Austell	
	<i>New Sink G5</i>	<i>New Sink G4</i>
Feldspar	0	5
Quartz	44	40
Mica (Zinnwaldite & Muscovite)	6	6
Tourmaline	5	3
Kaolinite	45	42

5.3.3.4.2 The effect of varying the particle size fraction on the recovery of lithium-bearing minerals from New Sink G4

In this study many parameters such as pH, collector dosage and PSD were varied in order to obtain optimal floatation conditions. The effects on the level of lithium using the two particle size fractions; 53µm to 250µm and 250µm to 500µm can be seen in Figure 5:28. The finer particle size fraction was able to recover a slightly higher lithium concentration after froth flotation separation, achieving 0.2 wt.% Li₂O and 51% recovery, compared to the coarser fraction, 0.19 wt.% Li₂O and a lower recovery of 28%. The recoveries identified that the finer PSD (53µm to 250µm) yielded a greater lithium recovery of 51%; this is suggested to be due to the increased liberation of the minerals from the kaolin ore, hence it was easier to extract lithium from the expanded mineral structure.

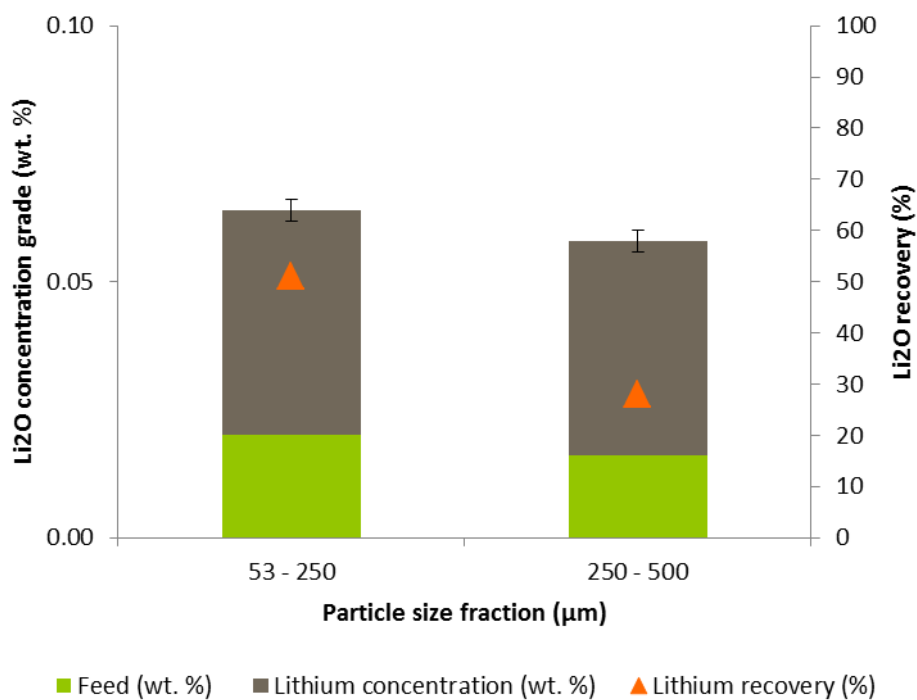


Figure 5:28 Recovery of Li_2O for New Sink G4 using froth flotation at different particle size distributions as a function of 200g/t collector, 500g/t depressant at pulp pH 1.5.

Table 5:22 Recovery of Li_2O for the New Sink G4 using froth flotation as a function of 200g/t collector, 500g/t depressant at pulp pH 1.5

PSD (μm)	Grade (%)			Recovery (%)		
	Li_2O	Rb_2O	Fe_2O_3	Li_2O	Rb_2O	Fe_2O_3
53 - 250	0.04	0.2	4.5	51	23	40
250 - 500	0.04	0.2	4.6	28	12	18

The chemical analysis shown in Table 5:23 can be seen for the PSD between 53μm to 500μm. From these results the PSD did not significantly affect the recovery as there is no significant difference observed. For the New Sink G4 material rubidium is also present in the lithium concentrate at concentration of approximately 0.2 %.

Table 5:23 Chemical analysis of New Sink G4 concentrate *tested by ICP

Metal oxide (%)	PSD (μm)	
	53-250	250-500
SiO ₂	56.5	55.9
Al ₂ O ₃	29.0	28.1
K ₂ O	6.43	6.84
Rb ₂ O	0.16	0.17
Fe ₂ O ₃	4.54	4.57
TiO ₂	0.44	0.42
MgO	0.86	0.91
CaO	0.57	0.64
Li ₂ O*	0.02	0.02
SUM	98.5	97.6

5.3.3.4.3 The effect of varying the pH on the recovery of lithium-bearing minerals from New Sink G4

In Figure 5:29 the recovery of Li₂O can be seen using froth flotation at pulp pH as a function of 200g/t collector, 250g/t depressant at pH between 1.4 to 2.3. The results show that less than 0.1 wt.% of lithium was recovered, with recoveries between 36 and 67%. Figure 5:25 shows the chemical composition for the pH 1.5 and 2.3 for the finer PSD (53 μm to 250 μm) which showed that Rb₂O and Fe₂O₃ were also observed in the flotation concentrates. For pH 1.5 the following metal oxides were detected; 0.02 wt.% Li₂O, 0.1% Rb₂O and 2.6% Fe₂O₃. For pH 2.3 slightly higher metal oxides for Li₂O and Fe₂O₃ were observed of 0.04 wt.% Li₂O, 3.2% Fe₂O₃ but Rb₂O remained at 0.1%.

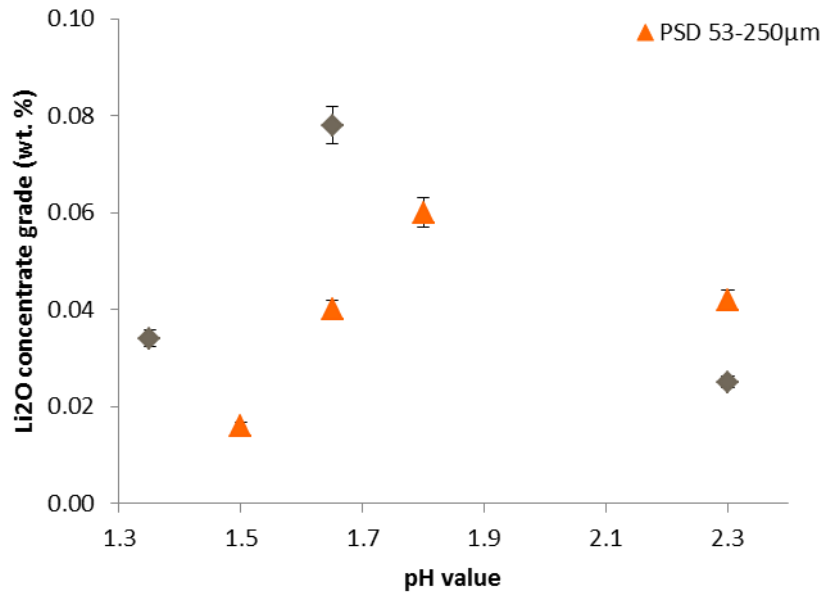


Figure 5:29 Recovery/ grade of Li₂O for New Sink G4 using froth flotation as a function of 200g/t collector, 250g/t depressant at pulp pH 1.4 - 2.3.

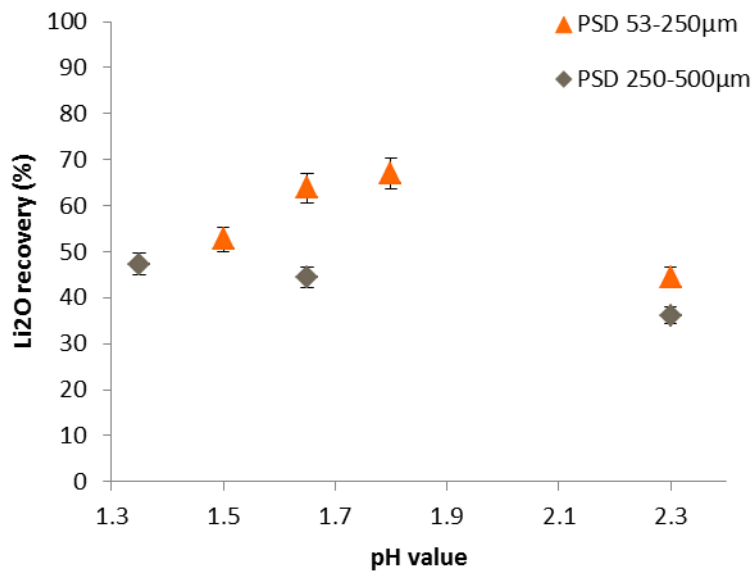


Figure 5:30 Recovery of Li₂O for New Sink G4 using froth flotation as a function of 200g/t collector, 250g/t depressant at pulp pH 1.4 - 2.3.

Table 5:24 Chemical analysis of New Sink G4 lithium concentrate for PSD 53-250 μ m *tested by ICP

Metal oxide (%)	pH value	
	1.5	2.3
SiO ₂	48.4	57.8
Al ₂ O ₃	28.2	30.1
K ₂ O	3.4	3.2
Rb ₂ O	0.1	0.1
Fe ₂ O ₃	2.6	3.2
TiO ₂	0.2	0.3
MgO	1.1	1.0
CaO	0.9	0.8
<i>Li₂O*</i>	<i>0.02</i>	<i>0.04</i>
SUM	92.3	99.5

5.3.3.4.4 The effect of varying the reagent dosages on the recovery of lithium-bearing minerals for New Sink G4

5.3.3.4.4.1 Particle size fraction 53 μ m to 250 μ m

The effect of varying collector and depressant dosage level on froth flotation performance can be seen in Figure 5:31 Li₂O grade for New Sink G4 using froth flotation as a function varying collector and depressant dosages at pH 1.5. and Figure 5:32 The highest lithium concentrate grade was achieved at 0.04 wt.% Li₂O when using 30g/t of collector and 40g/t depressant with a recovery of 55%. A relatively high lithium

grade of 0.04 wt.% Li_2O was also found when using 100g/t of collector and 500g/t depressant with a recovery of 51%.

No clear trend was observed for the New Sink G4 sample, as all of the flotation concentrates were very low. It was expected that the higher collector dosages would corresponds to a higher lithium concentration grade, this is because large collector amounts can bind more effectively to lithium mica minerals changing their surface properties. This could be due to the inability of the collectors to adsorb with the molecule as the particles are not liberated or that low levels of zinnwaldite were present in the sample. The structure for zinnwaldite is compact and from previous studies we know that lithium is in the centre of the molecule (Nomura, 2002). Manning (1996) suggested that over time weathering would alter zinnwaldite to muscovite, the chemical composition of the samples also found higher concentrations for iron compared to lithium, which suggested a higher level of muscovite present.

Table 5:25 Optimum recoveries using froth flotation at pulp pH 1.5 for PSD (53 μm to 250 μm) in New Sink G4.

Collector (g/t)	Depressant (g/t)	Grade (%)			Recovery (%)		
		Li_2O	Rb_2O	Fe_2O_3	Li_2O	Rb_2O	Fe_2O_3
30	40	0.04	0.1	1.3	55	79	97
100	500	0.04	0.1	1.4	51	55	93

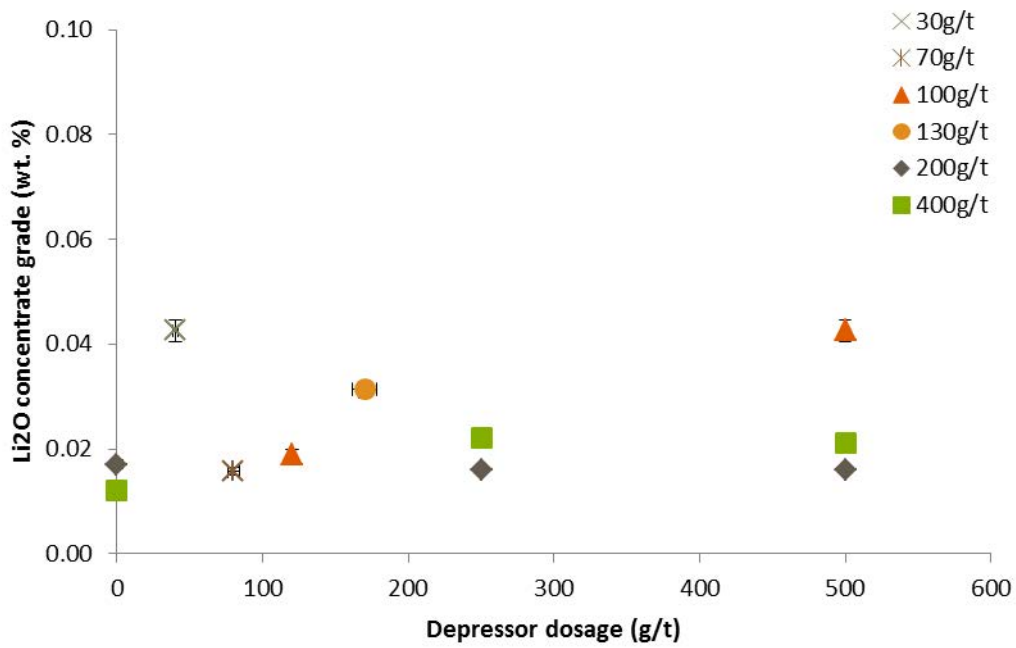


Figure 5:31 Li₂O grade for New Sink G4 using froth flotation as a function varying collector and depressant dosages at pH 1.5.

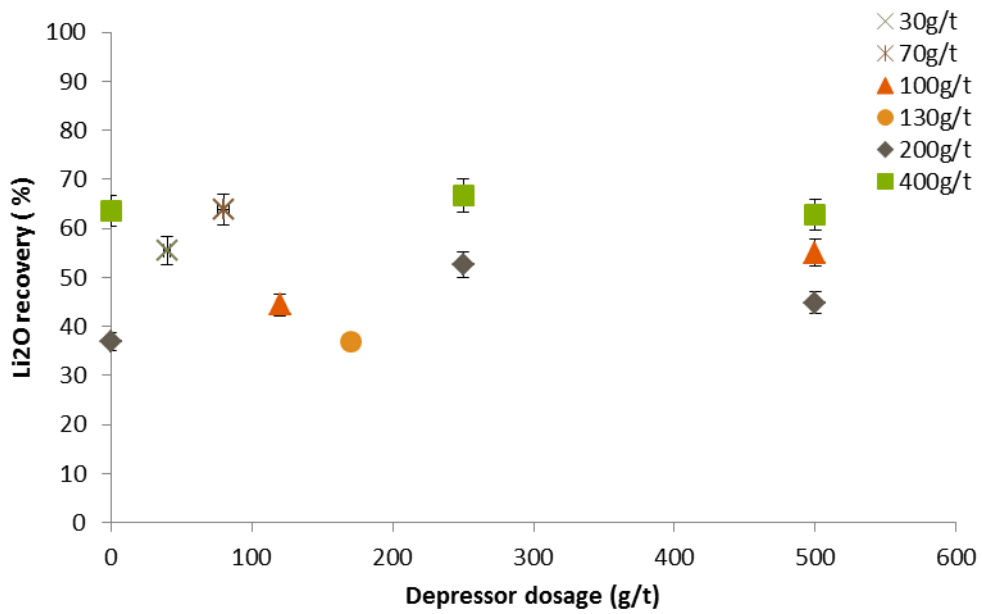


Figure 5:32 Li₂O recoveries for New Sink G4 using froth flotation as a function varying collector and depressant dosages at pH 1.5.

5.3.3.4.4.2 Particle size fraction 250µm to 500µm

The effects of varying collector and depressant dosage level on froth flotation performance can be seen in Figure 5:33 and Figure 5:34. The highest lithium concentrate grade was achieved at 0.16 wt.% Li₂O when using 400g/t of collector and 250g/t depressant with a recovery of 67%.

Table 5:26 Optimum recoveries for New Sink G4 using froth flotation as a function varying collector and depressant dosages at pulp pH 1.5.

Collector dosage (g/t)	Depressant dosage (g/t)	Grade (%)			Recovery (%)		
		Li ₂ O	Rb ₂ O	Fe ₂ O ₃	Li ₂ O	Rb ₂ O	Fe ₂ O ₃
200	500	0.08	0.1	2.0	60	10	69
400	250	0.15	0.1	1.0	67	92	99

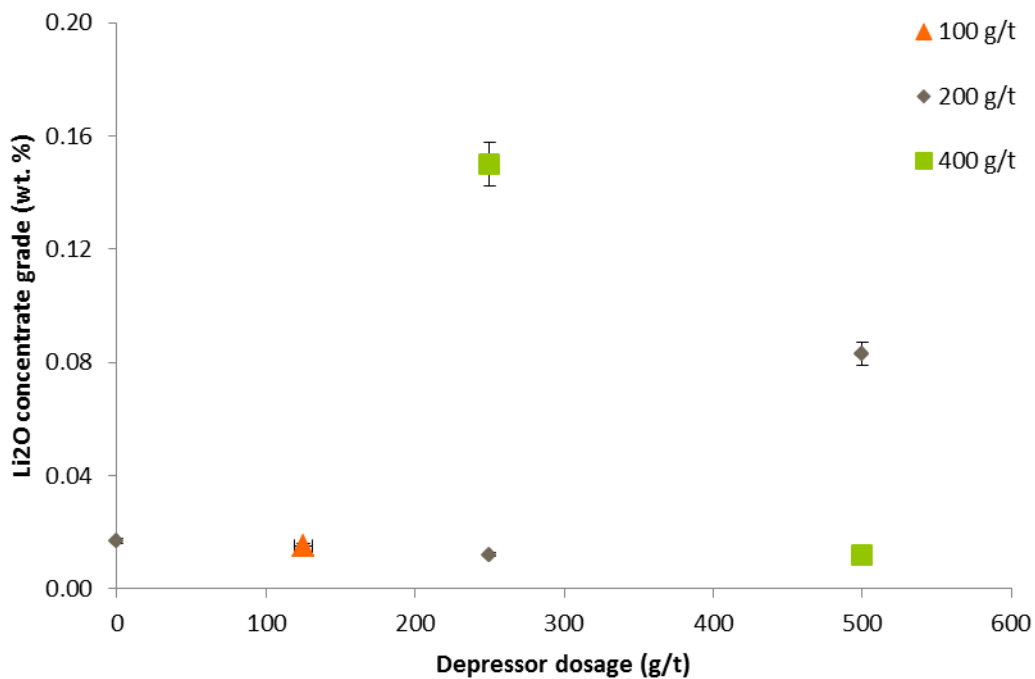


Figure 5:33 Li₂O grade for New Sink G4 using froth flotation as a function varying collector and depressant dosages at pH 1.5.

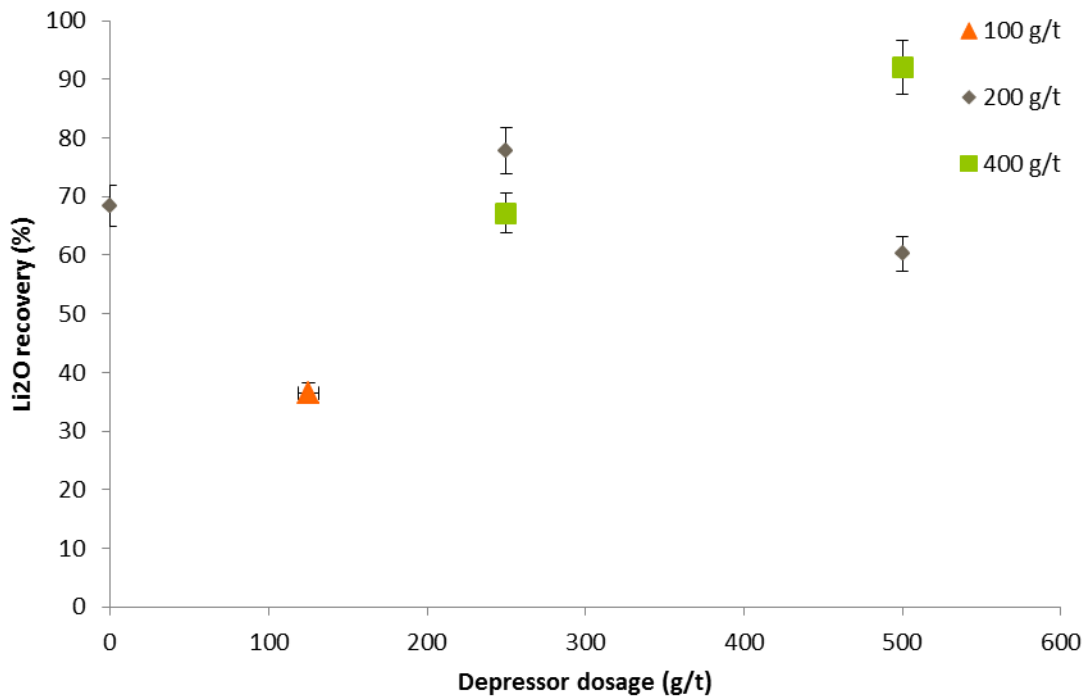


Figure 5:34 Li₂O recovery for New Sink G4 using froth flotation as a function varying collector and depressant dosages at pH 1.5.

5.3.3.5 Stope 13 G4 and Blackpool G4

An investigation into the recovery of lithium from the grade 4 material obtained from Stope 13 and Blackpool pit via froth flotation separation were compared in this section. From the previous low lithium recoveries (>0.1wt.%) obtained for the New Sink G4 material, the Stope 13 G4 and Blackpool G4 were not anticipated to produce commercial quantities of the lithium (4.0 wt.% Li₂O). Thus recovery of lithium from the Stope 13 G4 and Blackpool G4 materials was not an exhaustive investigation in comparison to previous material investigated (Beauvoir, New Sink G5 and New Sink G4).

5.3.3.5.1 Recovery of lithium via froth flotation separation of the Stope 13 G4

5.3.3.5.1.1 Effects of varying particle size on flotation separation

Stope 13 G4 (0.02 wt.% Li₂O) was investigated to recover lithium, using froth flotation separation. Figure 5:35 shows the lithium concentrate grade and recoveries. As it can be seen that >0.1 wt.% Li₂O was recovered in the samples, with lithium recoveries up to 60%. Table 5:27 provide the grades and recoveries for Li₂O, Rb₂O and Fe₂O₃.

Table 5:27 Recovery for Stope 13 G4 material via froth flotation on various pH pulp as a function 500g/t depressant and 400g/t collector at pulp pH 2.0

PSD (μm)	Grade (%)			Recovery (%)		
	Li ₂ O	Rb ₂ O	Fe ₂ O ₃	Li ₂ O	Rb ₂ O	Fe ₂ O ₃
53-250	0.03	0.3	3.3	62	7	17
250-500	0.04	0.3	6.5	16	15	40

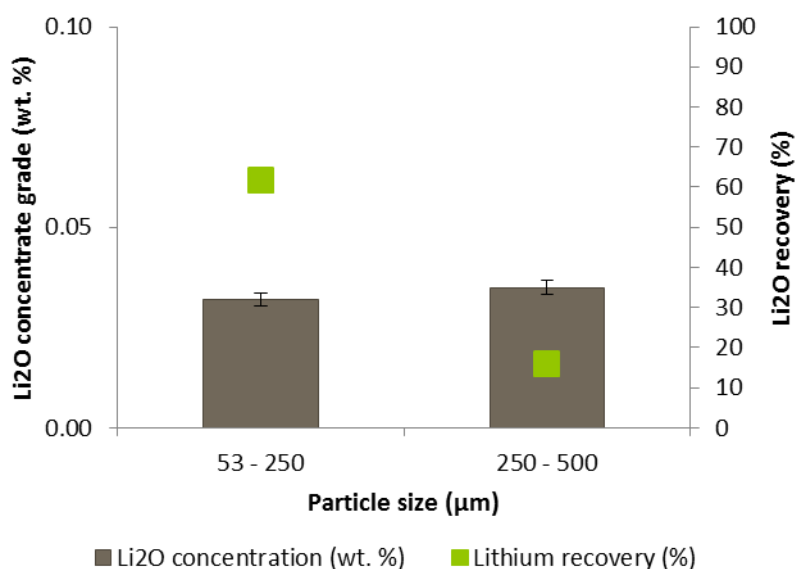


Figure 5:35 Li₂O recovery for Stope 13 G4 using froth flotation as a function 500g/t depressant and 400g/t collector at pulp pH 2.0

5.3.3.5.1.2 Effects of pulp pH on flotation separation

In Figure 5:36 Li₂O recovery for Stope 13 G4 using froth flotation as a function 250g/t depressant and 200g/t collector for PSD (53µm to 250µm). can be seen. From Table 5:27 it can be seen that when using 200g/t collector and 250g/t depressant at pH 2.0 slightly higher lithium grades and recoveries were achieved; 0.03 wt.% Li₂O, 0.4% Rb₂O and 3.8% Fe₂O₃ in the recoveries 59%, 23% and 53%, respectively.

Table 5:28 Recovery for Stope 13 G4 material via froth flotation on various pH pulp as a function 200g/t depressant and 250g/t collector for PSD (53µm to 250µm).

pH	Grade (%)			Recovery (%)		
	Li ₂ O	Rb ₂ O	Fe ₂ O ₃	Li ₂ O	Rb ₂ O	Fe ₂ O ₃
1.5	0.02	0.3	2.7	26	7	17
2.0	0.03	0.4	3.8	59	23	53

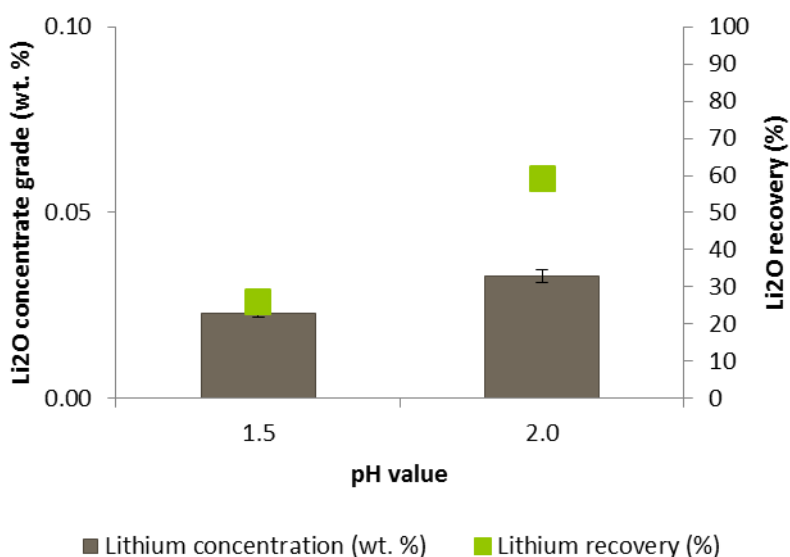


Figure 5:36 Li₂O recovery for Stope 13 G4 using froth flotation as a function 250g/t depressant and 200g/t collector for PSD (53µm to 250µm).

5.3.3.5.1.3 Effects of reagent concentration on flotation separation

In Figure 5:37 the effect of the reagent dosages on metal concentration grade can be seen, for the flotation separation using collector dosages of 200g/t and 400g/t and depressant dosages of 250g/t and 500g/t on the PSD 53µm to 250µm. There was no significant difference observed between varying the reagents dosages from this study.

5:29 Recovery for Stope 13 G4 material via froth flotation on various reagent dosages, pulp pH 2.0.

No.	Collector dosage (g/t)	Depressant dosage (g/t)	Grade (%)			Recovery (%)		
			Li ₂ O	Rb ₂ O	Fe ₂ O ₃	Li ₂ O	Rb ₂ O	Fe ₂ O ₃
1	200	250	0.03	0.4	3.8	59	23	53
2	400	500	0.03	0.4	3.3	16	15	40

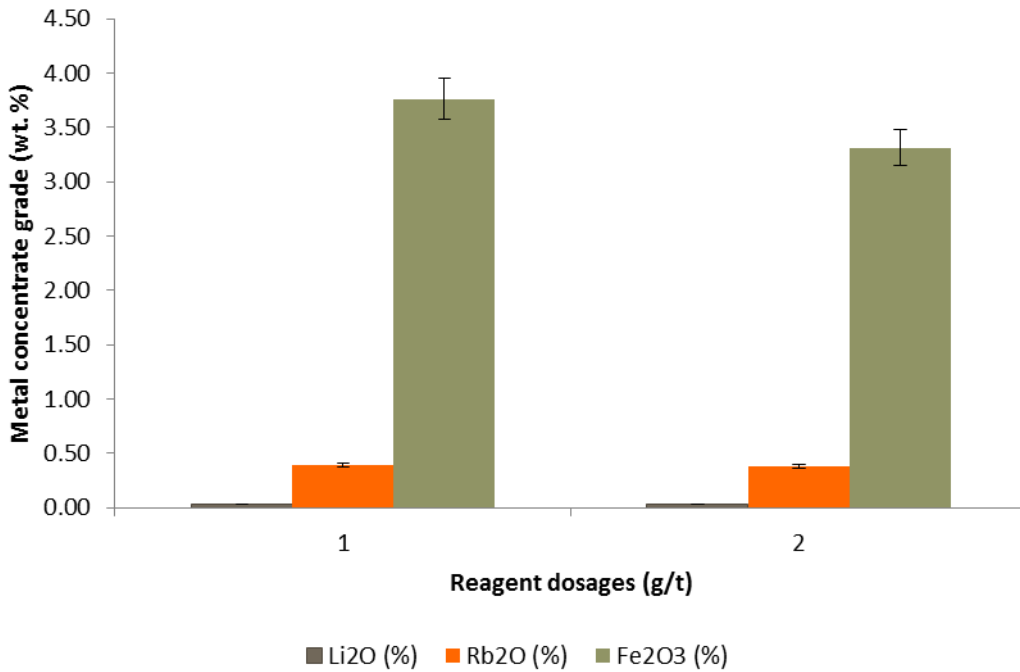


Figure 5:37 Li₂O recovery for Stope 13 G4 using froth flotation on various reagent dosages, pulp pH 2.0.

5.3.3.5.2 Recovery of lithium via froth flotation separation of the Blackpool G4 material

The Blackpool G4 material contained up to 0.08wt.% Li_2O in the particle size fraction: 53 μm to 250 μm . Recovery via froth flotation separation, recovering up to lithium concentrates of 0.03 wt.% Li_2O at a pulp pH of 1.5 and 200g/t of collector, 250g/t of depressant. In Table 5:30 the metal grades and recoveries can be seen. No significant difference was observed between the metal grades for Li_2O , Rb_2O and Fe_2O_3 .

Table 5:30 Recovery for Blackpool G4 material via froth flotation on various PSD.

PSD (μm)	Grade (%)			Recovery (%)		
	Li_2O	Rb_2O	Fe_2O_3	Li_2O	Rb_2O	Fe_2O_3
53-250	0.03	0.2	5.6	96	43	75
250-500	0.03	0.2	5.6	69	39	89

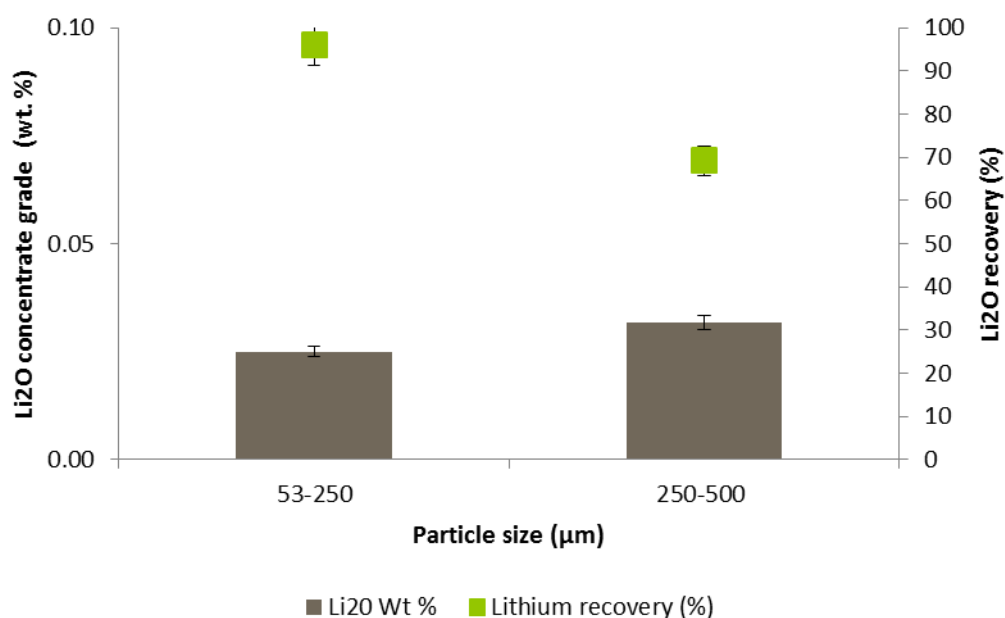


Figure 5:38 Li_2O recovery for Blackpool G4 using froth flotation on various reagent dosages, pulp pH 1.5.

5.3.4 Summary of froth flotation separation

The St Austell deposits contained low amounts of Li_2O , with the most promising sample New Sink G5 material containing 0.07 wt.% Li_2O in the particle size fraction $35\mu\text{m}$ to $250\mu\text{m}$. The grade 5 material showed fully kaolinised granite, as full kaolinisation of all of the feldspar within the sample had taken place. The material was highly malleable thus deemed as the most suitable for separation via froth flotation, in comparison the grade 4.

The New Sink G5 material, the optimum results were achieved when using the finer PSD ($53\mu\text{m}$ to $250\mu\text{m}$), 200g/t collector and 250g/t depressant at pH 1.5. The lithium concentrate contained; 0.47 wt.% Li_2O , 0.5% Rb_2O and 12.9% Fe_2O_3 with the recoveries 90% Li_2O , 94% Rb_2O and 90% Fe_2O_3 . For the New Sink G4 material, although the mineralogical analysis estimated that approximately 6% mica was found, as the material was not completely kaolinised it contained 5% feldspar. The grade 4 material can be described as malleable with some degree of friability. The flotation concentrates for all of the New Sink G4 material were less than 0.2 wt.% Li_2O , the highest lithium concentrate (0.15wt.% Li_2O with a recovery of 42%) was found within the coarser PSD ($250\mu\text{m}$ to $500\mu\text{m}$), 400g/t collector and 250g/t depressant at pH 1.5.

From this study it can be concluded that although the St Austell deposits could be slightly upgraded via froth flotation to achieve lithium concentrations grades up to 0.5 wt.% Li_2O for New Sink G5, they cannot be established as a commercial lithium resource as lithium concentrates of 4.0 wt.% would need to be achieved (Bauer, 2000).

5.4 Magnetic Separation of Kaolin Waste Material From St Austell in the UK

5.4.1 Introduction

High intensity magnetic separation was used to separate any paramagnetic minerals from the lithium concentrate for the New Sink Grade 5 sample. Two techniques were investigated in this study; dry magnetic separation and wet magnetic separation. Dry magnetic separation takes feed and uses a magnetic field to alter paramagnetic particle trajectories when passing over a high intensity induced roll magnetic separator, leading them into separate hoppers. Wet high intensity magnetic separation (WHIMS) separates materials based upon their relative magnetic susceptibilities (Kelland, 1973; Chelgani, 2015). The main contaminant in the St Austell material was altered muscovite. To improve the separation efficiency of the material and the lithium concentrate grade magnetic separation was investigated. Muscovite has non-magnetic properties, so any unaltered muscovite mica would be separated from the zinnwaldite mica (slightly paramagnetic) (Chelgani, 2015). For this study a schematic of the two-stage separation process used can be seen in Figure 5:39.

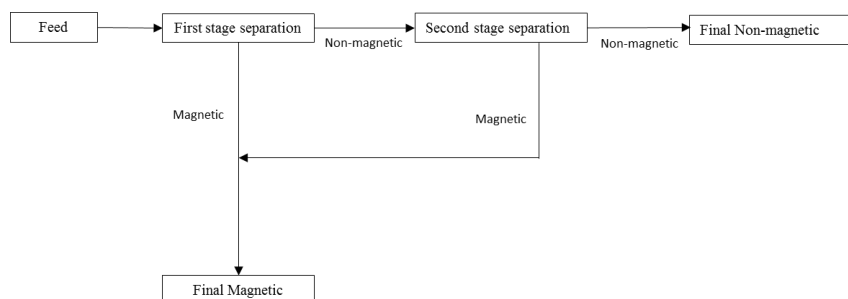


Figure 5:39 Schematic of two-stage separation process using WHIMS.

5.4.2 Experimental procedure

Wet high intensity magnetic separation (WHIMS) was carried out using a (BoxMag-Rapid Ltd, Rapid Magnetic Ltd, England). The separator was operated at 0.8 Tesla magnetic field strength and a current of 5 amps, in the open gap of the unit. A 1 mm metal wedge wire matrix was inserted into the gap to give capture sites for any paramagnetic mineral particles (Fe rich micas, iron oxides, tourmaline) and to provide the magnetic field gradient necessary to achieve a separation. The suspension (15% by weight) consisted of mineral particles in tap water, which was poured in a controlled manner through the magnetic matrix. The material was separated into two fractions; magnetic and non-magnetic, which were dried and weighed. The fractions were analysed for lithium by ICP-OES, for other metals by XRF and for other mineral phases via XRD.

5.4.3 Results and discussion

5.4.3.1 The effect of varying the particle size fraction using WHIMS for the New Sink G5 material

In Figure 5:40 the lithium concentrations for the wet magnetic separation techniques using 0.8 Tesla can be seen. Three particle size fractions were investigated in this study; 53µm to 250µm, 250µm to 500µm and 500µm to 710µm.

Each particle size fraction showed similar trends between the magnetic and non-magnetic fractions, of achieving higher lithium content in the magnetic fraction. The greatest difference was observed in the particle size fraction 250µm to 500µm,

approximately 0.1 wt.% Li₂O was recovered in the magnetic fraction and 0.02 wt.% Li₂O recovered in the non-magnetic fraction. In the particle size fraction 500µm to 710µm higher lithium concentrations were observed of 0.12 wt.% Li₂O in the magnetic fraction, although the non-magnetic fraction also achieved a higher lithium concentration of 0.08 wt.%. The recovery for the magnetic fraction were low between 28 to 34% Li₂O, thus suggesting that an efficient separation was not achieved. The chemical analysis can be seen in Table 5:32.

Table 5:31 Magnetic product grade and recovery of New Sink G5 using WHIMS (0.8 Tesla).

PSD (µm)	53 - 250		250 - 400		500 - 710	
	Grade	Recovery	Grade	Recovery	Grade	Recovery
Magnetic	0.06	30	0.09	28	0.12	34
Non-mag	0.04	70	0.02	72	0.08	66

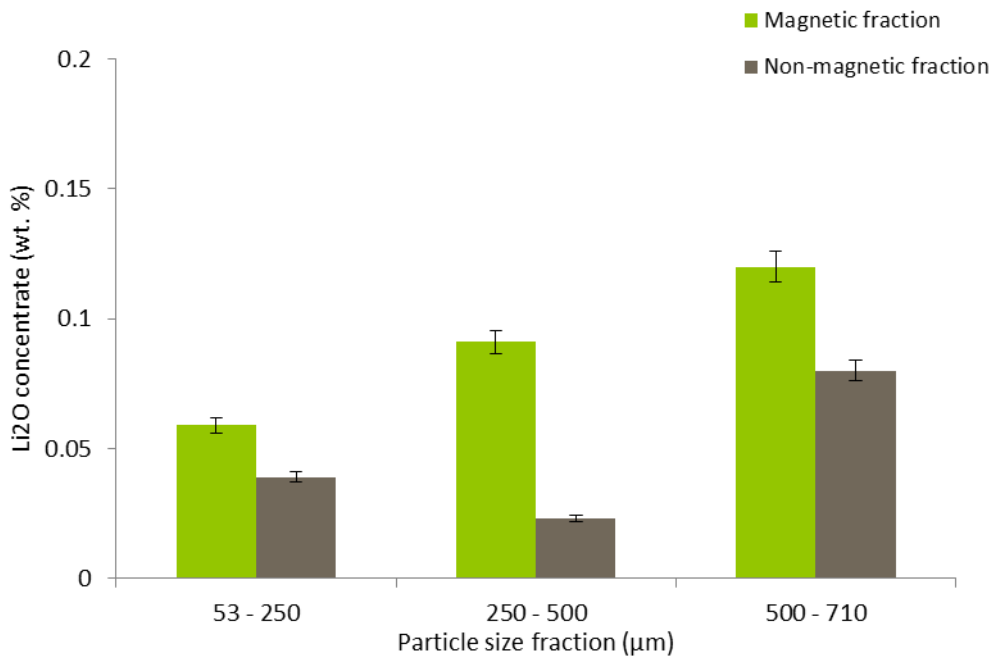


Figure 5:40 Lithium concentrations for varying particle size fractions using WHIMS (0.8 Tesla).

Table 5:32 Chemical analysis of the G5 material separation products at magnetic field of 0.8 Tesla for WHIMS, *tested by ICP.

Metal oxide (%)	PSD (250 - 500µm)		PSD (500 - 710µm)	
	<i>Magnetic</i>	<i>Non-magnetic</i>	<i>Magnetic</i>	<i>Non-magnetic</i>
SiO ₂	70.1	75.0	65.6	71.0
Al ₂ O ₃	12.3	11.8	14.0	13.8
K ₂ O	7.0	6.9	7.7	7.5
Rb ₂ O	0.2	0.2	0.2	0.2
Fe ₂ O ₃	7.3	4.8	8.5	5.4
TiO ₂	1.0	0.5	1.0	0.5
CaO	0.7	0.2	1.2	0.3
<i>Li₂O*</i>	<i>0.09</i>	<i>0.02</i>	<i>0.12</i>	<i>0.08</i>
SUM	98.7	99.4	98.3	98.8

The X-ray diffraction analysis can be seen in Figure 5:41 and Figure 5:42 for the magnetic and non-magnetic samples. The graphs show very similar peaks suggesting that WHIMS using 0.8 Tesla did not efficiently separate the minerals. Zinnwaldite was identified through characteristic peaks at 18, 27, 34 and 56 degrees. Large distinct peaks for the mineral quartz were seen at 21, 27 and 50 degrees. The peak at 27 degrees represents the SiO₂ bond, which is present in both of the minerals.

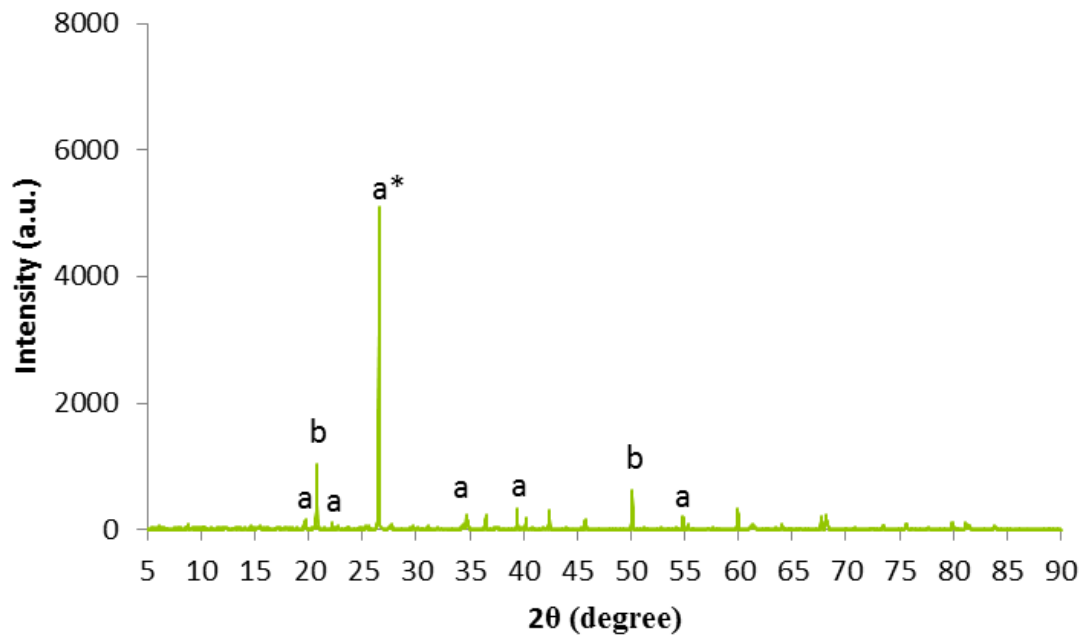


Figure 5:41 XRD pattern of New Sink G5 material showing magnetic fractions after WHIMS separation, (a) zinnwaldite, (b) quartz, (a*) zinnwaldite and quartz.

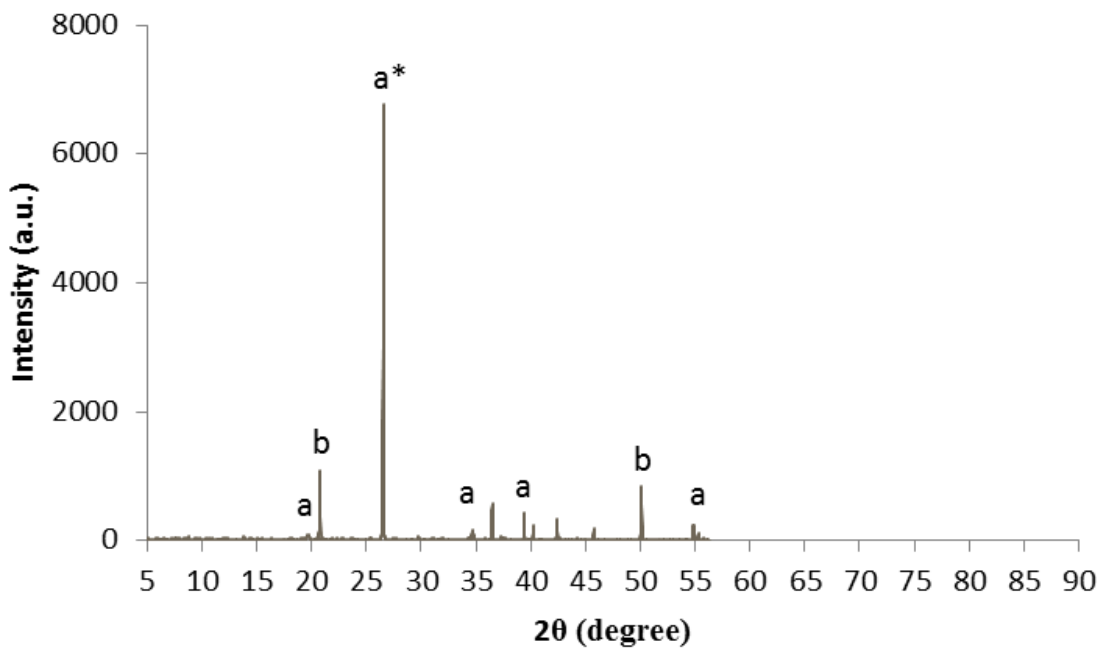


Figure 5:42 XRD pattern of New Sink G5 material showing non-magnetic fractions after WHIMS separation, (a) zinnwaldite, (b) quartz, (a*) zinnwaldite and quartz.

5.4.3.2 The effect of varying the particle size fraction using Dry Magnetic separation for the New Sink G5 material

Dry magnetic separation was used on the particle size fraction 710 μ m to 1700 μ m using a magnetic field strength of 1.2 Tesla. In Table 5:33 the chemical analysis of the material for the magnetic and non-magnetic fraction can be seen, 0.06 wt.% Li₂O in the magnetic fraction. A lower separation of the minerals efficiency for lithium was achieved, of 10% and 90% for the magnetic and non-magnetic fractions, respectively. The dry magnetic separation processes were limited to the strength of the magnetic field, the samples displayed weaker magnetic properties at 1.2 Tesla. It also shows less iron content in the non-magnetic fraction (4.6%). The XRD patterns are shown in Figure 5:43 and Figure 5:44, no significant difference was observed between the two fractions, with the exception of the peak at 27 degrees, which showed a decrease in the SiO₂ in the non-magnetic fraction, also identified by chemical analysis, Table 5.33.

Table 5:33 Chemical analysis of the G5 material separation products at magnetic field of 1.2 Tesla for dry magnetic separation, *tested by ICP.

Metal oxide (%)	PSD (710 - 1700 μ m)	
	<i>Magnetic</i>	<i>Non-magnetic</i>
SiO ₂	78.3	72.6
Al ₂ O ₃	9.6	10.9
K ₂ O	4.5	5.3
Rb ₂ O	0.1	0.2
Fe ₂ O ₃	5.5	4.6
TiO ₂	0.5	0.5
<i>Li₂O*</i>	<i>0.06</i>	<i>0.04</i>
SUM	99.1	94.1

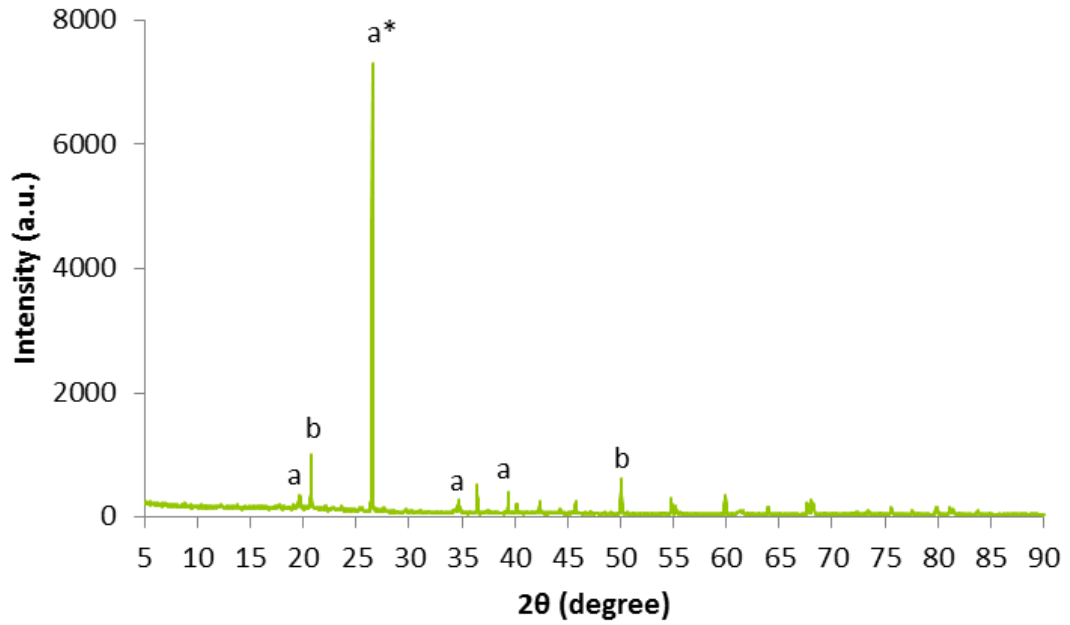


Figure 5:43 XRD pattern of New Sink G5 material showing magnetic fractions after dry magnetic separation, (a) zinnwaldite, (b) quartz, (a*) zinnwaldite and quartz.

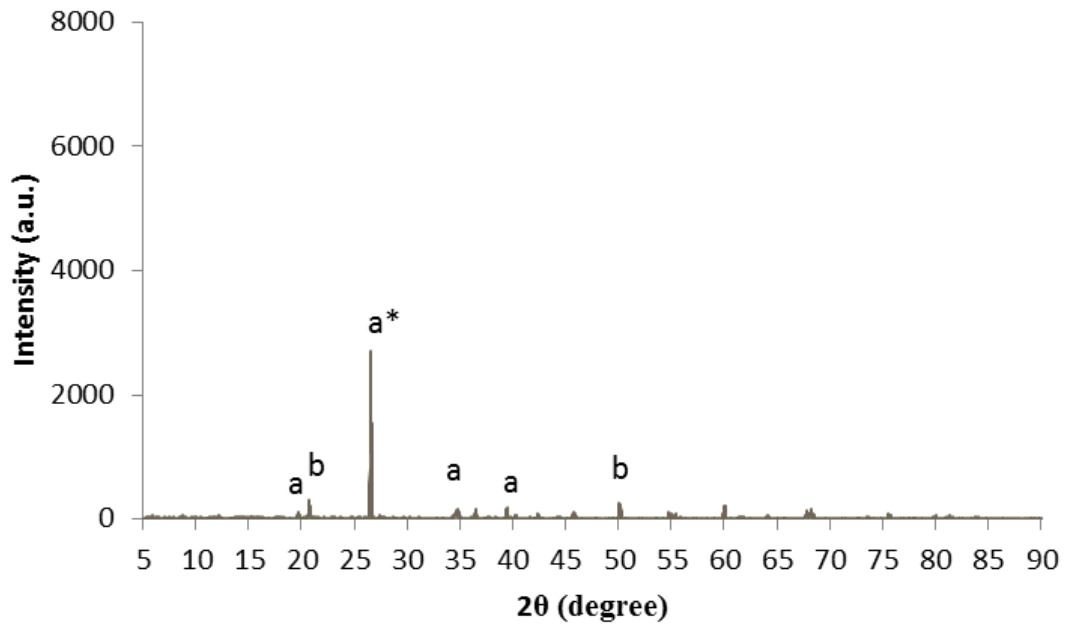


Figure 5:44 XRD pattern of New Sink G5 material showing non-magnetic fractions after dry magnetic separation, (a) zinnwaldite, (b) quartz, (a*) zinnwaldite and quartz.

5.4.3.3 The effect of varying the particle size fraction using WHIMS for the New Sink lithium concentrate

Further investigations were carried out to upgrade the highest lithium concentrations obtained from froth flotation separation on particle size fraction 53 μ m to 250 μ m. The two samples investigated using WHIMS were; New Sink Grade 5 and New Sink Grade 4, containing 0.5 and 0.04 wt.% Li₂O, respectively. In Figure 5:45 the results for New Sink Grade 5 showed an increase to 0.6 wt.% Li₂O in the magnetic fraction, an increase of 0.1 wt.% Li₂O. It was interesting to observe that for the magnetic and non-magnetic fractions a similar trend to that of the feed was observed, a difference of around 0.03 wt.% Li₂O was found.

For the New Sink Grade 4 sample an increase of 0.08 wt.% Li₂O was observed, although this was greater it was still not enough to process on an economical scale. Kawatra (2009) stated that the operating parameters of WHIMS are highly sensitive and that the presence of additional protons, collectors and depressants could interfere with the kaolin mining waste material or the metals' matrix magnetic properties. Magnetic separation did not perform as well as in studies carried out by Jandova (2010) using zinnwaldite concentration of 1.21% Li. It can be suggested that this is due to altered lithium-rich muscovite most likely to be a contaminant in the sample.

Table 5:34 Magnetic product grade and recovery of lithium concentrate using WHIMS (0.8 Tesla).

	New Sink G5				New Sink G4			
	Grade (%)		Recovery (%)		Grade (%)		Recovery (%)	
	Li ₂ O	Rb ₂ O						
Magnetic	0.5	0.5	51	70	0.08	0.2	53	82
Non-magnetic	0.6	0.4	49	30	0.04	0.1	47	18

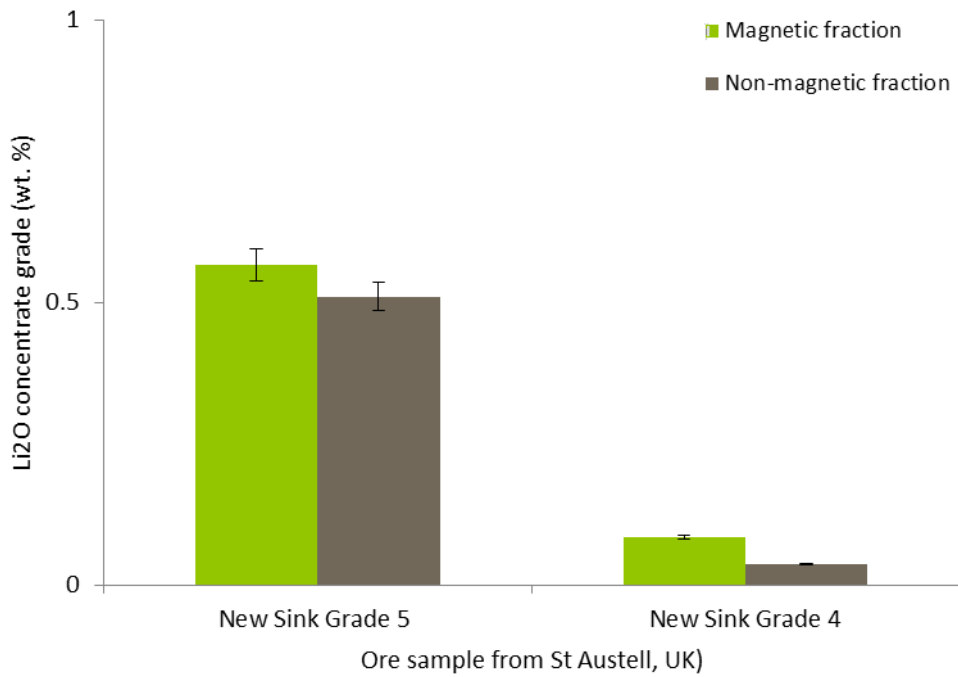


Figure 5:45 Lithium concentrate grades for the ore sample from St Austell (UK) using WHIMS.

5.4.4 Summary on magnetic separation technique

Magnetic separation was not effective in achieving high lithium contents, when separating the New Sink G5 flotation concentrate using WHIMS (at magnetic field strength of 0.8 Tesla). It is suggested that the poor efficiency in separation was due to the presence of muscovite in the sample, which acts as a contaminant in the separation process. As muscovite has non-magnetic properties, any unaltered muscovite mica would be separated from the zinnwaldite mica (slightly paramagnetic) to further improve the separation efficiency and concentrate lithium grade Chelgani, 2015).

In the study by Siame (2011) a lower content of muscovite (0.13%) was present in the sample provided by Goonvean Ltd. Using electron-microprobe analysis on individual mica grains Siame estimated that the majority of the sample contained zinnwaldite (3.88% Li_2O) and a smaller content of muscovite (0.13%). Siame found that the zinnwaldite flotation concentrate was able to be further concentrated to 2.1% Li_2O , 0.7% Rb_2O and 7.4% Fe_2O_3 with a recovery of 73%, 67% and 77%, respectively, when using WHIMS at a magnetic field strength of 1.95 Tesla.

5.5 Electrostatic separation of kaolin waste material from St Austell, UK

5.5.1 Introduction

Ullmann (2005) stated that electrostatic separation is based on the differences in the surface electrical properties of types of materials the most significant being the surface conductivity and the associated ability to gain, lose or retain charges. Electrostatic separation can improve material grades in the kaolin industry, as the material can be selectively charged and subsequently separated upon application of external electrical forces. Iuga (2004) provided an in-depth evaluation of different electrostatic techniques on their effectiveness for the removal of pegmatite micas from feldspars, concluding that particle size was the major influence on the effectiveness of roll-type separators. In this study the particle size fraction between 710 to 1700 μm was used to achieve greater separation efficiency.

5.5.2 Experimental procedure

An electrostatic separator (HT Electrostatic separator, BoxMag-Rapid Ltd., England) was used to separate the minerals at an operating voltage of 12keV. Dry material was fed into the vibratory hopper connected to the electrostatic separator, and two fractions were collected; non-conductive (insulator) and conductive. The samples were analysed by ICP-OES/XRF/XRD.

5.5.3 Results and discussion

The results for the New Sink Grade 5 sample can be seen in Table 5:35. The lithium recovered in both of the hoppers; insulator and conductor were not efficient as we were only achieved 0.05%. Electrostatic separation was found to not upgrade the feed at all. It was suggested that due to the surface conductivity of component minerals being too similar to achieve an effective separation (Inculet, 1985; Cohen, 2005). The micas; muscovite and zinnwaldite have very similar structural and physical properties, thus it was not likely to achieve an effective separation and therefore this investigation campaign was stopped. The mica has a crystal structure consisting of aluminium silicate sheets weakly bound together by layers of positive ions; thus allowing the structure to contain high dielectric strength, high insular strength and resistance to corona discharge.

Table 5:35 Electrostatic separation technique employed to recovery lithium bearing minerals for New Sink G5 samples.

Separator Technique	Physical property	Particle size fraction (μm)	Li ₂ O (%)
Electrostatic	Insulator	710 – 1700	0.05
	Conductor	710 – 1700	0.05

Table 5:36 Chemical composition of New Sink G5 material electrostatically separated *tested by ICP.

Metal oxide (%)	PSD (710 – 1700 μm)	
	<i>Insulator</i>	<i>Conductor</i>
SiO ₂	83.3	75.8
Al ₂ O ₃	7.44	13.6
K ₂ O	3.64	4.14
Rb ₂ O	0.1	0.1
Fe ₂ O ₃	3.67	4.64

TiO ₂	0.5	0.4
CaO	0.15	0.28
<i>Li₂O*</i>	<i>0.05</i>	<i>0.05</i>
SUM	98.9	99.0

5.6 Overall conclusion of the separating techniques

The recovery of lithium-bearing minerals such as lepidolite and zinnwaldite, from kaolinised material was investigated using physical separation techniques such as; froth flotation, gravity separation and magnetic separation. The kaolin waste material obtained from Beauvoir in France (0.89 wt.% Li₂O) showed promising results for commercial usage on a laboratory scale. The final flotation concentrate for the PSD of 53µm to 400µm, contained 4.5% Li₂O, 2.6% Rb₂O and 1.5% Fe₂O₃ in the recoveries 88%, 71% and 26%, respectively. The operating conditions for the flotation were pH 1.5, 80g/t depressant and 200g/t collector. The waste materials obtained from the Beauvoir hydrocyclone underflow are suggested to be a potential source of lithium, when compared to hard rock extraction of other pegmatite deposits, as the mineral is already liberated from the ore via previous processing stages. By utilising the hydrocyclone underflows as a potential source of lithium, the operational costs of the process are reduced due to not accruing additional mining or grinding costs.

Research on the St Austell material indicated that for the lithium found in the waste materials from Karlake and Blackpool area, whilst it is present, is only at levels (> 0.1 wt.% Li₂O). Processing of the material by froth flotation separation in this study did not achieve economical lithium levels, thus it would not be economically viable to process

the material using the existing chemical extraction processes to produce lithium carbonate. The St Austell waste materials would need to be crushed and milled prior to flotation treatment would increase the lithium recovery. Other separating techniques such as magnetic separation techniques (both dry and wet) and electrostatic separation were not successful, when separating lithium bearing minerals from kaolin waste material. The poor results are suggested to be due to high concentrations of iron found within the sample, present in the mineral muscovite. Both zinnwaldite and the impurity, muscovite, had similar structural and physical properties. The results were inconclusive, it is suggested that higher field strengths to separate the minerals could improve the recovery but this would require high costs, thus considered not an economical process.

CHAPTER 6

EXTRACTION PROCESSES FOR LITHIUM CONCENTRATE

6.1 Introduction

The extraction of lithium from mineral micas and pegmatites has been investigated for many years, it has been seen as the most expensive and critical aspect of recovering lithium from waste material. Previously, studies investigated extraction methods such as: sulphuric and hydrochloric acid leaching, which was reported by Distin and Phillips (1982), on non-kaolinised pegmatite with a significant lithium mica content, due to the presence of the lithium-bearing mineral amblygonite. The geological area studied was outside of the St Austell kaolin extraction area and as kaolin mining did not take place there in this study it was not pursued further. Other extraction processes included; the gypsum process which was investigated by Jandova (2009). At present the acid extraction and gypsum process are not considered economical due to the chemical costs and energy usage, thus are not being developed at an industrial scale. In this study, the gypsum process was investigated for the Beauvoir lithium concentrate, 4.1 wt.% Li_2O , as it contained higher Li_2O concentrations when compared to the St Austell concentrates New Sink Grade 5 lithium concentrate of 0.5 wt.% Li_2O . Due to the low levels of Li_2O in the Imerys St Austell deposits the gypsum process was not deemed suitable.

Other lithium extraction processes have also been previously studied such as bioleaching. In a study by Rezza (2001) the recovery of lithium from spodumene by bioleaching was investigated. Bioleaching utilises naturally occurring microorganisms to extract lithium from the mineral, thus this process is considered environmentally friendly and potentially low cost. Through this study an innovative extraction process was developed for lepidolite using the heterotrophic fungi, *Aspergillus niger* (*A. niger*). The lepidolite concentrate investigated was processed from kaolin waste material from the mining site in Beauvoir, France, due to the higher lithium recovery. The bio-extraction processes were also investigated using mineral grade specimens of pure lepidolite. The St Austell material was not investigated due to poor lithium recoveries.

6.2 Gypsum process

6.2.1 Introduction

The gypsum process was investigated as a comparative study to the studies of Jandova (2010) and Siame (2011) both found recovery efficiencies of above 90% for zinnwaldite concentrates ($\text{KLiFeAl}(\text{AlSi}_3)\text{O}_{10}(\text{F},\text{OH})_2$), containing around 1.0 wt.% lithium. Although the process used very high calcining temperatures, between 850 to 1050°C, thus it was not seen as economically viable and at present would not be able to sustain as a profitable process in the views of Imerys and the authors.

In this study two materials, were investigated following the gypsum process; Beauvoir lithium mica concentrate (4.1 wt.% Li_2O) obtained from Imerys Ltd contained the lithium-bearing mineral lepidolite ($\text{KLi}_2\text{Al}(\text{Si}_4\text{O}_{10})(\text{OH},\text{F})$) and the mineral specimen grade pure lepidolite (5.6 wt.% Li_2O) obtained from Northern Geological Suppliers Ltd.

Rieder (1998) described both lepidolite and zinnwaldite as trio-octahedral with different crystal structures, lepidolite as a light mica containing substantial lithium content between 3.0 to 7.7% Li_2O , whereas zinnwaldite is a dark mica containing lithium between 2.0 and 5.0% Li_2O (Garrett, 2004; Reider, 1998).

6.2.2 Experimental procedure

The lithium concentrate (20g) was mixed with calcium sulphate (10g) in a ratio of 2:1 before calcining for 60 minutes in a muffle furnace. The particle size range was between 53 to 400 μm . The temperatures used for calcination were; 850 and 900°C. After allowing the calcined product to cool down, the sinters (20g) were then water leached with distilled water (250mL) in a thermostat controlled stirred glass reaction vessel, at a temperature of 90°C for 30 minutes. The liquid to solid ratio was 10:1. The solutions were diluted to 1000mL and then analysed by AAS for lithium content and the solids were filtered, dried and weighed.

6.2.3 Results and discussion

6.2.3.1 Effect of heat treatment on Beauvoir lithium concentrate

The Beauvoir lithium concentrate supplied from Imerys contained the lithium-bearing mineral lepidolite ($\text{KLi}_2\text{Al}(\text{Si}_4\text{O}_{10})(\text{OH},\text{F})$), which contained a lithium concentration of 4.1 wt.% Li_2O . The crystal structure of the lepidolite, seen in Figure 6:1, shows the complex arrangement of the atoms in the lepidolite crystal structure lattice. To increase the efficiency of the water leach extraction process heat treatment was applied to the Beauvoir lithium concentrate, in Figure 6:2 and Figure 6:3 the lithium concentrate can

be seen before and after heat treatment at 850°C for 60 minutes. In Figure 6:3 the smaller size distribution of the particles could be explained by a structural volume expansion of the mineral due to the treatment with high temperatures and subsequently delamination of the mica platelets thus allowing easier access to the lithium atoms when leaching.

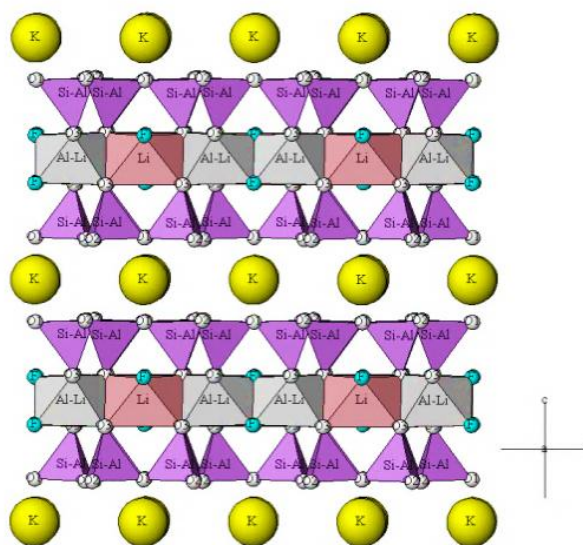


Figure 6:1 Crystal structure of the lepidolite taken from Crystal Structure Gallery, National Institute of Advanced Industrial Science and Technology (Nomura, 2002).

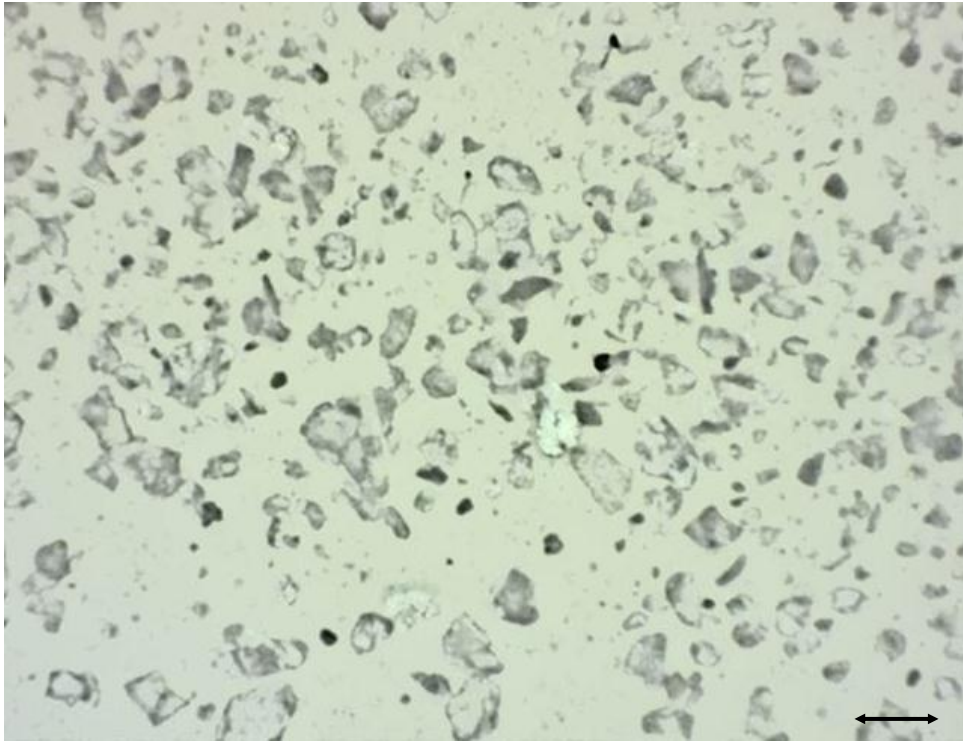


Figure 6:2 Optical microscope image of Beauvoir lithium concentrate untreated, magnification x10, scale 2.65cm.

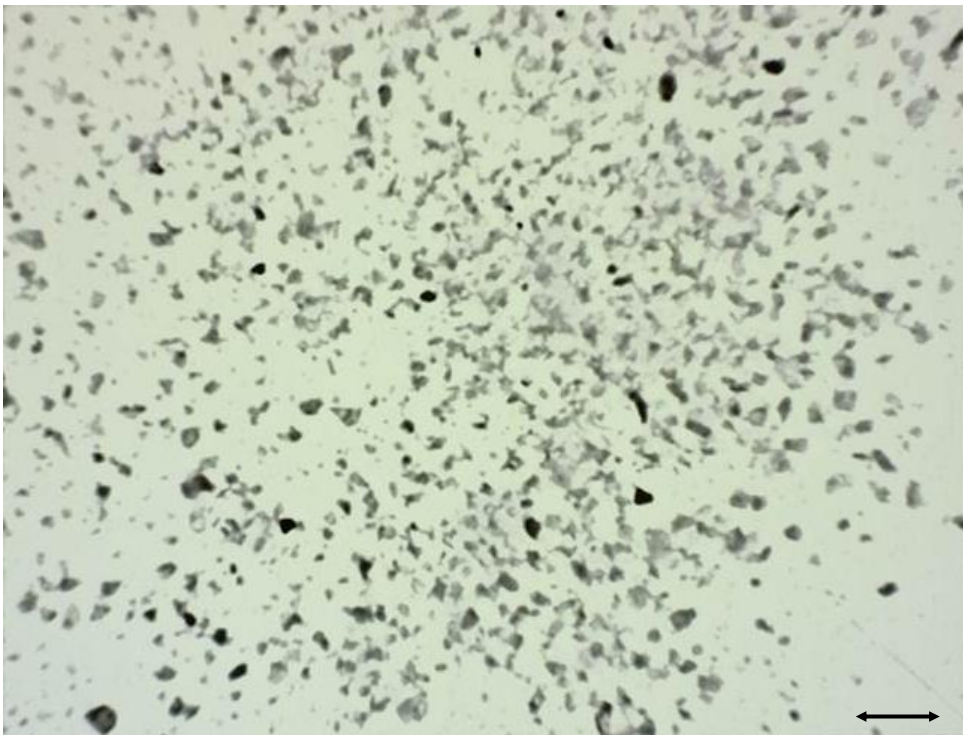


Figure 6:3 Optical microscope image of Beauvoir lithium concentrate heat treated at 850°C for 60 minutes, magnification x10, scale 2.65cm.

In Figure 6:4 and Figure 6:5 the XRD analysis for Beauvoir lithium concentrate can be seen for before and after heat treatment, respectively. The main changes observed were the increased intensity of the peaks upon heat treatment, which suggested a change in crystallinity of the lepidolite mineral structure. The figures show that the peaks for zinnwaldite. The main change observed for the heat treatment sample at 35 and 62 degrees, large peaks intensities were observed for the heat treated concentrate. At 35 degrees an increase of 63 a.u. was observed for the heat treated concentrate which had a final peak intensity of 75 a.u. Also at 62 degrees an increase of 8 a.u. for the heat treated concentrate to 26 a.u was observed. Siame (2011) also observed similar results between the lithium concentrate before and after heat treatment for zinnwaldite at 800°C, with the main changes being the increase in peak intensity. From the XRD patterns it is evident that the crystal structure of the concentrate has been altered due to the heat treatment.

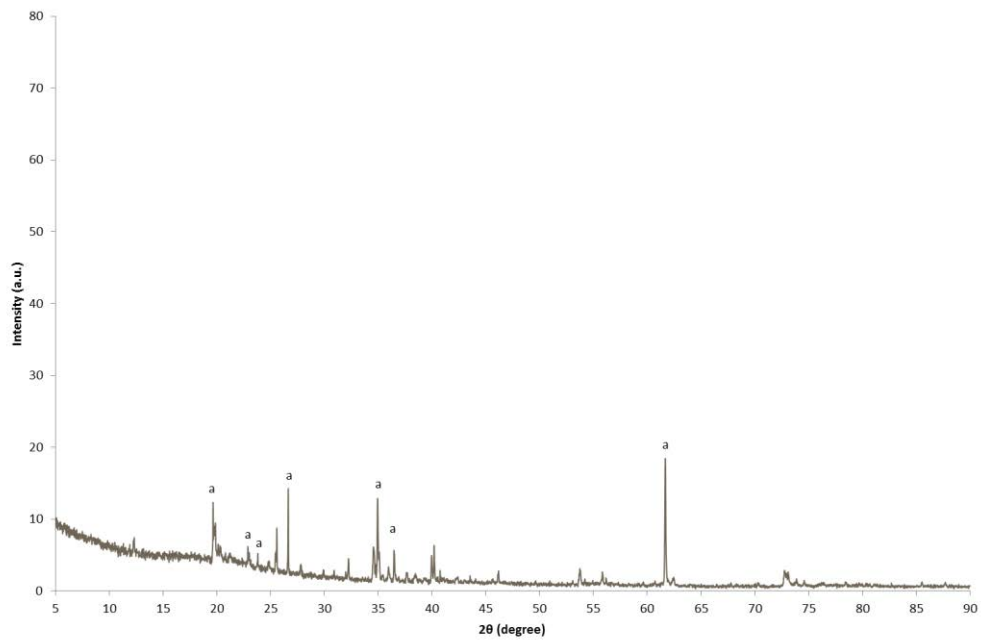


Figure 6:4 XRD pattern of Beauvoir lithium concentrate (untreated) for the PSD 53µm to 250µm, (a) zinnwaldite.

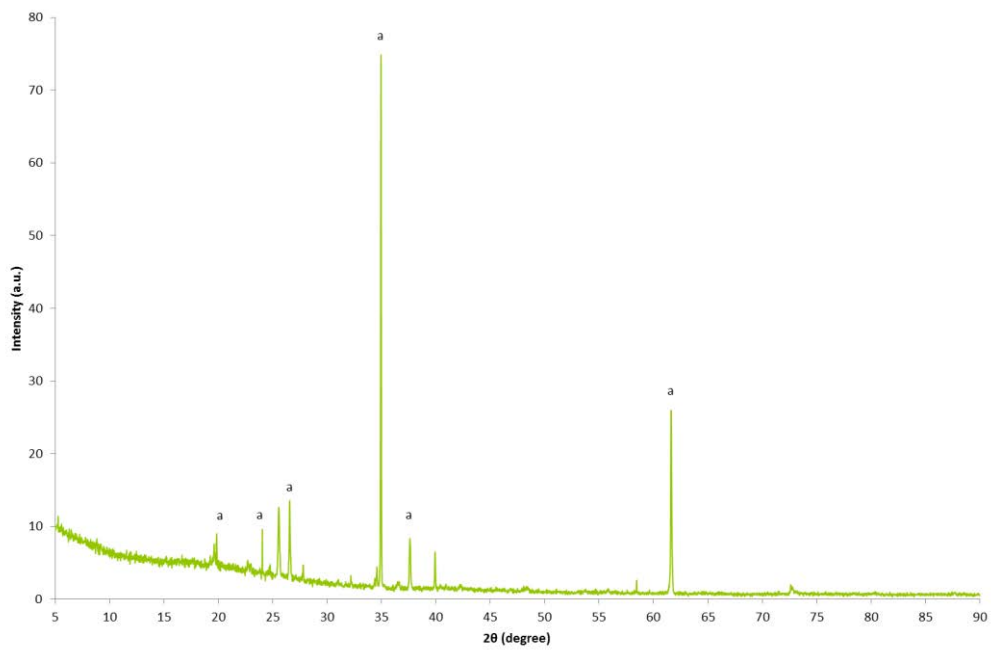


Figure 6:5 XRD pattern of Beauvoir lithium concentrate heat treated to 850°C for 60 minutes, for the PSD 53µm to 250µm, (a) zinnwaldite.

6.2.3.2 Lithium extraction of the heat treated Beauvoir lithium concentrate

The results shown in Figure 6:6 represent the metal concentrations leached into the solution for the gypsum process (calcined with CaSO_4) at varying calcination temperatures, 850°C and 900°C, as well as the recovery rates from lithium-bearing mineral lepidolite. At 850°C, the lithium concentration achieved in the solution was low at 5mg/L, whereas when a significantly higher concentration of lithium was extracted when calcined temperatures at 900°C, 72mg/L. The lithium recoveries for both temperatures was very low, achieving only up to 12%.

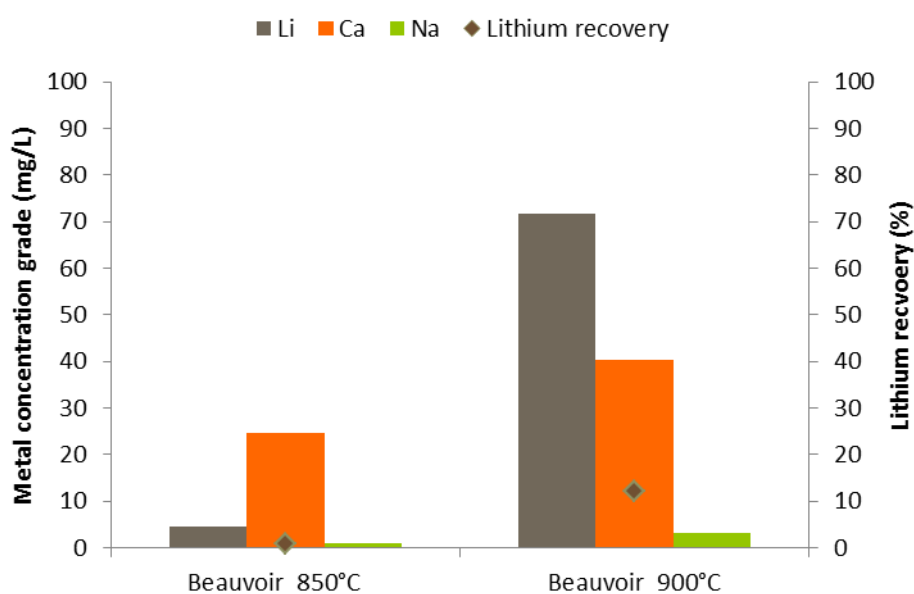


Figure 6:6 Results for the gypsum process with Beauvoir lithium concentrate at varying calcination temperatures.

As shown in Table 6:1, the studies by Siame (2011) and Jandova (2009; 2010) also investigated the recovery of lithium from the lithium-bearing mineral zinnwaldite. Similar results were found by Siame (2011) of low lithium recoveries at 850 and 900°C achieving below 5% and 25%, respectively. However when the calcining temperature

was increased to above 900°C a significant lithium recovery was achieved, at 1050°C approximately 85% lithium recovery was detected. This was suggested to be due the formation of the compound LiKSO_4 , a leachable lithium compound (2011). The study by Jandova (2009; 2010) also identified the formation of LiKSO_4 when extracting lithium from zinnwaldite, at calcination temperatures between the range 900 to 1050°C.

In this study, the gypsum process was investigated as a comparative study to the studies investigated by Siame (2011) and Jandova (2010; 2009); which investigated the lithium-bearing mineral zinnwaldite. The material was milled to a particle size of approximately 90% less than 100µm. The mineral investigated in this study was lepidolite; which contained a different mineralogical structure to zinnwaldite (Cundy, 1959).

In Table 6:2 a comparison of the results from this study and the study by Siame (2011) can be seen. The lower temperatures were not expected to yield high lithium recoveries which were confirmed. The Beauvoir lithium concentrate investigated contained a particle size distribution of approximately 90% less than 330µm. This could explain the lower recovery when calcining at 850°C and 900°C, recovering 0.8% and 12%, respectively. Further milling of the lithium concentrate and calcining at higher temperatures, of above 900°C, were not investigated as although there was a greater potential for lithium recovery which could be optimised, it would not be cost effective in the view of Imerys. Thus, the gypsum extraction process was not deemed as economical to process on a larger scale, mainly due to the high costs of the extraction process.

Table 6:1 Comparison of lithium extraction processes from various studies, using the gypsum method, * estimate.

	This study	Jandova (2009)	Jandova (2010)	Siame (2011)	Siame (2011)
Mineral	Lepidolite	Zinnwaldite	Zinnwaldite	Zinnwaldite	Zinnwaldite
Lithium (%)	0.89	1.40	1.21	0.96	0.96
Additives	CaSO ₄	CaSO ₄ , Ca(2005) ₂	CaCO ₃	CaSO ₄	Na ₂ SO ₄
Calcination temperature (1988)	850	950	825	1050	850
Calcination time (minutes)	60	60	60	60	60
Leach temperature (1988)	90	90	90 to 95	85	85
Leach time (minutes)	30	10	30	60	30
Water-to-calcine ratio	10:1	10:1	5:1	10:1	10:1
Lithium recovery (%)	12	96	90	84	>90
Liquor Li concentration (g/L)	0.1	0.7	0.4	0.2	~1*

Table 6:2 Comparison of the effect of temperature on lithium recovery via gypsum process.

Calcining temperature (°C)	Lithium recovery (%)	
	This study	Siame (2011)
500	-	0.81
850	0.77	0.83
900	12	24
950	-	52
1050	-	84

X-ray diffraction analysis was used to analyse the structural changes to the mineral after calcination. In Figure 6:7 XRD pattern of Beauvoir lithium concentrate and CaSO₄ calcined at 900°C for 60 minutes can be seen. In Figure 6:8 the XRD pattern for the sample after water leaching at 90°C for 30 minutes. The large peaks at 25 and 31 degrees are seen in both samples, although the intensity of the peak at 25 degrees decreases by 261 a.u. after leaching, thus observing a peak intensity of 1195 a.u. which can be explained by the addition of CaSO₄. There are also smaller peaks aligning at 39, 41, 49 and 56°C, thus indicating that similar thermal decomposition of the mineral sample has occurred with the resultant oxides formed being of a similar structure and chemical composition.

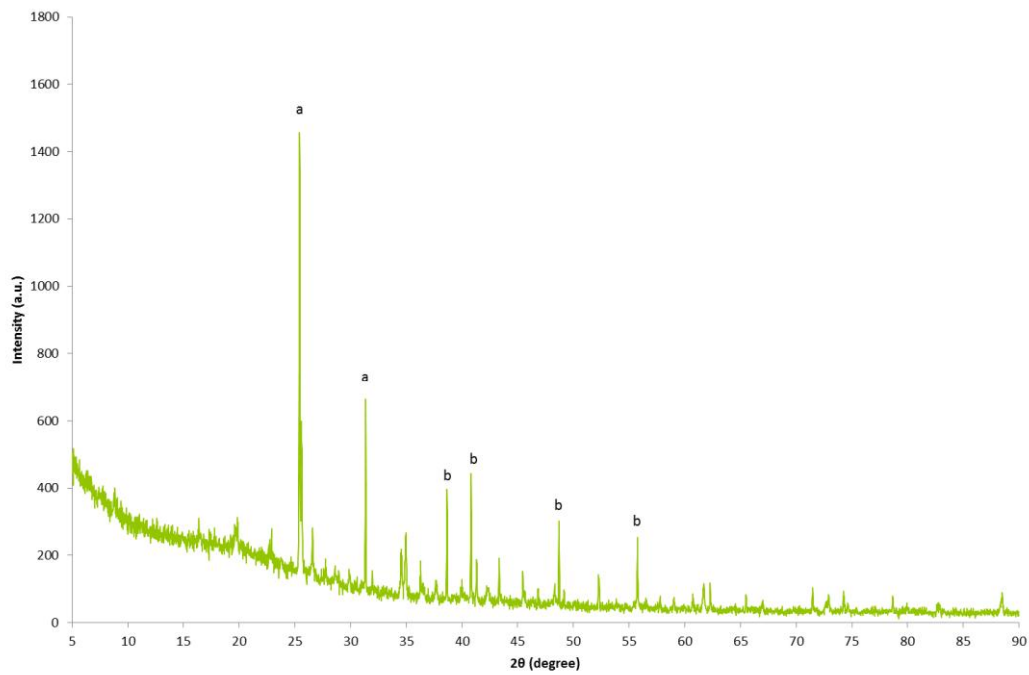


Figure 6:7 XRD pattern of Beauvoir lithium concentrate and CaSO_4 calcined at 900°C for 60 minutes, (a) CaSO_4 , (b) oxides.

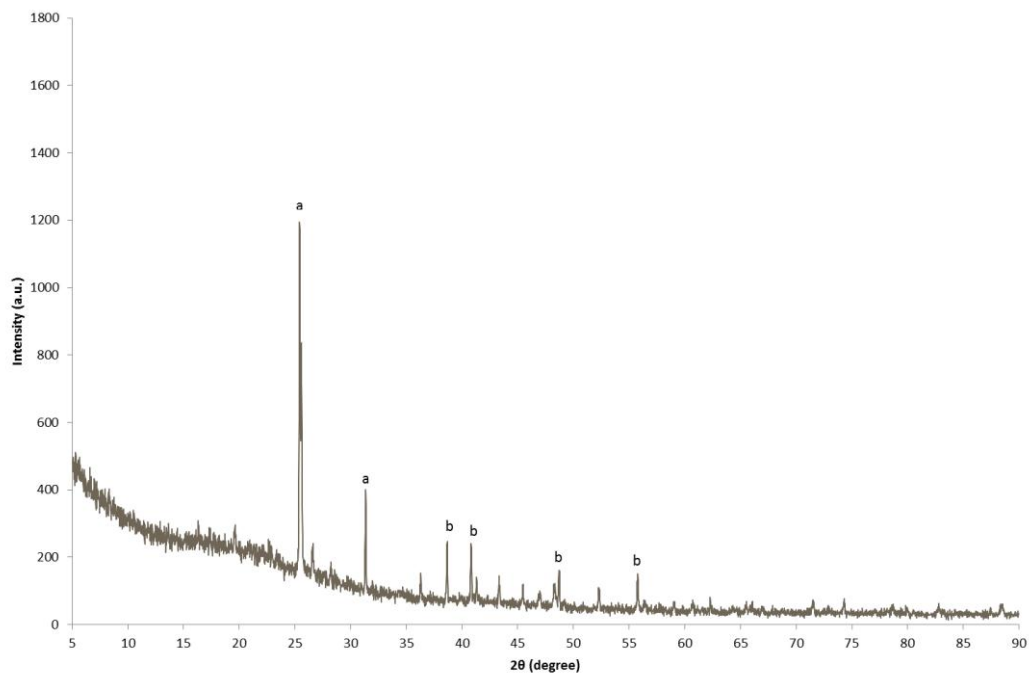


Figure 6:8 XRD pattern of Beauvoir lithium concentrate and CaSO_4 calcined at 900°C for 60 minutes and then leached with water at 90°C for 30 minutes, (a) CaSO_4 , (b) oxides.

6.2.3.3 Lithium extraction of the mineral specimen grade of pure lepidolite

In Figure 6:9 the XRD of the untreated mineral specimen grade pure lepidolite can be seen, characteristic peaks are observed at 20, 34 and 61 degrees with relative intensities of 780, 800 and 500 a.u confirming the presence of lepidolite in Figure 6:10 the X-ray diffraction of pure lepidolite and CaSO_4 after calcination at 850°C for 60 minutes. The changes observed suggested that heating the pure lepidolite at 850°C had altered the mineral structure. Other characteristic peaks at 20, 35, and 62 degrees in the samples the peaks were less intense in Figure 6:10. Two new peaks found which were due to the addition of CaSO_4 . The peaks observed at 25 and 31 degrees, showed an intensity of 1673 a.u. and 554 a.u., respectively.

Figure 6:11, the XRD pattern for pure lepidolite and CaSO_4 calcined at 850°C and then water leached at 90°C for 30 minutes can be seen. The XRD patterns are almost identical to Figure 6:10, with the exception of the peak intensity for the large peaks at 25 and 31 degrees. The peak at 25 degrees showed the greatest difference, for Figure 6:10 the intensity read 1673 a.u. whereas for Figure 6:11, 1233 a.u. thus after leaching the intensity decreased by 440 a.u. This could be explained as an effect of leaching the mineral and the chemical removal of soluble lithium species formed during the calcination process.

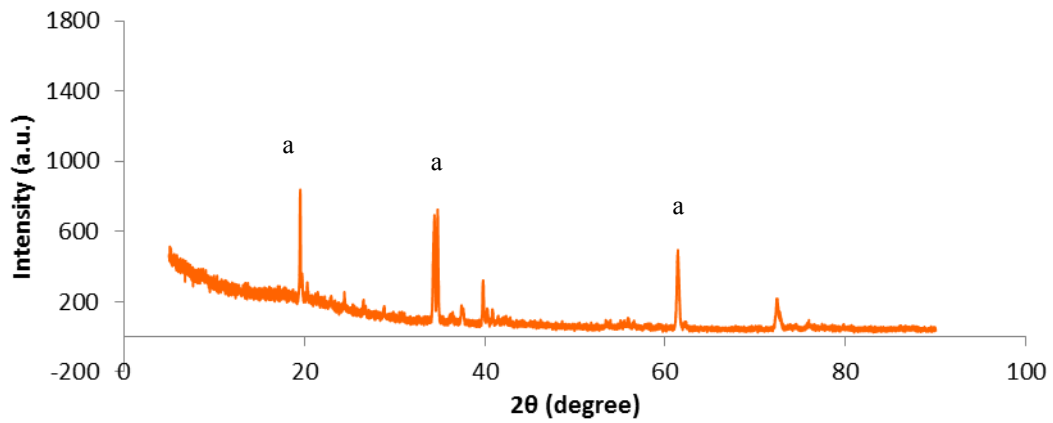


Figure 6:9 XRD pattern of mineral specimen grade pure lepidolite untreated, (a) lepidolite.

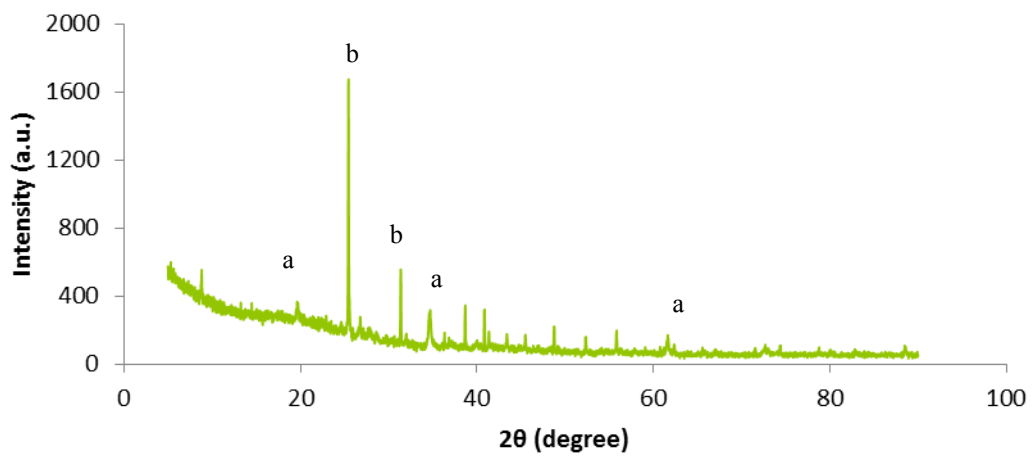


Figure 6:10 XRD pattern of pure lepidolite and CaSO_4 after calcination at 850°C for 60 minutes, (a) lepidolite, (b) CaSO_4 .

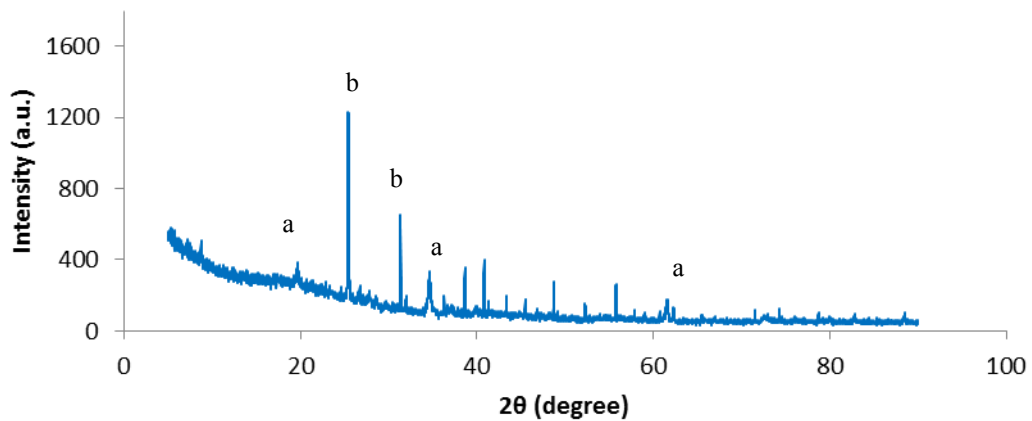


Figure 6:11 XRD pattern of pure lepidolite and CaSO_4 calcined at 850°C and then water leached at 90°C for 30 minutes, (a) lepidolite, (b) CaSO_4 .

In Figure 6:12 the results of the gypsum process on lithium extraction can be seen on the mineral lepidolite; the leach liquors were analysed by AAS to test for Li, Ca, Fe and Na. There was a significantly large difference observed for the efficiency of lithium extraction when the temperature increased from 850°C to 900°C. A lithium concentration of 95mg/L when calcining the material at 900°C compared to 24mg/L at 850°C.

It can be concluded that higher calcination temperatures play a vital role in lithium extraction. The study by Siame (2011) also found that when minerals were calcined above 900°C, significant changes were observed in the structure as well as higher lithium extraction, due to the formation of a leachable lithium compound, LiKSO_4 , as well as the formation of higher surface area due to mica delamination.

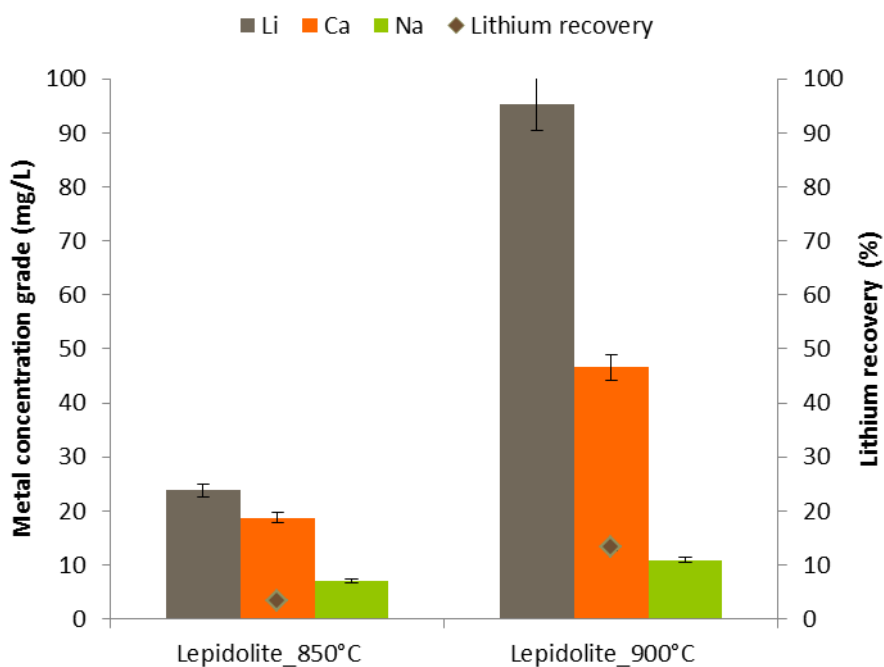


Figure 6:12 Metal extraction results for the gypsum method for lepidolite, the experiments were analysed three times, RSD <105%.

6.2.4 Summary of gypsum process

In order to efficiently precipitate the calcined material to lithium carbonate from the water leached calcine using the gypsum method, the process needed to achieve a lithium concentration of 9 g /L. This allows selective precipitation of lithium and prevents other elements from co-precipitating, such as: sodium and potassium which would act as impurities reducing the efficiency of the extraction process (Jandova, 2009). In this study using the Beauvoir lithium concentrate only achieved 71.72 mg/L of lithium in solution, when calcined at 900°C. To improve the efficiency of the extraction process a number of considerations would need to be investigated such as; higher temperatures of up to 1050°C would be required to potentially alter the lepidolite, further milling of the concentrate to create greater surface area to enhance the effects of leaching, investigate a choice of additive including: CaSO_4 , CaCO_3 and NaSO_4 , as well as the duration for each stage; calcination and water extraction. At present the lithium prices as a commodity show little sign of rising in the near future despite an increase in the demand, hence the extraction process would need to be low capital cost as well as operational costs. When taking into consideration all of the suggested variables to further improve the efficiency of the extraction process and the extra costs involved for the process to be potentially industrially attractive, it was not deemed economically efficient or technically viable to continue to the lithium solution to the precipitation stage for lepidolite. Imerys considered the gypsum process initially investigated to be marginally economical when considering the costs; hence any more milling to lepidolite or higher temperatures used would make the process uneconomical and also give it high a carbon footprint.

6.3 Organic acid leaching of lithium micas

6.3.1 Introduction

Lithium micas have been leached using industrial acids (Distin & Phillips, 1982) through chemical leaching (Napier-Munn, 2006) but little has been done in the field of bioleaching for lithium-bearing minerals. Organic acids leaching was investigated in this study as a proof of principle, as previous studies by Rezza (2001; 1997) also showed positive results for extracting lithium from spodumene when utilising microorganisms, such as; *A. niger*. Rezza (1997) found that the microorganisms produced organic acids such as; oxalic, citric and gluconic acids as part of their cellular metabolisms. These acids were suggested to have a certain roles in the leaching mechanism of lithium extraction from the minerals (Rezza, 2001). Santhiya (2005) and Strasser (1994) also found that bioleaching using *A.niger* produced high-yield oxalic acid.

This study investigated the potential of using organic acids for lithium dissolution, in order to further understand the role of organic acids types in the extraction process utilising heterotrophic microorganisms. Leaching metals from pegmatite ores, using heterotrophic microorganisms, has been investigated in a few studies such as; Vandevivere (1994). The study stated that silicates undergo natural weathering as a result of micro-organisms produced organic acids such as: oxalic acid ($H_2C_2O_4$) and citric acid ($C_6H_8O_7$).

The Beauvoir lithium concentrate investigated was made up of the following three minerals; albite, lepidolite and quartz in percentages of 35, 25 and 25%, respectively.

The remainder of the concentrate, 15%, was made up of: feldspar, topaz, kaolinite, muscovite, amblygonite and kyanite. The lepidolite mineral contained a concentration of 4.1 wt.% Li_2O . A mineral specimen grade pure lepidolite was also investigated, it contained 5.6 wt.% Li_2O .

6.3.2 Experimental procedure

The mineral specimen grade pure lepidolite (5.6 wt.% Li_2O) and Beauvoir lithium concentrate (4.1 wt.% Li_2O) were leached using organic acids in stirred flasks using 10% (w/v) pulp density and acid concentrations between 1 to 5% (w/v). The Beauvoir lithium concentrate was also heat treated prior to leaching at a temperature of 850°C for 60 minutes. Leaching experiments were conducted at 25, 40 and 70°C to evaluate the effect of temperature on the leaching process for up to 3 hours. Aliquots of 6mL were taken every hour over a period of 3 hours, the samples were filtered and then analysed. The dissolved lithium and iron concentrations were analysed by AAS and the pH reading were taken during the leaching process.

6.3.3 Results and discussion

6.3.3.1 Effect of using water as a leachant as a benchmark study

The lithium concentrations of the solutions when leaching with sterilised tap water were investigated for the mineral specimen grade pure lepidolite (5.6 wt.% Li_2O) and Beauvoir lithium concentrate (4.1 wt.% Li_2O). As shown in Table 6:3 after 10 days of leaching at ambient temperature (25°C) the lithium concentration in solution for the Mineral specimen grade pure lepidolite was 0.04mg/L and for the Beauvoir lithium

concentrate was 0.03mg/L. As lepidolite is a silicate mineral the lithium ion is covalently bonded within the structure of the mineral thus unlike lithium in its salt form the lithium-bearing mineral is not very soluble in water at room temperature.

Table 6:3 Extraction of lithium mica using water as a leachant.

	Particle size range (μm)	Li in solution (mg/L)	Fe in solution (mg/L)	pH
Sterilised tap water	-	0	0	7.6
Mineral specimen grade of pure lepidolite	< 212	0.04	<1.0	7.9
Beauvoir lithium concentrate	53 - 400	0.03	<1.0	7.8

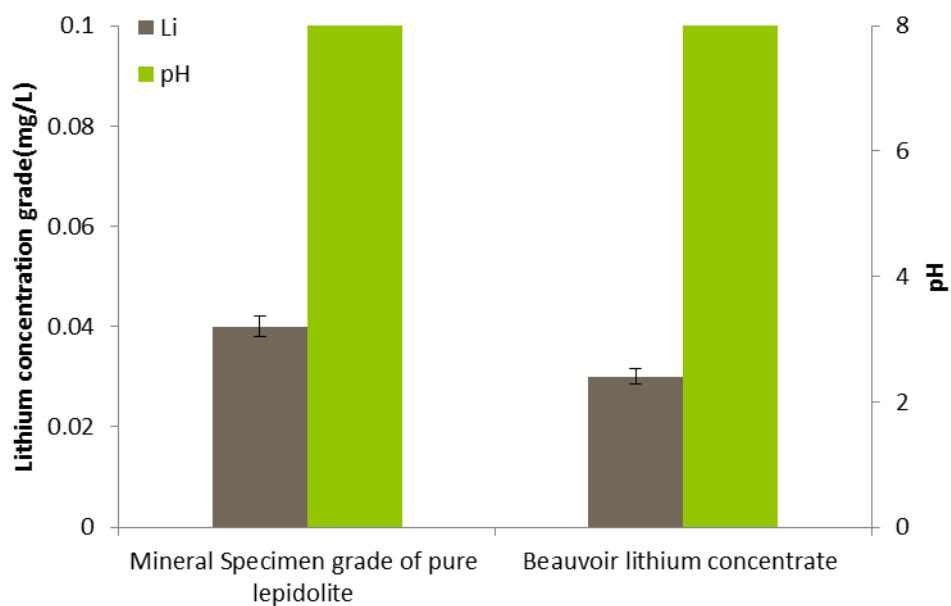


Figure 6:13 Extraction of lithium mica using water as a leachant, RSD <10%.

6.3.3.2 Effect of Oxalic acid concentration on leaching efficiency

The effect of oxalic acid concentration on leaching the Beauvoir lithium concentrate was investigated at 25°C, using concentrations of 1 and 5 % (w/v). The results are shown in Figure 6:14, both experiments saw an increase in lithium into solution over 3 hours. A higher lithium concentration of 3.5 mg/L was observed in the solution when using an oxalic acid concentration of 5 wt.%, which was significantly greater when compared to using a concentration of 1 wt.%, with a difference of 2.8 mg/L. The difference observed is suggested to be due to an increased number of H⁺ ions present in the higher acid concentration, which oxidise the metal within the mineral to produce higher lithium concentration in solution. The recovery rates shown in Figure 6:15 were very low for the acid concentrations, with the highest at 0.4 % for the concentration of 5 wt.% oxalic concentration.

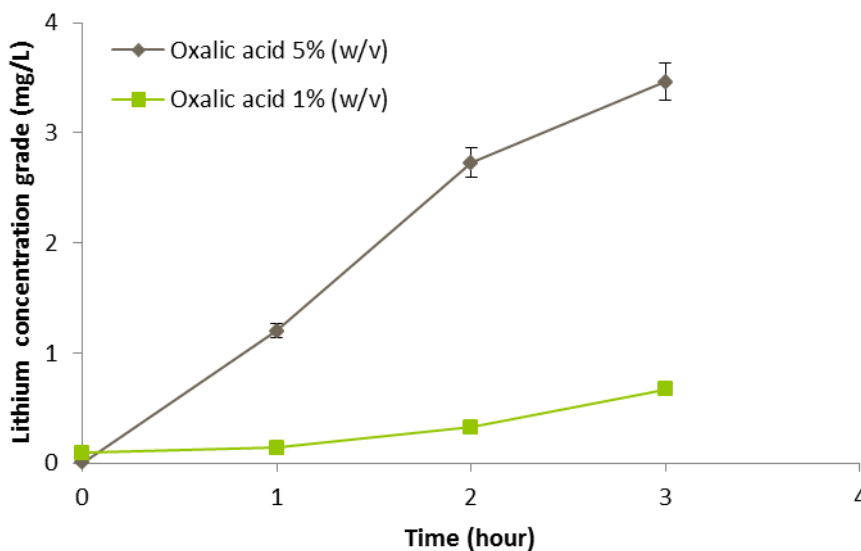


Figure 6:14 Lithium concentration in solution for the Beauvoir lithium concentrate leached at 25°C, with oxalic acid at varying acid concentrations, RSD < 10%.

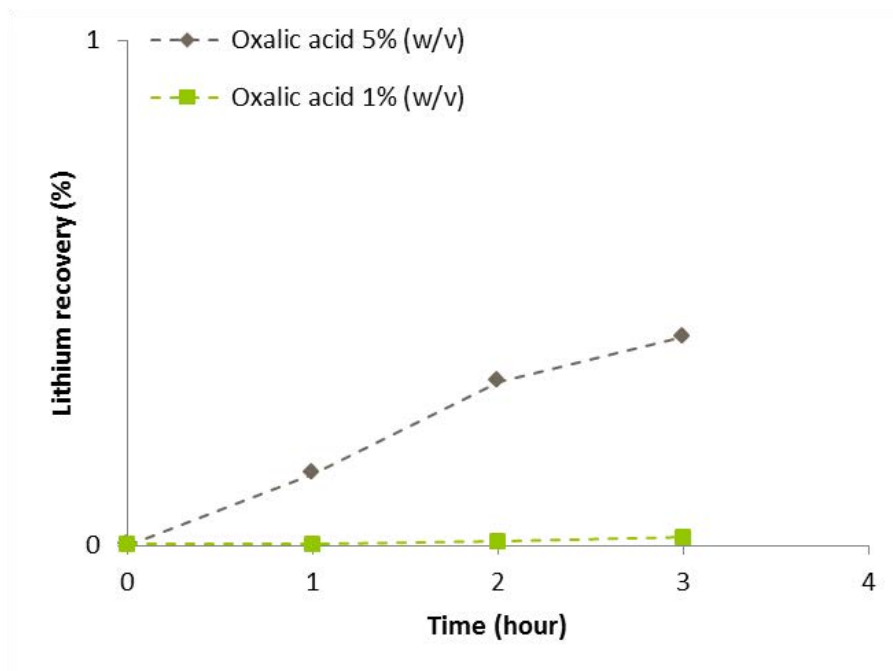


Figure 6:15 Lithium recovery for the Beauvoir lithium concentrate leached at 25°C, with oxalic acid at varying acid concentrations.

6.3.3.3 Effect of oxalic acid solution temperature on leaching efficiency

In Figure 6:16, the effect of temperature on the leaching efficiency of the Beauvoir lithium concentrate when using a concentration of 1% (w/v) oxalic acid can be seen, the temperatures investigated were 25, 40 and 70°C. It was expected that at higher leaching temperatures the lithium concentration in solution would increase, due to the reaction kinetic of the leaching process (Napier-Munn, 2006).

The highest lithium concentration in solution was detected when leaching at 70°C, after 3 hours up to 12mg/L was detected in the leach liquor. This gave an increase of 11 mg/L over the leaching time, initially only 0.95 mg/L of lithium was detected [as a safety pre-caution the mineral and acid were in contact before the temperature was

achieved]. For the experiments using the leaching temperatures of 25 and 40°C only 1 and 3 mg/L were detected in the in the leach liquor, respectively. In Figure 6:17, when leaching with 5% (w/v) oxalic acid concentration 29mg/L was detected in the leach liquor, at a temperature of 70°C. Whereas for the lower leaching temperatures of 25 and 40°C, lithium extraction were at lower concentrations of 4 and 6 mg/L, respectively. As reported, the increase in lithium extracted at higher temperatures can be explained by reaction kinetics, in this study an overall an increase of 25mg/L was observed when leaching at 25°C compared to when leaching at 70°C. From these results it can be assumed that the increased temperatures had a greater effect on the amount of lithium in solution when compared to increasing the concentration of the leachant, in this case oxalic acid. Figure 6:18 and Figure 6:19 show the recovery rates for the oxalic acid concentrations of 1 and 5% (w/v), at the varying temperatures. The results also showed that as the temperature increased the extraction of lithium from the mineral also increases the recovery efficiency, however the lithium recoveries are very poor, these results agree with finding by Jandova (2010).

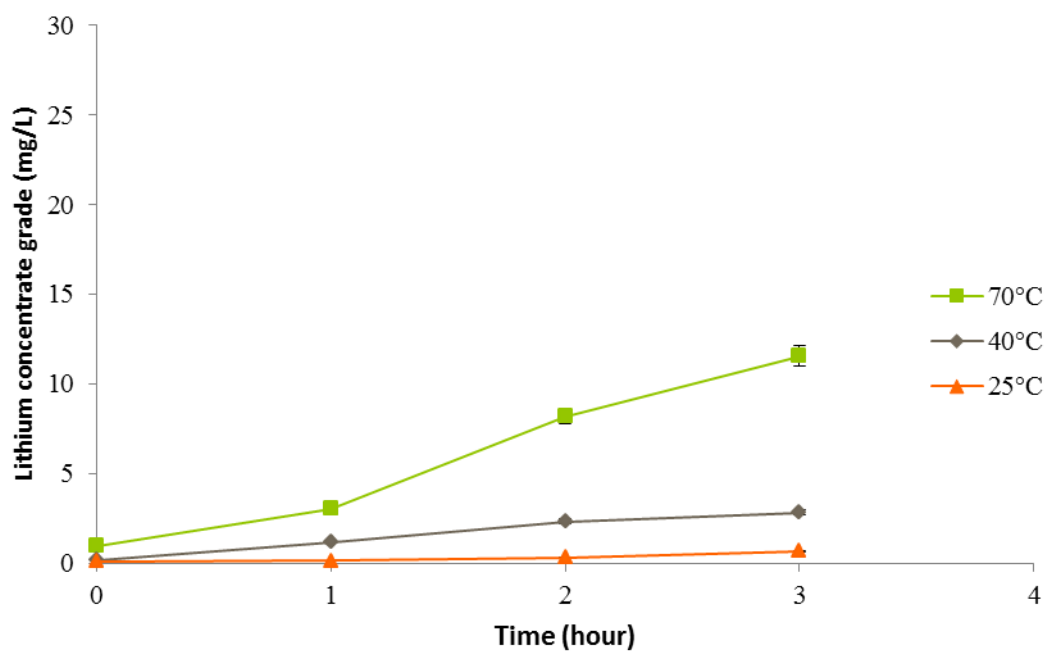


Figure 6:16 Lithium concentration in solution for the Beauvoir lithium concentrate leached with oxalic acid (1% w/v) at varying temperatures, RSD <10%.

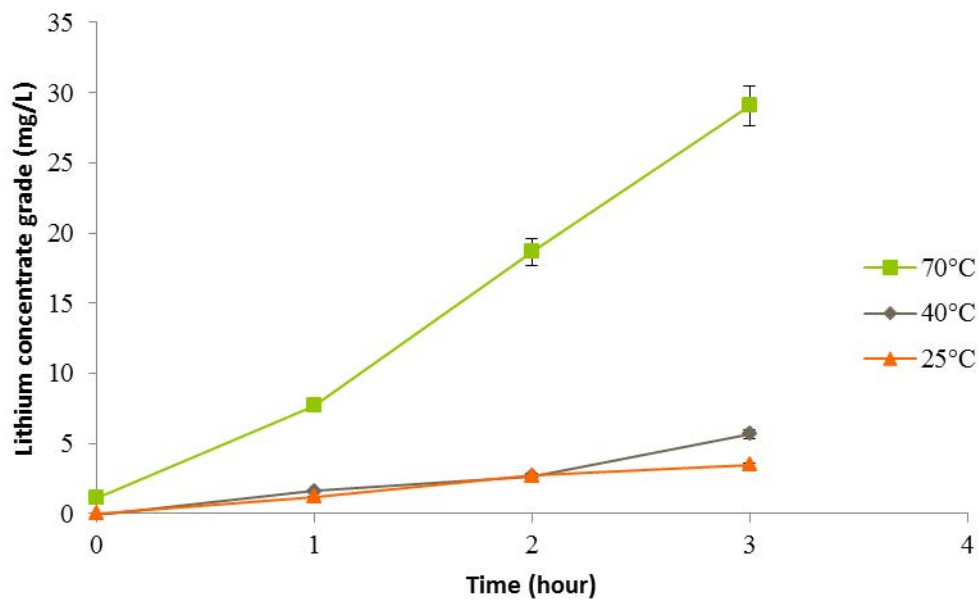


Figure 6:17 Lithium concentration in solution for the Beauvoir lithium concentrate leached with oxalic acid (5% w/v) at varying temperatures, RSD <10%.

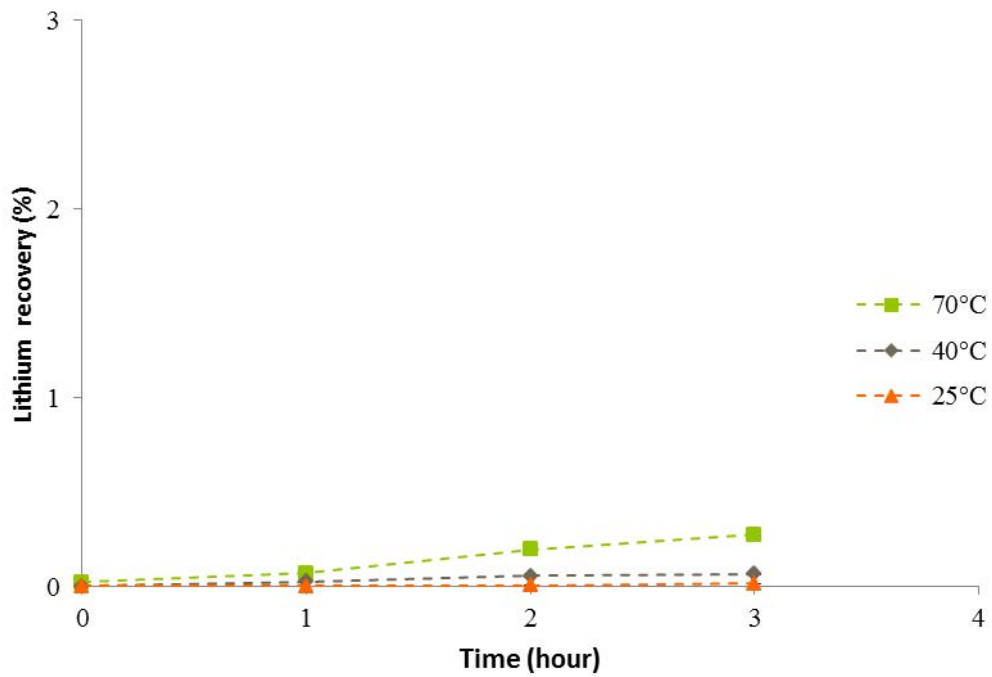


Figure 6:18 Lithium recovery for the Beauvoir lithium concentrate leached with oxalic acid (1% w/v) at varying temperatures.

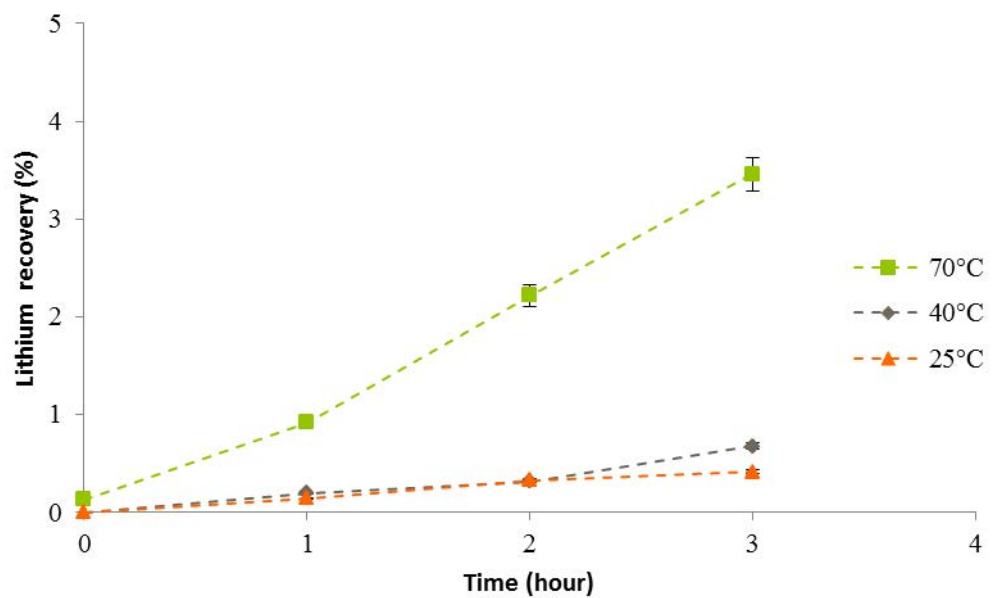


Figure 6:19 Lithium recovery for the Beauvoir lithium concentrate leached with oxalic acid (5% w/v) at varying temperatures.

6.3.3.4 Effect of pre-treatment on the leaching efficiency

The effect of thermal pre-treatment on leaching the Beauvoir lithium concentrate was investigated using oxalic acid at concentrations of 1 and 5% (w/v), as well as at varying temperatures of 25, 40 and 70°C. The concentrate was heat treated at 850°C for 60 minutes prior to leaching.

6.3.3.4.1 Varying the oxalic concentration

In Figure 6:20 and Figure 6:21 the heat treated Beauvoir lithium concentrate was leached with oxalic acid concentrations of 1 and 5% (w/v) at 25°C. The lithium concentrate was investigated under two conditions; heat treated (HT) prior to leaching and untreated (UT). When leaching the lithium concentrate with 1% (w/v) oxalic acid, the heat treated concentrate was significantly more reactive with the oxalic acid; 58mg/L was observed in the leach liquor after a leaching period of 3 hours, whereas for the untreated concentrate only 0.7 mg/L was detected after 3 hours. In comparison, the heat treated concentrate showed significantly greater lithium dissolution in shorter periods of time, after 1 hour of leaching 36 mg/L was detected in the leach liquor. In Figure 6:21 the results for the increased oxalic acid concentration of 5 wt.% are shown, again the heat treated Beauvoir lithium concentrate showed significantly greater results for the lithium extraction, 84 mg/L after 3 hours.

Heat treatment of the lithium concentrate prior to leaching, increased the surface area contained within the mineral structure, hence it gave better mineral/acid reaction conditions. Figure 6:22 and Figure 6:23 show that this also increased the leaching

efficiency of the process, although at 25°C the recovery rates were still low. The highest lithium recovery was 10% this was for 5% (w/v) oxalic acid heat treated.

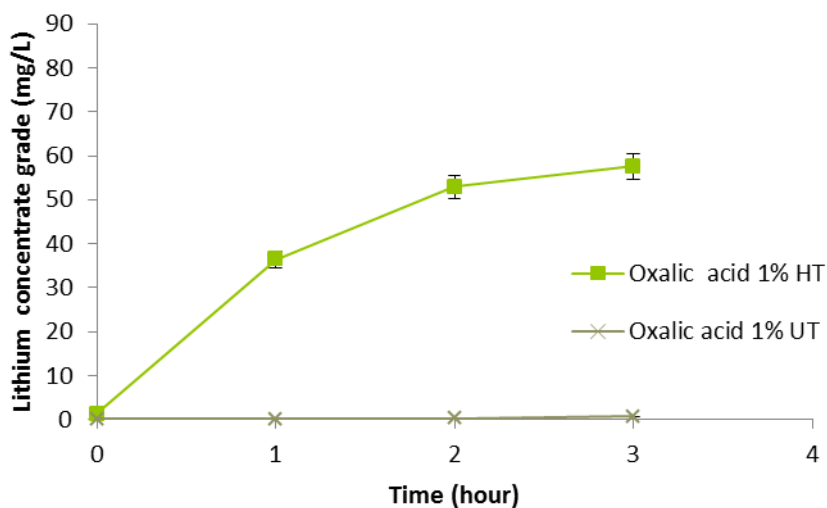


Figure 6:20 Lithium concentration in solution for the Beauvoir lithium concentrate leached with 1% (w/v) oxalic acid, the concentrate was heat treated (HT) and untreated (UT) prior to leaching at 25°C, RSD <10%.

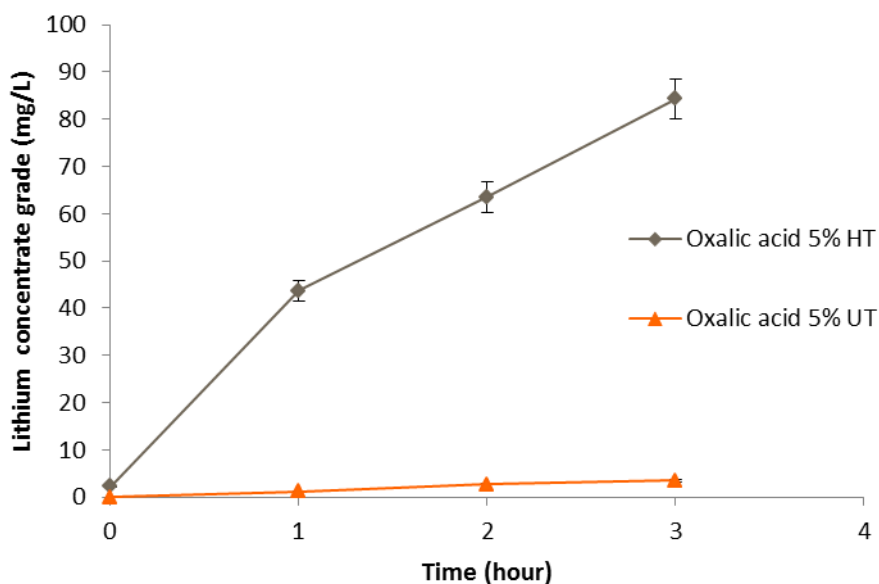


Figure 6:21 Lithium concentration in solution for the Beauvoir lithium concentrate leached with 5% (w/v) oxalic acid, the concentrate was heat treated (HT) and untreated (UT) prior to leaching at 25°C, RSD <10%.

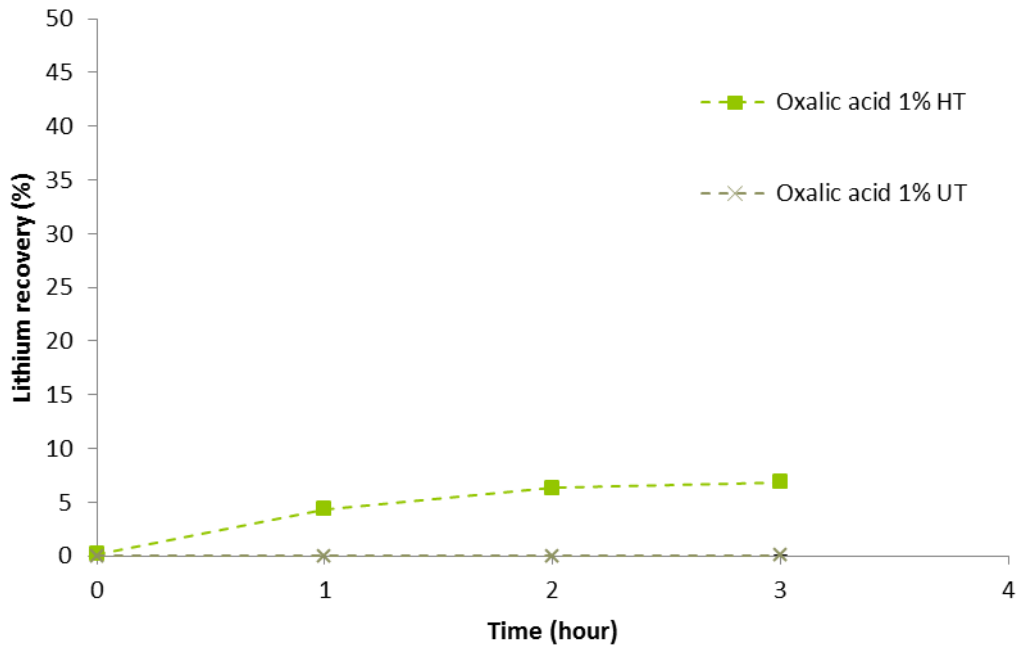


Figure 6:22 Lithium recovery for the Beauvoir lithium concentrate leached with 1 wt.% oxalic acid, the concentrate was heat treated (HT) and untreated (UT) prior to leaching at 25°C.

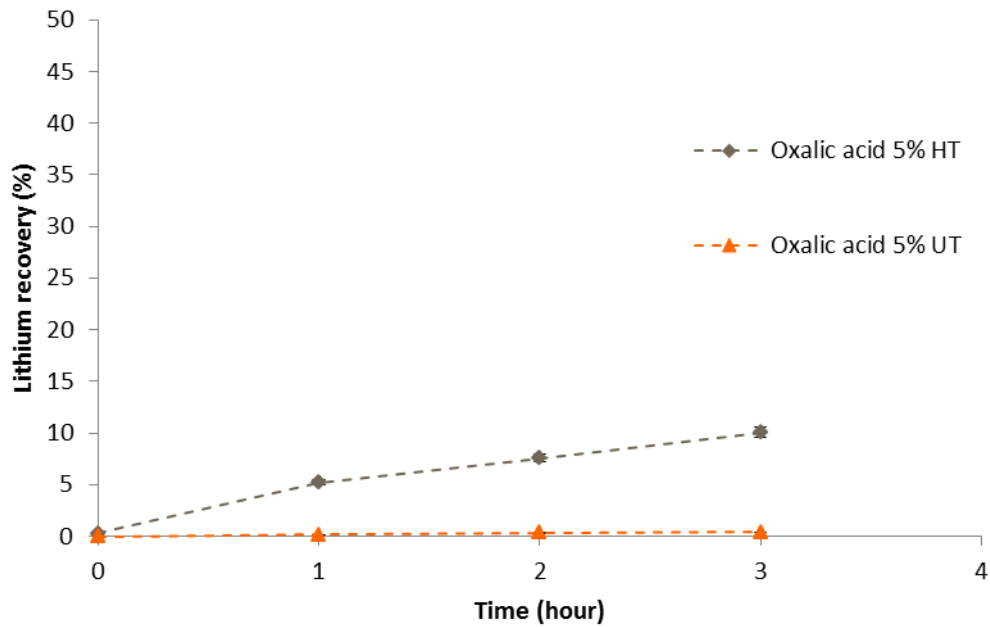


Figure 6:23 Lithium recovery for the Beauvoir lithium concentrate leached with 5 wt.% oxalic acid, the concentrate was heat treated (HT) and untreated (UT) prior to leaching at 25°C.

6.3.3.4.2 The effect of leaching on heat treated Beauvoir lithium concentrate

In Figure 6:24 and Figure 6:25 it can be seen that the heat treated Beauvoir lithium concentrate was leached using oxalic acid concentrations of 1 and 5% (w/v) at the temperatures: 25, 40 and 70°C. Due to safety pre-cautions the leachant was added to the concentration and then heated to the required temperature.

The results in Figure 6:24 agreed with previous observations, when increasing the leaching temperature, as the lithium concentration in solution increased with leaching temperature. The highest amount of lithium detected was after 3 hours for the highest leaching temperature of 70°C and was 186 mg/L. After the first hour of leaching the lithium concentrations increased steadily, reaching 141, 168 and 186 mg/L after 1, 2 and 3 hours of leaching, respectively. In Figure 6:25, the final leach liquor for the varying temperatures of; 25, 40 and 70 were 84, 198 and 424 mg/L, respectively. Comparing the lithium concentration for the final leach liquor, when leaching at 40°C an increase of 114 mg/L was observed in comparison to leaching at 25°C, when leaching at 70°C this further increased to 340 mg/L. The highest lithium concentration found when leaching at 70°C, after 3 hours of leaching was 424 mg/L. This was significantly greater than leaching the untreated Beauvoir concentrate under similar conditions, which achieved only 29 mg/L as shown in Figure 6:17. The recovery rates for the experiments are shown in Figure 6:26 and Figure 6:27, it shows for 1% (w/v) oxalic acid concentration it was only possible able to achieve 7, 14 and 22% recovery for the temperatures 25, 40 and 70°C, respectively, although in Figure 6:27 a lithium recovery of 51% for the experiment carried out at 70°C was observed.

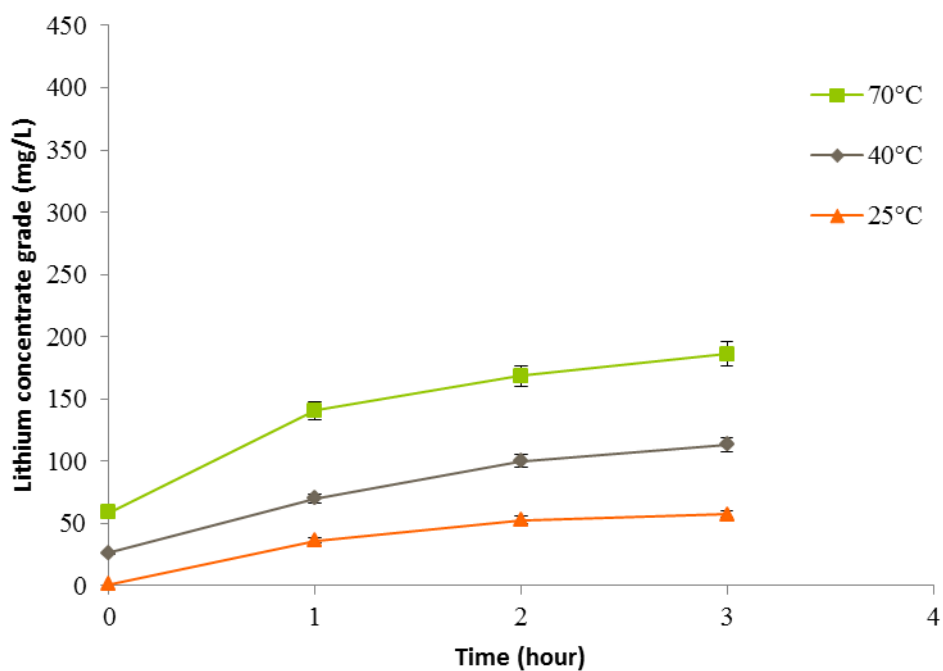


Figure 6:24 Lithium concentration in solution for the Beauvoir lithium concentrate (heat treated) leached with oxalic acid (1% w/v) at varying temperatures, RSD <10%.

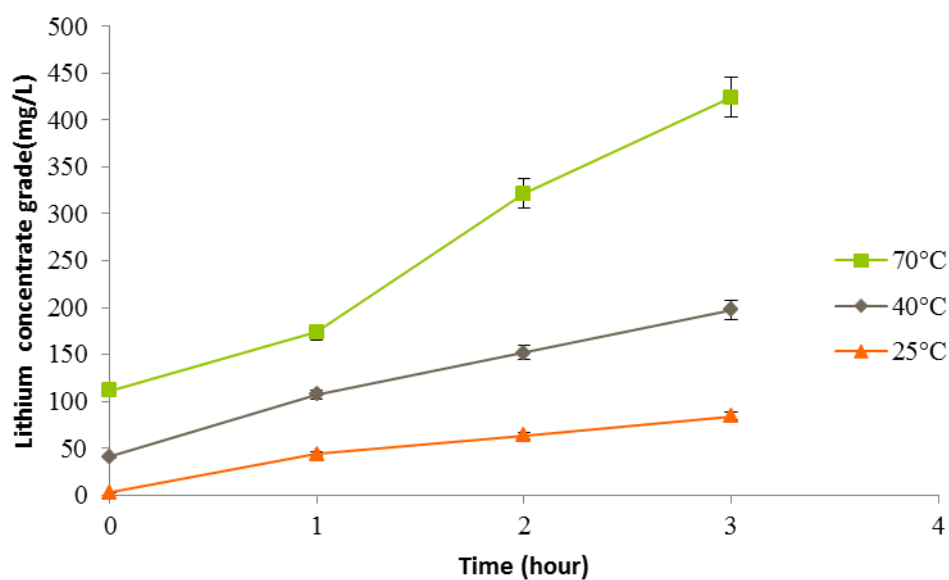


Figure 6:25 Lithium concentration in solution for the Beauvoir lithium concentrate (heat treated) leached with oxalic acid (5% w/v) at varying temperatures, RSD <10%.

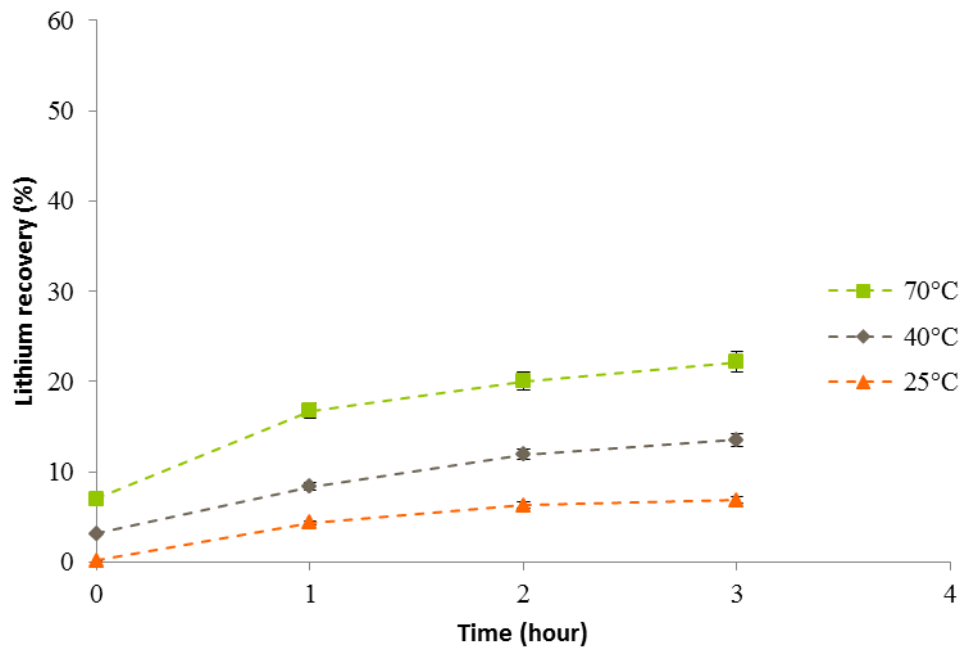


Figure 6:26 Lithium recovery for the Beauvoir lithium concentrate (heat treated) leached with oxalic acid (1% w/v) at varying temperatures.

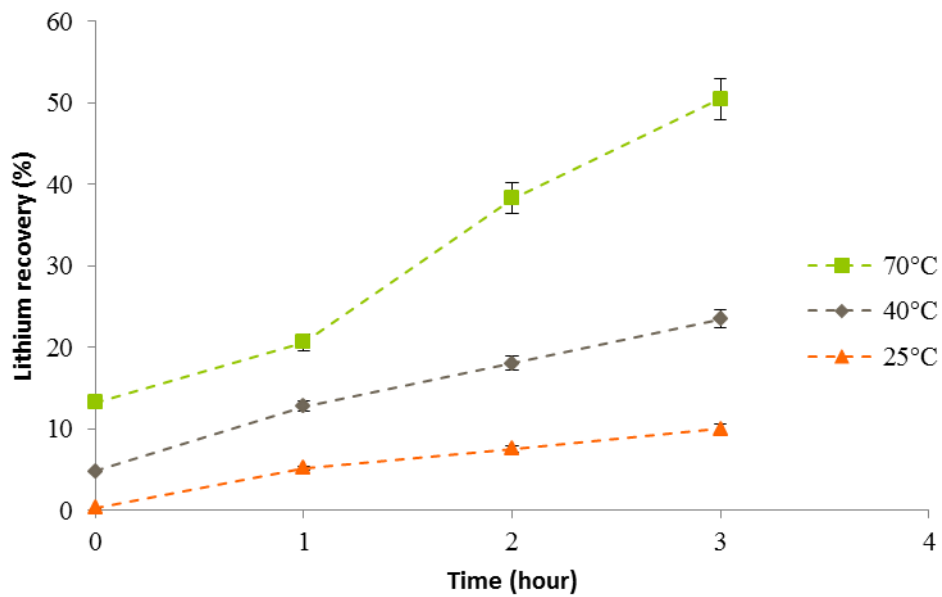


Figure 6:27 Lithium recovery for the Beauvoir lithium concentrate (heat treated) leached with oxalic acid (5% w/v) at varying temperatures.

In Figure 6:28 a comparison between the effects of prior heat treatment and leaching temperature can be seen. The heat treated mineral leached at 25°C gave three times the amount of lithium into solution compared to the untreated mineral leached at 70°C, showing that heat treatment to the mineral prior to leaching had a significant effect on the amount of lithium leached into solution. It can be suggested that heat treatment to the mineral expanded the lattice structure, which allowed an easier dissolution of lithium into solution suggesting that heat treatment made the lithium mineral more soluble. This was also reported by Fang (2002) when heating lepidolite to temperature up to 1120°C.

Table 6:4 Size of lepidolite crystal at various heat-treatment temperature (Fang, 2002).

Temperature (°C)	950	1000	1060	1080	1100	1120
Average diameter (µm)	0.58	0.90	1.76	2.87	4.09	5.15
Average thickness (µm)	0.20	0.24	0.38	0.53	0.56	0.60
Aspect ratio	2.90	3.75	4.63	5.42	7.32	8.52

A positive result was also observed for the untreated lithium concentrate leached at both 25°C and 70°C, which showed the potential for extracting lithium using oxalic acid. Santhiya (2005) found that oxalic acid was produced when bioleaching with *A. niger*, thus the investigation showed the potential for extraction of lithium using bioleaching processes.

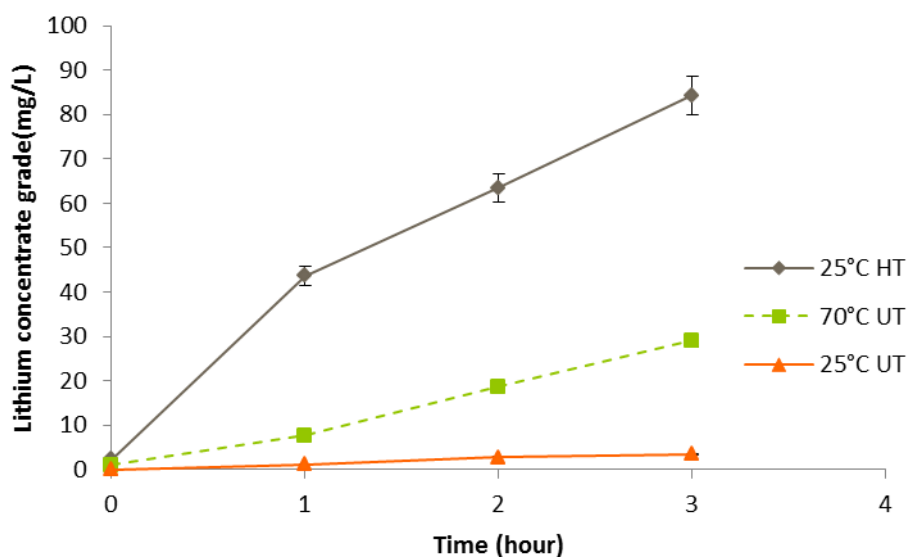


Figure 6:28 Lithium concentration for the Beauvoir lithium concentrate leached with oxalic acid (5% w/v) at varying temperatures RSD <10%. Heat treated (HT) and untreated (UT) Beauvoir concentrates.

6.3.3.5 Effect of Citric acid on the lithium leaching efficiency using the Beauvoir lithium concentrate

The effect of leaching Beauvoir lithium concentrate was investigated using citric acid as the leachant at an acid concentration of 5% (w/v), citric acid was chosen as the fungi *A. niger* is commonly known to produce citric acid as well as oxalic acid (Rezza, 2001). Citric acid has been successful in the leaching of low grade lithium ores (Mehdi, 2013).

6.3.3.5.1 Varying the temperature

Leaching experiments were carried out for the heat treated Beauvoir lithium concentrate with a citric acid concentration of 5% (w/v), at temperatures of 25 and 40°C. In Figure 6:29 it can be seen that the leaching at 40°C achieved a greater amount of lithium dissolution, when compared to 25°C. The lithium recovery for the experiments was very

low, only achieving up to 0.1%. The lithium dissolution was similar to the leaching experiments using oxalic acid concentration of 5% (w/v). Other authors have stated that increasing the reaction temperature in lithium extraction from mineral ores would increase the overall efficiency (Jandová., 2010; Yan, 2012).

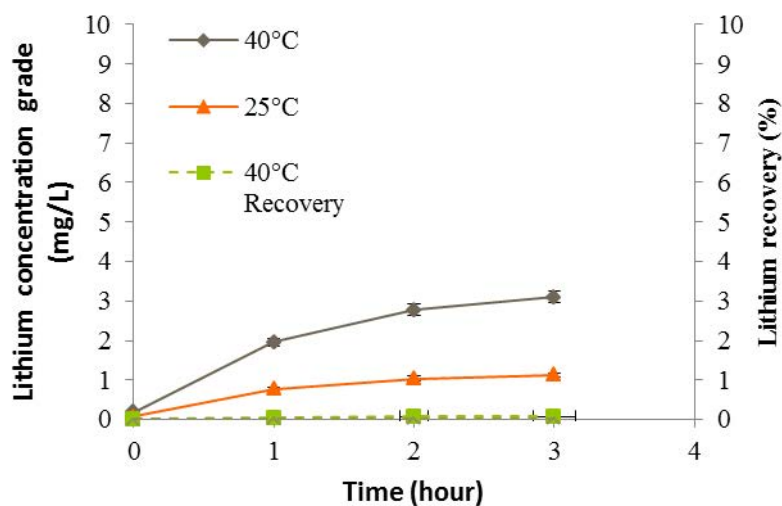


Figure 6:29 Lithium concentration and recovery for the Beauvoir lithium concentrate (untreated) leached with citric acid (5% w/v) at varying temperatures, RSD <10%.

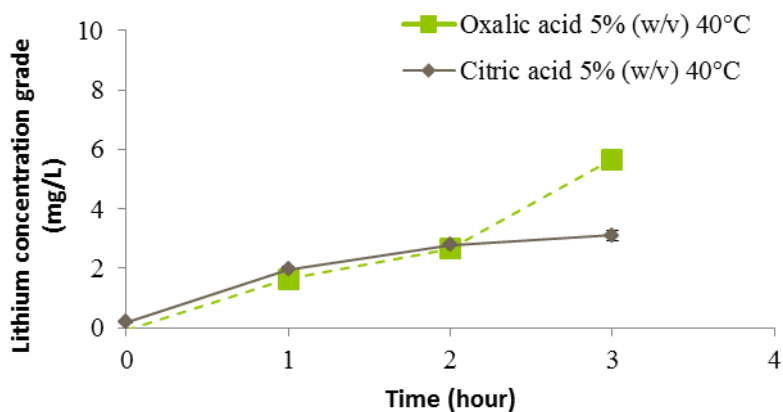


Figure 6:30 Comparison of lithium concentration for the Beauvoir lithium concentrate (untreated) leached with oxalic and citric acid (5% w/v) at 40°C, RSD <10%.

6.3.3.5.2 Effect of heat treatment of Beauvoir lithium concentrate prior to leaching efficiency

The Beauvoir lithium concentrate was heat treated at 850°C for 2 hours prior to leaching to assess the effect of thermal pre-treatment on leaching efficiency. The leachant used was citric acid in a concentration of 5% (w/v) and leaching temperatures of 25, 40 and 70°C were investigated. In Figure 6:31 it can be seen that an increase in leaching temperature also shows an increase in the lithium concentration, after 3 hours of leaching the lithium concentration was 123 mg/L when leaching at 70°C and 78 mg/L at 25°C. The recovery rates for the experiments were only up to 3% for the experiment at 70°C, making the process economically unattractive.

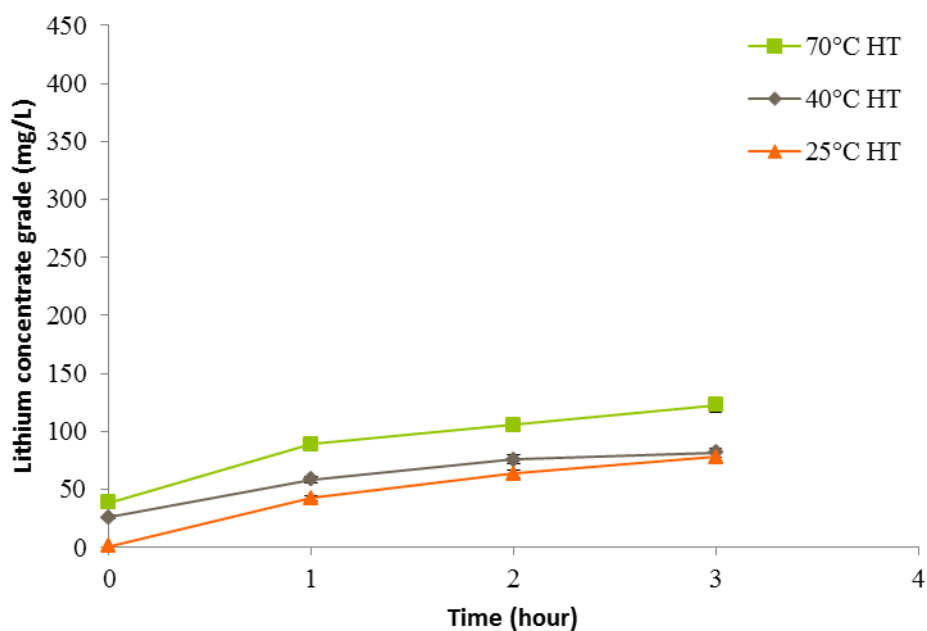


Figure 6:31 Lithium concentration in solution for the Beauvoir lithium concentrate (Heat treated) leached with citric acid (5 % w/v) at varying temperatures, RSD <10%.

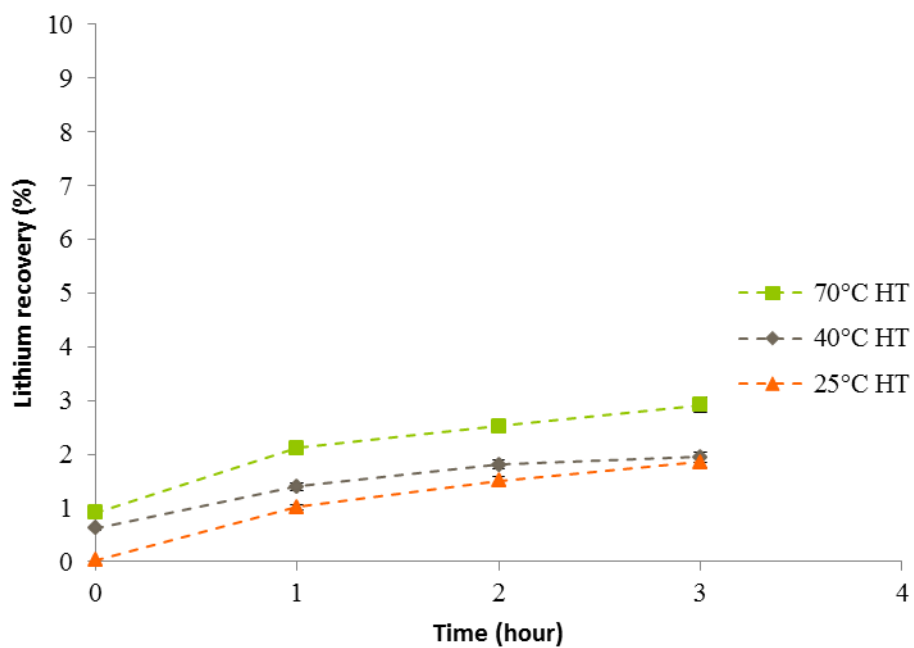
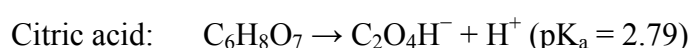
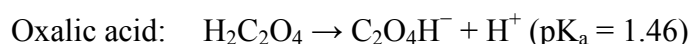


Figure 6:32 Lithium recovery for the Beauvoir lithium concentrate (Heat treated) leached with citric acid (5% w/v) at varying temperatures.

6.3.4 Summary of organic acid process

The results from this study showed that oxalic acid had a stronger dissociation, when compared to citric acid. Both organic acids produce H^+ ions as shown in the equations below, for oxalic acid, the oxalate ligand is formed.



Oxalic and citric acid leaching reformers at temperatures of $70^\circ C$ can be seen in Figure 6:33 and Figure 6:34. Using 1% (w/v) oxalic acid concentration achieved a greater lithium extraction after 3 hours of leaching when compared to a concentration of 5% (w/v) citric acid. The highest lithium concentrate grade was when leaching using a concentration of 5% oxalic acid at $70^\circ C$, 424mg/L after 3 hours with a lithium recovery of 51%. When using a concentration of 1% oxalic acid at $70^\circ C$, 186mg/L after 3 hours with a lithium recovery of 22%.

To optimise the process, lower leaching temperatures were investigated, as an increase in process energy requirements for lithium extraction which in turn means an increased operational cost of the leaching process. In Figure 6:35 and Figure 6:36, lower temperatures of $40^\circ C$ comparing the leachates; oxalic acid and citric acid (concentration of 5% w/v) leaching heat treated Beauvoir lithium concentrate. After 3 hours of leaching oxalic acid was more efficient at extraction lithium into solution with a lithium level of 198 mg/L and recovery rate of 24%.

The organic acid results from this study agreed with the study by Rezza (2001, 1997). Rezza found that when bioleaching the lithium-bearing mineral spodumene with *A.niger*, the leach liquor contained higher concentrations of oxalic acid, observing 8.0mM of oxalic acid and 0.09mM of citric acid in the solution after 30 days. Also studies by Sun (2012) and Li et al (2010) found oxalate leaching to recover cobalt and lithium from spent lithium-ion batteries. Organic acids investigated were oxalic, citric and malic acids, with a preference to oxalic acid as it is more easily soluble in water.

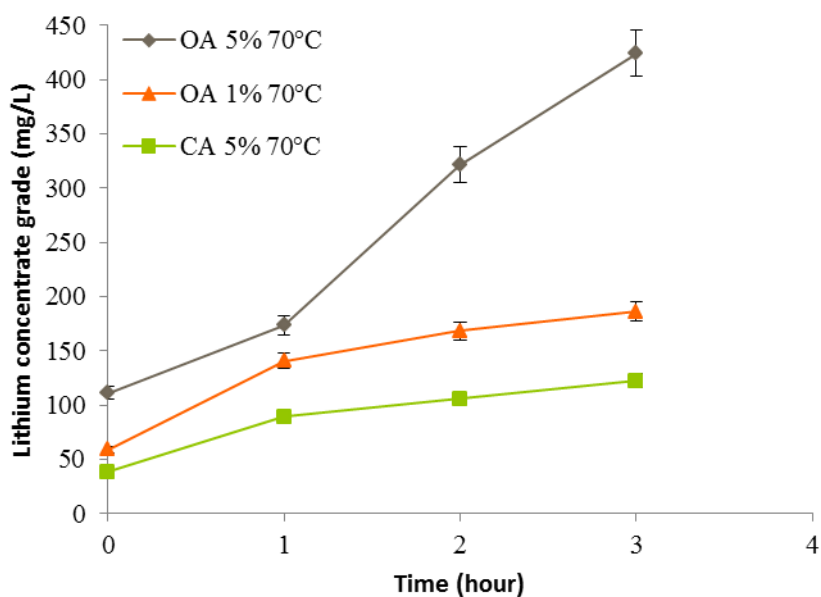


Figure 6:33 Comparison of lithium concentration in solution for the Beauvoir lithium concentrate (Heat treated) leached with oxalic and citric acids (5% w/v) at 70°C, RSD <10%.

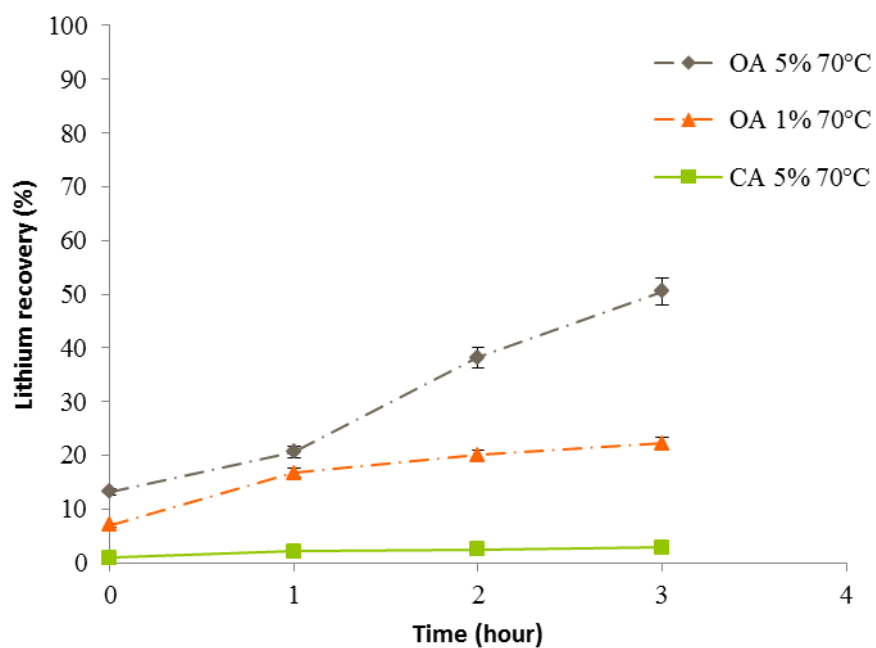


Figure 6:34 Comparison of lithium recovery for the Beauvoir lithium concentrate (Heat treated) leached with oxalic and citric acids (5% w/v) at 70°C.

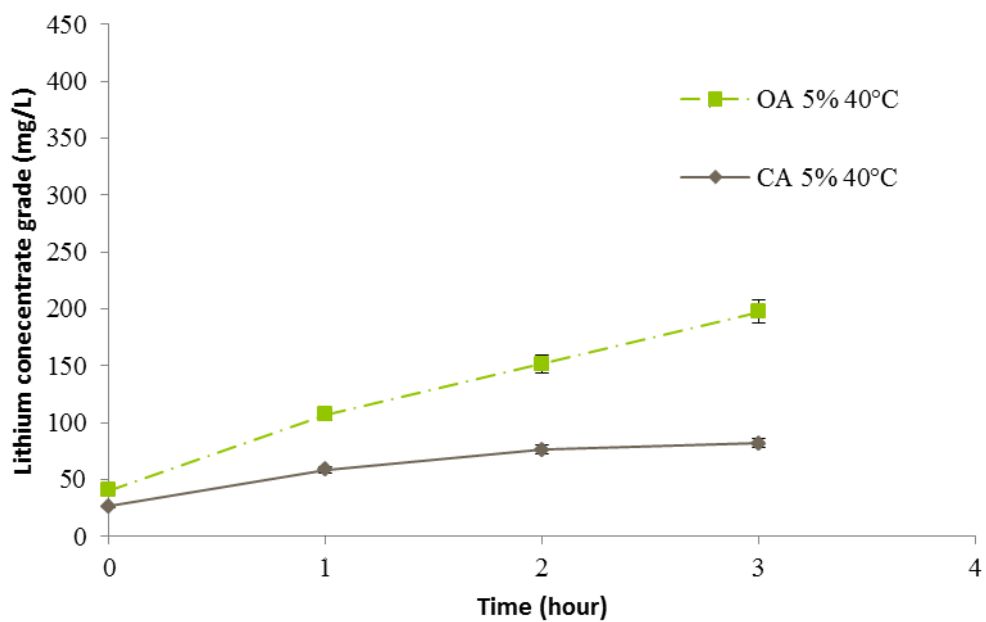


Figure 6:35 Comparison of lithium concentration for the Beauvoir lithium concentrate (heat treated) leached with oxalic and citric acid (5% w/v) at 40°C, RSD <10%.

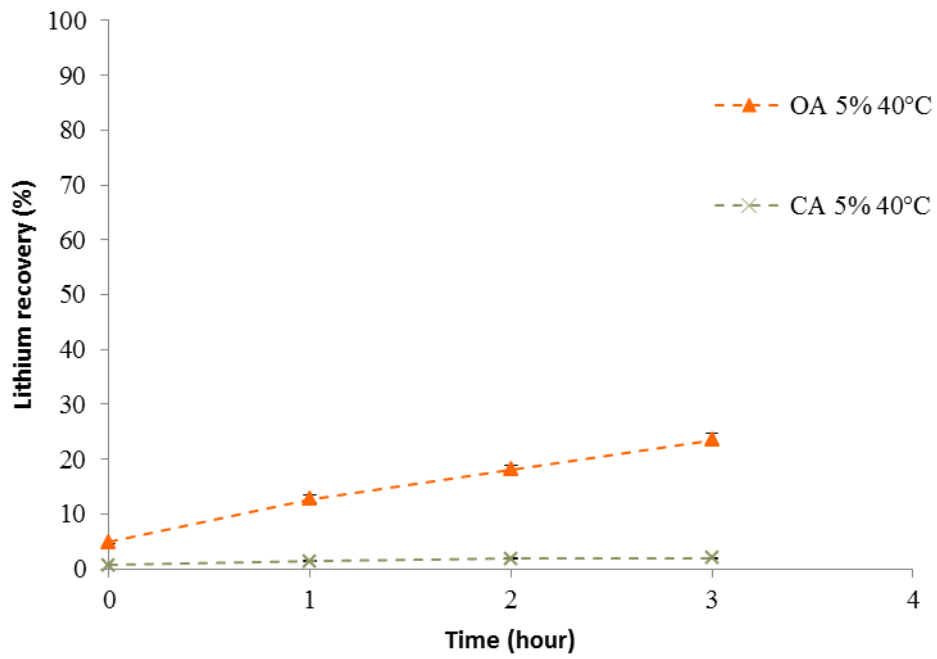


Figure 6:36 Comparison of lithium recovery for the Beauvoir lithium concentrate (heat treated) leached with oxalic and citric acid (5% w/v) at 40°C.

6.4 Mine water analysis from kaolin sites

6.4.1 Introduction

This section investigated the potential presence of microorganisms in the water samples from Imerys kaolin mine sites, by analysing the lithium concentrations in waste water. The potential presence of microorganisms or lithium in the water would suggest that biological dissolutions could already be taking place around the site, facilitating the extraction of lithium from the mineral. As bioleaching utilises naturally occurring microorganisms to leach the desired metal into solution, the extraction process is potentially economical viable as well as environmentally friendly due to not involving new microorganisms to the microbial ecosystem, thus reducing risk factors and making the process. In studies by Rezza (2001; 1997) three naturally occurring microorganisms (*A. niger*, *P. purpurogenum* and *R. rubra*) were identified from the lithium-bearing mineral spodumene, concluding that these were naturally occurring in mine sites.

6.4.2 Experimental procedure

The water samples analysed in this study were obtained from the Beauvoir mine site in France and the St Austell sites in the UK. The samples were analysed by AAS to detect metal concentrations, including: Li, Fe, Ca, K and Na. These metals are commonly found in microbial communities, thus their presence could suggest interesting microorganisms are present in the water around the mine site. The samples were also analysed using flow cytometry to detect the presence and size of microorganisms and get a better understanding of the environment. Flow cytometry measures and analyses characteristics of particles such as single particles and cells. To determine the presence of DNA particles a permanent cell dye was used to stain the DNA particles, SYTO 62. To prepare the sample vials; 10 μ m of SYTO 62 (200 μ M) was added a mixture of 50 μ L of the sample and 1mL of filtered H₂O. The vials were placed in a tray and then covered using foil, due to SYTO 62 being light sensitive. The tray was placed in an oven at 37°C for 30 minutes. The samples were then analysed by running the solution through the flow cytometer.

6.4.3 Beauvoir mine water analysis

The Beauvoir mine site in France had two main sites where water was sampled from; the mine and the nearby lake. In Figure 6:37 images of the two sites are shown. The sites were chosen as they were in close proximity to the mine where the kaolin was extracted and the mica wastes were stored.



Figure 6:37 Left image: Mine site in Beauvoir, France. Right image: lake near the mine in Beauvoir, France.

6.4.3.1 Metal content analysis

The pH reading of the samples was taken on site, for the mine it was 6.0 and the lake was slightly lower at 6.6. The samples were then isolated and analysed for their metal content, the results are shown in Table 6:5. The samples were analysed using AAS, the lake water (0.13 mg/L) contained slightly higher lithium concentration compared with the mine water, 0.09 mg/L. The lower levels of lithium concentration in the mine water can be explained by the DNA count, showing both the dead and live cells. The DNA content for the mine water sample was 917 cells per μL and a higher cell count of 1765 per μL for the DNA particles in the lake sample. This suggested that the microbial community was present and may play a role in the possible extraction lithium into solution. Flow cytometry was also used to plot the growth of bacterial species over the leaching period. As shown in Figure 6:38, the DNA particles are found within the red gate labelled R1, it was determined that 26.6% of the samples was from the DNA particles. To exclude debris and background, a standard gate was applied to each

sample, the gate was chosen from previous analysis which determined where cell particles were found in the samples.

Table 6:5 Summary of the results for mine water sampled from Beauvoir, France, *tr: trace.

Sample	Site in Beauvoir	pH	Metal concentration (mg/L)					DNA count
			<i>Li</i>	<i>Fe</i>	<i>Ca</i>	<i>K</i>	<i>Na</i>	Cells per μ L
1	Mine water	6.0	0.09	tr	5.8	2.3	2.6	917
2	Lake water	6.6	0.13	tr	4.4	3.7	2.2	1765

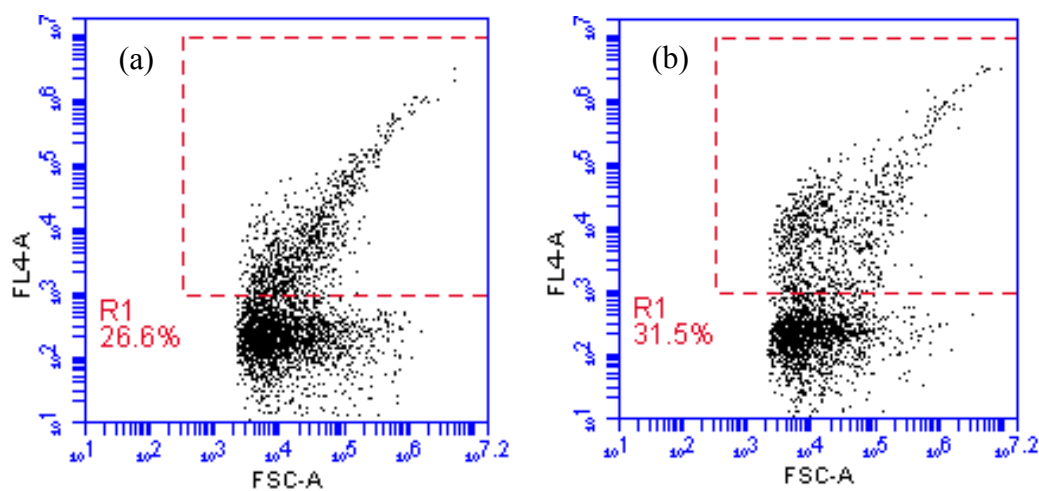


Figure 6:38 Density plot of (a) Mine water and (b) Lake water from Beauvoir stained with SYTO62 showing DNA count (FL4A) vs cell size (FSC-A).

6.4.4 St Austell mine water analysis

6.4.4.1 Mine water sample 1

In St Austell, six mine water samples of approximately 1.5L were collected earlier in the year, in January 2013. The sites chosen were from various locations within the Karslake and Blackpool pits as shown in Table 6:6 where high lithium micas may be present.

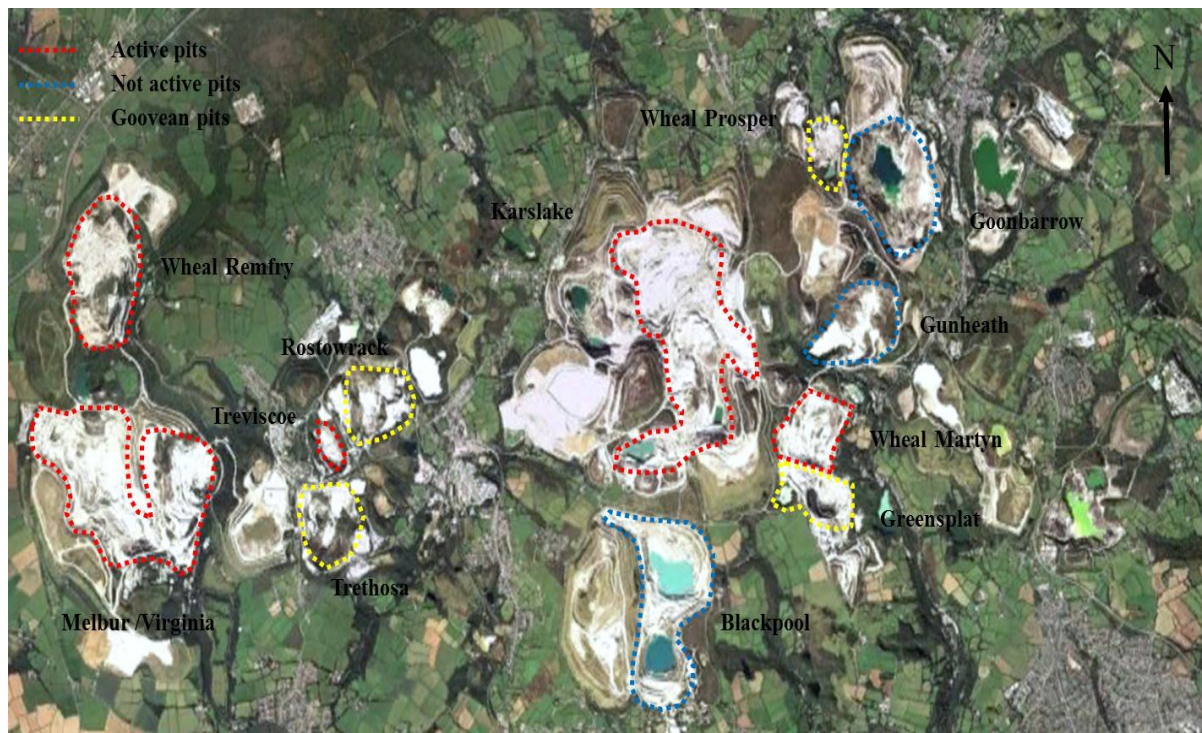


Figure 6:39 Map of St Austell showing the UK Hydrous Kaolin Platform operations site taken in 2010 (Hirtzig, 2010).

Table 6:6 shows the results for the metal concentrations and water pH, the water samples were analysed by AAS to detect for; Li, Fe, Ca, K, Na and Mn. Trebal refinery water gave interesting results, as it had the lowest pH reading of 2.85 and the highest concentration of lithium 0.14 mg/L, Figure 6:40. The sample was taken from a stream

running off a processing site, which could explain a high iron concentration of 2.19 mg/L. As well as the Fe present being associated with microorganisms another suggestion was the Fe observed could be a residue coming from the process site nearby. The second mine water sample of interest was the Dubbers dam overflow water. Although it had lower concentration of iron 0.01 mg/L, the lithium concentration was 0.1 mg/L. The Dubbers dam overflow water sample was taken from a mica dam, where natural occurring water is found. It also has a low pH reading of 3.60 suggesting the possible presence of microorganisms.

Table 6:6 Analysis of the mine water samples taken from various locations within St Austell (UK), RSD <10%, *tr: trace.

Sample	St Austell sites	pH	Metal concentration (mg/L)					
			<i>Li</i>	<i>Fe</i>	<i>Ca</i>	<i>K</i>	<i>Na</i>	<i>Mn</i>
1	Melbur refinery, process water	5.5	0.07	tr	3.6	2.0	8.6	tr
2	Hosepool 25P, process water	5.4	0.09	tr	1.2	1.2	4.3	tr
3	Hendra pit	5.3	0.08	tr	2.4	1.4	8.5	tr
4	Refiner hosepool	4.8	0.07	tr	3.3	1.6	8.2	tr
5	Trebal refinery	2.9	0.14	2.2	4.1	0.6	6.3	tr
6	Dubbers dam overflow	3.6	0.10	0.0	2.6	1.2	16.6	tr

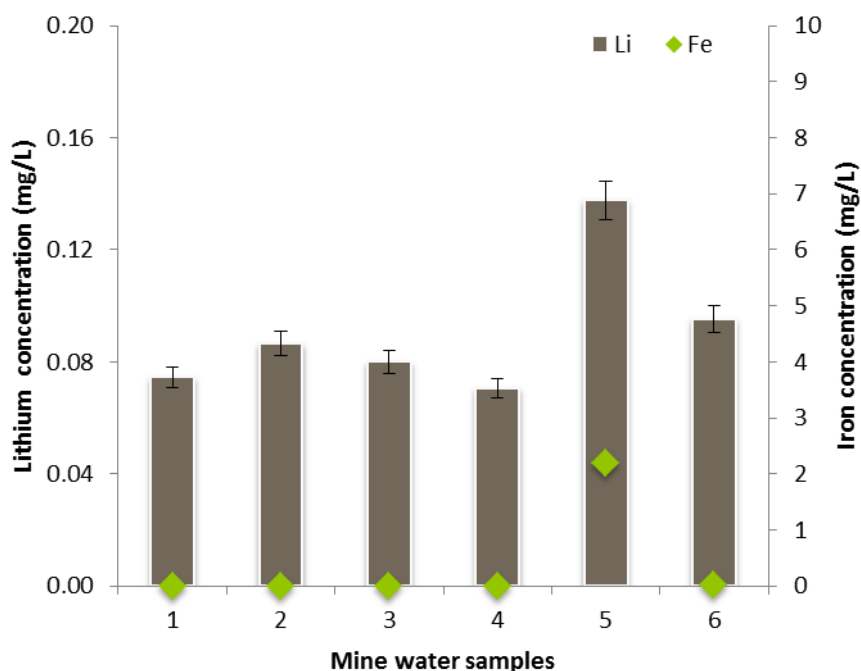


Figure 6:40 Iron and lithium analysis of the mine water samples taken from Imerys Ltd St Austell sites. .

6.4.4.2 Mine water sample 2

During the late summer of 2013 mine water and soil residue samples were taken from various locations in St Austell. The season was chosen to observe the change in water quality and potential microbial activity over the year. The samples were analysed for their pH readings, metal content and DNA content. In Table 6:7 the results for each sample can be seen. The lithium concentrations were very low for these samples; it was interesting to find that the Ca, K and Na were higher in Table 6:7 when compared to the samples in Table 6:6, suggesting that these metals may play a role in any bioleaching. Higher iron concentrations were found for the mine water samples taken from the Tanks, suggesting that it could be a by-product of the plant processes.

Table 6:7 Results for water and soil residue samples, analysed by Guardian labs, UK. The iron content was analysed at the University of Birmingham. *tr: trace.

Sites in St Austell	pH	Metal concentration (mg/L)								
		<i>Li</i>	<i>Fe</i>	<i>Ca</i>	<i>K</i>	<i>Mg</i>	<i>Na</i>	<i>SO₄²⁻</i>	<i>Si</i>	<i>Al</i>
Mine water										
Little Johns	7.4	tr	tr	8	11	6	27	60	3	tr
Hydrocyclone underflow										
Goverseth Refiner waste	5.0	tr	tr	12	40	10	95	259	4	tr
Dubbers Dam-Mica water	5.8	tr	tr	5	10	5	24	46	3	3
Stream										
Trebal Refinery Water	5.5	tr	tr	20	23	17	145	446	7	tr
Little Johns' Residue	6.4	tr	tr	7	10	6	27	55	3	3
Dorothy Pit	5.8	tr	tr	7	31	7	38	97	3	3
Plant Effluent To Rocks	5.1	tr	0.52	18	19	15	143	420	6	5
Tank 806										
Plant Water 140 Site Tank	5.2	tr	0.53	25	25	19	165	590	8	9
107										
Soil Residue										
Dorothy pit	-	tr	tr	6	10	4	21	14	2	tr
Little Johns pit	-	tr	tr	7	10	6	27	57	3	3
Treviscoe South	-	tr	tr	2	5	3	5	tr	tr	3

6.4.5 Using mine water as a leachant

Bioleaching processes require natural occurring microorganisms to extract metals into solution. For this study the mine water sample previous analysed were investigated as leachants for a potential bioleaching processes on the Beauvoir lithium concentration. The processes were designed to replicate the natural processes occurring on the mine site.

6.4.5.1 Experimental procedure

Bioleaching experiments were performed in shake flasks containing 5g of the mineral sample and 100mL mine water. A blank flask was also prepared using only mine water, 100mL. The flasks were incubated at 100 rpm at a temperature of 25°C. A sample of 10mL was taken at regular intervals then filtered and diluted with purified water. The samples were analysed for lithium, iron, potassium and sodium by AAS. The samples were also analysed using flow cytometry to monitor the microbial population and pH readings were also taken.

6.4.5.2 Results and discussion

6.4.5.2.1 Trebal refinery water

Trebal refinery water was used as a leachant for the experiment as it contained a higher lithium concentration of 0.14 mg/L, iron concentration of 2.2 mg/L and a low pH value of 2.9, thus it suggested the possible presence of microorganisms in the local environment. The mineral samples investigated were Beauvoir lithium concentrate (4.1 wt.% Li₂O) and the St Austell sample, New Sink G5 (0.5 wt.% Li₂O).

6.4.5.2.1.1 Effect of leaching Beauvoir lithium concentrate

The bioleaching experiments were carried out on Beauvoir lithium concentrate containing 4.1 wt.% Li₂O at a temperature of 25°C. In Figure 6:41 it can be seen that a positive correlation was observed for the Beauvoir lithium concentration upon bioleaching with only the mine water, achieving an increase of 0.29 mg/L over the 16 days. The positive results are possible indicator that some lithium bioleaching may be

taking place, the flow cytometry results also agree with this as an increase in DNA particles can be seen in over the duration of days as well as the change in pH observed, Table 6:8. The flow cytometry data produced indicated that bacterial populations increased dramatically during leaching,

Table 6:8 DNA count detected within the leach liquors during the mine water leaching extraction process, an average of three experiments, RSD < 10%.

Day	pH	Lithium (mg/L)	DNA Count (cells per μL)
0	2.9	0.14	200
4	3.4	0.14	514
7	3.5	0.20	635
11	3.8	0.29	1303
16	3.9	0.43	1670

In Figure 6:42 it can be seen that during the bioleaching of Beauvoir lithium concentrate, an initial decrease in the iron content in the leach liquor was observed, which then increased again in day 16, 0.24 mg/L, thus suggesting that microorganisms could be undergoing redox reactions.

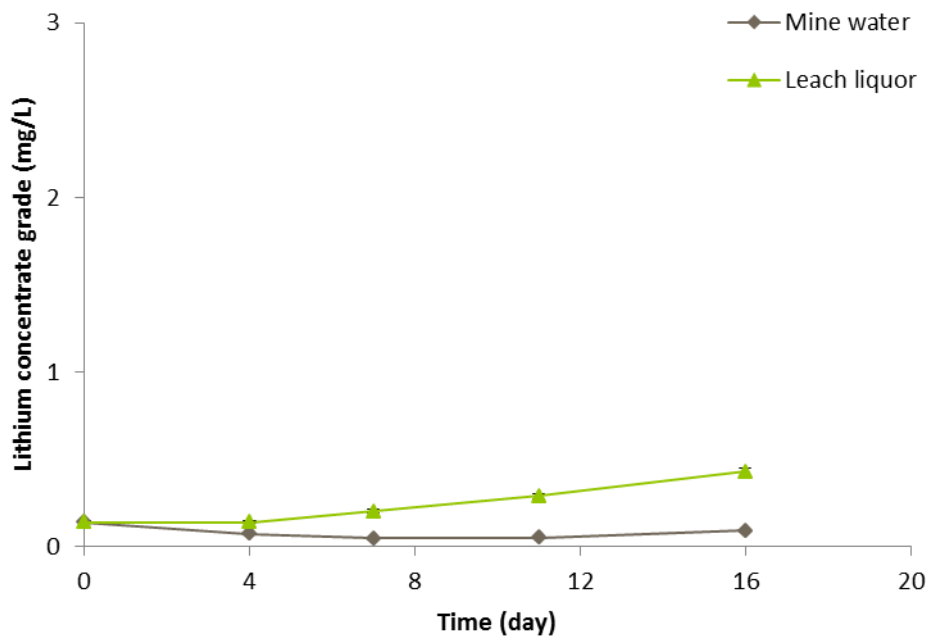


Figure 6:41 Lithium concentration in solution for the Beauvoir lithium concentrate contacted with mine water at 25°C RSD <10%.

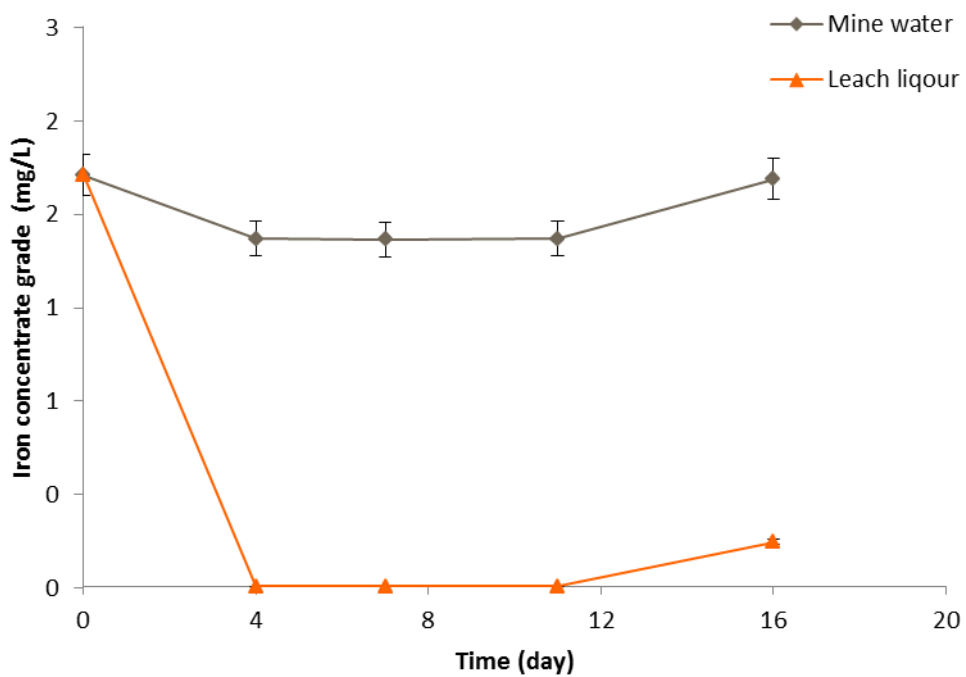


Figure 6:42 Iron concentration in solution for the Beauvoir lithium concentrate contacted with mine water at 25°C RSD <10%.

Overall the results showed that Trebal refinery water was capable of leaching lithium from the Beauvoir lithium concentrate, as up to 0.47 mg/L was extracted into the bioleach solution over a period of 16 days, showing an increase of 0.33 mg/L. In Figure 6:42 it can be seen that the DNA count over the leaching period increased over the 16 days; detecting up to 1670 cells per μL . Flow cytometry was used to detect the presence of microorganisms through DNA count. This technique does not distinguish between dead or live cells, thus the cell concentration either stays constant or increases. The increase in DNA count suggested that a growth in the microbial population was being observed which could play a potent role in the extraction of lithium into the leach liquor.

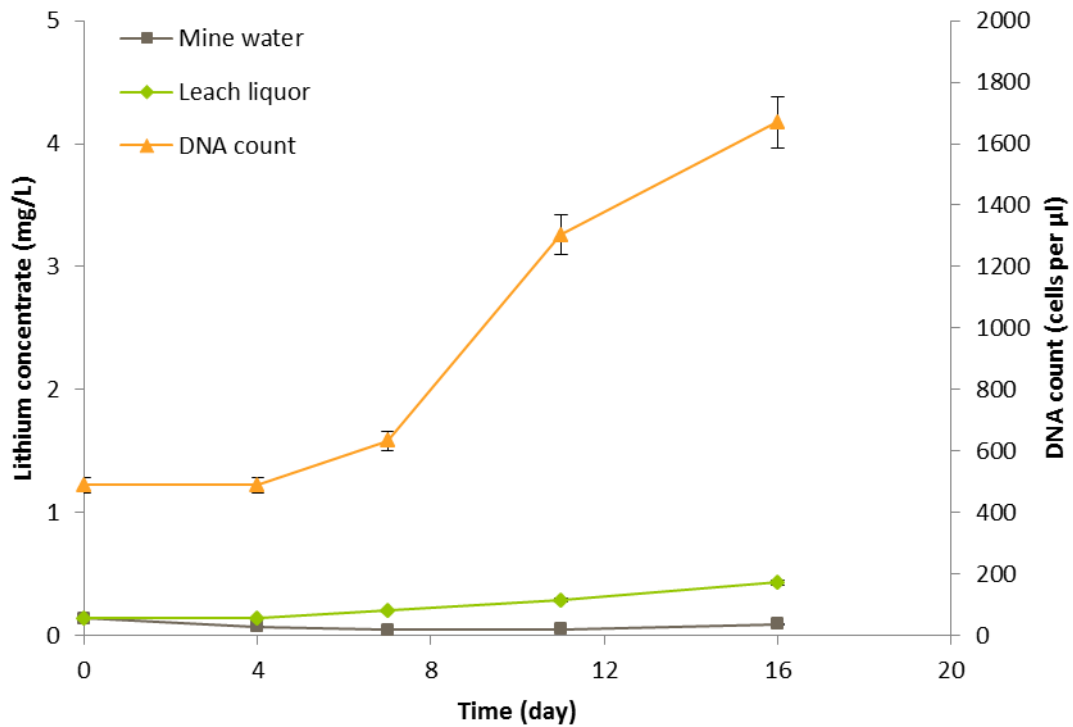


Figure 6:43 Lithium concentration in solution and DNA count for the Beauvoir lithium concentrate contacted with mine water at 25°C RSD <10%.

6.4.5.2.1.2 New Sink G5

The bioleaching process for the New Sink G5 sample, containing up to 0.08 wt.% Li_2O showed positive results when extracting lithium into solution. Two particle size fractions were investigated; 53 to 250 μm and 250 to 500 μm over a period of 16 days, it was expected that the smaller sized samples would have higher surface contact area hence increase the amount of lithium that could react with the leaching solution. Both of the experiments showed a similar pattern in the amount of lithium extracted into solution. A slow growth in lithium dissolution was observed over the duration of 16 days. On day 16, the amount of lithium extracted in solution was increased to 0.1 mg/L for both particle size fractions after detecting 0.05 wt.% Li_2O on days 4, 7 and 11. Therefore it can be suggested that the slow growth may be due to a lag phase of the microorganisms as the New Sink G5 samples showed potential for bioleaching, the analysis could not be continued due to restricted time.

When compared to bioleaching the Beauvoir lithium concentrate which achieved 0.43 mg/L after 16 days, the New Sink G5 sample showed lower lithium concentrations of 0.1 mg/L. This can be explained by the lithium content of the two samples, Beauvoir lithium concentrate contained 4.1 wt.% Li_2O whereas the New Sink G5 sample contained a much lower amount of lithium concentration of 0.08 wt.% Li_2O .

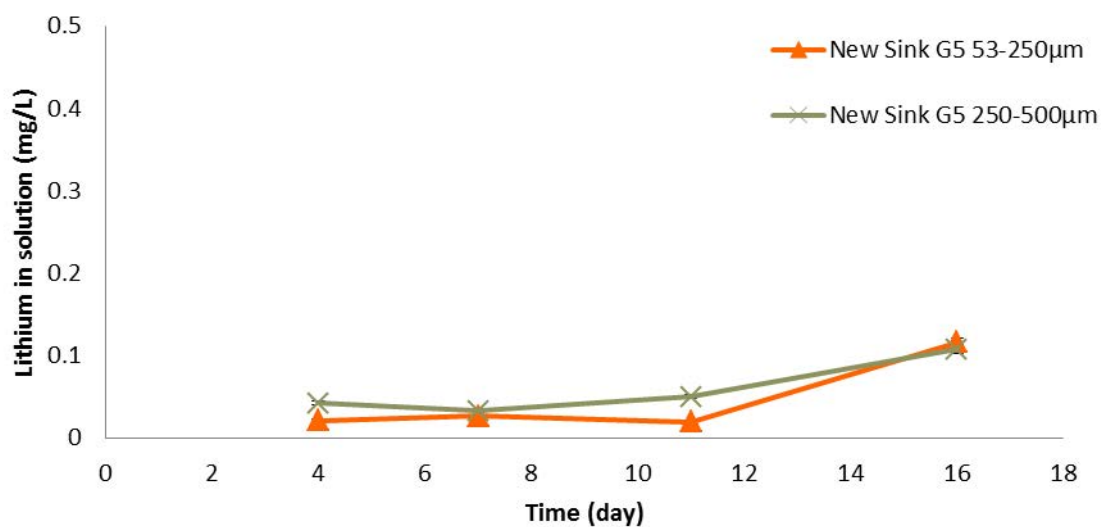


Figure 6:44 Lithium in solution when bioleaching New Sink G5 sample in Trebal refinery water, each data point is an average of three experiments.

6.4.5.2.2 Dubbers dam mine water

Dubbers dam overflow water was used as a leachant for an experiment, as it contained a higher lithium concentration of 0.10 mg/L, iron concentration of 0.01 mg/L and a low pH value of 3.6 as seen in Table 6:9. These results suggested also the possible presence of microorganisms in the local environment.

Table 6:9 Analysis of the mine water samples taken from Dubbers dam, within St Austell (UK) , each data point is an average of three readings, RSD <10%.

Sample	St Austell Sites	pH	Metal concentration (mg/L)				
			<i>Li</i>	<i>Fe</i>	<i>Ca</i>	<i>K</i>	<i>Na</i>
6	Dubbers dam, overflow water	3.60	0.10	0.01	2.63	1.16	16.61

In Figure 6:45 the lithium extracted from the Beauvoir lithium concentrate, 4.1 wt.% Li_2O over 13 days can be seen. The amount of lithium extracted from the Beauvoir lithium concentrate using mine water leaching was fairly constant, fluctuating between 0.1 to 0.2 mg/L. The highest amount of lithium was recorded on day 3, at 0.17 mg/L of lithium. After this the lithium readings remained fairly stable. Iron was not traceable in any of the leach solution throughout the study. The pH readings showed a fluctuating pH range from 3.6 to 7.0 for Beauvoir lithium concentrate.

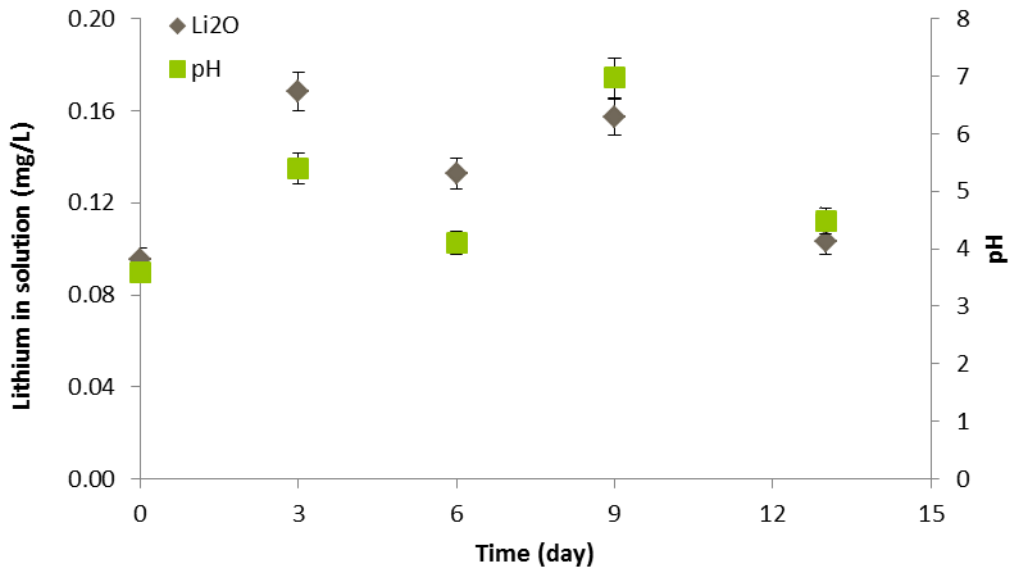


Figure 6:45 Lithium in solution when bioleaching Beauvoir lithium concentrate in Dubbers dam, each data point is an average of three experiments.

6.5 Biological leaching

6.5.1 Introduction

Bioleaching utilises a similar concept to chemical leaching, except for the part that the process is induced by the microbial metabolisms through a direct and indirect mechanism of extractive bio-hydrometallurgy (Buckley, 2012; Devasia, 2004). As bioleaching uses naturally occurring microorganisms, it is seen as an economically viable process. Collaboration was formed with Professor Jana Kadukova at the Technical University in Kosice, Slovakia, specialist in Biometallurgy as part of this study. Rezza (2001; 1997) investigated the extraction of lithium from lithium-bearing minerals, spodumene, using *Aspergillus niger* (*A. niger*). *A. niger* was isolated as a naturally occurring microorganism from spodumene mineral deposits. Collaborative research investigated the bioleaching using *A. niger* and the lithium-bearing mineral, lepidolite, found in the Beauvoir lithium concentrate.

Bioleaching occurs when micro-organisms that are naturally associated with certain ore bodies are utilised to alter the oxidation state of metals and dissolve them into solution; pH is good for selectivity of certain minerals. This solution is then processed to recover the desired metals. Previous studies have investigated the biological leaching of lithium, but these are mainly aimed at treatment of waste batteries or concentrated mineral spodumene (2.9 to 7.7% Li₂O). In this study, bioleaching lithium-bearing mineral was investigated following the success of extracting lithium from spodumene using *A. niger* (2001). After 30 days of leaching up to 0.4 mg/l of dissolved lithium was detected,

suggesting direct contact between the mineral and the microorganism was responsible for lithium extraction into solution.

A list of lithium-bearing minerals along with their lithium concentrations can be seen in Table 6:10. In this study, bioleaching processes using *A. niger* were applied to extract lithium from micas such as Lepidolite and Zinnwaldite as these were identified in the kaolin mining waste material for France and the UK, respectively. To further improve the efficiency of the method, the research also investigated by-products formed.

Table 6:10 Lithium-bearing minerals and their lithium concentrations ^atheoretical maximum (Garrett, 2004).

Lithium-bearing minerals	Li₂O concentration (wt.%)
Spodumene	3-7
Lepidolite	3-8 ^a
Zinnwaldite	2-5
Beauvoir lithium concentrate	4.1
Mineral specimen grade of pure lepidolite	5.6

6.5.2 Preliminary research (carried out by TUKE)

The initial research was carried out in collaboration with Dr Jana Kadukov at the Technical University of Kosice (TUKE) in Slovakia. The Beauvoir lithium concentrate was investigated with various micro-organisms in order to extract lithium. A detailed study on the bio-accumulation of the Beauvoir lithium concentrate was performed. A variety of microorganisms were used such as; bacteria, actinomycetes, fungi and yeasts. The presence of iron and copper found in water around polymetallic sulphide mines lead to the discovery and use of acidophilic bacteria (Buckley, 2007).

6.5.2.1 Effect using acidophilic bacteria in rich-nutrient medium

The Beauvoir lithium concentrate (2g) was bioleached using acidophilic bacteria, a culture of *A. ferrooxidans* and *A. thiooxidans*, to extract lithium. The bacteria were cultivated at 30°C. The experiments were carried out in a rich-nutrient medium for 35 days. The abiotic factors of the environment, including light, temperature, and atmospheric gases, were under the same conditions. The rich-nutrient medium contained all nutrients necessary for bacterial growth according to Karavaiko (1988) a source of reduced sulphur was provided for the microorganisms.

During the experiment the pH and the lithium content were recorded using a pH meter and AAS, respectively. Initially the pH value of the rich-nutrient medium was adjusted to pH 1.5 as *A. ferrooxidans* are most active and thus able to reproduce in the pH range 1.5 to 3.5. If the pH of the medium is below 1.0 the reproduction will be inhibited (Crundwell, 2003; Torma, 1976). Readings were then taken out regular intervals throughout the duration of the experiment. After the first 10 days, the pH of the rich-nutrient media decreased to pH 1.0, at day 20 the reading increased back up to pH 1.6 which remained *generally* constant, until the end of the experiment. Throughout the experiment no presence of lithium was detected in solution using AAS analysis (Manning & Grow, 1997).

6.5.2.2 Effect using acidophilic in low-nutrient medium

A low-nutrient medium containing a culture of acidophilic bacteria was used to leach lithium from the Beauvoir lithium concentrate (2g). The low-nutrient medium was

composed of diluted sulphuric acid to which elemental sulphur as an energy source for bacterial growth was added. The experiment was allowed to continue for a longer period of time, 206 days. During the bioleaching the pH slowly decreased from pH 1.5 to pH 0.82, which was measured on day 206.

In Figure 6:46 the lithium extraction and pH of the experiment over 206 days can be seen. The amount of lithium in solution was also analysed over the period of time, on day 21, 0.04 mg/L of lithium in solution was detected. The lithium extraction process continued very slowly, on day 206, 0.62 mg/L of lithium in solution was detected. It can be concluded that the acidophilic bacteria used in these experiments were not effective at extracting lithium from Beauvoir lithium concentrate. Hence acidophilic bacteria do not bioleach the mineral efficiently to develop as an economic process route to follow.

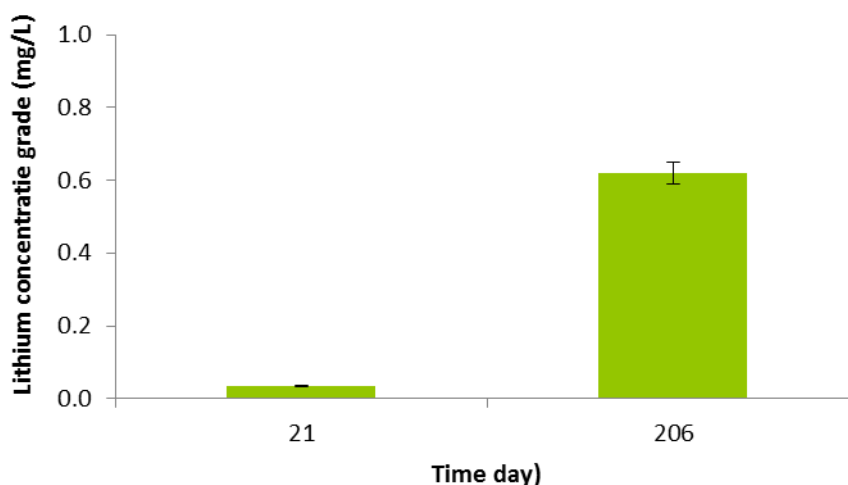


Figure 6:46 Lithium content observed in a low-nutrient medium containing a culture of acidophilic bacteria was used to leach lithium from the Beauvoir lithium concentrate, carried out in collaboration with TUKE.

6.5.2.3 Effect using heterotrophic fungi in low-nutrient medium

Other microorganisms investigated, to extract lithium from the Beauvoir lithium concentrate, were heterotrophic fungi of *A. niger* group. *A. niger* is the most common species of the genus *Aspergillus*. It is known as a common contaminant of food due to favouring condition at room temperature.

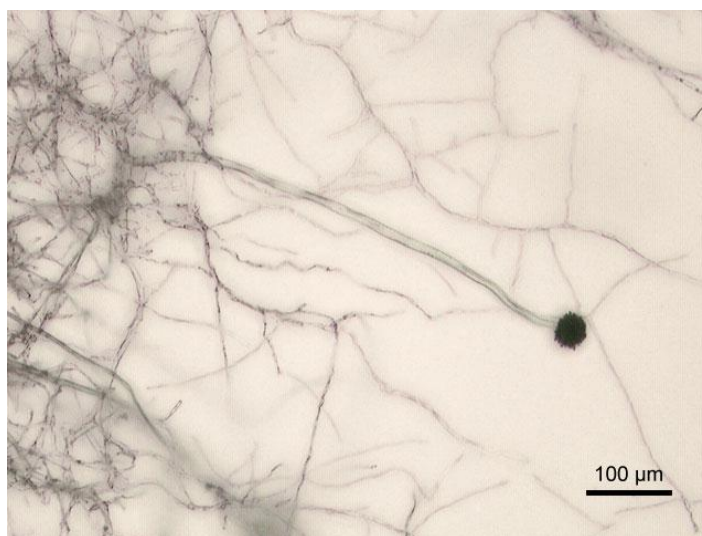


Figure 6:47 *A. niger* grown on Sabouraud agar taken from (JGI, 2012).

A low-nutrient medium composed of glucose with a small amount of $(\text{NH}_4)_2\text{SO}_4$ was used as the bioleaching medium. Karavaiko (1988) reported that this kind of media was the most appropriate for microbial growth. For the experiments, 12-day-old spores of *A. niger* were used. The initial pH of the bioleaching medium was 5.5, so was not adjusted as *A. niger* works best under these conditions. The experiments were allowed to continue for 42 days at 30°C. During the bioleaching process, a rapid pH decrease was observed down to pH 3.8 on day 3. The pH continued to decrease and gave a reading of pH 2.85, measured on day 42. During the bioleaching process lithium was not detected in the solution using AAS.

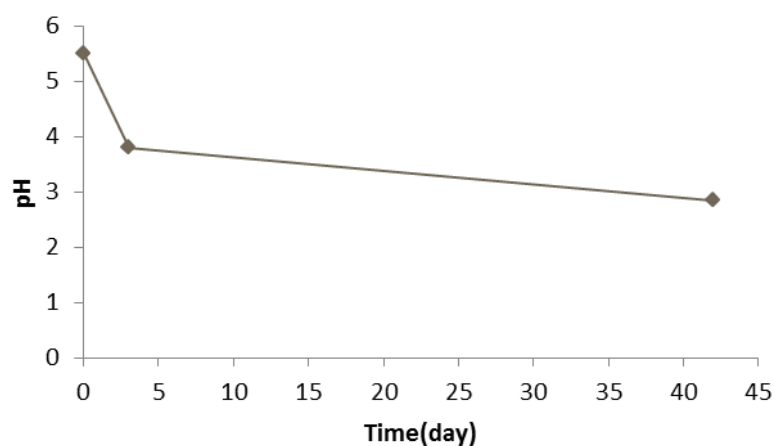


Figure 6:48 pH changes observed in a low-nutrient medium containing *A. niger* bioleaching the Beauvoir lithium concentrate over 42 days, carried out in collaboration with TUKE.

The biomass was treated with nitric acid, to determine the lithium present in the biomass. Although lithium was not found in the biomass at the end of the experiment, the solid and liquid phases were separated by centrifugation. Thus it can be assumed that in this case bio-accumulation is occurring. Based on the AAS analysis of solid residue, the amount of lithium released and accumulated into the biomass was determined to be 37%, this was achieved by melting at 850°C and then dissolving in diluted HCl (1:1) and measured by AAS. The Beauvoir lithium concentrate was analysed using SEM before and after bioleaching, these can be seen in Figure 6:49 and Figure 6:50. The SEM analysis showed a change in the structure of the mineral after bioleaching, the mineral appeared to be liberated and larger flat structures of the minerals can be seen in Figure 6.51.

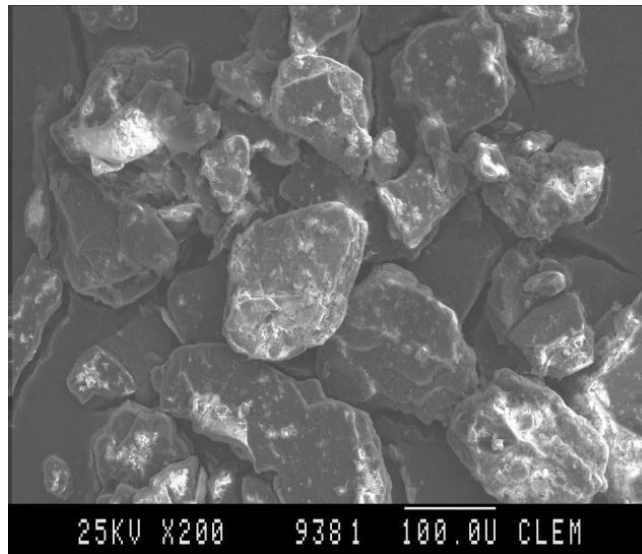


Figure 6:49 SEM of Beauvoir lithium concentrate before bioleaching with *A. niger*, taken in TUKE.

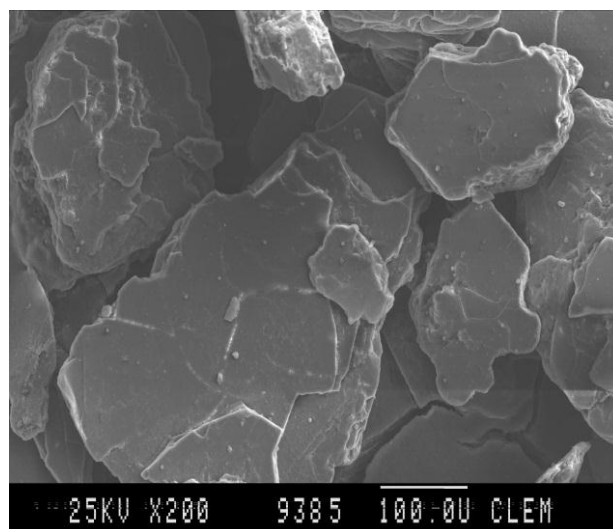


Figure 6:50 SEM of Beauvoir lithium concentrate after bioleaching *A. niger* taken in TUKE.

6.5.3 Bioleaching with *A. niger*

This section investigated utilising *A.niger* to extract lithium from low grade lepidolite, which was previously not seen as an economical process. *A. niger* was selected as it had previously shown success when bioleaching spodumene to extract lithium in the study by Rezza (2001) as well as the work in collaboration with TUKE.

The aims of this study were to obtain a better understanding of the mechanism and how the efficiency of the process could be improved. The duration of the experiments was up to 90 days, although for most of the experiments the maximum duration was 30 days due to laboratory limitations.

The following bioleaching mechanisms were investigated, under a controlled environment to understand the lithium extraction process in greater detail:

- **Direct and indirect**, *contact between the microorganism and mineral.*
- **Aerobic and Anaerobic**, *the condition of the experiment.*

6.5.3.1 Direct bioleaching under aerobic conditions

Direct leaching involves direct contact between the microorganism and the mineral, in this case *A. niger* and the mineral. Studies conducted by Rezza (2001) and Karavaiko and Tzaplina (1988) indicated that *A. Niger* undergoes a direct bioleaching mechanism, which solubilises the lithium into solution. Their study does not consider whether the process was a direct aerobic or anaerobic, thus this study investigated these two options in order to understand the mechanism better. The minerals investigated were a mineral specimen grade pure lepidolite and Beauvoir lithium concentrate. As a control parameter, the mineral concentrate was investigated under two conditions; pre-treated in an autoclave to sterilise the mineral and with no prior treatment. This was to ensure that there were no other microorganisms present within the mineral, were contributing towards the lithium extraction process.

6.5.3.1.1 Experimental procedure

A suspension of *A. niger* (0.5mL) grown for 10 days on a Potato Dextrose Agar (PDA) Petri dish was used to bioleach the minerals (5g,) in a sterile 500mL sterile conical flask containing 100mL of sterilised water. The experiments were repeated to assess two conditions; pre-treatment (sterilisation) of the mineral and no treatment of the mineral. All of the experiments were carried out in sets of three to test for reliability and validity. The flasks were set up on a rotary shaker at 200rpm at a temperature of 30°C. Aliquots (6mL) of the leach liquor were sampled for metal content weekly. The aliquots were centrifuged at 6000rpm for 10 minutes to separate the biomass from the leach liquor. The leach liquor was analysed using the AAS for metal content in parts per million. The solids were dried and weighed.

6.5.3.1.2 Results and discussion

6.5.3.1.2.1 Mineral specimen grade pure lepidolite

In Figure 6:51 lithium extraction is reported when bioleaching the mineral specimen grade pure lepidolite with *A. niger* at ambient temperature, each data point was an average of three experiments (<10% RSD). Figure 6:51 shows the amount of lithium detected in the bioleach solution for a period of four weeks. A positive correlation was observed for the lithium extracted over four weeks. After week 1, the sterilised and non-sterilised samples both contained lithium concentrations of 7 mg/L in the leach liquor. Following this in week 2, the lithium concentration detected almost doubled for both of the experiments. A slightly greater concentration of 2 mg/L was observed for the non-sterile experiment, 14.9 mg/L. This trend continued to week 4, a slight increase for the

amount of lithium extracted in the non-sterile sample was observed, 33 mg/L. The lithium recoveries for the sterile and non-sterile experiments were 9 and 12%, respectively. During the four weeks there was no traceable amount of iron content in the leach liquors.

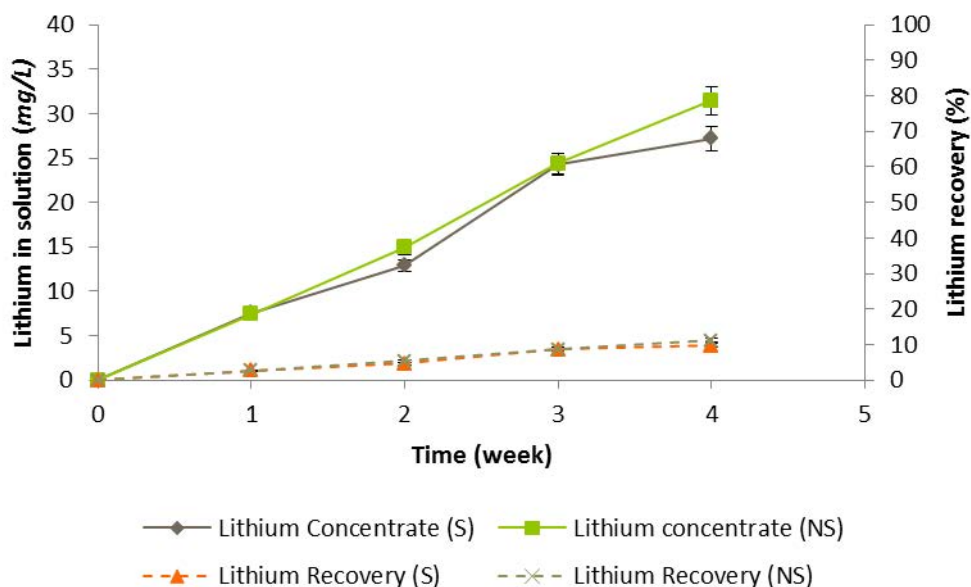


Figure 6:51 Lithium in solution when direct bioleaching mineral specimen grade pure lepidolite with *A. niger* at 25°C <10% RSD, S: sterilised, NS: non-sterilised.

The aerobic experiments were repeated to analyse data over a longer period of time (12 weeks). Instead of taking weekly aliquots, aliquots of the leach liquor were taken every 4 weeks. Over the 12 weeks period, an increase of lithium was observed, up to 125 mg/L for the sterile sample and 123 mg/L for the non-sterile.

The increase in lithium concentration could be explained by the microbial growth in the medium (enriched with *A.niger*), *A.niger* is known to produce oxalic and citric acid (Santhiya, 2005) which is suggested to extract lithium from minerals into solution (Rezza, 2001). Therefore, it is suggested that the increased dissolution of lithium into

solution could be due to an increase observed in the microbial population. Microorganisms experience four phases during their life cycle; lag, growth, stationary and death phase. In Figure 6:52 it can be seen that the first two phases of the cycle; lag and growth phase are present. After a relatively slow, growth the microorganisms started to acclimatise to the new conditions and multiply at the end of 12 weeks when 123 mg/L was detected in the leach liquors for both the sterilised and non-sterilised samples, with a lithium recovery of 45% and 44% in the samples, respectively. Due to laboratory constraints, the experiments were not able to be continued after this period, so it was not possible to observe the next two stages of the microbial cycle (stationary and death phase of cells). It can be expected that if the process was continued longer, higher lithium recoveries would be achieved.

There was a negligible difference between the sterile and non-sterile mineral sample results, suggesting that the mineral has limited contact with microorganisms prior to leaching and it can be assumed *A. niger* was responsible for the changes in lithium concentrations observed. It was interesting to note that the iron concentration remained at 0 mg/L until week 12 when 0.2 mg/L was observed in the leach liquor samples, although the pH reading remained fairly constant at a pH of 8.0.

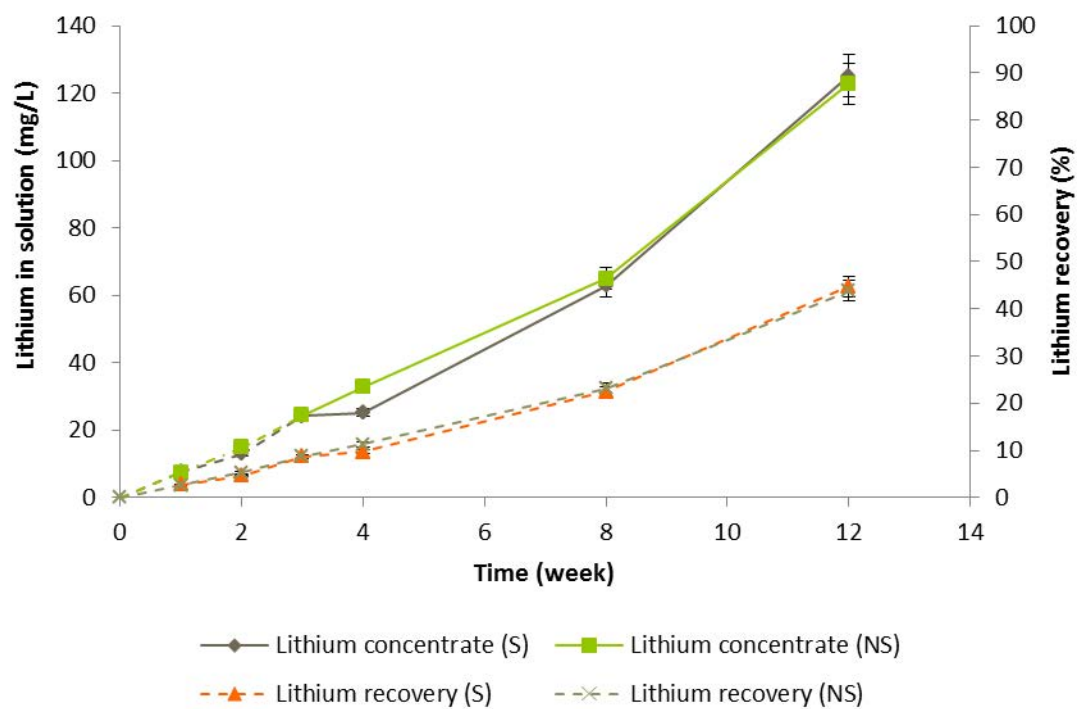


Figure 6:52 Lithium in solution when directly bioleaching mineral specimen grade pure lepidolite with *A. niger* at 25°C. <10% RSD, S: sterilised, NS: non-sterilised.

Table 6:11 Results for direct bioleaching experiment under aerobic conditions, S = sterile and NS= non-sterile.

Time (week)	Lithium concentration (mg/L)		Iron concentration (mg/L)		pH		Lithium recovery (%)	
	S	NS	S	NS	S	NS	S	NS
4	27.2	32.8	-	-	7.9	7.9	9	12
8	62.8	64.9	-	-	8.0	8.0	23	23
12	125.2	122.8	0.2	0.2	7.9	7.9	45	44

6.5.3.1.2.2 Beauvoir lithium concentrate bioleaching

When using the Beauvoir lithium concentrate (particle size range of 53 μ m to 400 μ m), a lower lithium concentration was observed in the leach solution. Over a period of four weeks, the lithium extraction peaked at 2.4 mg/L for the non-sterile experiment, as shown in Figure 6:53. It is suggested that the non-sterile experiment was able to produce a higher amount of lithium extraction due to the microorganisms already present in the sample. Rezza (1997) stated that the microorganism including *Penicillium*, *Aspergillus*, were found to be present in mined spodumene; flow cytometry analysis confirmed this as DNA particles were found in the Beauvoir mine water.

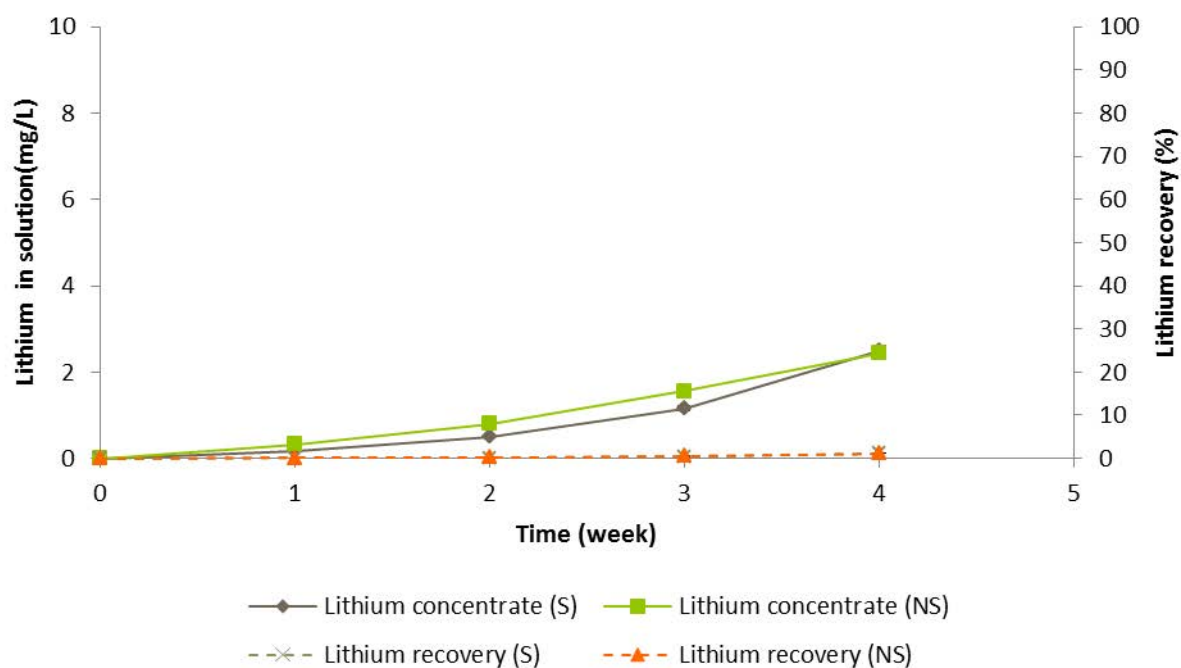


Figure 6:53 Lithium in solution for direct bioleaching under aerobic conditions Beauvoir lithium concentrate with *A. niger* at 25°C, <10% RSD, S: sterilised, NS: non-sterilised.

The experiment was continued for a further 4 weeks and then analysed in week 8. Figure 6:54 shows the lithium extraction over the period of 8 weeks. Initially a slow rate of lithium extraction was observed, until week 4 where a spike for the non-sterile sample, 7.3 mg/L was observed. At week 8, 14.7 mg/L of lithium was observed for the non-sterile experiment and 10.4 mg/L for the sterile experiment. The slow rate of extraction up until week 4 suggests that the leaching microorganisms are undergoing a lag phase, where they adapt to the new condition before a growth phase can be seen. The growth phase is observed in week 8 as greater amounts of lithium were extracted in the solution. Each week no iron was detected in the leach solution.

Table 6:12 Results for direct bioleaching experiment under aerobic conditions, S = Sterile and NS = Non-sterile.

Time (week)	Lithium concentration (mg/L)		Iron concentration (mg/L)		pH		Lithium recovery (%)	
	<i>S</i>	<i>NS</i>	<i>S</i>	<i>NS</i>	<i>S</i>	<i>NS</i>	<i>S</i>	<i>NS</i>
4	2.5	2.4	-	-	6.9	7.1	1.2	1.2
8	4.6	5.9	-	-	6.8	6.7	2.3	2.9
12	12.7	11.7	0.1	0.2	6.7	6.6	6.2	5.7

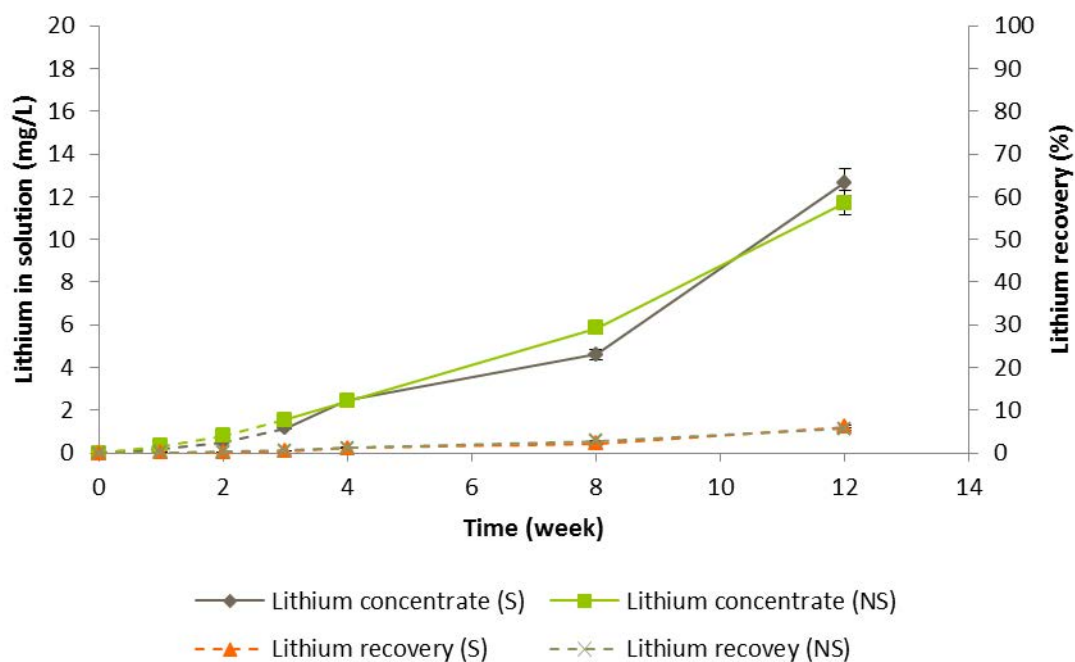


Figure 6:54 Lithium in solution for direct bioleaching under aerobic condition of the Beauvoir lithium concentration using *A. niger* 12 weeks. RSD<10%. S: sterilised, NS: non-sterilised.

6.5.3.2 Direct bioleaching under anaerobic conditions

Direct bioleaching under anaerobic conditions was investigated using mineral specimen grade pure lepidolite and Beauvoir lithium concentrate. The process involved direct contact between *A. niger* and the mineral in a controlled environment.

6.5.3.2.1 Experimental procedure

A polyethylene bag (Aldrich Atmosbag) inflated with nitrogen (N₂) provided a de-oxygenated environment, an indicator was used to detect for the presence of oxygen. The conical flasks were placed in the bag, which was then re-filled with N₂ and then

sealed. The rotary shaker was set at 30°C and 200rpm. The experiments were analysed over a period of four weeks, weekly aliquots were taken. The aliquots were centrifuged and then analysed to determine their metal content using the AAS and pH readings were taken.

6.5.3.2.2 Results and discussion

For the mineral specimen grade of pure lepidolite, positive results were observed over the period of four weeks when direct bioleaching with *A. niger*, whereas for the Beauvoir lithium concentrate no lithium was detected in the leach liquors. This could be due to the lower lithium content in the mineral as well as a longer lag phase.

Table 6:13 summarises all of the results, including the iron concentrations over the weeks. Iron was not detected until week 4 (0.8 mg/L for the sterile sample and 0.6 mg/L for the non-sterile). The pH readings remained fairly constant at 8.0. The anaerobic experiment for the Beauvoir lithium concentrate was not successful, no lithium or iron were detected in solution over the period of time.

In Figure 6:55 it can be seen that the lithium concentration in solution for both the sterile and non-sterile lepidolite mineral. Over 4 weeks 37 mg/L for the non-sterile mineral is extracted into solution. The sterile mineral also gives a similar amount of lithium dissolution, 34 mg/L. There was no significant difference between the sterilised and non-sterile mineral leaching behaviour, suggesting that for the non-sterile lepidolite mineral there were no other microorganisms involved in the extraction process. The lithium recoveries achieved were between 12 to 13 % after four weeks of bioleaching, which was much lower than that achieved under aerobic conditions, 45%. This

suggested that aerobic conditions are more favourable, as the microorganisms needed oxygen in order to cultivate.

Table 6:13 Results for the direct bioleaching experiment for lepidolite under anaerobic conditions for week 4, S = Sterile and NS = Non-sterile.

Time (week)	Lithium concentration (mg/L)		Iron concentration (mg/L)		pH		Lithium recovery (%)	
	<i>S</i>	<i>NS</i>	<i>S</i>	<i>NS</i>	<i>S</i>	<i>NS</i>	<i>S</i>	<i>NS</i>
	1	12.8	14.6	-	-	7.6	7.9	4.6
2	20.4	20.5	-	-	7.9	7.9	7.3	7.3
3	29.6	28.8	-	-	7.7	7.8	10.6	10.3
4	33.7	37.2	0.8	0.6	7.3	7.7	12.0	13.3

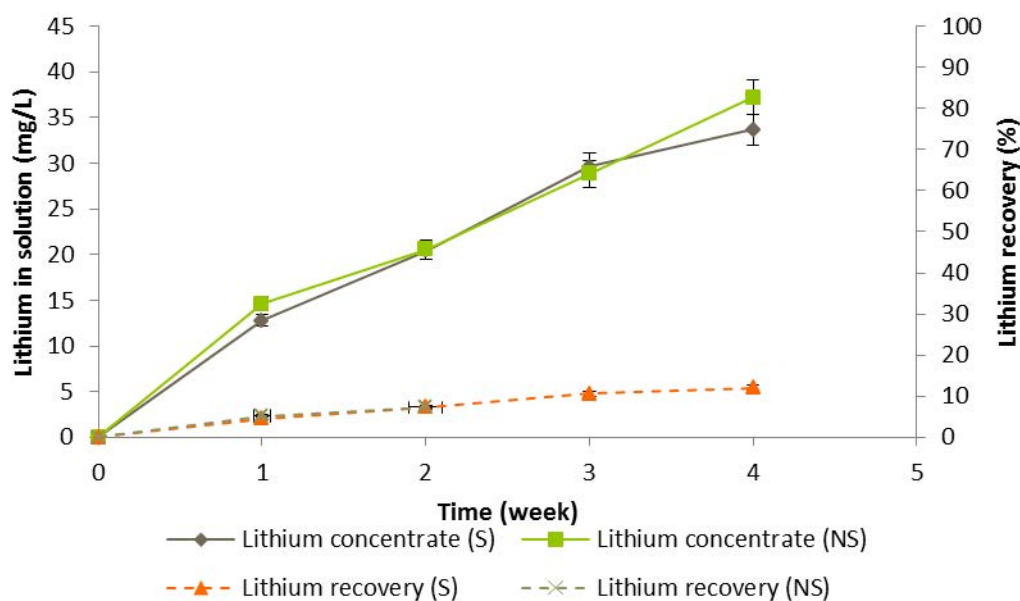


Figure 6:55 Direct Bioleaching of the Pure lepidolite using *A. niger* over a period of 4 weeks, each data points is an average of three experiments, which are each analysed three times RSD<10%.

6.5.3.3 Indirect bioleaching under aerobic conditions

Indirect bioleaching was investigated to determine the mechanism involved in extracting lithium from the mineral into solution. For indirect processes there must be no contact between the mineral and microorganism. All flasks were sealed, to ensure that the experiment was carried out in a sterilised environment. Schinner (1993) reported that heterotrophic microorganisms generally leach metal through an indirect bioleaching process.

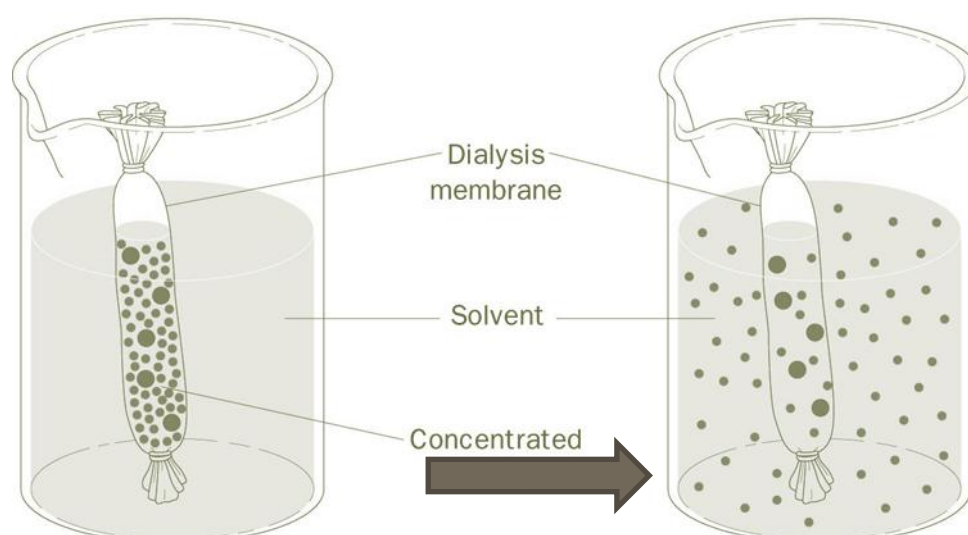


Figure 6:56 Schematic diagram for indirect leaching using dialysis tubing (adapted from SOS03, 2011).

6.5.3.3.1 Experimental procedure

The non-sterile minerals were placed within dialysis tubing prior to leaching. The dialysis tube prevented any contact between the mineral and the microorganism, *A. niger*. The tube was made from semi-permeable material, allowing lithium leached from the mineral into the solution. The flasks were placed on a rotary shaker which was set to 30°C and 200 rpm. The experiments were analysed over a period of four weeks. Weekly

aliquots were centrifuged and then analysed to determine their metal content using AAS and pH readings were taken.

6.5.3.3.2 Results and discussion

6.5.3.3.2.1 Indirect bioleaching of mineral specimen grade pure lepidolite

The indirect bioleaching was carried out under aerobic conditions; the mineral was bioleached for duration of 8 weeks. Figure 6:57 shows the lithium content in solution for the weeks: 1,2,3,4 and 8. The mineral specimen grade pure lepidolite shows the greatest potential in lithium extraction over the period of 8 weeks achieving 33 mg/L in solution with a recovery of 12%. The results of the leaching experiments agree with Rezza (2001), concluding that a greater amount of lithium was achieved in the direct bioleaching process. For the mineral specimen grade pure lepidolite in direct bioleaching 65 mg/L in solution was detected, whereas for the in-direct process although positive, it was only 33 mg/L.

Table 6:14 Chemical analysis of indirect bioleaching for mineral specimen grade of pure lepidolite.

Time (week)	Lithium concentration (mg/L)	Iron concentration (mg/L)	pH	Lithium recovery (%)
1	11.3	0	7.8	4.0
2	13.0	0	7.8	4.6
3	17.8	0	7.6	6.4
4	18.1	0	8.0	6.5
8	32.5	0.1	8.1	11.6

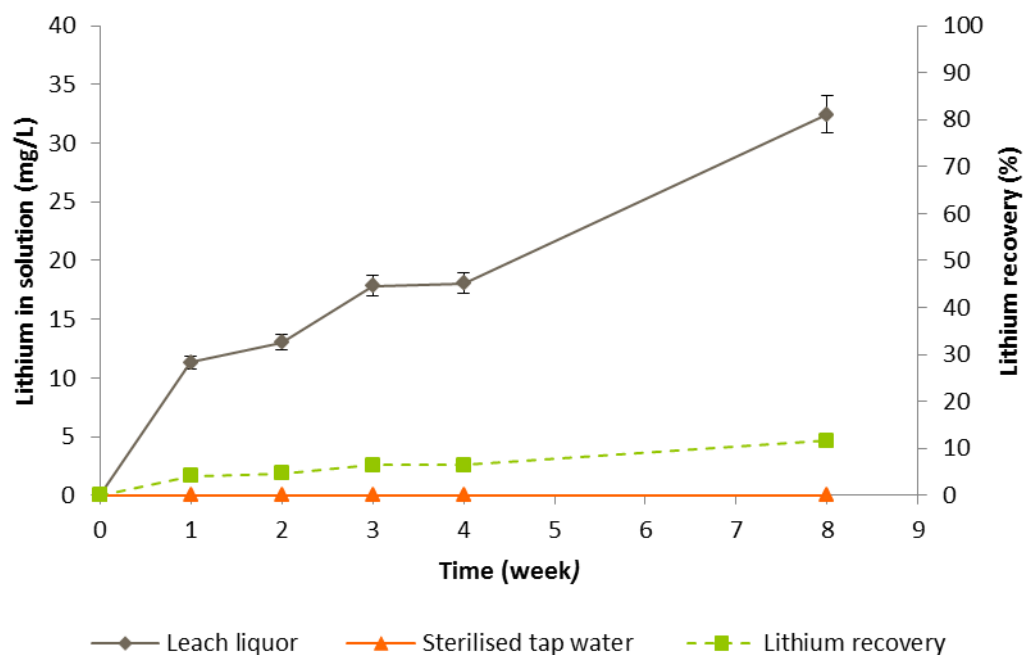


Figure 6:57 Indirect bioleaching mineral specimen grade pure lepidolite using *A. niger*. Each data points is an average of three experiments, which are each analysed three times RSD<10%.

6.5.3.3.2 Indirect bioleaching of Beauvoir lithium concentrate

The indirect bioleaching was carried out under aerobic conditions; the mineral was bioleached for duration of 8 weeks, Table 6:15 summarises the metal content detected in the solution for week 4 and 8. In Figure 6:58 a slow lithium extraction can be seen, achieving 0.3 mg/L of lithium concentration in solution after 8 weeks. With directly bioleaching it was observed at 6 mg/L, which suggested *A. niger* favoured direct bioleaching.

Table 6:15 Chemical analysis of indirect bioleaching for Beauvoir lithium concentrate

Time (week)	Lithium concentration (mg/L)	Iron concentration (mg/L)	pH	Lithium recovery (%)
1	0	0	6.8	0

2	0	0	6.9	0
3	0.01	-	6.8	0
4	0.2	-	6.8	0.1
8	0.3	0.1	6.9	0.1

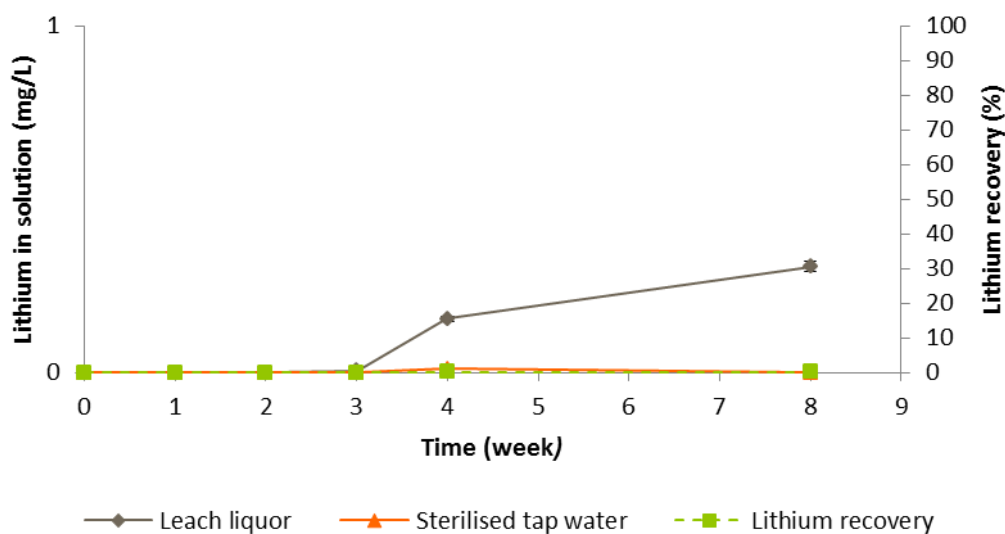


Figure 6:58 Indirect bioleaching Beauvoir lithium concentrate using *A. niger*. Each data points is an average of three experiments, which are each analysed three times RSD<10%.

6.5.4 Summary of bioleaching results

In this study, the optimum extraction of lithium was from direct bioleaching, under aerobic conditions. The results agreed with the study by Rezza (2001, 1997), as when extracting lithium from spodumene (6.9 wt.% Li_2O) a higher lithium concentrate in solution was produced via direct (mineral to microorganism) bioleaching processes.

In this study for the mineral specimen grade pure lepidolite (5.6 wt.% Li_2O), two mineral samples were analysed; pre-sterilisation of the mineral and no prior treatment to the mineral before bioleaching. This was carried out to determine whether the results

were due to the process parameters. After 4 weeks of bioleaching the lithium extracted in to solution was between 27 mg/L for the sterile mineral sample and 33 mg/L for no prior treatment to the mineral, the recovery rates were 9% and 12%, respectively. After a further 12 weeks of directly bioleaching under aerobic conditions, a significant increase of lithium in solution was observed at 125mg/L and 123 mg/L for the sterile and non-sterile conditions, respectively. The lithium recovery after 12 weeks was approximately 45% and 44% for the sterile and non-sterile conditions, respectively. There was a negligible difference observed between the sterile and the non-sterile conditions suggested *A.niger* was responsible for the lithium extraction into solution.

The Beauvoir lepidolite was able to extract 12mg/L of lithium in to solution after 12 weeks of direct bioleaching under aerobic conditions, recovery rate of 6%. This lower concentration, when compared to the mineral specimen grade of lepidolite, could be due to the larger particle size distribution (53 μ m to 400 μ m) used for Beauvoir, whereas for lepidolite the particle size distribution was less than 212 μ m. Finer particles provide a larger surface area for leaching and, thus are expected to have increase reactions rates. Previous studies using bioleaching of low grade ores have found a smaller particle size distribution to be more effective in leaching the desired metal (Olubambi, 2009). Other suggestions for the low lithium content could be due to the flotation reagent coating the surface of the mineral or inhibiting bioleaching, as well as other minerals present in the sample inhibiting bioleaching.

The main advantages of the bioleaching process are that it does not require high temperatures or strong chemical reactions, unlike the gypsum process. In many cases, the microorganisms used to recover the desired metal are found occurring naturally

within the mineral deposit and the surrounding mining operation. The extraction process is less energy intensive and can be developed into an economically viable process route. As well as the economic advantage of using *A. niger*, it is also beneficial for the local environment, as a new microorganism would not be introduced thus avoiding the risk of unknown factors affecting the ecosystem.

Organic acids leaching was also investigated in this study as a proof of principle, as previous studies by Rezza (2001; 1997) found that the microorganisms produced organic acids such as; oxalic and citric acids as part of their cellular metabolisms. From this study and the research in collaboration with TUKE, it can be concluded that oxalic acid was much more effective than citric acid at leaching lithium from lepidolite. In this study, 50% of lithium was recovered, when leaching heat treated lithium concentrate with oxalic acid (5% w/v) at a temperature of 70°C, achieving 424mg/L after 3 hours, although it would be more cost effective to leach lepidolite at lower temperatures of 25°C. When using the 5% concentration of oxalic acid a 3.5 mg/L of lithium was extraction into solution with a lithium recovery of 0.4%, from the Beauvoir lithium concentrate after 3 hours.

Following this study, Imerys is applying to build a pilot plant, securing funding through the Innovative UK grant. Suggestions for further research would be to develop a heap leaching process to maintain low costs. Further research would be required to optimise the leaching time and oxalic acid strength for lithium recovery on a larger scale.

CHAPTER 7

CONCLUSION AND RECOMMENDATIONS

7.1 Conclusion

Primary resources for lithium, mainly located in South America and China, are expected to be insufficient to meet the expanding demand for lithium applications (Fox-Davies, 2013). Jaskula (2015) estimated an approximate yearly increase of 10% due to lithium applications.

This thesis investigated the development of an economical process to recovery lithium from kaolin mining wastes material in the UK and Europe at reduced environmental impact securing a potential strategic supply of this element. The two main process routes investigated were; mineral processing in order to recover the lithium-bearing mineral and bioleaching to extract the metal from the mineral to produce a saleable lithium final product. A novel extraction process was developed, utilising microorganisms to extract lithium into solution. The process showed potential to reduce extraction costs, improve efficiency and ultimately recover an important raw material from resources within the UK (and Europe), reducing the environmental impact compared to existing supplies from hard rock mining and salt extraction in South America and China.

7.2 Characterisation

Lithium-bearing minerals such as lepidolite and zinnwaldite were identified by Imerys in the Beauvoir kaolin waste material as well as the St Austell granites. The lithium-bearing mineral in Beauvoir granites is lepidolite, chemical formula $K(\text{Li Al})_3(\text{Al Si})_4\text{O}_{10}(\text{FOH})_2$, a pink to greyish mineral of the mica group. It can contain between 3.3 and 7.7% Li_2O and often contains 3.0 to 5.0% rubidium and caesium oxides. Sources have been considered as economic to process by conventional means if they contain 3.0 to 4.0% Li_2O (Wietelmann, 2000). Zinnwaldite is a variant of lepidolite with a relatively high iron content, chemical formula $\text{KLiFeAl}(\text{AlSi}_3)\text{O}_{10}(\text{F,OH})_2$, typically it can contain between 2.0 to 5.0 wt.% Li_2O (Garrett, 2004).

7.3 Recovery

The recovery of lithium-bearing minerals, using principally froth flotation, was investigated. The maximum lithium grade recovered for the Beauvoir waste material was 5.0 wt.% Li_2O . For the Beauvoir waste material (hydrocyclone underflow) the lithium recoveries were dependent on the particle size distribution of the product being fed into the flotation cells. Optimum conditions were obtained when using the conditioning parameters: 80g/t of depressant and 200g/t collector. For the finer particle size fractions, a higher lithium concentrate grade was found at a lower pulp pH of 1.5, 4.8 wt.% Li_2O and a 70% recovery. In comparison, the coarser particle size fraction achieved higher lithium recovery at pH 2.5, 4.9 wt.% Li_2O and a 74% recovery.

Additional Rb_2O was identified as a significant by-product of the froth flotation process. In the lithium concentrate of particle size range of 53 μm to 400 μm , pH 1.5, 80g/t

depressant and 200g/t collector, the following oxides were reported, 4.5% Li_2O , 2.6% Rb_2O and 1.5% Fe_2O_3 at recoveries of 88%, 71% and 26%, respectively. Jaskula (2013) reported that a 3.5% increase in rubidium usage was observed in 2012 from 2011, due to increases in lithium exploration creating rubidium as a by-product and it can be expected that the commercial applications for rubidium will expand.

The maximum lithium grade recovered for the St Austell material using froth flotation was 0.47 wt.%, for the particle size fraction of $53\mu\text{m}$ to $250\mu\text{m}$ and a pulp pH of 1.5. This study indicated that for the lithium found in the St Austell waste materials from Karslake and Blackpool area, whilst it is present, is only at levels (> 0.5 wt.% Li_2O) that would make a traditional mineral processing approach uneconomic; (i.e. processing by froth flotation and chemical recovery of lithium carbonate). It is suggested that the St Austell waste materials would need to be crushed and milled prior to flotation treatment to increase the lithium recovery, although this extra stage would add additional costs to the recovery process. Other separating techniques such as wet/dry magnetic separation techniques and electrostatic separation were not successful when separating lithium bearing minerals from kaolin waste material. The poor results (< 0.1 wt% Li_2O) are suggested to be due to high concentrations of iron found within the sample, present in the mineral muscovite. Both zinnwaldite and the impurity, muscovite, had similar structural and physical properties. From the results obtained it was not sufficient to draw reliable conclusive but it was indicated that at low field strengths it was not possible to efficiently separate the minerals. It is suggested that this could be improved using higher field strengths but as this would require high costs, it is not considered an economical viable process.

Thus the waste materials obtained from the Beauvoir hydrocyclone underflow are suggested to be a potential source of lithium, when compared to hard rock extraction of other pegmatite deposits, as the mineral is already liberated from the ore via previous processing stages. Hence the operational costs of the process are reduced, due to not accruing additional mining or grinding costs.

7.4 Extraction

Worldwide, lithium is either recovered from brines or is extracted from mineral resources (spodumene) through mineral processing to produce a concentrate; thermal processing of the concentrate and then leaching to mobilise lithium into solution (Vu, 2013). The processing of mineral resources from pegmatites is costly and has a high environmental impact, as it involves roasting of a concentrated mineral with strong acid or base to release the lithium for leaching into aqueous solution. Once in solution the lithium may be easily recovered through precipitation of a carbonate. Whilst economic for some reserves, processing has a high environmental impact and the overall cost of this process is substantially affected by the energy requirements of the mining, grinding, physical separation and high temperature roasting. (Siame, 2011; Jandova, 2010).

In a comparative study, extraction processes for lithium using conventional chemical processes were investigated. Using the Beauvoir lithium concentrate only achieved 71.72 mg/L of lithium in solution, when calcined at 900°C. In order to selectively extract lithium a lithium concentration of 9g/L would be required. The low levels of lithium (>9g/L) concluding that chemical extraction is possible, but would require a complex flowsheet.

Previous studies highlighted biological leaching of lithium for treatment of waste batteries or concentrated spodumene and bio-accumulation of lithium by microorganisms (bacteria, actinomycetes, yeasts and filamentous fungi) signposts the potential of bio-leaching as a method for lithium extraction (Rezza, 2001).

In this study, a novel bioleaching process to extract lithium from the lithium-bearing mineral, lepidolite and zinnwaldite was developed. Previously this method has been used extensively in the mining industry for the recovery of copper, uranium, cobalt and gold from low grade ores not economic to process by conventional mineral processing techniques, but it has not been previously applied to other metals; hence the physical engineering of a system is not new but the interactions and biology of the system are novel. The study demonstrated the ability of fungi of the *Aspergillus niger* group to leach lithium from the lepidolite mica in significant quantity and at a significant rate; laboratory bioleaching of lepidolite produced concentrations of 32mg/l of lithium into solution after 4 weeks, recovery of 12%. After a further 8 weeks, 125mg/L of lithium in solution was detected with a recovery of 45%. The initial step is bio-accumulation where the microbial community is allowed to reproduce and then can leach lithium into solution in larger volumes. These results are a strong indication of technical and commercial feasibility for the proposed process, taking capital and operating costs known for copper bio-heap leaching and lithium refining from leach liquor used in conventional operations.

The bioleaching process has the potential to be low cost, involving no movement or additional processing of the kaolin waste before extraction of lithium, compared to the gypsum process. It offers an additional income stream from the existing kaolin

processing operations for Imerys and provide a secure supply of lithium for the UK (and Europe) into the long term future. Imerys plans to trial the extraction process at pilot scale, to determine the operational efficiency data necessary for full economic evaluation as well as assessing the impact interactions with the natural environment to be fully assessed. Data generated may well indicate the extraction of other high value metals is possible using this technique; Be, V, Ge, Rb, Y, Nb, Ta, W and Rare Earths.

7.5 Recommendations

The further recommendations from the research can be summarised as follows:

- To optimise the extraction process conditions via bioleaching on a pilot scale, through in-situ heap leaching applied to mineral processing waste stockpiles at 500 tonne scale to allow interaction with the natural environment to be examined as well as measuring recovery rates.
- To study the microbial population responsible for lithium solubilisation at the mine site and the leaching bioreaction to identify the microbes; using biochemical, molecular microbiology and flow cytometry assays, thus allowing an accurate study of the microbial-mineral interactions to be found.
- To investigate the extraction of lithium from the leach liquor and chemically refined to lithium carbonate or hydroxide as a commodity product.

REFERENCES

Amarante, M. M. (1999). Processing a spodumene ore to obtain lithium concentrates for addition to glass and ceramic bodies. *Minerals Engineering*, 12(4), 433-436.

Amer, A. M. (2008). The Hydrometallurgical Extraction of Lithium from Egyptian Montmorillonite-Type Clay. *Aqueous Processing*, 60(10), 55-57.

Ancia, D. B. A. (2010). [Allier Processing the "Stone" ore using flotation method].IMERYYS

Ancia, D. B. A. (2010). [UK Platform Li Recovery through a flotation process of Cyclones under-flow].IMERYYS

Anzaplan, D. (2013) Alternative Lithium mineral Processign Concepts *dorfner ANZAPLAN*.

Astle, T. (2009). Lithium - Hype of Substance [Press release].

Averill, W. A., & Olson, D. L. (1978). A review of extractive processes for lithium from ores and brines. *Energy*, 3(3), 305-313.

Backhurst, J. F. R. (2002). Particle Technology and Separation Processes. In Elsevier, *Flotation Coulson and Richardson's Chemical Engineering* (5th ed., Vol. 2).

Barbic, F. (2012). Intensification of Biochemical Leaching Process Through Application of Mine Water *International Mine Water Association*, 1, 223-229.

Bauer, U. W. R. J. (2000). Lithium and Lithium Compounds In Ullmann's (Ed.), *Encyclopedia of Industrial Chemistry*

Baylis, R. (2013). *Evaluating and forecasting the lithium market from a value perspective*. Paper presented at the Lithium Supply & Markets Las Vegas.

Box, S. (2012). *Lithium Industry* Paper presented at the Signals for decision makers, Chile

Brandt, F., & Haus, R. (2010). New concepts for lithium minerals processing. *Minerals Engineering*, 23(8), 659-661.

Buckley, M. and Rowson, N.A. (2007). *Biohydrometallurgy* Presentation. School of Chemical Engineering. University of Birmingham

Chehreh Chelgani, S., Leibner, T., Rudolph, M., & Peuker, U. A. (2015). Study of the relationship between zinnwaldite chemical composition and magnetic susceptibility. *Minerals Engineering*, 72, 27-30.

Chen, Y., Mariba, E. R. M., Van Dyk, L., & Potgieter, J. H. (2011). A review of non-conventional metals extracting technologies from ore and waste. *International Journal of Mineral Processing*, 98(1-2), 1-7. doi: 10.1016/j.minpro.2010.10.001

Clarke, G. (2012). Lithium supply-How much can the market digest? *Objective Capital's Rare Earths, Speciality & Strategic Metals Investment* (pp. p14). United Kingdom.

Clayton, G. D. and F. E. Clayton (eds.). *Patty's Industrial Hygiene and Toxicology*: 3rd ed. New York: John Wiley Sons, 1981-1982., p. 4936.

Cohen, H. E. (2005). Physical Separation Processes. *Ullmann's Chemical Engineering and Plant Design, Volumes 1-2* (pp. 934-937). John Wiley & Sons.

- Crocker, L. (1988). Lithium and its recovery from low-grade Nevada clays. *Bulletin (USA)*.
- Crundwell, F. K. (2003). How do bacteria interact with minerals? *Hydrometallurgy*, 71(1-2), 75-81.
- Cundy, E. K. (1960). The Occurrence of Zinnwaldite in Cornwall. *Clay Minerals Bulletin*, 4, 151-156.
- Cytec. (2002). *Mining chemical handbook*: CYTEC
- Dill, H. G. (2015). Pegmatites and aplites: Their genetic and applied ore geology. *Ore Geology Reviews*, 69(0), 417-561.
- Distin, P. A., & Phillips, C. V. (1982). The Acid Extraction of Lithium from the Granites of South West England. *Hydrometallurgy*, 9, 1-14.
- Dresler, W. J.; Reilly, I. G. ; Laffin, S.; Egab, E. (1998). The Extraction of Lithium Carbonate from a Pegmatite Deposit in Manitoba, Canada *Light Metals* (pp. 1303-1308). Warrendale, PA, USA.
- Ebensperger, A., Maxwell, P., & Moscoso, C. (2005). The Lithium Industry: Its Recent Evolution and Future Prospects. *Resources Policy*, 30(3), 218 - 231.
- Evans, K. (2008). An abundance of Lithium Raleigh.
- Fang, P.-A., & Wu, Z.-P. (2002). Effect of microstructural evolution on the mechanical properties of lepidolite based glass-ceramics. *Journal of the European Ceramic Society*, 22(8), 1381-1385.

Felix Brandt, R. H. (2010). New concepts for lithium minerals processing. In *Minerals Engineering* (Vol. 23, pp. 659-661). Retrieved 4 10, 2012.

Fox-Davies. (2013). The Lithium Market

Garrett, D. E. (2004). Part 1 - Lithium. In D. E. Garrett (Ed.), *Handbook of Lithium and Natural Calcium Chloride* (pp. 1-235). Oxford: Academic Press.

Goodbody, A. (2014). Hydrocyclones for classification in Mineral Processing *Mining*

Gruber, P. W., Medina, P. A., Keoleian, G. A., Kesler, S. E., Everson, M. P., & Wallington, T. J. (2011). Global Lithium Availability. *Journal of Industrial Ecology*, 1-16.

Hawkes, J. R. (1987). The lithium potential of the St Austell Granite *British Geological survey*

Hirtzig, J. M. P. and J. Michel, P. H. (2010). *Geology of the Cornish Kaolin Deposit*. St Austell: IMERYS CERAMICS.

Hooper, R. (2012). Lithium project geological samples. IMERYS (Ed.).

Inculet, I. (1985). Electrostatic Charges on Clays. . *IEEE Transactions on Industry Applications*, 23 - 25.

Iuga, A., Cuglesan, I., Samuila, A., Blajan, M., Vadan, D., & Dascalescu, L. (2004). Electrostatic separation of muscovite mica from feldspathic pegmatites. *Industry Applications, IEEE Transactions on*, 40(2), 422-429.

- J. Jandová; Vu, H. B., J.; Vaculíková, L.; Goliáš, V. (2013). Lithium and rubidium extraction from zinnwaldite by alkali digestion process: Sintering mechanism and leaching kinetics. *International Journal of Mineral Processing*, 123, 9-17.
- Jandova, J., Vu, H. N., Belkova, T., Dvorak, P., & Kondas, J. (2009). Obtaining Li₂CO₃ from Zinnwaldite Waste. *Ceramics - Silikaty*, 53(2), 108 - 112.
- Jaskula, B. W. (2015). Lithium. In M. C. Summaries (Ed.), *U.S. Geological Survey* (pp. 648-4908). U.S.
- JGI. (2012). *Aspergillus niger* CBS 513.88. *United States Department of Energy*
- Karavaiko, G., Krutsko, V., Melnikova, E., Avakyan, Z., & Ostroushko, Y. I. (1980). Role of microorganisms in spodumene degradation. *Microbiology*, 49(3), 402-406.
- Karavaiko, G. I. G., R.S.; Pivovarova, T.A.; & Tzaplina, L. V., N.S. (1988). Biotechnology of metals. *Biohydrometallurgy*, pp. 29-41.
- Karimi, G. R. (2010). Bioleaching of copper via iron oxidation from chalcopyrite at elevated temperatures. *Food and Bioproducts Processing*, 88, 21-25.
- Kawatra, S. K. (2001). *Coal Desulfurization: High Efficiency Preparation Methods*: New York
- Kawatra, S. K. (2011). *Froth flotation - Fundamental Principles* Electronic
- Kelland, D. R., Oberteuffer, J. A., & Massachusetts Institute of, T. (1973). *Proceedings of the High Gradient Magnetic Separation Symposium : [Cambridge], Mass., 2.5.1973*. Cambridge.
- Kim, J. B. G. a. Y. (2010). Challenges for Rechargeable Li Batteries *Chemistry of Materials Review*, 22, 587-603.

- Konopacka, Z., & Drzymala, J. (2010). Types of particles recovery—water recovery entrainment plots useful in flotation research. *Adsorption*, 16(4-5), 313-320.
- Kroschwitz, J. I., & Howe-Grant, M. (1999). *Kirk-Othmer concise encyclopedia of chemical technology* (Vol. 16): Wiley New York.
- Lanzi, F. (2008). Geological modelling and economical pit optimisation tests. IMERYYS.
- Lestang, M. (2013). Imerys doe not know the crisis with operating a "geological anomaly" in Echassieres. *Auvergne*.
- Levich, B. (2009). A five year strategic outlook for the lithium industry. *Metal Bulletin*.
- Li, L., Dunn, J. B., Zhang, X. X., Gaines, L., Chen, R. J., Wu, F., & Amine, K. (2013). Recovery of metals from spent lithium-ion batteries with organic acids as leaching reagents and environmental assessment. *Journal of Power Sources*, 233(0), 180-189.
- Li, L., Ge, J., Wu, F., Chen, R., Chen, S., & Wu, B. (2010). Recovery of cobalt and lithium from spent lithium ion batteries using organic citric acid as leachant. *Journal of Hazardous Materials*, 176(1-3), 288-293.
- Li, L., Ge, J., Chen, R., Wu, F., Chen, S., & Zhang, X. (2010). Environmental friendly leaching reagent for cobalt and lithium recovery from spent lithium-ion batteries. *Waste Manag*, 30(12), 2615-2621. doi: 10.1016/j.wasman.2010.08.008
- Ltd, Merchant Research and Consultancy. (2014). Global lithium consumption to grow 9.5% through 2020. UK Market Publishers Ltd.
- Ltd, N. G. S. (2014). Petalite.

- Luong, V. T., Kang, D. J., An, J. W., Dao, D. A., Kim, M. J., & Tran, T. . (2014). Iron sulphate roasting for extraction of lithium from lepidolite *Hydrometallurgy*, 141(0), 8-16.
- McNulty, J., & Khaykin, A. (2009). Lithium: Extracting the details on the lithium market.
- Luong, V. T., Kang, D. J., An, J. W., Dao, D. A., Kim, M. J., & Tran, T. . (2014). Iron sulphate roasting for extraction of lithium from lepidolite *Hydrometallurgy*, 141(0), 8-16.
- Manning, D. (1996). Primary lithological variation in the kaolinized St Austell Granite, Cornwall, England *Journal of Geological Society*, 153, 827-838.
- Manning, T., & Grow, W. (1997). Inductively Coupled Plasma - Atomic Emission Spectrometry. *The Chemical Educator*, 2(1).
- May, M. et al. (1989). Processing of ores to produce tantalum and lithium. *Minerals Engineering*, 2(3), 299-320.
- Mehdi, I. (2013). Leaching of Zinc from low grade oxide ore using organic acid. *Physicochemical Problems of Mineral Processing*, 49(2), 547-555.
- Meshram, P., Pandey, B. D., & Mankhand, T. R. (2014). Extraction of lithium from primary and secondary sources by pre-treatment, leaching and separation: A comprehensive review. *Hydrometallurgy*, 150(0), 192-208.
- Miller, J., Khalek, N. A., Basilio, C., Shall, H., Fa, K., Forssberg, K., .Rao, K. (2007). *Flotation Chemistry and Technology of Nonsulfide Minerals*.
- MIR. (2008). The Trouble with Lithium 2. In M. I. Research (Ed.). France

- Mishra, D., Kim, D.-J., Ralph, D. E., Ahn, J.-G., & Rhee, Y.-H. (2008). Bioleaching of metals from spent lithium ion secondary batteries using *Acidithiobacillus ferrooxidans*. *Waste Manag*, 28(2), 333-338.
- Mortland, MM (1978). Development in Sedimentology. *International Clay Conference, Vol 6*. Amsterdam: Elsevier.
- McNulty, J., & Khaykin, A. (2009). Lithium: Extracting the details on the lithium market: Credit Suisse.
- Mulligan, C. N. (2004). Bioleaching of heavy metals from a low-grade mining ore using *Aspergillus niger*. *Journal of Hazardous Materials*, 110, 77-84.
- Murray, H. (2000). *Traditional and new applications for kaolin, smectite and palygorskite: A General Overview. Applied Clay Science*.
- Naden, J. (2012). *Sustainable use of natural resources* Nottingham Natural Environment Research Council.
- Napier-Munn, T. J. (2006). *Mineral Processing Technolgy* (T. Napier-Munn Ed. Seventh ed.): Elsevier
- Neijssel, O., Mattos, M. J. T. d., & Tempest, D. W. (Eds.). (1993). *Overproduction of Metabolites*. Germany: VCH.
- Nomura, K. (2002). Crystal Structure Gallery, National Institute of Advanced Industrial Science and Technology (AIST)
<https://staff.aist.go.jp/nomura-k/english/itscgallery-e.htm>

- Rezza, I., Salinas, E., Calvente, V., Benuzzi, D., & Tosetti, M. I. S. d. (1997). Extraction of lithium from spodumene by bioleaching. *Letters in Applied Microbiology*, 25(3), 172-176.
- Olubambi, P. A., Potgieter, J. H., Ndlovu, S., & Borode, J. O. (2009). Electrochemical studies on interplay of mineralogical variation and particle size on bioleaching low grade complex sulphide ores. *Transactions of Nonferrous Metals Society of China*, 19(5), 1312-1325.
- Osman, M. A., Ploetze, M., & Suter, U. W. (2003). Surface treatment of clay minerals ? thermal stability, basal-plane spacing and surface coverage. *Journal of Materials Chemistry*, 13(9), 2359. doi: 10.1039/b302331a
- Paulino, J. F., Busnardo, N. G., & Afonso, J. C. (2008). Recovery of valuable elements from spent Li-batteries. *J Hazard Mater*, 150(3), 843-849. doi: 10.1016/j.jhazmat.2007.10.048
- Pistilli, M. (2012). Lithium Deposit Types: Brine, Pegmatite and Sedimentary *Investing News*.
- Rezza, I., Salinas, E., Elorza, M., Sanz de Tosetti, M., & Donati, E. (2001). Mechanisms involved in bioleaching of an aluminosilicate by heterotrophic microorganisms. *Process Biochemistry*, 36(6), 495-500.
- Reider, M. (1998). Nomenclature of the micas. *The Canadian Mineralogist*, 36, 905-912.

Richardson, J. F., Harker, J. H., & Backhurst, J. R. (2002). Flotation *Coulson and Richardson's Chemical Engineering Volume 2 - Particle Technology and Separation Processes* ((5th Edition) ed., Vol. 2, pp. 62-67): Elsevier.

Roskill. (2012). Lithium Market. *Lithium Market 2014*.

Rowson, N. A. (2010). Mineral purification techniques, University of Birmingham.

Ryu, T., Lee, D.-H., Ryu, J. C., Shin, J., Chung, K.-S., & Kim, Y. H. (2015). Lithium recovery system using electrostatic field assistance. *Hydrometallurgy*, 151(0), 78-83.

Santhiya, D., & Ting, Y.-P. (2005). Bioleaching of spent refinery processing catalyst using *Aspergillus niger* with high-yield oxalic acid. *Journal of Biotechnology*, 116(2), 171-184.

Samková, R. (2009). Recovering Lithium Mica from the waste after mining Sn-W Ores through the use of flotation

Schinner, W. B. F. (1993). Leaching of metals with fungi. *Journal of Biotechnology*, 27(2), 91-116.

Serjeant, E.P., Dempsey B.; Ionisation Constants of Organic Acids in Aqueous Solution. International Union of Pure and Applied Chemistry (IUPAC). 1979. New York, New York: Pergamon Press, Inc., p. 989

Siame, E. (2011). *Recovery of Lithium from China Clay Waste Using a Combination of Froth Flotation, Magnetic Separation, Roasting and Leaching*. University of Exeter.

Siame, E., & Pascoe, R. D. (2011). Extraction of lithium from micaceous waste from china clay production. *Minerals Engineering*, 24(14), 1595-1602.

Smith, L., E. M. (2011). Global Lithium Market Outlook: Projects and Strategies to 2020 for a New Era of Demand.

Strasser, H. (1994). High-yield production of oxalic acid for metal leaching processes by *Aspergillus niger*. *FEMS Microbiology Letter*, 119, 365-370.

Subrahmanyam, E. F. (1988). *Froth Stability, Particle Entrainment and Drainage in Flootation- A review*. International Journal of Mineral Processing.

Strategically important metals: Government Response to the Committee's Fifth Report of Session 2010-12. (2011). In H. o. C. S. a. T. Committee (Ed.), (9th reopr ed.).

Survey, B. G. (2013). World Mineral Production 2009-2013 *Minerals Statistics*. UK.

Sun, L., & Qiu, K. (2012). Organic oxalate as leachant and precipitant for the recovery of valuable metals from spent lithium-ion batteries. *Waste Manag*, 32(8), 1575-1582.

Sylvester, P. J. (2010). *Use of the Mineral Liberation Analyzer (MLA) for Mineralogical studies of sediments and sedimentay rocks*. Paper presented at the Mineralogical Association of Canada Canada

Thompson, B. (2012). *Beauvoir kaolin and cassiterite oprations*. IMERYYS.

Thompson, C. A. (2011). *Mineral Commodity Summaries 2011*. Hauppauge, N.Y: Nova Science Publishers.

Torma, A. E., Gabra, G. G., Guay, R., & Silver, M. (1976). Effects of surface active agents on the oxidation of chalcopyrite by thiobacillus ferrooxidans. *Hydrometallurgy*, 1(4), 301-309.

Tsuruta, T. (2005). Removal and recovery of lithium using various microorganisms. *J Biosci Bioeng*, 100(5), 562-566.

U.S.Geological Survey. (2013). Mineral Commodity

- U.S.Geological Survey. (2008). Lithium. In USGS (Ed.).
- U.S.Geological Survey. (2011). Rare Earth Elements - End Use and Recyclability
- Ulrich Wietelmann, R. J. (2000). Lithium and Lithium Compounds. In *Ullmann's Encyclopedia of Industrial Chemistry*. Wiley-VCH.
- Vu, J. J. H. (2008). *Processing of zinnwaldite wastes to obtain lithium and rubidium compounds*. Paper presented at the Global Symposium on Recycling, Waste Treatment and Clean Technology, Mexico.
- Wagner, F. S. (2006). *Rubidium and Rubidium Compounds*: JohnWiley & Sons.
- Watson, H. H. R. J. (1962). *Introduction to Geology* (Second ed. Vol. 1). London and Basingstoke: The Macmillian Press.
- WS. (2013). Where is it Found and Produced
- Wills, B. A., & Napier-Munn, T. (2006). *Wills' Mineral Processing Technology: An Introduction to the Practical Aspects of Ore Treatment and Mineral Recovery* (7th ed.). Burlington: Butterworth-Heinemann.
- Yan, Q., Li, X., Wang, Z., Wu, X., Guo, H., Hu, Q., . . . Wang, J. (2012). Extraction of valuable metals from lepidolite. *Hydrometallurgy*, 117-118, 116-118.
- Yan, Q., Li, X., Wang, Z., Wu, X., Wang, J., Guo, H., Peng, W. (2012). Extraction of lithium from lepidolite by sulfation roasting and water leaching. *International Journal of Mineral Processing*, 110-111, 1-5.
- Yan, Q.-x., Li, X.-h., Wang, Z.-x., Wang, J.-x., Guo, H.-j., Hu, Q.-y., . . . Wu, X.-f. (2012). Extraction of lithium from lepidolite using chlorination roasting–water leaching

process. *Transactions of Nonferrous Metals Society of China*, 22(7), 1753-1759. doi: 10.1016/s1003-6326(11)61383-6

Yu, L.-x., Wang, H.-d., Qiu, G.-z., & Liang, D.-y. (2010). Comprehensive utilization of kaolin ore accompanying muscovite. *Journal of Central South University of Technology*, 17(5), 954-958. doi: 10.1007/s11771-010-0583-4

APPENDIX

List of conferences:

Biochemical Engineering Young Researchers (2014) University of Birmingham, UK.

23rd World Mining Congress (2013), Montreal, Canada.

23rd International Mining Congress & Exhibition of Turkey (2013), Antalya, Turkey.

Mineral Engineering Symposium (2013), East Midlands, UK.

2nd International Conference on Environmental Pollution & Remediation (2012),
Canada.

List of publications:

Iqbal, Z. and Rowson N.A. (2013) Recovery of Lithium rich micas from mineral waste,
23rd World Mining Congress, Montreal, Canada.

Iqbal, Z. and Rowson N.A. (2013) Recovery of Lithium Rich Mica from Mineral
Waste, 23rd International Mining Congress & Exhibition of Turkey, Antalya, Turkey.

Iqbal, Z. and Rowson N.A. (2013) Recovery of Lithium Rich Micas from Mineral
Waste, Mineral Engineering Symposium, East Midlands, UK.

Iqbal, Z. and Rowson N.A. (2012) Lithium Recovery From Kaolin Mining Waste
Material, 2nd International Conference on Environmental Pollution & Remediation,
Canada.